

Natural Product Biosynthesis by *Streptomyces venezuelae*:  
Genetic Variants for Drug Discovery

by

Jeanna MacLeod

Submitted in partial fulfilment of the requirements for the  
degree Master of Science

at

Dalhousie University

Halifax, Nova Scotia

November 2017

© Copyright by Jeanna MacLeod, 2017

## TABLE OF CONTENTS

LIST OF TABLES .....	vi
LIST OF FIGURES .....	vii
ABSTRACT .....	xi
LIST OF ABBREVIATIONS AND SYMBOLS USED .....	xii
ACKNOWLEDGEMENTS .....	xiv
CHAPTER 1: INTRODUCTION .....	1
1.1    Natural Products .....	1
1.2    Biosynthesis of Natural Products .....	2
1.3    Streptomyces venezuelae as a Source of Natural Products .....	3
1.3.1    Jadomycin Biosynthesis .....	7
1.4    Project Aims .....	9
Chapter 2: ISOLATION OF NOVEL JADOMYCINS BY PRECURSOR-DIRECTED BIOSYNTHESIS .....	10
2.1    Jadomycin lactam analogue incorporating 4-(Aminomethyl)benzoic Acid.....	12
2.1.1 Introduction .....	12
2.1.2 Results and Discussion .....	13
2.2    Jadomycins incorporating 3-(Aminomethyl)benzoic Acid .....	16
2.2.1    Introduction .....	16
2.2.2    Results and Discussion .....	17
2.3    Isolation and Characterization of an 11-membered E-ring Jadomycin .....	25
2.3.1    Introduction .....	25
2.3.1    Results and Discussion .....	26
2.4    Conclusions .....	32
2.5    Experimental Methods .....	33
2.5.1    General .....	33
2.5.2    Jadomycin Production Methods .....	35

2.5.3	Jadomycin Purification Methods .....	35
2.5.4	Compound Characterization .....	37
2.5.5	Productions using 4-AMBA .....	39
2.5.6	Productions using 3-AMBA .....	41
2.5.7	Productions using 8-aminooctanoic acid .....	48
CHAPTER 3: PRODUCTION OF C-GLYCOSIDIC JADOMYCINS .....		52
3.1	Natural Product Glycosylation .....	52
3.2	Synthetic Biology and Combinatorial Biosynthesis within Gene Clusters .....	53
3.3	Natural Product C-Glycosylation .....	55
3.3.1	C-Glycosyltransferase Toolbox .....	55
3.3.2	UrdGT2 Characteristics .....	57
3.4	Heterologous Expression of UrdGT2 for C-glycoside Jadomycin Production ..	57
3.4.1	Introduction .....	57
3.4.2	Results and Discussion .....	58
3.5	Conclusions .....	71
3.6	Experimental Methods .....	74
3.6.1	General Laboratory Procedures .....	75
3.6.2	Vector Construction .....	81
3.6.3	Mutant Preparation .....	89
3.6.4	Jadomycin Production Conditions .....	94
3.6.5	Jadomycin Purification Methods .....	95
3.6.6	Extract Characterization .....	95
CHAPTER 4: EXPLORATION OF SILENT BIOSYNTHETIC GENE CLUSTERS ..		96
4.1	Cryptic and Silent Biosynthetic Gene Clusters .....	96
4.2	Regulation of Biosynthesis .....	98
4.2.1	LuxR Family .....	99

4.3	Cryptic Gene Cluster Selection .....	101
4.4	Cryptic Gene Cluster Activation .....	103
4.4.1	Generation of pLuxR Mutant of <i>S. venezuelae</i> .....	103
4.4.2	Evaluation of Natural Product Biosynthesis .....	105
4.5	Conclusions .....	110
4.6	Experimental Methods .....	111
4.6.1	General Laboratory Procedures .....	111
4.6.2	Vector Construction .....	112
4.6.3	Mutant Preparation.....	113
4.6.4	Production Conditions .....	114
4.6.5	Natural Product Purification Methods .....	115
4.6.6	Natural Product Analysis and Characterization .....	117
CHAPTER 5: CONCLUSIONS .....		118
REFERENCES .....		120
APPENDIX I: Supplementary Information for Chapter 2.....		131
7.1	Jadomycin 4-AMBA Amide (1) Data .....	131
7.2	Jadomycin 3-AMBA Data.....	134
7.2.1	Jadomycin 3-AMBA Acetate Major (2a).....	134
7.2.2	Jadomycin 3-AMBA Acetate Minor (2b).....	137
7.2.3	Jadomycin 3-AMBA 3a-Methoxy (3).....	141
7.2.4	Jadomycin 3-AMBA Lactam (4) .....	145
7.3	Jadomycin Undec Data.....	149
7.3.1	Jadomycin Undec Major (5a).....	149
7.3.2	Jadomycin Undec Minor (5b).....	155
7.3.3	Jadomycin Undec Open E-ring Analogues (6, 7).....	157
APPENDIX II: Supplementary Information for Chapter 3 .....		160

8.1	UrdGT2 Gene and Protein Sequences.....	160
8.2	Control Production Analysis .....	161
APPENDIX III: Supplementary Information for Chapter 4 .....		164
9.1	Control Compound Data .....	164
9.2	Supplemental Production Data.....	164

## LIST OF TABLES

Table 1. Biosynthetic gene clusters in <i>Streptomyces venezuelae</i> ISP5230 as identified by antiSMASH 3.0.....	4
Table 2. Changes in chemical shift at the 3a-position and adjacent protons across the characterized 3-AMBA Jds.....	20
Table 3. Notable trends observed through the series of unsubstituted extended E-ring jadomycins. ....	30
Table 4. NMR assignment for 1 (700 MHz, MeOD).....	40
Table 5. NMR assignment for 2a (700 MHz, MeOD).....	43
Table 6. NMR assignment for 2b (700 MHz, MeOD).....	44
Table 7. NMR assignment for 3a (700 MHz, MeOD).....	45
Table 8. NMR assignment for 3b (700 MHz, MeOD).....	46
Table 9. NMR assignment for 4 (700 MHz, MeOD).....	47
Table 10. NMR assignment for 5a (700 MHz, MeOD).....	50
Table 11. NMR assignment for 5b (700 MHz, MeOD).....	51
Table 12. Selection of bacterial polyketide C-glycosyltransferases involved in secondary metabolism.....	56
Table 13. Methods for heterologous gene complementation in <i>Streptomyces</i> .....	59
Table 14. List of bacterial strains and plasmids used in Chapter 3.....	74
Table 15. List of primers used in Chapter 3.....	75
Table 16. Collection of LAL-family activators involved in positive secondary metabolite regulation. ....	100
Table 17. LuxR genes identified within the <i>S. venezuelae</i> BGC.....	101
Table 18. Cluster R6 genes and putative functions.....	103
Table 19. List of bacterial strains and plasmids used in this study.....	111

## LIST OF FIGURES

Figure 1. Natural products associated with <i>S. venezuelae</i> biosynthetic gene clusters.....	5
Figure 2. Jadomycin biosynthesis; assembly of the aromatic backbone, incorporation of the amino acid, biosynthesis and transfer of the dideoxysugar. ....	8
Figure 3. Jadomycons 4-AMBA congeners.....	13
Figure 4. (A) Structure of 1 with diastereotopic C1' protons; (B) <sup>1</sup> H NMR spectrum illustrating downfield shifted A-ring protons; (C) HMBC correlation of H4 to the 3a carbonyl. HSQC correlations of 4AMBA jadomycin amide 1' CH <sub>2</sub> protons. ....	15
Figure 5. Jadomycin production with 3-(aminomethyl)benzoic acid. ....	16
Figure 6. (A) Key COSY and HMBC correlations supporting the structural characterization of 2a; (B) Key HBMC correlations from H3a to the acetate branch C2 and the 3-AMBA C1'. ....	19
Figure 7. (A) Jadomycin F (JdF, F) and doxorubicin (Dox); (B) IC <sub>50</sub> values of 2a, 2b, 3, 4, versus positive controls Dox and JdF in 231-CON and 231-TXL breast cancer cells. P ≤ 0.05, n ≥ 4. In 231-CON cells, the IC <sub>50</sub> value is significantly different versus that of † all 3-AMBA Jds, # Dox, JdF, 3, and 4, and \$ all other treatments; in 231-TXL cells, the IC <sub>50</sub> value is significantly different versus that of ‡ Dox, JdF, and 2, as determined by one-way ANOVAs, followed by Bonferroni's multiple comparison tests. *The IC <sub>50</sub> value of the treatment is significantly higher in the 231-TXL versus 231-CON cells, as determined by unpaired t tests; (C) fold-resistance values of Jds and Dox, measuring the relative resistance of the 231-TXL cells to each drug treatment versus 231-CON cells, n ≥4. *P ≤ 0.05, the value is significantly lower than that of Dox, as determined by a one-way ANOVA, followed by Bonferroni's multiple comparison test. ....	22
Figure 8. (A) Previously characterized jadomycons with unsubstituted, extended E-rings; (B) production of Jd Undec from 8-aminooctanoic acid. ....	25
Figure 9. Incorporation of amino acid to form a hemiaminal center. Further decarboxylation and cyclization to Jd Undec scaffold or E-ring open jadomycin analogues; where R is a proton or l-digitoxose and n is 7. ....	26
Figure 10. Structure of 5a, illustrating important (A) <sup>1</sup> H- <sup>13</sup> C HMBC correlations (solid arrows), and (B) <sup>1</sup> H- <sup>1</sup> H COSY correlations (bold lines); key <sup>1</sup> H- <sup>13</sup> C HMBC spectrum correlations from (C) H3a, (D) H6'. ....	28
Figure 11. High resolution fragmentation of 5a [M+H] <sup>+</sup> to [M+H - digitoxose] <sup>+</sup> and (inset) from [M+H - digitoxose] <sup>+</sup> to [phenanthroviridin+H] <sup>+</sup> . ....	29

Figure 12. Jd Undec 3a-O-methoxy analogue (6) and its deuterated isotopomer (6d) and the Jd Undec 3a-acetate analogue (7). .....	31
Figure 13. <i>S. venezuelae</i> growth and Jd production MSM with 3-AMBA and d-serine..	41
Figure 14. <i>S. venezuelae</i> growth and Jd production in MSM with 8-aminooctanoic acid and d-serine.....	48
Figure 15. l-digitoxose biosynthetic genes and their contributions to the dideoxysugar biosynthesis and transfer.....	53
Figure 16. Demonstrated UrdGT2 flexibility to donor and acceptor substrates; (inset) proposed jadomycin substrates and proposed donor substrate l-digitoxose shown in <sup>1</sup> C <sub>4</sub> and <sup>4</sup> C <sub>1</sub> conformers.....	57
Figure 17. l-digitoxose biosynthetic gene cluster in the jadS replacement and deletion <i>S. venezuelae</i> mutants.....	61
Figure 18. Jadomycin fragments ions used in precursor ion scans (PREC).....	65
Figure 19. <i>S. venezuelae</i> urdGT2 ( $\Delta$ jadS) culture analysis; (A) Jadomycin production growth curves; HPLC traces of (B) JdG crude extract, (C) JdDS crude extract; PREC 306 ion scans of (D) wild-type JdG crude extract and (E) <i>S. venezuelae</i> urdGT2 ( $\Delta$ jadS) JdG crude extract.....	66
Figure 20. JdG and JdDS productions of pKC1139-derived urdGT2 and jadS complemented <i>S. venezuelae</i> $\Delta$ jadS (SV_11Urd and SV_11JS, respectively); HPLC traces of (A) SV_11JS and (B) SV_11Urd; PREC 306 ion scans of (C) SV_11JS and (D) SV_11Urd.....	67
Figure 21. Growth and JdG production in integrative urdGT2 and jadS complemented <i>S. venezuelae</i> $\Delta$ jadS. (SV_52Urd and SV_52JS, respectively); SV_52JS JdG crude analysis by (B) HPLC and (D) LC-MS PREC 306 indicating formation O-glycosylated jadomycins, including jadomycin O-glucoside (C).....	69
Figure 22. Analysis of JdG and JdDS productions in SV_52Urd; HPLC traces of (A) JdG and (B) JdDS; PREC 306 scans of (C) JdG and (D) JdDS; ESI <sup>+</sup> non-selective scans of (E) JdG and (F) JdDS.....	70
Figure 23. pKC1139_jadQ::urdGT2::jadT construction; (A) EcoR1 and HindIII double restriction digest of transformant colony plasmid isolates; (B) Confirmatory data; undigested plasmid (coiled), ScaI digest (no digestion, coiled), NcoI digest (linearized plasmid), XbaI and HindIII double digest (3.1 kb drop out).....	84



Figure 24. Construction of pKC1139_jadQT; (A) jadT and jadQ PCR fragments for overlap extension; (B) jadQT overlap extension PCR product; (C) XbaI and HindIII double restriction digest of NEB 5-alpha transformant pKC1139_jadQT. ....	85
Figure 25. (A) XbaI/HindIII double digest of pSE34_urdGT2; (B) XbaI/HindIII double digest of pSE34_jadS. ....	86
Figure 26. EcoR1/HindIII double digests of pKC1139_urdGT2 and pKC1139_jadS. ....	87
Figure 27. (A) XbaI/XhoI double digest of pSET152 (1.8 kb dropout) and pSEE152 (2.1 kb dropout); (B) XbaI/KpnI double digest of pSEE152 plasmids. ....	89
Figure 28. 1-digitoxose biosynthetic genes of <i>S. venezuelae</i> wild-type, urdGT2( $\Delta$ jadS), $\Delta$ jadS. ....	89
Figure 29. (A) Colony PCR of wild-type and urdGT2( $\Delta$ jadS) <i>S. venezuelae</i> ; (B) Colony PCR <i>S. venezuelae</i> $\Delta$ jadS and wild-type. ....	91
Figure 30. (A) PCR of pKC1139_urdGT2, and gDNA from the SV_11JS and SV_11Urd transformants, amplified using permE* primers; (B) PCR of gDNA from the SV_11JS and SV_11Urd transformants, amplified using permE* Fwd primer and gene-specific Rev primer. ....	92
Figure 31. (A) PCR of gDNA from the SV_WT5 and SV_52DS transformants, amplified using permE* primers; (B) PCR of gDNA from the transformants SV_52JS, SV_52Urd, and SV_WUrd, amplified using insert-specific primers. ....	92
Figure 32. JdG and JdDS productions of pKC1139-derived urdGT2 and jadS complemented <i>S. venezuelae</i> $\Delta$ jadS. (SV_11Urd and SV_11JS, respectively). ....	94
Figure 33. JdG productions of pSEE152 (empty) control strains of <i>S. venezuelae</i> wild-type (SV_WT5) and <i>S. venezuelae</i> $\Delta$ jadS SV_52DS. ....	95
Figure 34. (Inset) organization of the genes in Cluster R6; biosynthesis of indolocarbazoles from tryptophan. ....	102
Figure 35. Vector construction; (A) R6 LuxR fragment and downstream flanking region PCR fragments for overlap extension; (B) digestions of NEB 5-alpha transformant pKC1139_R6 LuxR(OE) to confirm plasmid identity; (C) ermE* PCR fragment from pSE34; (D) XbaI and NdeI double digestion of NEB 5-alpha transformant pKC1139_R6 pLuxR to confirm plasmid identity. ....	104
Figure 36. Mutant confirmation; (A) PCR using permE* primers; (B) PCR using LuxR cassette flanking primers. ....	105

Figure 37. Comparative analysis of R6 and WT paired productions; (A) TLC of WT and R6 extract from dl-W supplemented productions; (B) TLC of R6 extract from non-supplemented and dl-W supplemented productions; (C) HPLC trace of R6 extract from dl-W supplemented production; (D) HPLC trace of WT extract from dl-W supplemented production. ....	106
Figure 38. NMR spectra of RFM productions with 5F-W supplementation ( <sup>19</sup> F:470 MHz). ....	108
Figure 39. Jadomycin production crude material HPLC traces. JadDS productions with ethanol shock from (A) WT and (B) R6; JadDS productions without ethanol shock from (C) WT and (D) R6; JadG productions with ethanol from (E) WT and (F) R6; JadG productions without ethanol from (G) WT and (H) R6. ....	109

## ABSTRACT

Natural product biosynthesis in *Streptomyces venezuelae* ISP5230 was investigated in three ways. First, through precursor-directed jadomycin biosynthesis using non-proteinogenic amino acids (4-(aminomethyl)benzoic acid, 3-(aminomethyl)benzoic acid, 8-aminooctanoic acid), five novel jadomycins were isolated and characterized. Four novel jadomycins were evaluated for cytotoxic activity in drug-sensitive and drug-resistant cancer cells and a panel of six microbes. Next, jadomycin C-glycoside production was attempted by heterologous expression of *urdGT2* in place of the native O-glycosyltransferase, *jadS*. C-glycoside production was not observed from three complementation methods pursued. Finally, a *S. venezuelae* mutant was prepared to evaluate a silent biosynthetic gene cluster identified through genome mining. While the changes to the biosynthetic profile were apparent in the activator overexpression mutant, the major products detected were previously identified metabolites of tryptophan, including tryptophol. The studies demonstrated the pliability of *S. venezuelae* ISP5230 as a producer of natural products through manipulations to growth conditions, supplementation, and genetic variation.

## LIST OF ABBREVIATIONS AND SYMBOLS USED

$\epsilon$	Molar absorptivity
$\lambda_{\max}$	Wavelength of maximal absorbance
Abs	absorbance
ACN	acetonitrile
amu	Atomic mass unit
ATCC	American type culture collection
ATMA	Auto-tune and match
bm	Broad multiplet
bs	Broad singlet
Cam	Chloramphenicol
COSY	Correlation spectroscopy
CV	Column volume
d	doublet
DCM	Dichloromethane
dd	Doublet of doublets
ddH <sub>2</sub> O	Distilled, deionized water
DNA	Deoxyribonucleic acid
EDTA	ethylenediaminetetraacetic acid
EPI	Enhanced product ion
ESI	Electrospray ionization
EtOAc	Ethyl acetate
EtOH	Ethanol
H <sub>2</sub> O	Water
His <sub>6</sub> -tag	Histidine tag
HMBC	Heteronuclear multiple bond correlation spectroscopy
HPLC	High performance liquid chromatography
HRMS	High resolution mass spectrometry
HSQC	Heteronuclear single quantum coherence spectroscopy
ISP	International <i>Streptomyces</i> Project
Jd	Jadomycin
LB	Lysogeny broth
LC-MS	Liquid chromatography mass spectrometry
m	Multiplet
Mj	Major

Mn	Minor
<i>m/z</i>	Mass to charge ratio
MeOD	Deuterated methanol, methanol- <i>d</i> <sub>4</sub>
MeOH	Methanol
MS/MS	Tandem mass spectrometry
MSM	Minimal salt media
MYM	Maltose yeast media
NCI	National Cancer Institute (US)
NCI DTP	National Cancer Institute (US) Developmental Therapeutics Program
NIH	National Institute of Health (US)
NMR	Nuclear magnetic resonance
NMR-3	Nuclear magnetic resonance resource (Dalhousie University)
nOe	Nuclear Overhauser effect
NOESY	Nuclear Overhauser effect spectroscopy
NRC	National Research Council
NRC IMB	National Research Council Institute for Marine Biosciences
NRPS	Non-ribosomal peptide synthase
OD	Optical density
PKS	Polyketide synthase
ppm	Parts per million
PREC	Precursor ion
q	Quartet
RBS	Ribosomal binding site
<i>R<sub>f</sub></i>	Retention factor
RNA	Ribonucleic acid
rpm	Revolutions per minute
<i>R<sub>t</sub></i>	Retention time
RT	Room temperature
s	Singlet
t	Triplet
TAE	Tris base, acetic acid, EDTA buffer solution
TIC	Total ion chromatogram
TLC	Thin layer chromatography
UV-Vis	Ultra-violet/visible light

## **ACKNOWLEDGEMENTS**

Thanks to Dr. David Jakeman for the opportunity, the guidance, and the resources to do this work. I'd like to extend my gratitude to the members of the Jakeman Group that help in many ways, large and small: Stephanie Forget, Madison Carroll, Dr. Jian-She Zhu (current) along with Nicole Alward, Camilo Martinez-Farina and Dr. Andrew Robertson (past). Thank you to my committee members, Dr. Kerry Goralski and Dr. Tannis Jurgens, as well as to the Dalhousie College of Pharmacy and Department of Chemistry faculty, administrators, and staff for their help in facilitating my education. And finally, an enormous thank you to Kevin MacLeod and to both of our families for all the support as I entered and completed this degree.

## **CHAPTER 1: INTRODUCTION**

### **1.1 Natural Products**

Throughout history, compounds from nature have been used therapeutically in complex mixtures and with the progression of medicinal and pharmacological sciences, the bioactive natural products were isolated from the mixtures and used clinically.<sup>1-3</sup> Natural sources grew to become - and continue to be - a valuable tool in drug discovery and development.<sup>4</sup> Early natural products were predominantly from plant sources,<sup>1</sup> with microbial natural products being incidental providers of antibiotics in fermented or molded food and beverages;<sup>2</sup> however, in the growth of natural products research, bacterial and fungal sources provided hallmark compounds for infective disease treatments.<sup>5</sup> Microbes have become the predominant source of natural product drug therapies;<sup>2</sup> in fact, microbial sources are being identified as responsible for the production of select natural products previously identified from plant and marine animal sources.<sup>4,6</sup> Natural product research has contributed greatly to the development of antibacterial agents in particular, with 77% of antibiotics approved by the FDA since 2000 from natural product sources (natural products or derivatives), all of which were derived from microbes.<sup>2</sup>

With accelerating antimicrobial resistance, microbial sources are being sought as a source of novel antibiotics, due to the past success and to the unique chemical property space they provide.<sup>5</sup> While interest in typical bacterial natural product isolation methods from industry has waned due to the high cost of purification and the frequency of isolation of known compounds, novel approaches to access natural product diversity have renewed the field of research.<sup>7</sup> High-throughput screening based on the “One Species Many

Compounds” (OSMAC) approach of varying media compositions and growth conditions in addition to the many genome-based mining approaches have allowed for new chemistry to be discovered from previously studied bacteria.<sup>7-9</sup>

Natural products are successful sources of drug candidates, as they are designed through evolution to interact with biological systems.<sup>10</sup> Often they contain complex stereochemistry and many oxygen-containing moieties.<sup>11</sup> Therefore, finding new chemical entities (NCEs) from natural sources are desirable for the discovery of drugs with novel mechanisms of action for improved therapies against drug-resistant diseases (bacterial infections, aggressive cancers) or novel therapies for diseases for which there are no current treatments.

## **1.2 Biosynthesis of Natural Products**

Natural products are also referred to as secondary metabolites, as they are produced through separate cell machinery from primary metabolism, using primary metabolites (e.g. acetate, isoprene, amino acids, glucose) as precursors. These alternate pathways are highly regulated and are comprised of biosynthetic machinery with conserved domains, such as polyketide synthases (PKSs), non-ribosomal peptide synthetases (NRPSs), and terpene synthases (TSs).<sup>9,12</sup> Genes for biosynthesis of secondary metabolites are clustered on chromosomes or plasmids and often contain regulatory genes.<sup>7,13,14</sup> Natural products may be produced as a response to stress conditions or as a competitive survival strategy, therefore, they are a protective or defensive response to external stimuli.<sup>11,15,16</sup>



### 1.3 *Streptomyces venezuelae* as a Source of Natural Products

*Streptomyces* are a genus of Gram-positive bacteria which are prolific providers of natural products with therapeutic and commercial value, accounting for the production of approximately fifty percent of known antibiotics.<sup>17</sup> *Streptomyces venezuelae* ISP5230, ATCC 10712, (*S. venezuelae*) is a strain which was studied initially for its ability to produce chloramphenicol,<sup>18</sup> but more recently for its ability to produce the jadomycin family of compounds.<sup>19-21</sup> It is a fast-growing, sporulating species with a high G+C content and, fortunately, it is amenable to liquid culture conditions and genetic manipulation techniques, making it a relatively forgiving species to study.<sup>22</sup>

The genome of *S. venezuelae* ISP5230 was sequenced and was published in 2011.<sup>22</sup> The 8.22 Mb genome has been annotated with over 7000 predicted protein-coding genes. A sequence analysis was performed using the online antiSMASH 3.0 software,<sup>23</sup> and thirty-one biosynthetic gene clusters were identified (Table 1).

**Table 1.** Biosynthetic gene clusters in *Streptomyces venezuelae* ISP5230 as identified by antiSMASH 3.0

Cluster	Description	Nucleotides (NC018750.1)	Associated natural product(s)
Cluster R1	Ectoine	237842-248258	
Cluster R2	Terpene	274553-325254	Geosmin <sup>24</sup>
Cluster R3	T1PKS-T3PKS-NRPS	504136-604067	Venemycin, Watasemycin, Isopyochelin <sup>25,26</sup>
Cluster R4	Lantipeptide-Terpene	614220-645285	Isodauc-8-en-11-ol <sup>27</sup>
Cluster R5	Lantipeptide	707463-730315	Venezuelin <sup>28</sup>
Cluster R6	Indole	867489-890695	
Cluster R7	Other	1020853-1073914	Chloramphenicol <sup>18</sup>
Cluster R8	Other	2055965-2096690	
Cluster R9	Siderophore	2791630-2806751	
Cluster R10	Lasso peptide	3408328-3430687	
Cluster R11	Other	4387707-4451900	
Cluster R12	Butyrolactone	4522206-4533171	Gaburedins <sup>29</sup>
Cluster R13	Cf_saccharide-Melanin	4984388-5019228	
Cluster R14	Butyrolactone	5476839-5502716	
Cluster R15	Thiopeptide	5526743-5557501	
Cluster R16	T3 PKS	5785193-5826323	Unknown <i>m/z</i> 425 <sup>30</sup>
Cluster R17	Siderophore	5869901-5883169	
Cluster R18	Siderophore	5936046-5950407	
Cluster R19	Bacteriocin (Peptide)	6331621-6361866	
Cluster R20	Butyrolactone-T2pks	6493381-6531550	Jadomycin <sup>19,20</sup>
Cluster R21	Other	6657180-6759607	
Cluster R22	NRPS-Cf_fatty_acid- Ladderane	6683678-6856821	
Cluster R23	NRPS	6760862-6856821	
Cluster R24	Terpene	7020725-7084124	2-Methylisoborneol <sup>24</sup>
Cluster R25	Bacteriocin (Peptide)	7128838-7139692	
Cluster R26	T2pks (Spore Pigment, 83%)	7409956-7464101	
Cluster R27	Melanin	7484949-7495338	
Cluster R28	NRPS	7698646-7760938	Foroxymithine <sup>31</sup>
Cluster R29	Terpene	7788497-7809951	
Cluster R30	Alkylresorcinol (T3pks)	7946146-7987237	
Cluster R31	Terpene-Nrps	8189935-8226158	

Nine of these clusters are associated with one, or several, characterized natural products (Figure 1), and one is associated with an uncharacterized natural product with a  $m/z$  of 425. The remaining identified gene clusters are putative, bearing limited homology to reported gene clusters or sub-clusters, suggesting they encode genes to produce secondary metabolites with novel chemistry. These uncharacterized clusters include PKSs, NRPS, and TSs, along with interesting hybrid gene clusters. The exploration of these clusters will be discussed further in Chapter 4.

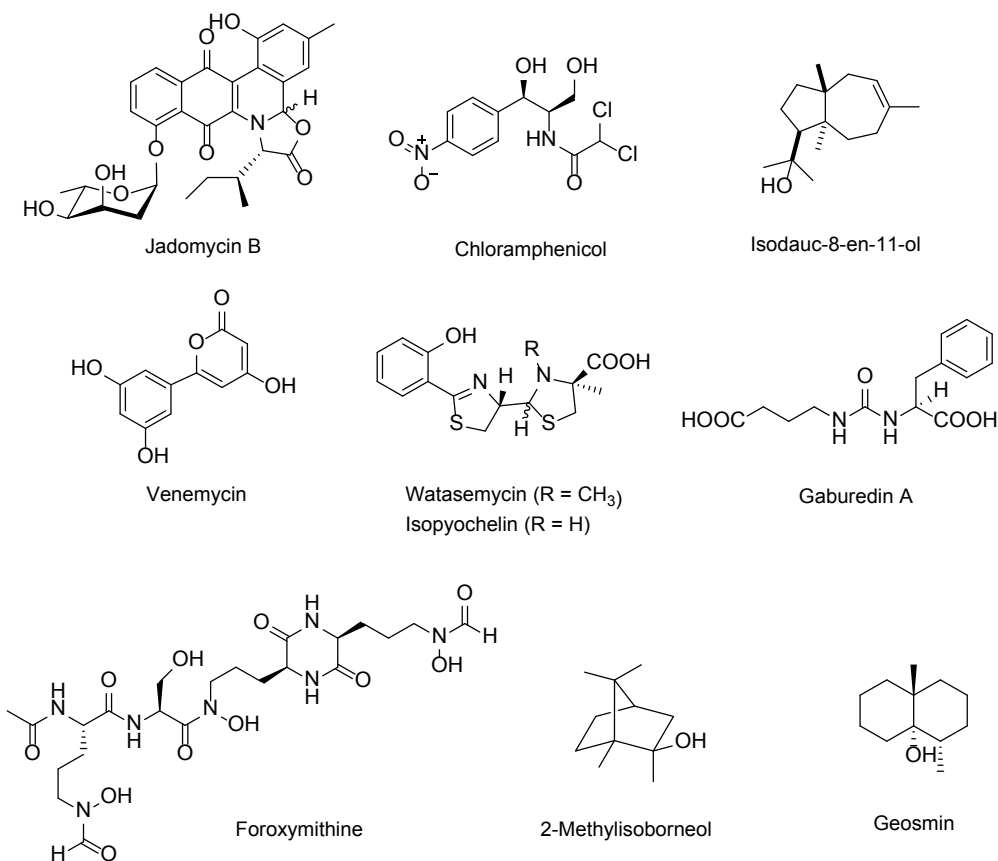


**Figure 1.** Natural products associated with *S. venezuelae* biosynthetic gene clusters.

Chloramphenicol is a clinically relevant natural product, originally isolated from another strain of *Streptomyces venezuelae* and re-isolated by Leo Vining (Dalhousie University)

from *S. venezuelae* ISP5230.<sup>32</sup> In studying chloramphenicol biosynthesis in *S. venezuelae*, Doull *et al.* serendipitously discovered jadomycin A, an angucycline polyketide, in a heat-shocked fermentation which turned purple.<sup>19</sup> Jadomycin B (Figure 1), the glycosylated form of jadomycin A, was discovered in subsequent cultures.<sup>33,20</sup>

Foroxymithine is a known siderophore, isolated from an iron deficient culture of *S. venezuelae* in a rationally-designed culturing strategy based upon identification of NRPS genes homologous to the peucechelin biosynthetic gene cluster.<sup>31</sup> The gaburedins are a family of  $\gamma$ -aminobutyrate-derived ureas isolated from a mutated strain of *S. venezuelae* in which a transcriptional repressor, identified by genome mining, was inactivated. Gaburedin A (Figure 1) was the major component of the six identified analogues.<sup>29</sup> Geosmin and 2-methylisoborneol (2-MIB) are terpene secondary metabolites commonly produced in soil-borne actinomycetes.<sup>34</sup> The terpene synthases for these volatile compounds were identified through genome analysis and subsequent gene inactivation, where sven\_RS01290 disruption abolished geosmin production and sven\_RS35205 disruption abolished 2-MIB production.<sup>24</sup>

Recent reports from the Bibb and Challis groups identified several natural products through comparative transcriptional analysis of *S. venezuelae* wild-type and a *bldM* deletion strain, where *bldM* is a regulator involved in morphological differentiation.<sup>25,26,35</sup> The venemycins, small chlorinated polyketides were produced in the  $\Delta bldM$  mutant in limited quantities, but in isolable yields in another mutant overexpressing a LuxR activator gene sven\_RS36965 under a constitutive promoter.<sup>25</sup> A 2-hydroxyphenylthiazoline BGC, which exhibited increased transcription in the  $\Delta bldM$  mutant, was heterologously

expressed in *S. coelicolor* M1152, yielding isolation of the known non-ribosomal peptide siderophores thiazostatin and watasemycin, and the novel C-methylated isopyochelin.<sup>26</sup>

In a CRISPR-Cas9 knock-in study, a bi-directional promoter was inserted between a type III PKS gene (sven\_RS 26635) and a cytochrome P450 gene (sven\_RS26640). The mutant produced pigmented products on solid media, and analysis of the ethyl acetate extract revealed a unique peak in the UV chromatogram and a major peak in the mass spectrum with  $m/z$  425 which were not observed in the wild-type extract.<sup>30</sup> A structure has not yet been reported.

Finally, two of the biosynthetic gene clusters identified in *S. venezuelae* have been studied through heterologous expression of the structural genes with their predicted substrates. Isodauc-8-en-11-ol is a sesquiterpene alcohol identified in an evaluation of a terpene cyclase encoded by sven\_RS02645 with its predicted substrate, farnesyl pyrophosphate.<sup>27</sup> Similarly, venezuelin was characterized through expression of the NRPS sven\_RS02980 and its substrate peptide in *E. coli* and co-incubated, resulting in the mature peptide.<sup>28</sup>

### **1.3.1 Jadomycin Biosynthesis**

The jadomycins are an interesting family of compounds, as they are glycosylated with a rare dideoxysugar, L-digitoxose, and they have an amino acid incorporated into the aromatic angucycline backbone; these locations provide an interesting opportunity for structural activity relationship studies. The biosynthesis of the jadomycin backbone and the L-digitoxosyl sugar nucleotide are detailed in Figure 2, noting that the functions of these biosynthetic enzymes have been inferred through homology to characterized

enzymes and have not been evaluated individually. An amino acid is non-enzymatically incorporated, giving a final oxazolone ring with the amino acid side chain as the R-group.

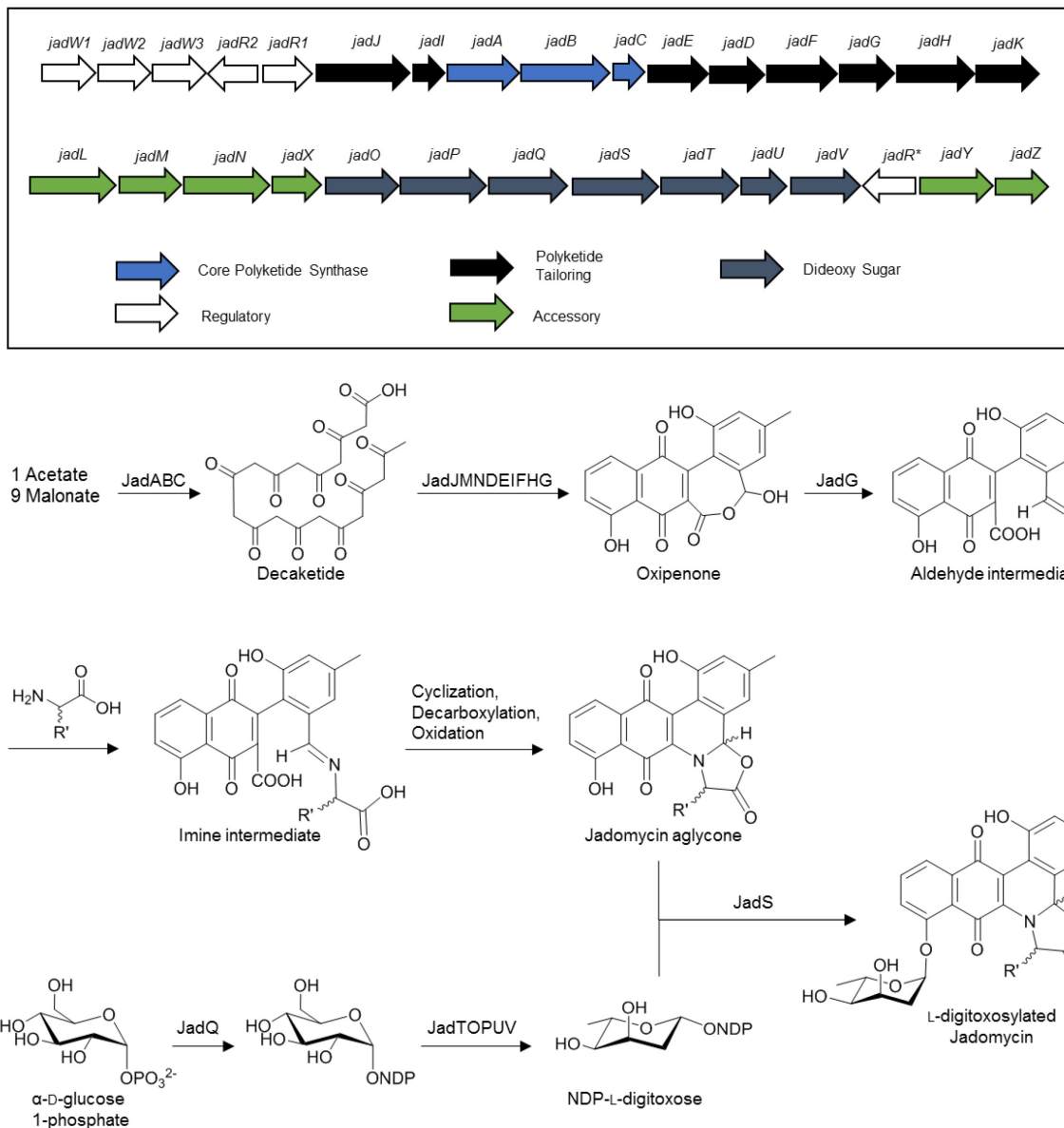


**Figure 2.** Jadomycin biosynthesis; assembly of the aromatic backbone, incorporation of the amino acid, biosynthesis and transfer of the dideoxysugar.

## 1.4 Project Aims

This thesis was conducted in three project arms, detailed in the succeeding three chapters and introduced briefly here. First, production of novel jadomycins was investigated by precursor-directed biosynthesis using non-proteinogenic amino acids, selected to probe the non-enzymatic cyclization of the E-ring. Second, the production of *C*-glycosylated jadomycin analogues was explored by combinatorial biosynthesis, through heterologous expression of a *C*-glycosyltransferase in place of the native *O*-glycosyltransferase, with the aim of generating hydrolytically stable jadomycin *C*-glycosides to screen for anti-cancer activity. And third, *S. venezuelae* secondary metabolite production was explored through the activation of an uncharacterized biosynthetic gene cluster. The overexpression strain was evaluated for novel natural products.

## CHAPTER 2: ISOLATION OF NOVEL JADOMYCINS BY PRECURSOR-DIRECTED BIOSYNTHESIS

Polyketides (PKs) are a vast and structurally diverse group of natural products which are an important source of medicines with antibiotic, anti-parasitic, immunosuppressant, and antitumor activity.<sup>36,37</sup> The structural intricacy of polyketides arises from highly-controlled assembly and tailoring of the simple biosynthetic units, acetate and malonate. Polyketides are classified as Type I, II, or III based on their biosynthetic origins from modular- or iterative-type PK synthases (PKS).<sup>36</sup> Type II PKSs are iterative synthases which typically use malonyl extender units to generate polyaromatic natural products.<sup>38</sup> The jadomycins (Jds) are type-II polyketides, classified within the large decaketide angucycline group of natural products which also contains the landomycins, urdamycins, and gilvocarcins.<sup>39</sup> The Jds differ from the other angucyclines in that their unique biosynthesis involves the non-enzymatic incorporation of an amino acid into the polyaromatic core.<sup>33,40</sup>

This non-enzymatic amino acid incorporation permits assimilation of a range of substituents into the angucycline backbone simply by including the amino acid as the only nitrogen source in liquid culture. The preparation and characterization of a large library of jadomycin analogues using proteinogenic and non-proteinogenic amino acids has been performed by the Jakeman group in the last twelve years.<sup>21,41-54</sup> Until recently, the range of chemistry for jadomycin incorporation was principally limited by the metabolism characteristics of *S. venezuelae*; if the amino acid was an inadequate nitrogen source for *S. venezuelae*, the cells could not proliferate and therefore natural product synthesis could not proceed. To overcome this, it was discovered that including an established nitrogen source at a reduced concentration in the culture media with the selected precursor amino acid



facilitated both *S. venezuelae* proliferation and jadomycin production with incorporation of the selected precursor amino acid.<sup>52</sup> Furthermore, the supplemental amino acid (D-serine) was not biosynthetically incorporated into the jadomycin, so siphoning of biosynthetic effort is not a limitation to the method.

Based on this culture method, jadomycin biosynthesis were performed using each of three amino acids which were insufficient as sole nitrogen sources for *S. venezuelae*, but were incorporated in jadomycin productions supplemented with D-serine. In each, jadomycin productions were performed using *S. venezuelae* VS1099, a mutant with an apramycin disruption cassette inserted into the *jadW<sub>2</sub>* repressor gene for improved jadomycin production<sup>55</sup> and monitored at 600 nm (OD<sub>600</sub>) to quantify cellular proliferation and at 526 nm (Abs<sub>526</sub>) to approximate the production of the coloured jadomycins.

## 2.1 Jadomycin lactam analogue incorporating 4-(Aminomethyl)benzoic Acid

Excerpts taken from Robertson, A.W.; MacLeod, J.M.; MacIntyre, L.W.; Forget, S.M.; Hall, S.R.; Bennett, L.G.; Correa, H.; Kerr, R.G.; Goralski, K.B.; Jakeman, D.L. *Submitted to J. Org. Chem.* **2017**. Manuscript ID jo-2017-02823e.

### 2.1.1 Introduction

The jadomycin polyketide backbone terminates in the formation of dehydrorabelomycin, a substrate for post-PKS enzyme catalysis that transforms the dehydrorabelomycin into the oxepinone, which is subsequently opened by JadG to produce an aldehyde intermediate (Figure 2).<sup>38,56</sup> It is with this aldehyde that the amino acid present in the growth medium reacts non-enzymatically to finally deliver the cyclized B- and E-rings.<sup>44,49,57</sup> The presence of a cyclized E-ring has been prevalent in all previously characterized jadomycin congeners.<sup>21</sup>

With the aim to probe the structural diversity permissible from non-enzymatic amino acid incorporation, 4-(aminomethyl)benzoic acid (4-AMBA) was selected for study. It was postulated that the 4-AMBA amino group would react with the aldehyde biosynthetic intermediate to form an imine but the rigid benzyl moiety would prohibit E-ring cyclization with the carboxylate group (Figure 3). It was anticipated that a longer-lived imine intermediate would allow for novel chemistry to occur. Indeed, five new jadomycin analogues (Figure 3) were identified and described from cultures with 4-AMBA. The first two natural products identified possessed reactive hemiaminal centers to compensate for the inability to cyclize (Jd 4-AMBA hydroxy and 3a-O-methyl) and two further congeners (Jd 4-AMBA acetate and pyruvate) demonstrated a previously unreported post type-II PKS core carbon-carbon bond formation. Biosynthesis of the jadomycin polyaromatic core is

highly specific, with no C-C branching being observed in any of the previously isolated analogues [isolated and characterized by A.W. Roberston]. Lastly, a lactam variant (**1**) was identified, proposed to be a product of spontaneous oxidation of the dynamic hemiaminal congeners at the 3a-position [isolated and characterized by J.M. MacLeod].

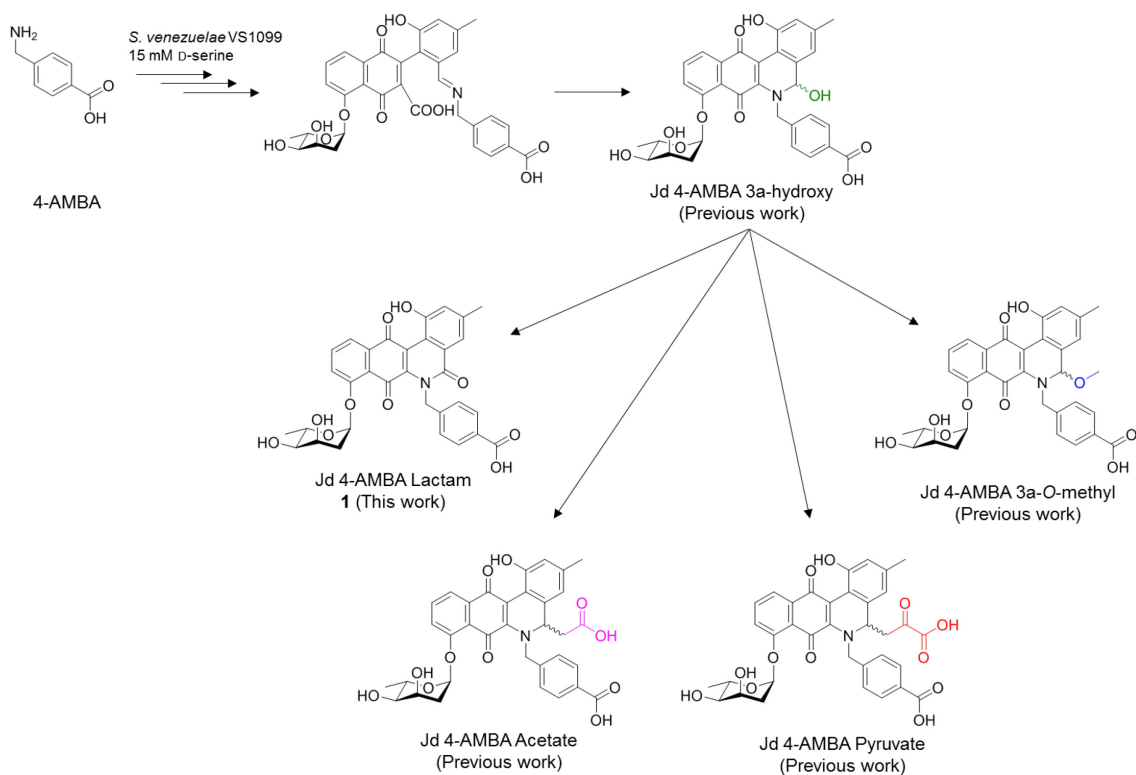


**Figure 3.** Jadomycins 4-AMBA congeners.

### 2.1.2 Results and Discussion

Cultures were carried out using previously established bacterial growth conditions with 4-AMBA (60 mM),<sup>58</sup> but *S. venezuelae* was unable to proliferate with 4-AMBA as the sole nitrogen source, so a modified procedure was implemented with co-supplementation of a second amino acid. Cultures with D-serine (15 mM) and 4-AMBA (60 mM) promoted *S. venezuelae* growth and natural product production. TLC analysis of the culture extract identified several new colored compounds that did not correspond to the previously

reported D-serine jadomycin analogue (JdDS).<sup>59</sup> [Culture and processing performed by L. MacIntyre and A.W. Robertson]

During the purification of a red *O*-methyl jadomycin analogue, an orange compound was observed by TLC with a similar  $R_f$ . This compound was separately purified by normal phase prep-TLC and two rounds of reverse phase prep-HPLC, after which 1.2 mg was characterized by HRMS and NMR analysis. The  $^1\text{H-NMR}$  spectrum indicated a glycosylated jadomycin-like compound in which the chemical shifts H4 and H6 ( $\delta_{\text{H4}} = 7.96$ ,  $\delta_{\text{H6}} = 6.94$ ) of the A-ring were shifted downfield compared to that of **1** ( $\delta_{\text{H4}} = 6.97$ ,  $\delta_{\text{H6}} = 6.85$ ), likely owing to the presence of an adjacent carbonyl group (Figure 4B). Only one diastereomer was observed, which is unusual for jadomycons as they typically possess a 3a-stereocenter. The observation of an HMBC correlation between the H4 ( $\delta_{\text{H}} = 7.57$ ) and C3a ( $\delta_{\text{C}} = 164$ ) (Figure 4C) supported a structure of jadomycin 4AMBA-lactam (**1**) with oxidation of the 3a position, consistent with reported data for a previously isolated lactam derivative.<sup>53</sup> HRMS analysis identified an  $m/z$  of 584.1640 corresponding to  $\text{C}_{32}\text{H}_{26}\text{NO}_{10}$  and consistent with the proposed  $[\text{M-H}]^-$  of **1**.  $^1\text{H-NMR}$ , HMBC, and  $^1\text{H-}^1\text{H}$  COSY analysis confirmed the intact core jadomycin polyaromatic backbone, the presence of the L-digitoxose glycosylation at the 12-position, and the incorporation of the 4-AMBA moiety. Interestingly, the C1' methylene protons behaved very differently; where the peak for H1'b was broadened and gave weak HSQC correlations while H1'a was a sharp doublet (Figure 4D). These protons had a weak COSY correlation, and phased negative in the edited-HSQC, confirming their identification as diastereotopic methylene protons.

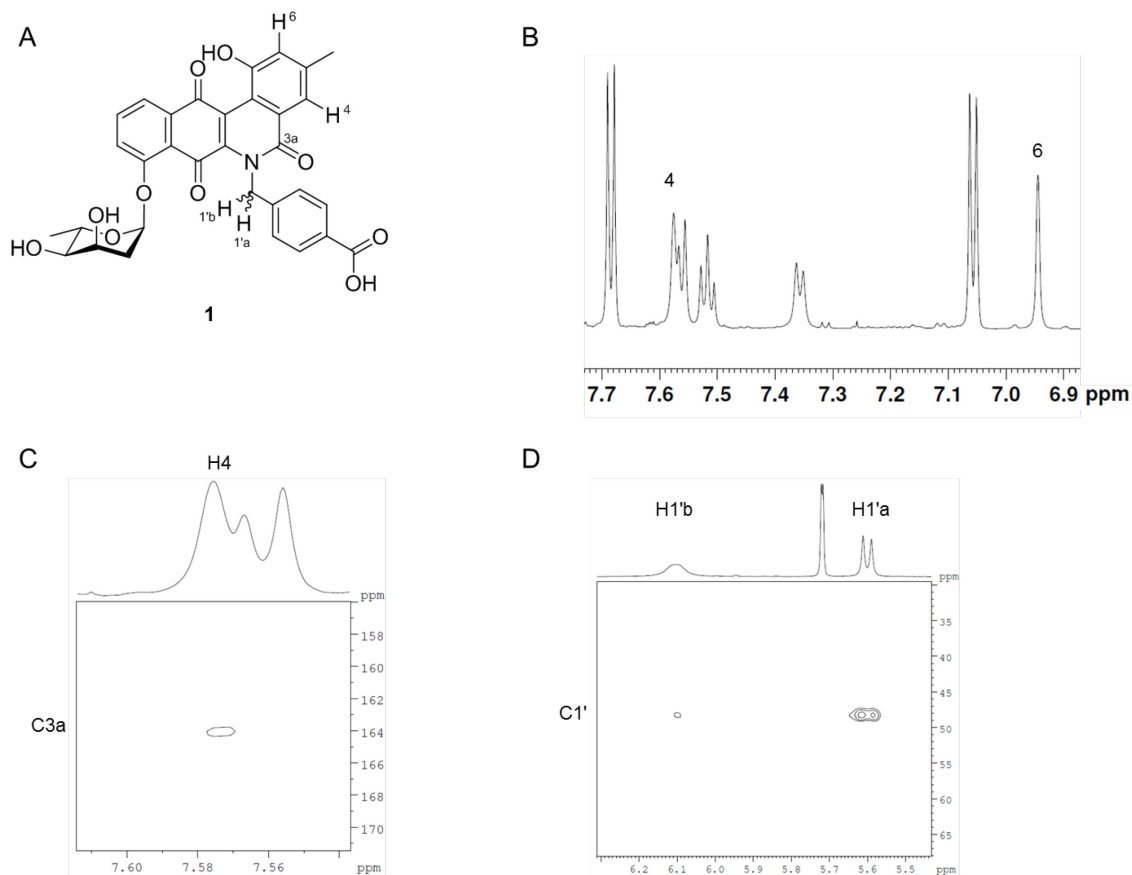


**Figure 4.** (A) Structure of 1 with diastereotopic C1' protons; (B)  $^1\text{H}$  NMR spectrum illustrating downfield shifted A-ring protons; (C) HMBC correlation of H4 to the 3a carbonyl. HSQC correlations of 4AMBA jadomyacin amide 1'  $\text{CH}_2$  protons.

While NMR characterization was performed in MeOD, alternate deuterated solvents were used in attempts to obtain spectra with a sharper 1'b signal, but the jadomyacin amide analogue had limited solubility in a variety of solvents (acetone, chloroform, acetonitrile, deuterium oxide) and unfortunately broke down to a dark green compound when solubilized in *N,N*-dimethylformamide.

## 2.2 Jadomycins incorporating 3-(Aminomethyl)benzoic Acid

Excerpts taken from Robertson, A.W.; MacLeod, J.M.; MacIntyre, L.W.; Forget, S.M.; Hall, S.R.; Bennett, L.G.; Correa, H.; Kerr, R.G.; Goralski, K.B.; Jakeman, D.L. *Submitted to J. Org. Chem.* **2017**. Manuscript ID jo-2017-02823e.

### 2.2.1 Introduction

The isolation of a series of structural congeners where the hemiaminal center was not only oxidized, but also subjected to a biosynthetically unusual post-PKS C-C bond forming step<sup>52</sup> informed the decision to further examine this phenomenon and whether it was limited to those particular 4-AMBA analogues, or if *S. venezuelae* could be induced to accomplish this C-C bond formation in other Jd congeners. The isolation of three new Jd congeners with C3a C-C branching, solvent substitution, and oxidation (Figure 5) was accomplished through incorporation of 3-(aminomethyl)benzoic acid (3-AMBA) into the jadomycin scaffold. The identification of the acetate-branched congener indicates there is a broader substrate specificity for the C-C bond forming step within the *S. venezuelae*.

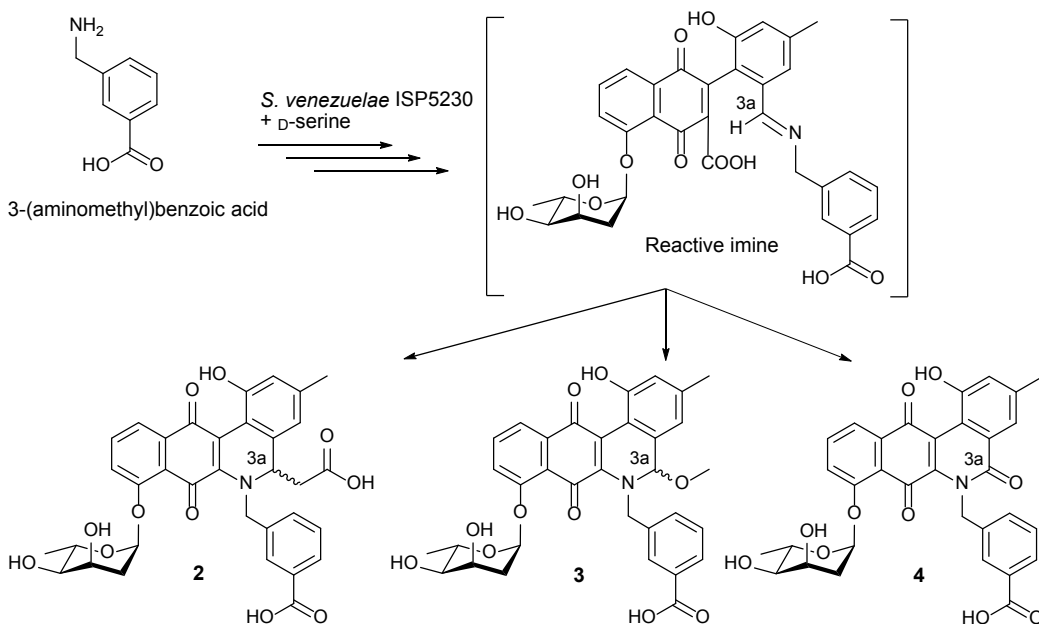


**Figure 5.** Jadomycin production with 3-(aminomethyl)benzoic acid.

### 2.2.2 Results and Discussion

Jadomycin productions were performed as previously described,<sup>52</sup> culturing *S. venezuelae* ISP5230 VS1099 in minimal media with 3-AMBA (60 mM) and supplementing with D-serine (15 mM). The productions continued for 96 hours, extending the typical Jd production duration due to modest absorbance values at 526 nm ( $A_{526}$ ) at 48 hours, where  $A_{526}$  values approximate the concentration of the coloured Jds in the production media (Figure 13). After 96 hours, the production media was coloured deep purple. Crude extract was generated by silica-phenyl flash chromatography. Analysis of the crude methanolic extract by TLC identified three major coloured spots, one red and two violet. These were anticipated to be novel open E-ring Jd congeners, as the natural product colouration and relative polarity were consistent with the previously characterized 4-AMBA jadomycins.<sup>52</sup>

The material was crudely purified by preparative TLC to generate three fractions, each enriched with one of the major coloured compounds initially identified by TLC. These coloured fractions were examined by LC-MS using ESI- scans to assign the natural product identity. The two polar, violet compounds had masses corresponding to Jd 3-AMBA 3a-acetate (**2**) and the red material was identified as Jd 3-AMBA 3a-*O*-methyl (**3**) (data not shown). Subsequent <sup>1</sup>H NMR data indicated that the two violet compounds were in fact separable diastereomers of the 3a-acetate analogue (**2a**, **2b**). Largely, Jds are isolated and characterized as a mixture of the C3a diastereomers. The diastereomers form upon E-ring cyclization (Figure 2) and readily interconvert through a ring-opening/recyclizing mechanism.<sup>57</sup> In **2**, the inability to interconvert between diastereomers facilitated the individual isolation and characterization of the isomers **2a** and **2b**.

There was no evidence of a 3a-pyruvate branched analogue, as was observed in the 4-AMBA system;<sup>52</sup> the crude culture material was revisited to probe for that analogue by LC-MS, but no evidence of its formation has been obtained. Interestingly, the major products by TLC appeared to be the violet 3a-acetate congener (**2a**) and not the red 3a-O-methyl (**3**), whereas in the 4-AMBA system, the major natural product was the 3a-O-methyl analogue.<sup>52</sup>

#### *Isolation and Characterization of Jadomycin 3-AMBA Acetate*

The violet compounds were further purified for characterization by preparative TLC and size exclusion chromatography. The isolated diastereomers had a 100:72 ratio of the major diastereomer (**2a**) to the minor diastereomer (**2b**). The high-resolution mass spectrum of **2a** provided an  $m/z$  of 628.1824 [M-H]<sup>-</sup>, corresponding to the presumed chemical formula C<sub>34</sub>H<sub>30</sub>NO<sub>11</sub>. The compound was characterized completely by NMR (Table 5). The COSY spectrum showed correlations characteristic of the L-digitoxosyl and the angucycline (H9-11, H4-6) backbone spin systems (Figure 6A). COSY correlations also established the connectivity of the H3a (triplet) to the branched acetate C2 methylene protons to support C-C branching. The structure was further corroborated by HMBC correlations from H3a to the branched acetate C2 and the C1' of the amino acid (Figure 6B). Incorporation of the intact 3-AMBA into the Jd structure was supported by COSY correlations across H6'-8' and HMBC correlations within the benzyl ring and to the carboxylic acid (C5') and C1' methylene. Similar data supported the characterization of the minor diastereomer **2b**. NMR data for the assignments were consistent with the previously characterized 4-AMBA acetate jadomycin analogue.<sup>52</sup>



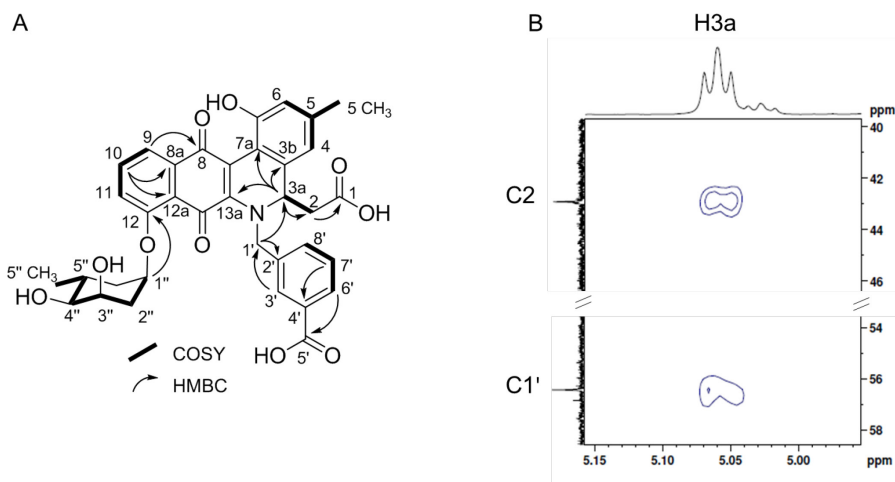


**Figure 6.** (A) Key COSY and HMBC correlations supporting the structural characterization of **2a**; (B) Key H3a correlations from H3a to the acetate branch C2 and the 3-AMBA C1'.

#### *Isolation and Characterization of Jadomycin 3-AMBA 3a-O-Methyl*

The red 3a-*O*-methyl (**3**) was also purified for characterization by preparative TLC and size exclusion chromatography. Due to the dynamic nature of the C3a in **3**, separation of diastereomers was not feasible and, as such, the mixture of diastereomers was characterized with an observed 1:1 Mj:Mn ratio. HRMS of **3** provided an  $m/z$  of 600.1853 [M-H]<sup>-</sup>, consistent with the chemical formula C<sub>33</sub>H<sub>30</sub>NO<sub>10</sub>. To demonstrate the rapid exchange of the C3a substitution, **3** was also re-suspended in methanol-*d*<sub>4</sub> (MeOD) to generate **3d** (Figure S22) for HRMS analysis. The formation of **3d** proceeded readily, as evidenced by a +3 increase in the observed  $m/z$  to 603.2044 [M-H]<sup>-</sup> corresponding to a chemical formula of C<sub>33</sub>H<sub>27</sub>D<sub>3</sub>NO<sub>10</sub> (Figure S24). The COSY and HMBC correlations observed in the NMR spectra of **2** established similar connectivity of the jadomycin backbone and 3-AMBA incorporation presented in Figure 2; the COSY spectrum outlined spin systems for the *L*-digitoxosyl, angucycline (H9-11, H4-6), and 3-AMBA (H6'-8') backbones and the HMBC correlations established connectivity through the 3-AMBA to

the H3a. There were notable differences in the chemical shifts of the 3a-position and adjacent protons (Table 2) as a result of the electronegative *O*-methyl substitution, in agreement with the previously characterized 4-AMBA 3a-*O*-methyl jadomycin.<sup>52</sup> The H3a multiplicity was observed here as singlet, contrasting with the triplet H3a observed in the acetate-branched analogues.

**Table 2.** Changes in chemical shift at the 3a-position and adjacent protons across the characterized 3-AMBA Jds.

Jd	$\delta_{\text{C or H}}$					
	C3a	H3a	H4	H6	H1'a	H1'b
<b>2a</b>	64.8	5.06	6.39	6.61	4.86	5.74
<b>2b</b>	64.8	5.03	6.39	6.62	4.81	5.78
<b>3Mj</b>	91.6	5.58	6.63	6.82	4.95	5.75
<b>3Mn</b>	91.6	5.56	6.62	6.81	5.15	5.57
<b>4</b>	163.9	N/A	7.91	7.20	5.67	6.22

#### *Identification, Isolation, and Characterization of Jadomycin 3-AMBA Lactam*

A portion of the crude material was reserved at -30°C for several months. Subsequent analysis of this crude material by TLC permitted identification of a new orange spot of similar polarity to **3**, suggesting formation of the lactam analogue by spontaneous oxidation during storage.<sup>52,53</sup> This orange material was purified in a similar fashion to **3** to yield jadomycin 3-AMBA lactam (**4**). An *m/z* of 584.1542 [M-H]<sup>-</sup> was consistent with the expected molecular formula C<sub>32</sub>H<sub>26</sub>NO<sub>10</sub>. By NMR, only one diastereomer was observed, indicative of a loss of chirality at C3a. The H4, H6, and H1'(a,b) were shifted dramatically downfield relative to congeners **2** and **3** (Table 2), consistent with literature data for the previously characterized lactam jadomycons.<sup>52,53</sup> The downfield shift of H1'(a,b) provided

evidence of C1' proximity to C3a, as HMBC correlations supporting connectivity of the 3-AMBA moiety were not observed.

#### *Cytotoxic and Anti-Microbial Activity*

Breast cancers are stratified for treatment based on the expression of estrogen receptor (ER), progesterone receptor (PR), and human epidermal growth factor receptor 2 (HER2). Jds have previously demonstrated equal cytotoxicity in MCF7 (ER+, PR+, HER2-), BT474 (ER-, PR+, HER2+), SKBR3 (ER-, PR-, HER2+), and MDA-MB-231 (ER-, PR-, HER2-) breast cancer cell lines,<sup>60-63</sup> with the lattermost being the most difficult to treat clinically due to the lack of hormone receptor targets. Furthermore, metastatic breast cancer curability has been diminished by the development of multidrug resistance (MDR) within cancerous cells.<sup>64,65</sup> A major mechanism of MDR is the overexpression of ABCB1, a broad-spectrum multidrug efflux pump which expels chemotherapeutics from within the cell and renders treatments ineffective. ABCB1 is the best studied of the various ABC-transporters,<sup>66-68</sup> and its expression is increased after certain therapies, including taxanes and anthracyclines, which has been associated with further treatment failure.<sup>69,70</sup> Many Jd analogues are effective against MCF7 breast cancer cells and largely retain their potency in MDR MCF7 breast cancer cells that overexpress the ABC drug efflux transporters, including *ABCB1*.<sup>60</sup> In comparison, known ABC-transporter substrates such as doxorubicin (Dox, Figure 7A), etoposide, or mitoxantrone drugs lose their cytotoxic potency in these cells.<sup>60</sup>

The anti-cancer activity of compounds **2a**, **2b**, **3** and **4** was examined with a drug-sensitive MDA-MB-231 triple negative breast cancer cell line (231-CON) and a taxol-resistant variant cell line (231-TXL) using a MTT proliferation assay, with activity observed for all

analogues in the low micromolar range. Dox and jadomycin F (JdF, Figure 7A) were assayed in parallel to generate data for comparison to prior literature.<sup>60-62</sup> With the exception of **2**, the 3-AMBA Jd analogues were less potent cytotoxic agents compared to the positive control JdF, which we previously identified as one of the most potent cytotoxic Jds.<sup>60,61</sup> The IC<sub>50</sub> values of all jadomyjcins and control doxorubicin were significantly higher in the 231-TXL versus 231-CON cells (Figure 7B).

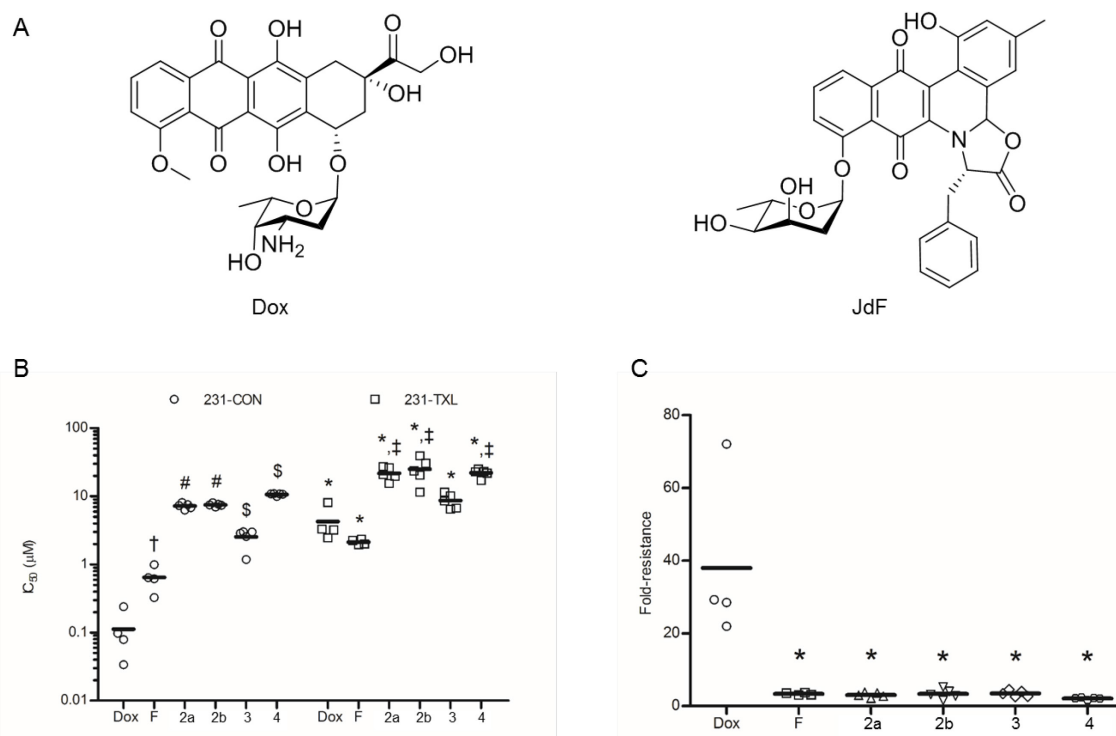


**Figure 7.** (A) Jadomycin F (JdF, F) and doxorubicin (Dox); (B) IC<sub>50</sub> values of **2a**, **2b**, **3**, **4**, versus positive controls Dox and JdF in 231-CON and 231-TXL breast cancer cells.  $P \leq 0.05$ ,  $n \geq 4$ . In 231-CON cells, the IC<sub>50</sub> value is significantly different versus that of † all 3-AMBA Jds, # Dox, JdF, **3**, and **4**, and \$ all other treatments; in 231-TXL cells, the IC<sub>50</sub> value is significantly different versus that of ‡ Dox, JdF, and **2**, as determined by one-way ANOVAs, followed by Bonferroni's multiple comparison tests. \*The IC<sub>50</sub> value of the treatment is significantly higher in the 231-TXL versus 231-CON cells, as determined by unpaired *t* tests; (C) fold-resistance values of Jds and Dox, measuring the relative resistance of the 231-TXL cells to each drug treatment versus 231-CON cells,  $n \geq 4$ . \* $P \leq 0.05$ , the value is significantly lower than that of Dox, as determined by a one-way ANOVA, followed by Bonferroni's multiple comparison test.

The 3-AMBA jadomycin analogues demonstrated the ability to retain their potency in MDR breast cancer cells, based on their inhibition of MDR 231-TXL versus drug-sensitive 231-CON cell proliferation. To quantify the resistance of the 231-TXL cells to the drug treatments, fold-resistance values were calculated.<sup>60</sup> None of the fold-resistance values for the Jds were significantly different from each other, and all were significantly lower than Dox (Figure 7C). While the IC<sub>50</sub> values of all Jd treatments were found to be significantly higher in the 231-TXL versus 231-CON cells, the calculated fold-resistance values showed that the 231-TXL cells were significantly more resistant to Dox (38-fold),<sup>71</sup> than the 3-AMBA Jd analogues (2.1-3.4-fold). In fact, the fold-resistance values of the 3-AMBA Jds were equivalent to that observed with JdF, and to the fold-resistance values reported previously when comparing similar *ABCBI*-overexpressing, MDR MCF7-TXL to drug-sensitive MCF7-CON cells.<sup>60</sup>

Alternate drugs effective in treating MDR cancers show similar small fold changes *in vitro*, such as the epothilone derivative ixabepilone, which demonstrated a 2.2-fold reduction in potency in *ABCBI*-overexpressing versus drug-sensitive colon carcinoma cells, whereas paclitaxel realized a 28-fold reduction.<sup>72</sup> This suggests that the minor fold-decreases in potency observed with the 3-AMBA jadomycins in 231-TXL versus 231-CON cells does not equate to their being inappropriate candidate-drugs for the treatment of such MDR cancers. These data suggest the anti-breast cancer activity of Jds is retained when the oxazolone ring of typical Jds such as JdF, is omitted, as in the 3-AMBA Jd analogues, albeit with decreased potency. [Assayed in collaboration with K.B. Goralski; analysis by S.R. Hall]

The 3-AMBA jadamycins **2a** and **2b** were also evaluated *in vitro* for biological activity against microbial pathogens. Samples were evaluated in a microbroth antimicrobial assay against three Gram-positive bacteria [methicillin-resistant *Staphylococcus aureus* (MRSA), *Staphylococcus warneri*, and vancomycin-resistant *Enterococcus faecium* (VRE)], two Gram-negative bacteria (*Proteus vulgaris* and *Pseudomonas aeruginosa*), and the yeast *Candida albicans*. The compounds had no measurable activity against these microbes ( $IC_{50} > 128 \mu\text{M}$  in all cases). [Assayed in collaboration with R.G. Kerr].

## 2.3 Isolation and Characterization of an 11-membered E-ring Jadomycin

Excerpts taken from MacLeod, J.M.; Martinez-Farina, C.F.; Jakeman, D.L. *Submitted to Can. J. Chem.* **2017**. Manuscript ID cjc-2017-0572.

### 2.3.1 Introduction

A series of jadomycins with unsubstituted, extended E-rings from 6- to 10-members (Figure 8A) have been isolated and characterized previously,<sup>42,43,51</sup> but attempts to produce an eleven-membered E-ring jadomycin analogue using 8-aminooctanoic acid as the sole nitrogen source in the *S. venezuelae* cultures were unsuccessful.<sup>51</sup> However, with the newly developed co-amino acid supplementation method for jadomycin productions using amino acids insufficient as sole nitrogen sources for bacterial growth of *S. venezuelae*,<sup>52</sup> the productions were re-attempted with 15 mM D-serine supplementation.

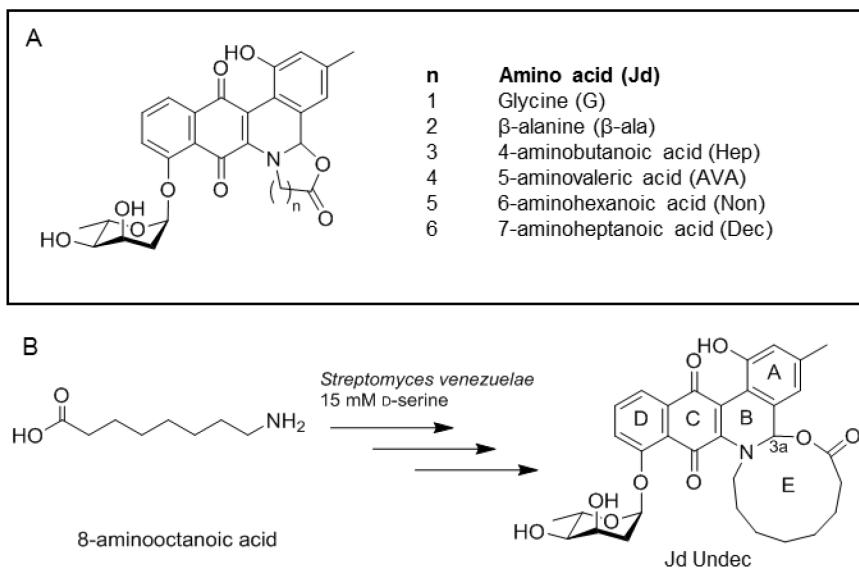


**Figure 8.** (A) Previously characterized jadomycins with unsubstituted, extended E-rings; (B) production of Jd Undec from 8-aminooctanoic acid.

Herein, we describe the isolation and characterization of the novel natural product, Jd Undec (**5**, Figure 8) using this approach. This further demonstrates both the flexibility of

the non-enzymatic incorporation of amino acids for E-ring formation in jadomycin biosynthesis and the value of co-amino acid supplementation-facilitated jadomycin production in broadening the repertoire of non-proteinogenic amino acids available to incorporate into the jadomycin structure through precursor-directed biosynthesis. Additionally, two Jd Undec analogues with open E-rings were also identified (Figure 9), one with a dynamic 3a-position (**6**) and another with a C-C branched acetate (**7**). These compounds emulate those observed in 4-AMBA jadomycin productions.<sup>52</sup>

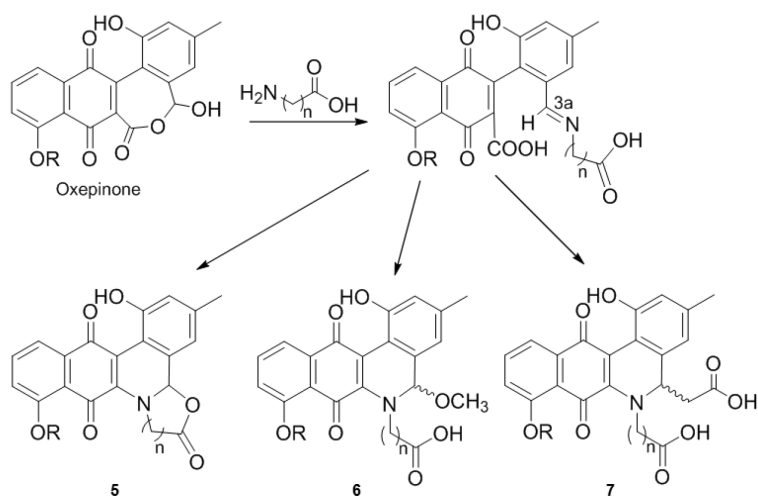


**Figure 9.** Incorporation of amino acid to form a hemiaminal center. Further decarboxylation and cyclization to Jd Undec scaffold or E-ring open jadomycin analogues; where R is a proton or L-digitoxose and n is 7.

### 2.3.1 Results and Discussion

*Streptomyces venezuelae* ISP2530 VS1099 demonstrated only limited proliferation and negligible jadomycin production in cultures with 8-aminooctanoic acid as the sole nitrogen source<sup>51</sup>, indicating the bacteria was incapable of effectively utilizing the compound as a nutrient source. Productions re-attempted using D-serine (15 mM) to support *Streptomyces*



proliferation displayed improved growth and natural product production compared to the non-supplemented production with 8-aminooctanoic acid (Figure 14).

#### *Isolation and Characterization of Jd Undec Major (5a) and Minor (5b) Diastereomers*

A violet compound appeared as the major natural product by TLC analysis. Comparative TLC analysis between the crude material and previously purified Jd DS established definitively that the major compound was not Jd DS. Typically, the non-enzymatic incorporation of the amino acid in jadomycin biosynthesis provides a mixture of diastereomers at the 3a-position (Figure 9), which are in a dynamic equilibrium with one another via B-ring opening and re-cyclization.<sup>57</sup> Generally, these diastereomers are inseparable or, where separated, re-equilibrate to a mixture. However, due to large ring size in Jd Undec and the resolution of the preparative HPLC separation, the major (**5a**) and minor (**5b**) diastereomers were successfully separated for individual characterization. The ratio of isolated major and minor diastereomers was 100:57, with isolated yields of 2.8 mgL<sup>-1</sup> and 1.6 mgL<sup>-1</sup>, respectively. This ratio of diastereomers emulates the values for Jadomycin Dec, the 10-membered E-ring analogue, and isolated yields were also comparable.<sup>51</sup>

The compounds were purified through preparative TLC and HPLC and subsequently characterized by <sup>1</sup>H and <sup>13</sup>C NMR (Table 10, Table 11), HRMS, and UV-Vis analysis. The characteristic jadomycin A-ring, D-ring, and L-digitoxose spin systems were identified by <sup>1</sup>H-NMR and <sup>1</sup>H-<sup>1</sup>H COSY analysis (Figure 10A). HMBC analysis completed the polyaromatic core identification and confirmed the glycosylation of the 12-position with the L-digitoxose deoxysugar (Figure 10B). HMBC also indicated correlations from the H3a

of the jadomycin backbone to alkyl C1, C1' and C6' of the 8-aminooctanoic acid, confirming successful incorporation 8-aminooctanoic acid and cyclization of the E-ring (Figure 10C). This was also supported by an HMBC correlation from the H6'(a,b) to the C3a C13 (Figure 10D).

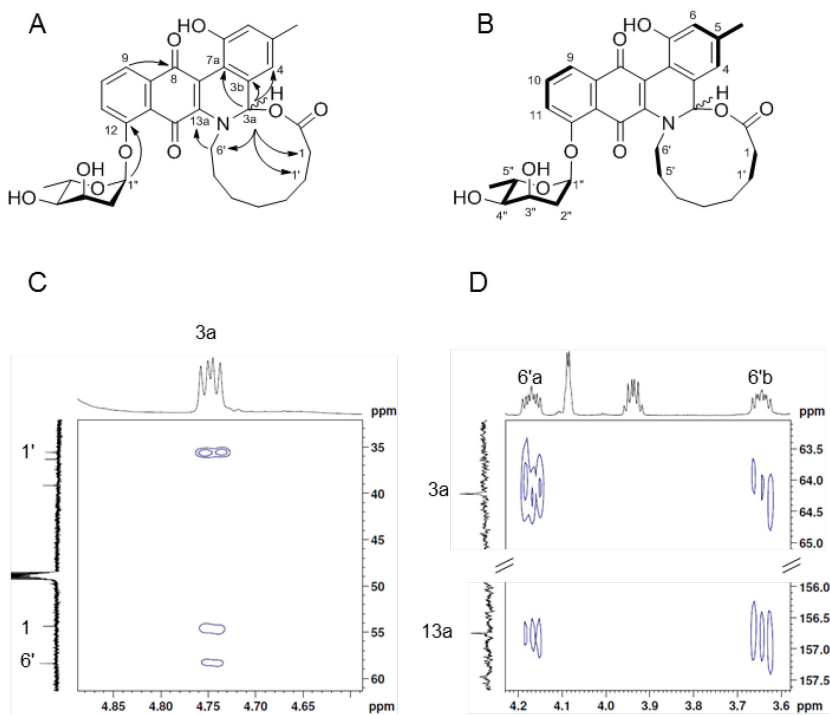


**Figure 10.** Structure of **5a**, illustrating important (A)  $^1\text{H}$ - $^{13}\text{C}$  HMBC correlations (solid arrows), and (B)  $^1\text{H}$ - $^1\text{H}$  COSY correlations (bold lines); key  $^1\text{H}$ - $^{13}\text{C}$  HMBC spectrum correlations from (C) H3a, (D) H6'.

High-resolution mass spectrometry (HRMS) analysis identified an  $m/z$  of 578.2385, corresponding to the  $[\text{M} + \text{H}]^+$  for the molecular formula  $\text{C}_{32}\text{H}_{35}\text{NO}_9$ . Further MS/MS experiments showed fragmentation to the aglycone and then to phenanthroviridin (Figure 11).

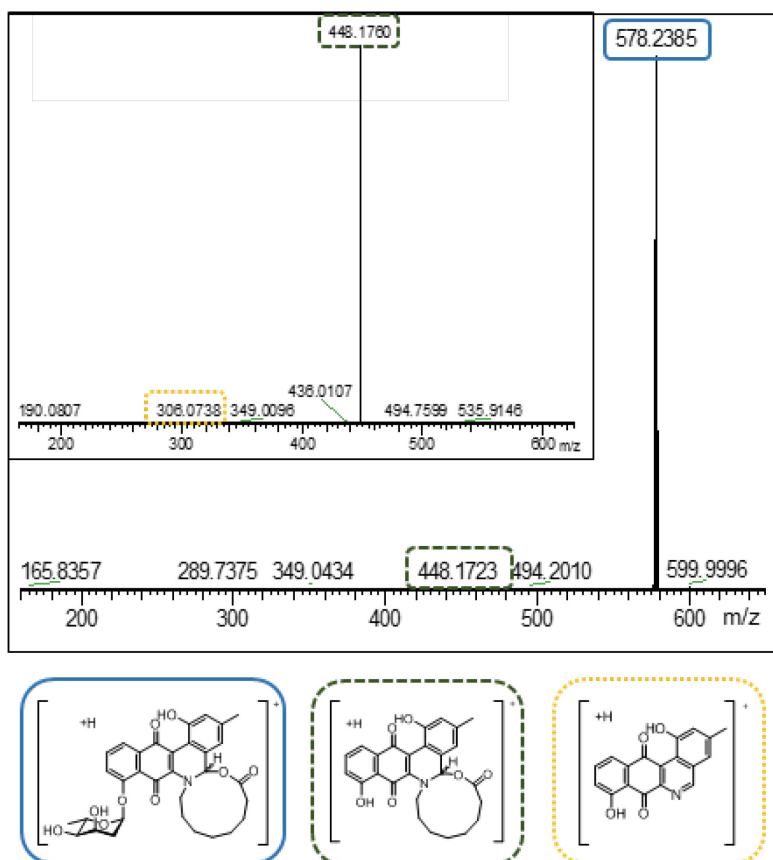


**Figure 11.** High resolution fragmentation of **5a**  $[M+H]^+$  to  $[M+H - \text{digitoxose}]^+$  and (inset) from  $[M+H - \text{digitoxose}]^+$  to  $[\text{phenanthroviridin}+H]^+$ .

In an attempt to determine the absolute configuration of the H3a in **5a**, 2D NOESY data were collected. While correlations were observed between the H3a and H1'b (Figure S46), further supporting that the 8-aminooctanoic acid had cyclized into the 11-membered E-ring, there were no conclusive NOESY correlations to support an *R*- or *S*- configuration for **5a**. Since the amino acid itself does not contain a stereocenter from which to infer the 3a-stereochemistry, further attempts to determine this configuration were not made.

Notably, the trends observed in the chemical shifts of the H3a and H1 and the  $\lambda_{\text{max}}$  wavelengths observed throughout the series of extended E-ring jadomycins (Jd Hep, AVA,

Non, and Dec) were consistent in Jd Undec, as shown in Table 3.<sup>51</sup> These reflect the nature of the chemical environment of the large ring structures due to their inherent flexibility.

**Table 3.** Notable trends observed through the series of unsubstituted extended E-ring jadomycins.

Jadomycin	H3a Chemical Shift (ppm)	H1 Chemical Shift (ppm)	$\lambda_{\max}$ wavelength (nm)
Hep <sup>51</sup>	5.64 (Mj), 5.61 (Mn)	2.29	524
AVA <sup>49</sup>	5.64 (Mj), 5.61 (Mn)	2.19	522
Non <sup>51</sup>	5.62 (Mj), 5.59 (Mn)	2.24	522
Dec <sup>51</sup>	4.72 (Mj), 4.66 (Mn)	3.48, 3.40 <sup>a</sup>	551
<b>5a</b>	4.75	3.51, 3.42 <sup>a</sup>	553
<b>5b</b>	4.63	3.43, 3.35 <sup>a</sup>	555

<sup>a</sup> Diastereotopic protons no longer overlap

#### *Identification of Open E-Ring Analogues of Jad Undec*

Two minor constituents of the crude material were purified in limited quantities by preparative TLC and preparative HPLC. The colouration and polarity of the compounds, relative to the major natural product **5**, suggested these to be analogues of Jd Undec in which the E-ring was open and the 3a-position has been methoxylated (**6**) and branched with acetate (**7**) (Figure 9). A red compound (<1 mgL<sup>-1</sup>) was established by HRMS to be the Jd Undec dynamic 3a-*O*-methoxy (**6**, Figure S53). The assignment was confirmed by re-suspending **6** in MeOD to generate **6d** (Figure 12) by nucleophilic solvent substitution and observing a +3 shift in the *m/z* corresponding to the exchange of -OCH<sub>3</sub> to -OCD<sub>3</sub> (Figure S54).

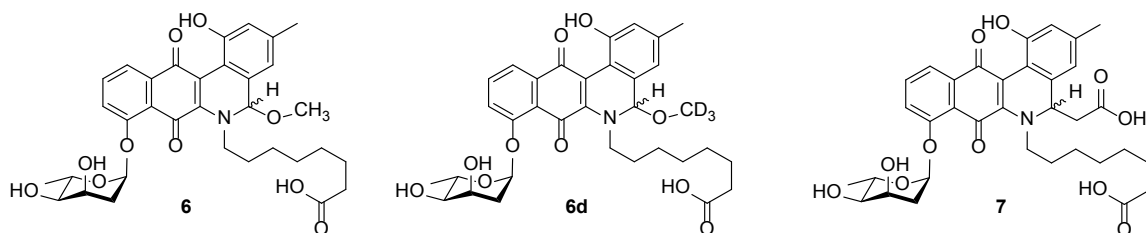


**Figure 12.** Jd Undec 3a-*O*-methoxy analogue (**6**) and its deuterated isotopomer (**6d**) and the Jd Undec 3a-acetate analogue (**7**).

A second, violet compound ( $<500 \mu\text{gL}^{-1}$ ) with a lower  $R_f$  than Jd Undec was identified by HRMS as Jd Undec acetate (**7**, Figure S55). Comparable C3a derivatized compounds were isolated in jadomycin productions with 4-AMBA and 3-AMBA.<sup>52,73</sup> These analogues have been implicated as shunt products resulting from nucleophilic substitution of the reactive hemiaminal center produced during amino acid incorporation into the jadomycin scaffold (Figure 9). In incorporating an amino acid for which the intramolecular E-ring cyclization is sterically hindered, the reactive hemiaminal becomes available for substitution, yielding opportunities for derivatization. Unfortunately, the purity and isolated yield of **6** and **7** were insufficient for complete characterization.

#### *11-aminoundecanoic acid and 12-aminododecanoic acid productions*

Small scale productions were conducted using the co-amino acid supplementation methodology using D-serine with longer unsubstituted linear amino acids, 11-aminoundecanoic acid and 12-aminododecanoic acid, in attempts to produce jadomycons with fourteen- and fifteen-membered E-rings, respectively. However, these productions showed reduced cell growth and negligible production of coloured compounds, namely due to the limited solubility ( $<10 \text{ mM}$ ) of the long chain amino acids in the production media at pH levels conducive to cell proliferation. We anticipate that resolving the limited

solubility of these long-chain amino acids, larger ringed systems could be produced through biosynthetic incorporation.

## 2.4 Conclusions

In probing the non-enzymatic incorporation of amino acids into the jadomycin polyaromatic backbone and establishing the scope of the co-amino acid supplementation method, a series of jadomycins were identified and characterized. Incorporation of 4-(aminomethyl)benzoic acid and 3-(aminomethyl)benzoic acid (4-AMBA and 3-AMBA, respectively), amino acids unable to undergo the typical intramolecular cyclization associated with jadomycin biosynthesis, provided the development of jadomycins containing a reactive hemiaminal center. These hemiaminal intermediates were available for nucleophilic attack, permitting the generation of C3a oxidized, solvated and C-C branched jadomycin congeners (**1-4**). The structures of these congeners broaden the library of jadomycins omitting an E-ring and indicate that the yet-unconfirmed mechanism of the jadomycin C-C branching in *S. venezuelae* may have broad flexibility to polyketide substrates.

This work provides new biological data in exploring the structure-activity profile of the jadomycin family. While the E-ring omitting 3-AMBA jadomycins were less potent anti-breast cancer treatments than JdF, they similarly retained their potency in *ABCBI*-overexpressing, MDR 231-TXL versus drug-sensitive 231-CON cells. At this time, jadomycin analogues lacking the E-ring have not demonstrated cytotoxic potency equivalent to those with an E-ring, suggesting that ring may be crucial to the jadomycins' mechanisms of action.<sup>52,53</sup>

Further, the co-amino acid supplementation methodology was used to introduce 8-aminooctanoic acid, a non-proteinogenic amino acid which had previously been capable at maintaining only limited cell growth and non-detectable quantities of jadomycins, leading to the isolation and characterization of the new natural product, Jd Undec (**5**). Containing an eleven-membered E-ring Jd Undec further demonstrates both the flexibility of the non-enzymatic incorporation of amino acids for E-ring formation in jadomycin biosynthesis and the value of co-amino acid supplementation-facilitated jadomycin production in broadening the repertoire of non-proteinogenic amino acids available to incorporate into the jadomycin structure through precursor-directed biosynthesis.

## **2.5 Experimental Methods**

### **2.5.1 General**

All chemical and biological reagents were purchased from commercial sources and used without further purification. All solvents used in the described chromatographic methods were HPLC grade, unless otherwise indicated. The presence and purity of the jadomycin of interest was monitored by thin layer chromatography (TLC) using glass-backed, normal phase silica (250  $\mu\text{m}$  thickness) TLC plates. All media was prepared with distilled water and was sterilized by autoclaving at 121°C for 20 minutes. Apramycin (50  $\mu\text{g}/\text{mL}$ ) was added as indicated.

#### *General Bacteria Handling*

*Streptomyces venezuelae* strains were grown on MYM-agar at 30°C. Liquid cultures of MYM were inoculated from a sporulated lawn of *S. venezuelae* and grown at 30°C and 250 rpm. Spore solutions were prepared by harvesting spores from plates grown for a

minimum of 10 days, scraping the *S. venezuelae* lawn into sterile water, vortexing and vigorously shaking to separate spores, then filtering through sterile cotton wool. For preparation of glycerol stocks, the spores were immediately diluted 1:1 with 50% sterile glycerol. Alternatively, the spore solution was pelleted at 5000 g for 10 minutes, supernatant decanted, and the spores were re-suspended in sterile water before being diluted 1:1 with 50% sterile glycerol. The glycerol stocks were aliquoted and stored at -70 °C.

*E. coli* cultures were grown overnight at 37°C, 250 rpm in LB media with antibiotics as required, and stored as solutions supplemented with 25% glycerol at -70°C.

#### *Media recipes*

*Malt yeast maltose (MYM)*: 10 g malt extract, 4 g yeast extract, 4 g maltose, distilled water to 1.0 L, pH 7.0

*Malt yeast maltose agar (MYM-agar)*: 10 g malt extract, 4 g yeast extract, 4 g maltose, 15 g agar, distilled water to 1.0 L, pH 7.0

*Minimal salt media (MSM)*: 3.77 g MOPS, 0.4 g MgSO<sub>4</sub>, 9 mL salt solution, 4.5 mL trace mineral solution, 4.5 mL FeSO<sub>4</sub> solution (0.2% w/v), water to 1.0 L, pH 7.5

*Salt solution*: NaCl (1%, w/v) and CaCl<sub>2</sub> (1%, w/v) in water.

*Trace mineral solution*: ZnSO<sub>4</sub> (0.088%, w/v), CuSO<sub>4</sub> (0.0039%, w/v), MnSO<sub>4</sub> (0.00061%, w/v), H<sub>3</sub>BO<sub>3</sub> (0.00057%, w/v), and (NH<sub>4</sub>)<sub>6</sub>Mo<sub>7</sub>O<sub>24</sub> (0.00037%, w/v) in water.



### **2.5.2 Jadomycin Production Methods**

*S. venezuelae* VS1099 cultures were grown on MYM-apramycin agar incubated at 30°C until sporulation was observed. MYM growth media were inoculated with a patch of mycelia and spores and incubated at 30°C with shaking (250 rpm) for 16 – 20 hours. The cultures were monitored by microscope until the mycelia were fibrous. At that point, the cultured cells were pelleted (3750 rpm, 4°C) and the supernatant was drawn off. The cell pellet was re-suspended and washed twice with MSM media to remove the rich MYM media. The cells were then re-suspended in minimal MSM solution as an inoculum slurry.

The MSM production media was separately prepared with the required amino acid(s) and autoclaved, after which separately filter sterilized 30% glucose solution and separately autoclaved 9 mM phosphate solution were added. The re-suspended *S. venezuelae* slurry was then added to the production media to an optical density of 0.4-0.6 at 600 nm (OD<sub>600</sub>) using a SpectraMax Plus Microplate Reader (Molecular Devices). The production media was ethanol shocked (3%, v/v) to induce jadomycin production and incubated at 30°C with shaking (250 rpm). Production OD<sub>600</sub> and Abs<sub>526</sub> were monitored and the production media pH was corrected regularly to 7.5 using NaOH (5 M) or HCl (5 M) for the duration of the production period.

### **2.5.3 Jadomycin Purification Methods**

#### *Filtration*

Upon completion of the jadomycin production, the bacteria were removed from the solution by filtration through Whatman #5 filters, followed by 0.45 µm and 0.22 µm Millipore filters.

### *Flash chromatography*

Flash chromatography was performed using a Silisep™ prepacked phenyl columns (2 g or 12 g) purchased from Silicycle® that had been preconditioned with ddH<sub>2</sub>O (3 column volumes), methanol (4 column volumes), and again with ddH<sub>2</sub>O (4 column volumes). The production media filtrate was passed through the column followed by a ddH<sub>2</sub>O wash (1 column volume) to remove all water-soluble material. The crude natural product was eluted using 100% methanol (0.5-1 column volume). The solvent was removed *in vacuo*.

### *Automated flash chromatography*

A Biotage SP1™ unit was used to perform flash chromatography using pre-packed normal phase silica columns (25 g, 40 g, and 80 g) from SiliCycle®. Compounds were eluted using a methanol/dichloromethane solvent system using automated fraction collection with 254 nm detection.

### *Preparative thin layer chromatography*

Material was purified by preparative TLC (prep-TLC) using 20 × 20 cm glass backed, normal phase silica TLC plates (SiliCycle®, 250 μm, 1000 μm, or 2000 μm thickness). The natural product extract was brought up in minimal methanol and spotting onto the plate. The plate was eluted in a methanol/dichloromethane solvent system. When the plate had been completely developed, it was removed from the solvent to allow air-drying. Bands of interest were removed by scraping the silica from the plate. The compounds were then eluted from the silica using the same solvent system as was used for development. The solvent was then removed *in vacuo*.

### *Preparative high-performance liquid chromatography*

Semi-pure natural products were purified for characterization using preparative HPLC (prep-HPLC). The material was brought up in methanol and injected in 50-200  $\mu\text{L}$  volumes into a Millipore Waters prep-HPLC (717 Plus Autosampler, 486 Tunable Absorbance Detector, 600E Controller) with an Altex Ultrasphere-ODS 5 $\mu\text{m}$  C18 column (10 mm x 25 cm). The jadomycin separation was monitored at 254 nm. Prep-HPLC was conducted using a flow rate of 5.0  $\text{mLmin}^{-1}$  and a linear gradient of water (A) and methanol (B) from 95:5 to 5:95 A:B over 30.0 minutes, followed by a plateau at 5:95 A:B for 30.0 minutes, a linear gradient from 5:95 to 95:5 A:B over 10.0 minutes, and finally a re-equilibration at 95:5 A:B for 5.0 minutes.

### *Size-exclusion chromatography*

Jadomycins were finally purified for characterization by size exclusion chromatography using LH20 in methanol (10 g in 35 mL). Samples were solvated in minimal methanol to apply to column and were eluted with isocratic methanol at 1  $\text{mLmin}^{-1}$ .

## **2.5.4 Compound Characterization**

### *Ultra-violet-visible spectroscopy*

UV-Vis spectroscopy on novel jadomycin compounds was carried out on a SpectraMax Plus Microplate Reader (Molecular Devices) and analyzed using SoftMax® Pro Version 4.8 Software. Samples were dissolved in methanol, placed in a quartz cuvette (1 cm path length), and scanned over a 280 nm – 700 nm range (1 nm intervals). Two dilutions were to calculate extinction coefficients ( $\epsilon$ ) from maximal absorbance wavelengths ( $\lambda_{\text{max}}$ ).

### *High-performance liquid chromatography*

HPLC of purified jadomycin and extracts of various purity were performed using a Hewlett Packard Series 1050 instrument equipped with an Agilent Zorbax 5  $\mu\text{m}$  Rx-C18 column (15.0 cm  $\times$  4.6 mm). Injections were monitored at an absorbance of 254 nm. HPLC was conducted using a flow rate of 1.0 mLmin<sup>-1</sup> and a linear gradient from 90:10 A:B to 40:60 A:B over 8.0 min, followed by a plateau at 40:60 A:B from 8.0 to 10.0 min, and finally a linear gradient from 40:60 A:B to 90:10 A:B over 5.0 min with a. Buffer A is an aqueous solution containing 12 mM *n*-Bu<sub>4</sub>NBr, 10 mM KH<sub>2</sub>PO<sub>4</sub>, and 5% acetonitrile at pH 4.0 and Buffer B is 100% acetonitrile. Samples were analyzed by injecting 20  $\mu\text{L}$  aliquots with 10-100  $\mu\text{M}$  concentrations.

### *High-resolution mass spectrometry*

HRMS of jadomycins was performed on a Bruker Daltonics MicroTOF Focus Mass Spectrometer using an ESI+ or ESI- source, unless otherwise indicated. HRMS and MS/MS/MS of Jd Undec was performed on a Thermo Scientific Orbitrap LTQ Velos High Resolution Mass Spectrometer using an ESI+ source with fragmentation observed using 35.00 v CID.

### *Nuclear magnetic resonance spectroscopy*

NMR analyses of jadomycins were recorded using either a Bruker AV 500 MHz Spectrometer (<sup>1</sup>H: 500 MHz, <sup>13</sup>C: 125 MHz) equipped with an auto-tune and match (ATMA) broadband observe (BBFO) SmartProbe located at the Nuclear Magnetic Resonance Research Resource (NMR-3) facility (Dalhousie University) or a Bruker AVIII 700 MHz Spectrometer (<sup>1</sup>H: 700 MHz, <sup>13</sup>C: 176 MHz) equipped with a 1.7 mm probe

located at the Canadian National Research Council Institute for Marine Biosciences (NRC-IMB) in Halifax, Nova Scotia. The use of each is specified next to the appropriate spectra. Spectra were recorded in MeOD with chemical shifts given in ppm after calibrating to the residual solvent peak (MeOD: 3.31 ppm).

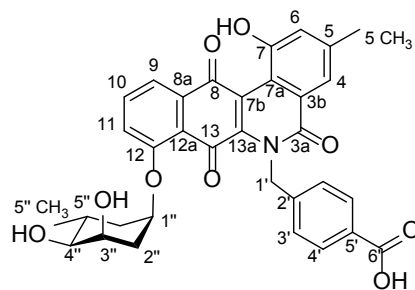
Structural characterization and signal assignments were accomplished using  $^1\text{H}$ -NMR chemical shifts and multiplicities,  $^{13}\text{C}$ -NMR chemical shifts,  $^1\text{H}$ - $^1\text{H}$  correlated spectroscopy (COSY),  $^1\text{H}$ - $^{13}\text{C}$  heteronuclear single quantum coherence (HSQC) spectroscopy,  $^1\text{H}$ - $^{13}\text{C}$  heteronuclear multiple bond correlation (HMBC) spectroscopy, and nuclear Overhauser effect 2D spectroscopy (2D NOESY).

#### **2.5.5 Productions using 4-AMBA**

The jadomycin production and flash chromatography to generate 4-AMBA natural product crude extract were performed by A.W. Robertson as described in manuscript SC-EDG-08-2017-003676. In purification of Jd 4-AMBA 3a-*O*-methyl, an orange compound with a similar  $R_f$  was observed by TLC analysis of the crude extract. The crude mixture (65 mg) was dissolved in minimal methanol and loaded onto preparative normal phase silica TLC plates (250  $\mu\text{m}$ ) and developed with DCM:MeOH (9:1). The orange band of interest was scraped from the plate and eluted with MeOH to give 6.7 mg of **1**. Further purification was accomplished through two successive rounds of semi-preparatory HPLC, as previously described in Section 2.5.3, yielding **1** as an orange solid (1.2 mg). TLC  $R_f$ : 0.48 (95:5 DCM:MeOH), HRMS (ESI): 584.1640 found, 584.1562 calculated for  $\text{C}_{32}\text{H}_{26}\text{NO}_{10}$  [ $\text{M} - \text{H}$ ]. NMR spectra to follow in Appendix I, see characterization table (Table 4) for numbering.

**Table 4.** NMR assignment for **1** (700 MHz, MeOD)

Position	$\delta$ $^1\text{H}$ (ppm)	Multiplicity (J (Hz))	$\delta$ $^{13}\text{C}$ (ppm)	COSY	HMBC
3a			164.1		
3b			136.3*		
4	7.57	s (obscured)	120.0	5-CH <sub>3</sub> , 6	3a, 5-CH <sub>3</sub>
5			143.9		
5-CH <sub>3</sub>	2.31	s	21.3	4, 6	4, 5, 6
6	6.94	s (broad)	125.4	4, 5-CH <sub>3</sub>	5-CH <sub>3</sub> , 7a
7			155.1*		
7-OH					
7a			118.2		
7b			113.8*		
8			182.3*		
8a			129.2*		
9	7.56	d (7.6, obscured)	121.5	10	11
10	7.51	t (7.9)	136.3	9,11	12
11	7.36	d (8.3)	120.6	10	9
12			155.2		
12a			122.1*		
13			180.2*		
13a			161.4*		
1' (a)	5.60	d (15.4)	49.6	1' (b)	2', 3'
1' (b)	6.10	s (broad)	49.6	1' (a)	None
2'			141.2		
3'	7.06	d (8.1)	128.2	4'	1', 3', 5'
4'	7.68	d (8.3)	130.6	3'	2', 3', 4', 6'
5'			138.2		
6'			174.7		
1''	5.72	d (2.8)	96.4	2'' (a, b)	3'', 5'', 12
2'' (a)	2.13	dt (3.5, 15)	36.2	1'', 2'' (b), 3''	None
2'' (b)	2.29	dd (obscured)	36.2	1'', 2''(a), 3''	1'', 3'', 4''
3''	4.03	d (3.2)	68.5	2'' (a, b), 4''	None
3''-OH					
4''	3.19	dd (obscured)	73.8	3'', 5''	3'', 5'', 5''-CH <sub>3</sub>
4''-OH					
5''	3.78	m	66.3	4'', 5''-CH <sub>3</sub>	5''-CH <sub>3</sub>
5''-CH <sub>3</sub>	1.11	d (6.1)	18.2	5''	4'', 5''

\*Assigned by  $^{13}\text{C}$  NMR only and signals may be interchanged.

### 2.5.6 Productions using 3-AMBA

MSM production media (2.0 L) was prepared with 3-(aminomethyl)benzoic acid (3-AMBA, 60 mM) and D-serine (15 mM). The production continued for 96 hours to allow for improved Abs<sub>526</sub> values (Figure 13).

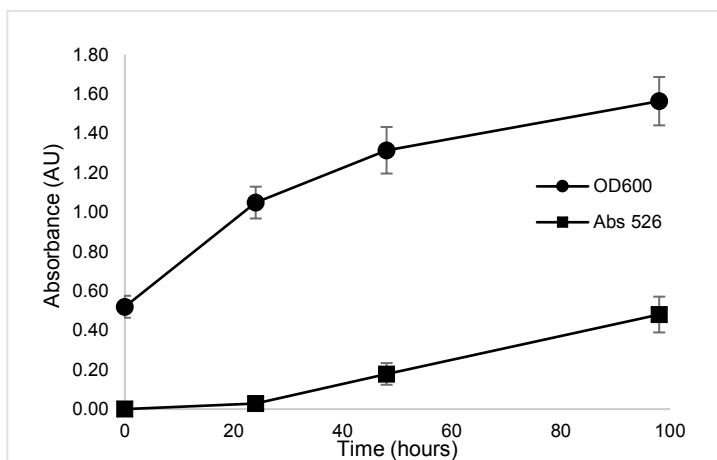


**Figure 13.** *S. venezuelae* growth and Jd production MSM with 3-AMBA and D-serine.

The jadomycin production media was clarified and passed through a pre-conditioned 12 g silica-phenyl flash column. The column was washed with water before eluting the crude natural product with methanol. The solvent was removed *in vacuo* to give 480 mg of crude extract.

The material was fractionated over a prepacked C<sub>18</sub> column (12 g, 70 mL). The material was reconstituted in minimal methanol, applied to the column and air-dried, then eluted with a stepwise gradient of the following solvents (100 mL), in order: water, 1:1 water:MeOH, MeOH, and ethyl acetate. The solvents were removed *in vacuo*. The crudely fractionated material was analyzed by TLC before proceeding. The C<sub>18</sub> fractionated material was purified by preparative TLC, using 20 × 20 cm glass backed, normal phase silica TLC plates (250 μm thickness). The material was re-suspended in minimal methanol.

The C<sub>18</sub> aqueous fraction (58 mg), enriched with **2a** and **2b**, was spotted onto four silica plates and the C<sub>18</sub> 1:1 water:MeOH fraction, enriched with **3** and **4**, (15 mg) was spotted onto three silica plates. All plates were developed twice in 5:95 MeOH:DCM and twice more in 10:90 MeOH:DCM. Following prep-TLC, 6.8 mg of violet **2a**, 6.1 mg of violet **2b**, 2.6 mg of red **3**, and 1.6 mg of orange **4** were isolated. Jadomycins were finally purified for characterization by size exclusion chromatography using LH20 in methanol. Following the LH20 separation, 3.8 mg of violet Jad 3-AMBA acetate major (**1a**), 2.7 mg of violet Jad 3-AMBA acetate minor (**1b**), 1.4 mg of red Jad 3-AMBA methoxy (**2**), and 0.9 mg of orange Jad 3-AMBA lactam (**3**) were isolated.

*Jadomycin 3AMBA Acetate Major (2a)*

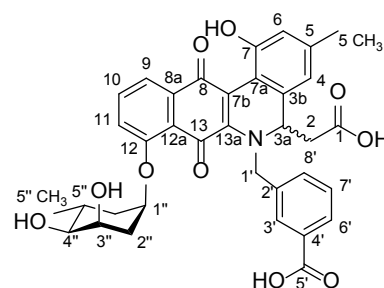
UV-Vis (2.0 × 10<sup>-4</sup> M, 8.0 × 10<sup>-4</sup> M, MeOH), λ<sub>max</sub> (ε) [(297 (9813), 325 (9252), 552 (1329)]; TLC Rf: 0.26 (9:1 DCM: MeOH); HPLC Rt = 8.748 min; NMR spectra to follow in Appendix I, see characterization table (Table 5) for numbering.



**Table 5.** NMR assignment for **2a** (700 MHz, MeOD)

3-AMBA Acetate 3a <sub>Mj</sub> ( <b>2a</b> )					
Position	$\delta$ <sup>1</sup> H (ppm)	Multiplicity (J (Hz))	$\delta$ <sup>13</sup> C (ppm)	COSY	HMBC
1			178.2		
2a	2.33	m	42.92	2b, 3a	1, 3a
2b	2.70	dd (8.0, 6.0)	42.92	2a, 3a	1, 3a, 3b
3a	5.06	t (6.7)	64.81	2a, 2b	2, 3b, 4, 7a, 13a
3b			134.27		
4	6.39	s	118.76	5-CH <sub>3</sub> , 6	3a, 5-CH <sub>3</sub> , 6, 7a
5			141.24		
5-CH <sub>3</sub>	2.19	s	21.09	4, 6	5, 6
6	6.61	s	119.39	4, 5-CH <sub>3</sub>	4, 5-CH <sub>3</sub> , 7a, 7
7			154.38		
7-OH					
7a			114.18		
7b*			112.5		
8			180.75		
8a			137.71		
9	7.83	m	121.15	10	8, 11
10	7.70	t (8.3)	136.59	9, 11	8a, 12, 12a
11	7.50	d (8.5)	119.89	10	10, 12, 13
12			155.86		
12a			120.88		
13			186.17		
13a			156.88		
1'a	5.74	d (15.1)	56.44	1'a	2', 3a, 8', 13a
1'b	4.86	d (15.1)	56.44	1'b	2', 3a, 8', 13a
2'			137.69		
3'	8.01	s	130.1	None	1', 6'
4'			139.62		
5'			175.24		
6'	7.84	m	129.78	7'	5', 8'
7'	7.26	t (7.6)	129.07	6', 8'	4'
8'	7.31	d (7.5)	130.72	7'	3'
1''	5.92	d (3.1)	96.47	2''a	3'', 5'', 12
2''a	2.18	m	36.40	1'', 2''b, 3''	None
2''b	2.35	m	36.40	2''a, 3''	None
3''	3.99	dd (2.8, 5.9)	68.43	2''a, 2''b, 4''	None
3''-OH					
4''	3.23	dd (2.8, 9.8)	74.14	3'', 5''	5'', 5''-CH <sub>3</sub>
4''-OH					
5''	3.91	m	66.49	4'', 5''-CH <sub>3</sub>	5''-CH <sub>3</sub>
5''-CH <sub>3</sub>	1.2	d (6.1)	18.30	5''	4'', 5''

\*Assigned by <sup>13</sup>C NMR only and signals may be interchanged.



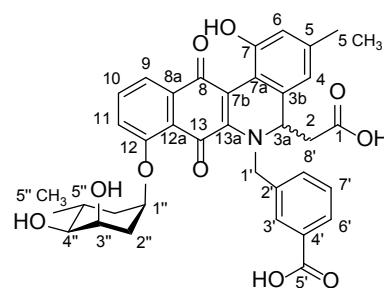
### *Jadomycin 3AMBA Acetate Minor (2b)*

UV-Vis ( $2.0 \times 10^{-4}$  M,  $8.0 \times 10^{-4}$  M, MeOH),  $\lambda_{\text{max}}$  ( $\epsilon$ ) [(298 (3981), 325 (5464), 381 (900), 552 (724)]; TLC R<sub>f</sub>: 0.37 (9:1 DCM: MeOH); HPLC R<sub>t</sub> = 8.781 min; NMR spectra to follow in Appendix I, see characterization table (Table 6) for numbering.

**Table 6.** NMR assignment for **2b** (700 MHz, MeOD)

3-AMBA Acetate 3a <sub>Mn</sub> ( <b>2b</b> )					
Position	$\delta$ <sup>1</sup> H (ppm)	Multiplicity (J (Hz))	$\delta$ <sup>13</sup> C (ppm)	COSY	HMBC
1			178.1		
2a	2.35	dd (6.2, 7.9)	42.9	2b, 3a	3a
2b	2.67	dd (7.9, 6.2)	42.9	2a, 3a	3a, 3b
3a	5.03	dd (6.6, 1.3)	64.77	2a, 2b	1, 1', 2, 3b, 4, 7a, 13a
3b			134.8		
4	6.39	s	118.79	5-CH <sub>3</sub> , 6	3a, 5-CH <sub>3</sub> , 6, 7a
5			141.27		
5-CH <sub>3</sub>	2.19	s	20.99	4, 6	4, 5, 6
6	6.62	s	119.33	4, 5-CH <sub>3</sub>	4, 5-CH <sub>3</sub> , 7a, 7
7			154.34		
7-OH					
7a			114.04		
7b*			114.26		
8			181.49		
8a			137.64		
9	7.85	d (7.9)	121.33	10	8, 11
10	7.7	t (8.3)	136.35	9, 11	8a, 12
11	7.48	d (8.3)	120.86	10	9, 12
12			156.47		
12a			120.97		
13			184.36		
13a			155.13		
1'a	5.78	d (15.1)	57.47	1'b	2', 3a, 13a
1'b	4.81	d (15.1)	57.47	1'a	2', 3a, 13a
2'			138.1		
3'	7.94	s	129.86	None	1', 5', 6', 8'
4'			139.51		
5'			175.10		
6'	7.81	d (7.7)	129.51	7	5'
7	7.25	t (7.7)	128.87	6'	4', 8'
8'	7.28	d (7.7)	130.68	None	3'
1''	5.88	d (3.4)	96.88	2''a	5'', 12
2''a	2.17	dt (3.8, 15.2)	36.28	1'', 2''b, 3''	None
2''b	2.40	dd (2.5, 15.2)	36.28	2''a, 3''	None
3''	4.03	d (3.1)	67.99	2''a, 2''b, 4''	None
3''-OH					
4''	3.24	dd (2.4, 6.7)	74.09	3'', 5''	5'', 5''-CH <sub>3</sub>
4''-OH					
5''	3.97	t (5.8)	66.42	4'', 5''-CH <sub>3</sub>	None
5''-CH <sub>3</sub>	1.22	d (6.6)	18.20	5''	4'', 5''

\*Assigned by <sup>13</sup>C NMR only and signals may be interchanged.



### *Jadomycin 3AMBA Methoxy (3)*

UV-Vis ( $2.5 \times 10^{-4}$  M,  $1.0 \times 10^{-3}$  M, MeOH),  $\lambda_{\max}$  ( $\epsilon$ ) [(287 (13313), 324 (3824), 389 (2696), 526 (1923)]; TLC R<sub>f</sub>: 0.80 (9:1 DCM: MeOH); HPLC R<sub>t</sub> = 8.987 min; NMR spectra to follow in Appendix I, see characterization table (Table 7, Table 8) for numbering.

**Table 7.** NMR assignment for **3a** (700 MHz, MeOD)

3AMBA Methoxy 3a <sub>Mj</sub> ( <b>3a</b> )					
Position	$\delta$ <sup>1</sup> H (ppm)	Multiplicity (J (Hz))	$\delta$ <sup>13</sup> C (ppm)	COSY	HMBC
3a	5.58	bs	91.6	None	1', 3b, 4, 6, 7a, 13a
3a-OCH <sub>3</sub>	3.2	bs	54.6	None	3a
3b			131.97		
4	6.63	bs	120.5	5-CH <sub>3</sub> , 6	3a, 6
5			141.54		
5-CH <sub>3</sub>	2.3	bs	21.02	4, 6	4, 5, 6
6	6.82	bs	120.67	4, 5-CH <sub>3</sub>	4, 7
7			154.88		
7-OH					
7a			114.2		
7b*			113.75		
8			183.45		
8a*			136.54		
9	7.83	d (7.2)	121.41	10	8
10	7.71	m	136.62	9, 11	12
11	7.53	t (9.2)	120.93	10	None
12			155.9		
12a*			121.52		
13*			185.37		
13a			154.86		
1'a	5.75	d (15.5)	58.92	1'b	2', 3a, 8'
1'b	4.95	d (15.5)	58.92	1'a	2', 3a, 8'
2'			138.57		
3'	7.94	s	130.08	None	5'
4'			136.55		
5'			175.15		
6'	7.82	d (obscured)	129.59	7'	None
7'	7.25	t (7.6)	129.16	6', 8'	4'
8'	7.31	d (7.6)	130.64	7'	None
1''	5.86	t (2.9)	96.63	2''a	None
2''a	2.19	m	36.26	1'', 2''b, 3''	None
2''b	2.41	dd (2.6, 15.1)	36.26	2''a, 3''	None
3''	4.08	dd (3.1, 6.3)	68.29	2''a, 2''b, 4''	None
3''-OH					
4''	3.27	dd (3.3, 9.9)	74.11	3'', 5''	None
4''-OH					
5''	3.91	m	66.43	5''-CH <sub>3</sub>	None
5''-CH <sub>3</sub>	1.18	d (6.2)	18.19	5''	4'', 5''

\*Assigned by <sup>13</sup>C NMR only and signals may be interchanged.

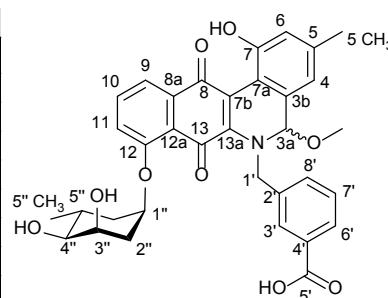
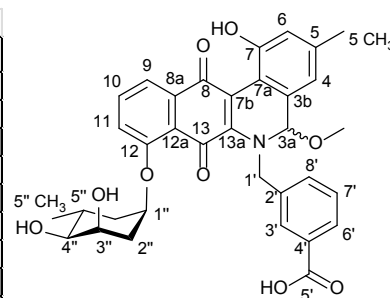


**Table 8.** NMR assignment for **3b** (700 MHz, MeOD)

3AMBA Methoxy 3a <sub>Mn</sub> ( <b>3b</b> )					
Position	δ <sup>1</sup> H (ppm)	Multiplicity (J (Hz))	δ <sup>13</sup> C (ppm)	COSY	HMBC
3a	5.56	bs	91.6	None	1', 3b, 4, 6, 7a, 13a
3a-OCD <sub>3</sub>	3.2	bs	54.6	None	3a
3b			131.97		
4	6.62	bs	120.5	5-CH <sub>3</sub> , 6	3a, 6, 7a
5			142.18		
5-CH <sub>3</sub>	2.3	bs	21.05	4, 6	4, 5, 6
6	6.81	bs	120.71	4, 5-CH <sub>3</sub>	4, 7
7			154.88		
7-OH					
7a			113.76		
7b*			113.75		
8			185.35		
8a*			136.60		
9	7.82	d (7.4)	121.45	10	8
10	7.70	m	136.40	9, 11	None
11	7.53	t (9.2)	120.80	10	12
12			156.3		
12a*			121.52		
13*			185.37		
13a			154.86		
1'a	5.57	d (15.4)	57.04	1'b	2', 3a, 8'
1'b	5.15	d (15.4)	57.04	1'a	2', 3a, 8'
2'			138.17		
3'	7.79	s	130.13	None	None
4*			136.55		
5*			175.15		
6'	7.76	d (7.2)	129.63	7'	None
7'	7.21	t (7.4)	129.06	6', 8'	None
8'	7.19	d (7.6)	131.09	7'	None
1''	5.86	t (2.9)	96.5	2''a	None
2''a	2.17	m	36.31	1'', 2''b, 3''	None
2''b	2.3	dd (3.1, 14.2)	36.31	2''a, 3''	3''
3''	4.00	dd (3.2, 6.3)	68.28	2''a, 2''b, 4''	None
3''-OH					
4''	3.23	dd (3.1, 9.8)	74.08	3'', 5''	5''
4''-OH					
5''	3.87	m	66.41	5''-CH <sub>3</sub>	None
5''-CH <sub>3</sub>	1.22	d (6.2)	18.2	5''	4'', 5''



\*Assigned by <sup>13</sup>C NMR only and signals may be interchanged.

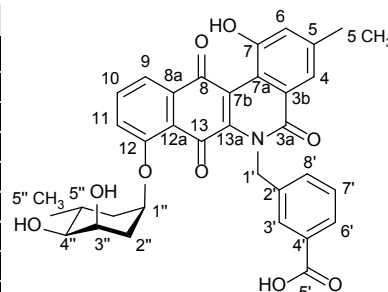
*Jadomycin 3AMBA Lactam (4)*

UV-Vis ( $2.5 \times 10^{-4}$  M,  $1.0 \times 10^{-3}$  M, MeOH),  $\lambda_{\max}$  ( $\epsilon$ ) [(264 (8954)]; TLC R<sub>f</sub>: 0.82 (9:1 DCM: MeOH); HPLC R<sub>t</sub> = 10.257 min; NMR spectra to follow in Appendix I, see characterization table (Table 9) for numbering.

**Table 9.** NMR assignment for **4** (700 MHz, MeOD)

3AMBA Lactam ( <b>4</b> )					
Position	$\delta$ <sup>1</sup> H (ppm)	Multiplicity (J (Hz))	$\delta$ <sup>13</sup> C (ppm)	COSY	HMBC
3a			163.9		
3b*			148.26		
4	7.91	d (1.2)	121.86	5''-CH <sub>3</sub> , 6	3a, 6, 7a
5			143.95		
5-CH <sub>3</sub>	2.47	s	21.29	4, 6	4, 5, 6
6	7.20	d (1.3)	125.2	4, 5''-CH <sub>3</sub>	4, 7a
7*			156.68		
7-OH					
7a			118.07		
7b*			115.19		
8			186.93		
8a*			129.1		
9	7.77	d (7.6)	121.88	10	8
10	7.67	t (8.4)	136.58	9, 11	12
11	7.51	d (8.4)	121.90	10	9
12			154.68		
12a*			120.68		
13*			170.3		
13a*			158.83		
1'a	5.67	d (15.4)	48.9	1'b	None
1'b	6.22	bs	48.9	1'a	None
2*			135.73		
3'	7.68	s	129.01	None	5'
4'			138.7		
5'			174.62		
6'	7.72	d (7.9)	129.45	7'	None
7'	7.24	t (7.7)	129.30	6', 8'	4'
8'	7.31	d (7.5)	131.00	7'	None
1''	5.82	d (3.0)	96.74	2''a	3'', 5''
2''a	2.19	dt (3.6, 15.2)	36.30	1'', 2''b, 3''	None
2''b	2.45	dt (2.8, 14.7)	36.30	2''a, 3''	None
3''	4.1	dd (3.3, 6.3)	68.48	4''	None
3''-OH					
4''	3.27	dd (3.0, 9.9)	74.06	3'', 5''	5''
4''-OH					
5''	3.84	m	66.38	4'', 5''-CH <sub>3</sub>	None
5''-CH <sub>3</sub>	1.18	d (6.1)	18.19	5''	4'', 5''

\*Assigned by <sup>13</sup>C NMR only and signals may be interchanged.



### 2.5.7 Productions using 8-aminooctanoic acid

MSM production media (0.75 L) was prepared with 8-aminooctanoic acid (60 mM) and D-serine (15 mM). The production continued for 72 hours (Figure 14).

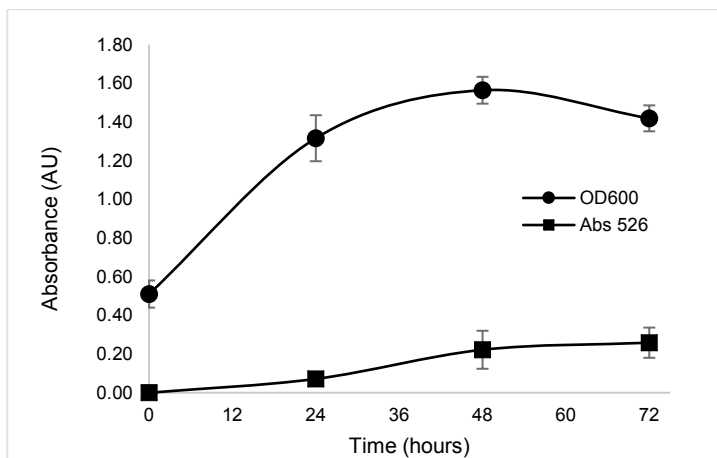


**Figure 14.** *S. venezuelae* growth and Jd production in MSM with 8-aminooctanoic acid and D-serine.

The jadomycin production media was clarified and passed through a pre-conditioned 12 g silica-phenyl flash column. The column was washed with water before eluting the crude natural product with methanol. The solvent was removed *in vacuo* to give 122 mg of crude extract.

The crude material was initially purified by prep-TLC using four plates (250  $\mu\text{m}$ ), developed with 5% MeOH in DCM. Following prep-TLC, 5.5 mg of the violet jadomycin (**5**) were isolated, in addition to 2.3 mg of red jadomycin (**6**) and 2.0 mg of a second violet jadomycin (**7**). Prep-HPLC was then performed on **5**, resulting in 1.2 mg of the major diastereomer (Jd Undec Major, **5a**) and 0.8 mg of the minor diastereomer (Jd Undec Minor, **5b**). Commonly, jadomycin 3a diastereomers are inseparable; however, due to the apparent size of the E-ring and the resolution of the preparative HPLC method, the major and minor

diastereomers of Jad Undec were separately collected for characterization. Prep-HPLC was also used in the purification of **6** and **7**, yielding 0.4 mg of **6** and 0.2 mg of **7**.

Jd Undec Major was characterized by NMR (in MeOD, Table 10), HRMS, UV, HPLC and TLC. Jd Undec Minor was characterized by NMR (in MeOD, Table 11), UV, MS, and TLC. The open E-ring Jd Undec analogues were characterized by HRMS (Figure S53, Figure S54, Figure S55).

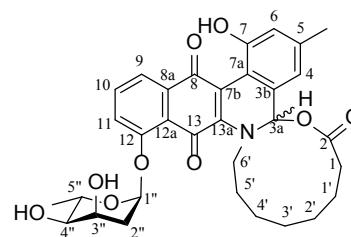
#### Jadomycin Undec Major (**5a**)

UV-Vis ( $8.67 \times 10^{-4}$  M and  $1.73 \times 10^{-4}$  M, MeOH),  $\lambda_{\max}$  (296 (9589), 326 (10305), 382 (1990), 553 (1347)); TLC  $R_f$ : 0.61 (9:1 DCM: MeOH); HPLC  $R_t$  = 8.279 min; NMR spectra to follow in Appendix I, see characterization table (Table 10) for numbering.

**Table 10.** NMR assignment for **5a** (700 MHz, MeOD)

Jd Undec 3a <sub>Mj</sub> ( <b>5a</b> )					
Position	$\delta$ <sup>1</sup> H (ppm)	Multiplicity ( <i>J</i> (Hz))	$\delta$ <sup>13</sup> C (ppm)	COSY	HMBC
1(a)	3.51	m	58.4	1(b), 1'(a)	1', 3a
1(b)	3.42	m	58.4	1(a), 1'(a)	1', 3a
2			182.9		
3a	4.75	dd (5.7, 9.3)	64.2	1'(a,b)	1', 6', 1, 3b, 4, 7a, 13a
3b			133.0		
4	6.60	s	119.2	6, 5-CH <sub>3</sub>	3a, 3b, 5-CH <sub>3</sub> , 6, 7a
5			140.8		
5-CH <sub>3</sub>	2.34	s	21.0	4, 6	4, 5, 6, 7a
6	6.72	s	119.4	4, 5-CH <sub>3</sub>	4, 5-CH <sub>3</sub> , 7, 7a
7			154.6		
7-OH					
7a			114.1		
7b			111.7		
8			179.6		
8a			119.7		
9	7.80	d (7.5)	120.3	10	8, 11
10	7.72	t (8.3)	136.6	9, 11	12, 12a
11	7.51	d (8.4)	120.9	10	9, 12, 13
12			155.6		
12a			137.6		
13			185.9		
13a			156.8		
1'(a)	1.92	m	35.6	1'(b)	1, 3a, 3b
1'(b)	1.79	m	35.6	1'(a)	1, 3a, 3b
2'	1.41	bm	27.6	None	3'
3'	1.41	bm	30.2	None	2'
4'	1.38	bm	30.7	None	3'
5'	1.79	m	31.4	6'(a,b)	None
6'(a)	3.64	m	54.4	6'(b)	3a, 13a
6'(b)	4.17	m	54.4	6'(a)	3a, 13a
1''	5.96	d (3.1)	96.2	2''(a,b)	3'', 5'', 12
2''(a)	2.38	dd (2.6, 15)	36.3	1'', 2''(b), 3''	1'', 3'', 4''
2''(b)	2.25	dt (3.5, 15)	36.3	1'', 2''(a), 3''	None
3''	4.09	d (3.0)	68.3	2''(a,b), 4''	None
3''-OH					
4''	3.30	dd (3.6, 10.2)	74.0	3'', 5''	3'', 5'', 5''-CH <sub>3</sub>
4''-OH					
5''	3.94	m	66.3	4'', 5''-CH <sub>3</sub>	3'', 5''-CH <sub>3</sub>
5''-CH <sub>3</sub>	1.23	d (6.6)	18.1	5''	4'', 5''

\*Assigned by <sup>13</sup>C NMR only and signals may be interchanged.



### Jadomycin Undec Minor (**5b**)

UV-Vis ( $8.67 \times 10^{-4}$  M,  $1.73 \times 10^{-4}$  M, MeOH),  $\lambda_{\max}$  (298 (16421), 320 (4550), 555 (2436));

TLC R<sub>f</sub>: 0.60 (9:1 DCM: MeOH); HPLC R<sub>t</sub> = 8.367 min; NMR spectra to follow in

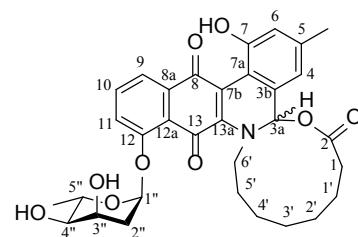
Appendix I, see characterization table (Table 11) for numbering.



**Table 11.** NMR assignment for **5b** (700 MHz, MeOD)

Jd Undec 3a <sub>Mn</sub> ( <b>5b</b> )					
Position	$\delta$ <sup>1</sup> H (ppm)	Multiplicity ( <i>J</i> (Hz))	$\delta$ <sup>13</sup> C (ppm)	COSY	HMBC
1(a)	3.43	m	58.3	1(b), 1'(a)	1', 3a
1(b)	3.35	m	58.3	1 (a)	1', 3a
2			182.9*		
3a	4.63	dd (6.9, 9.3)	63.9	1'(a,b)	1', 6', 1, 3b, 4, 7a, 13a
3b			134.0		
4	6.50	s	119.3	5-CH <sub>3</sub> , 6	3a, 3b, 5-CH <sub>3</sub> , 6, 7, 7a
5			140.9		
5-CH <sub>3</sub>	2.24	s	20.9	4, 6	4, 5, 6, 7a
6	6.62	s	119.5	4, 5-CH <sub>3</sub>	4, 5-CH <sub>3</sub> , 7, 7a
7			154.6		
7-OH					
7a			114.0		
7b			111.7*		
8			180.5		
8a			119.7*		
9	7.74	d (8.0)	121.4	10	8, 11
10	7.63	t (8.7)	136.7	9, 11	12, 12a
11	7.40	d (8.3)	121.1	10	9, 10, 12, 13
12			156.4		
12a			137.5		
13			184.5		
13a			155.4		
1'(a)	1.82	m	35.8	3a, 1'(b), 2'	1, 3a, 3b
1'(b)	1.69	m	35.8	3a, 1'(a), 2'	1, 3a, 3b
2'	1.28	m	30.1	1'(b)	3''
3'	1.23	m	27.5	None	2''
4'	1.23	m	30.6	None	None
5'	1.69	m	31.2	6'(a)	None
6'(a)	3.41	m	55.1	6'(b), 5'	5', 3a, 13a
6'(b)	4.21	m	55.1	6'(a), 5'	5', 3a, 13a
1''	5.83	d (3.3)	97.0	2''(a,b)	3'', 5'', 12
2''(a)	2.37	dd (2.4, 14.8)	36.2	1'', 2''(b), 3''	1'', 3'', 4''
2''(b)	2.14	dt (3.6, 14.8)	36.2	1'', 2''(a), 3''	None
3''	4.01	d (3.0)	67.9	2''(a, b), 4''	4''
3''-OH					
4''	3.21	dd (3.2, 9.8)	74.0	3'', 5''	3'', 5'', 5''-CH <sub>3</sub>
4''-OH					
5''	3.84	m	66.4	4'', 5''-CH <sub>3</sub>	1''
5''-CH <sub>3</sub>	1.14	d (6.7)	18.0	5''	4'', 5''

\*Assigned by <sup>13</sup>C NMR only and signals may be interchanged.



### Jadomycin Undec Methoxy (**6**)

TLC R<sub>f</sub>: 0.67 (9:1 DCM: MeOH); HPLC R<sub>t</sub> = 8.464 min.

### Jadomycin Undec Acetate (**7**)

TLC R<sub>f</sub>: 0.54 (9:1 DCM: MeOH); HPLC R<sub>t</sub> = 8.859 min.

## CHAPTER 3: PRODUCTION OF C-GLYCOSIDIC JADOMYCINS

### 3.1 Natural Product Glycosylation

Glycosylation is a common biological modification observed in many biomolecules and small molecules, such as proteins, nucleic acids, and secondary metabolites.<sup>74,75</sup> The addition of the carbohydrates generally serves to alter the physicochemical or biological properties of these molecules, but in natural products, glycosylation can directly alter or provide biological activity through enhanced target binding.<sup>74,76</sup>

A comprehensive analysis of bacterial natural products published recently by Thorson *et al* indicates 3426 of 15940 (21%) of secondary metabolites were glycosylated with one or several of 344 distinct carbohydrates.<sup>77</sup> Many of these sugars are deoxy-pyranoses which are derived from NDP-glucose or other glucose-derived metabolites, such as the dideoxy sugar L-digitoxose in jadomycin biosynthesis (Figure 15). These natural products include clinically relevant antibiotics such as erythromycin and vancomycin, anticancer drugs like doxorubicin, antifungals, and antiparasitics.<sup>76</sup> For anthracyclines in particular, the glycosylation highly impacts drug properties, where epirubicin, differing from doxorubicin only by the sugar, has improved activity and reduced cardiotoxicity.<sup>37</sup>

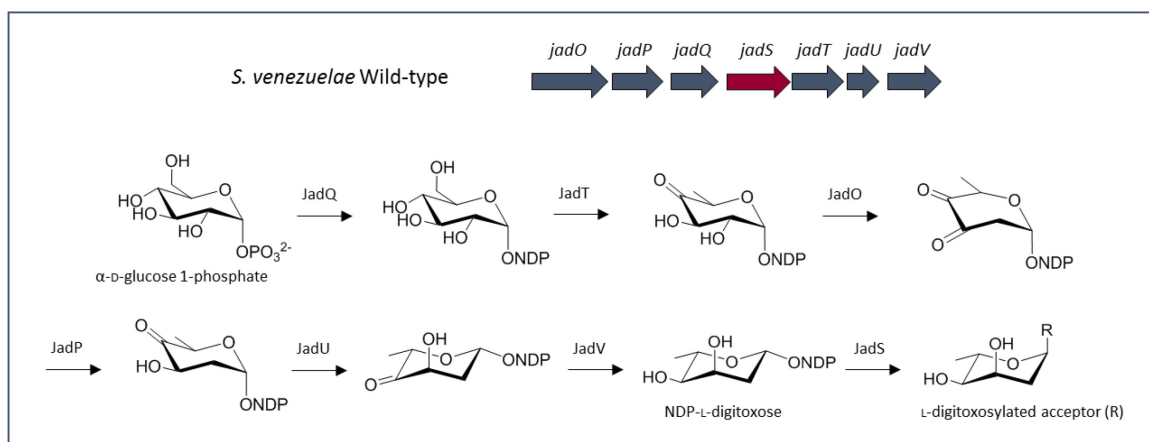


**Figure 15.** L-digitoxose biosynthetic genes and their contributions to the dideoxysugar biosynthesis and transfer.

### 3.2 Synthetic Biology and Combinatorial Biosynthesis within Gene Clusters

In bacterial natural products, appended sugars tend to be deoxygenated.<sup>78</sup> The biosynthetic genes for these sugars are often found in sub-clusters within the biosynthetic gene clusters for the secondary metabolite. The sugar diversity comes from the combinations of modifications to the precursor metabolite, including ketoreduction, C-, N- or O-alkylation, amination, or epimerization. Distinct genes (and therefore proteins) are responsible for each modification step, allowing deletions from/insertions into the sugar biosynthetic gene sub-cluster to affect the resultant glycosylated product.<sup>76</sup> This inherent modularity of natural product biosynthetic gene clusters lend themselves well to modifications by gene deletion, replacement, or modification through gene fusion or domain swapping.<sup>10</sup> While many natural products have desirable biological activity, they may also present difficult pharmacological properties (e.g. solubility, lipophilicity, toxicity) which can pose difficulty to alter through chemical synthesis or semi-synthesis due to the complexity of the natural products. Using synthetic biology to produce the desired natural product analogues with rationally modified biosynthetic genes, a process referred to as

combinatorial biosynthesis, is becoming a favourable alternative.<sup>10,79</sup> With the increasing availability of genomic sequences, the opportunities for heterologous expression and preparation of hybrid gene clusters through combinatorial biosynthesis are improving, widening the chemical space available for the discovery of these “unnatural” natural products.<sup>10</sup>

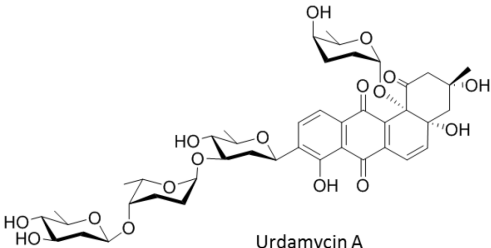
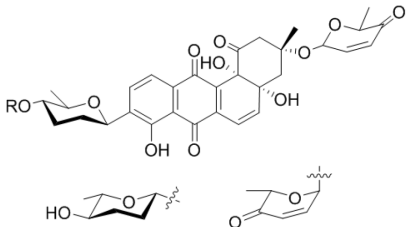
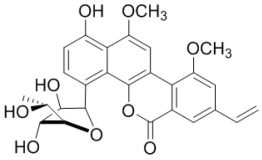
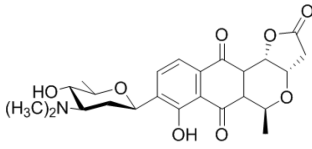
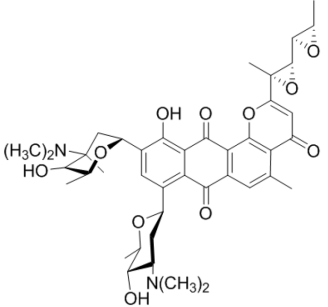
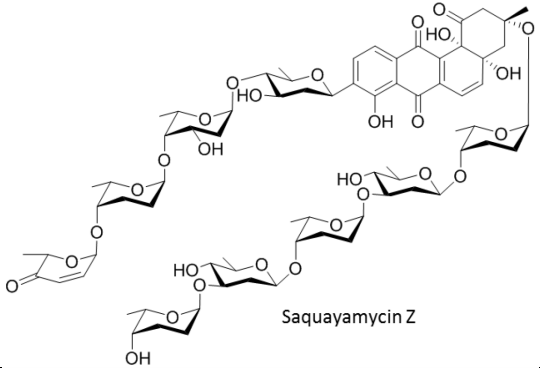
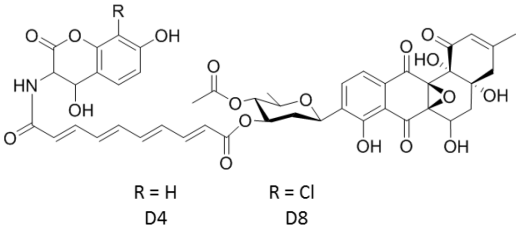
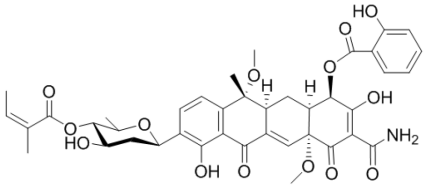
Glycosylation is performed principally by glycosyltransferases (GTs), enzymes which control the formation of a regio- and stereo-specific bond between an acceptor and a sugar donor substrate.<sup>76</sup> *O*-glycosylation is the most common, while *N*-, *C*-, and *S*-glycosylation also observed, but less frequently.<sup>74,78</sup> *C*-glycosylation is more desirable due to the stability to hydrolysis. Hydrolytic instability, as observed in the jadomycins, may limit the advancement of *O*-glycosylated natural products as clinical candidates.<sup>80</sup> GTs in NP biosynthetic gene clusters typically demonstrate increased flexibility to sugar donors and acceptor substrates than GTs involved in primary metabolism.<sup>74</sup> The combinatorial biosynthesis of known and novel deoxysugars has been demonstrated effectively by Salas and Mendez *et al*, including the production of a *C*-glycosylated pre-mithramycin through the combination of genes from three species of *Streptomyces*.<sup>81,82</sup> With an increasing deoxysugar gene “toolbox”, glycodiversification of secondary metabolites *in situ* to improve drug characteristics has become a novel method in natural product research.

### **3.3 Natural Product C-Glycosylation**

#### **3.3.1 C-Glycosyltransferase Toolbox**

Natural product C-glycosides are relatively rare in nature, making the pool of identified C-GTs limited, particularly in polyketide biosynthesis (Table 12). Within these identified C-GTs, only a few have demonstrated substrate flexibility. SsfS6 from *Streptomyces* sp. SF2575 is highly specific to its native anhydrotetracycline aglycone acceptor, but was able to transfer several sugar substrates<sup>83</sup> and GilGT similarly displayed flexibility to sugar donors.<sup>84</sup> One particular C-GT, UrdGT2, has been well-characterized through heterologous expression with apparent broad substrate specificity to both acceptors and sugar donors.<sup>85</sup>

**Table 12.** Selection of bacterial polyketide C-glycosyltransferases involved in secondary metabolism

C-glycoside(s)	C-GT (Species)	C-glycoside	C-GT (Species)
Urdamycins <sup>86</sup>	UrdGT2 <sup>85</sup> ( <i>Streptomyces fradiae</i> Tü2717)	Sch 47554, Sch 47555 <sup>&lt;sup&gt;87&lt;/sup&gt;</sup>	SchS7 <sup>88</sup> ( <i>Streptomyces</i> sp. SCC-2136 (ATCC 55186))
	Urdamycin A		Sch-47554
Gilvocarcins <sup>89</sup>	GilGT <sup>90</sup> ( <i>Streptomyces anandii</i> )	Medermycin <sup>91</sup>	Orf-8 <sup>92</sup> ( <i>Streptomyces</i> sp. AM-7161)
	Gilvocarcin V		Medermycin (Lactoquinomycin)
Hedamycin <sup>93</sup>	HedL, HedJ <sup>94</sup> ( <i>Streptomyces griseoruber</i> )	Saquayamycin, galtamycin <sup>95</sup>	SaqGT5 <sup>96</sup> ( <i>Micromonospora</i> sp. Tü6368)
	Hedamycin		Saquayamycin Z
Simocyclinone <sup>97</sup>	SimB7 <sup>98</sup> ( <i>Streptomyces antibioticus</i> Tü6040)	SF2575 <sup>99</sup>	SsfS6 <sup>83</sup> ( <i>Streptomyces</i> sp. SF2575)
	Simocyclinone R = H D4 R = Cl D8		SF2575

### 3.3.2 UrdGT2 Characteristics

UrdGT2 natively transfers D-olivose to produce urdamycin B, but has also been shown to transfer D-mycarose, D-rhodinose, and L-rhodinose (Figure 16).<sup>82,100,101</sup> UrdGT2 shows acceptor substrate flexibility within and outside of the angucycline class of natural products, having transferred D-olivose to prejadomycin and premithramycin, early biosynthetic polyaromatic products in landomycin and mithramycin biosynthesis, respectively.<sup>82,102</sup>

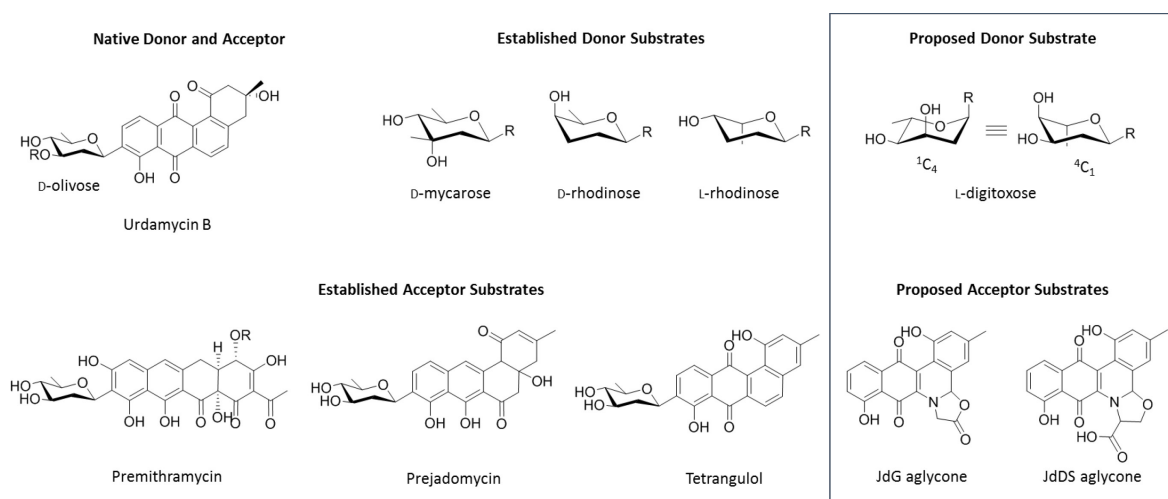


**Figure 16.** Demonstrated UrdGT2 flexibility to donor and acceptor substrates; (inset) proposed jadomycin substrates and proposed donor substrate L-digitoxose shown in <sup>1</sup>C<sub>4</sub> and <sup>4</sup>C<sub>1</sub> conformers.

## 3.4 Heterologous Expression of UrdGT2 for C-glycoside Jadomycin Production

### 3.4.1 Introduction

The jadomycins contain an *O*-glycosidic bond to L-digitoxose, the formation of which is catalyzed by JadS.<sup>103</sup> Since jadomycin aglycone and the established acceptor substrates of UrdGT2 share structural features, specifically hydroxylated polyaromatic rings with potential binding sites *ortho* or *para* to a phenolic OH group, favoured by many C-GTs,<sup>74</sup>

it is hypothesized that UrdGT2 could C-glycosylate jadomycins (Figure 16). It is also anticipated that UrdGT2 could accept NDP-L-digitoxose as a donor for C-glycosylation, based on the similar axial and equatorial substitution patterns to D-mycarose and D- and L-rhodinose, as shown in the  ${}^1C_4$  and  ${}^4C_1$  conformers in Figure 16.

Therefore, to direct the production of C-glycosylated jadomycins, the O-glycosyltransferase gene, *jadS*, was replaced with a homologous C-glycosyltransferase gene, *urdGT2* via several methods. First, through direct replacement by homologous recombination with a *jadQ::urdGT2::jadT* cassette and subsequently, through deletion of *jadS* and expression of *urdGT2* on two replicative vectors and an integrative vector. Jadomycin productions performed with the resultant *S. venezuelae* mutants were studied for the formation of a jadomycin C-glycoside.

### 3.4.2 Results and Discussion

#### *Preparation of urdGT2 complementation mutants*

The deletion of *jadS* and complementation with *urdGT2* was approached in four ways ( **Table 13**). First, a pKC1139 vector containing a *jadQ::urdGT2::jadT* cassette was used to generate an *urdGT2(ΔjadS)* mutant of *S. venezuelae*. Next, a *S. venezuelae ΔjadS* mutant was prepared for complementation with *urdGT2* on a replicative plasmid. Overall, three complementation strategies were exhausted with the *ΔjadS* mutant, each using a different vector; pSE34, pKC1139 (replicative), and pSEE152 (integrative). For each vector complementation strategy, a *jadS* variant was also prepared for control experiments to rescue production of O-digitoxosylated jadomycins.



**Table 13.** Methods for heterologous gene complementation in *Streptomyces*.

(Method) Description	Vector Description	Method Features (▲) and Disadvantages (▼)
(1) Homologous recombination to generate <i>S. venezuelae urdGT2(ΔjadS)</i>	pKC1139 <sup>104</sup> containing <i>jadQ::urdGT2(His)::jadT</i> cassette	<ul style="list-style-type: none"> <li>▲ Markerless, in-frame insertion/deletion</li> <li>▲ No selective pressure required to maintain mutant</li> <li>▲ <i>E. coli/Streptomyces</i> conjugation to introduce plasmid</li> </ul>
(2) Homologous recombination to generate <i>S. venezuelae ΔjadS</i>	pKC1139 containing <i>jadQ::jadT</i> cassette	<ul style="list-style-type: none"> <li>▲ Heterologous gene insertion into Jd gene cluster for co-transcription (Method 1 only)</li> <li>▼ Possible polar effects causing disruption of downstream gene transcription</li> <li>▼ Prolonged selection of double crossover mutant (4 weeks)</li> <li>▼ Potential disruption of translation or protein folding by His tag (Method 1 only)</li> </ul>
(2a) Complementation with replicative vector containing constitutive promoter	pSE34; <sup>105</sup> replicative plasmid containing <i>ermE*</i> promoter, high copy number replicon	<ul style="list-style-type: none"> <li>▲ Literature precedence for heterologous GT gene expression<sup>106,107</sup></li> <li>▲ Contains a strong, well- characterized constitutive promoter<sup>108</sup></li> <li>▲ Rapid selection of transformant (&lt;2 weeks)</li> <li>▲ High copy number replicon, pIJ101<sup>109</sup></li> <li>▼ Protoplast transformation into <i>S. venezuelae</i> is difficult</li> <li>▼ Thiostrepton selection required to maintain plasmid</li> <li>▼ <i>S. venezuelae</i> may readily develop <i>tsr</i> resistance<sup>110</sup></li> </ul>
(2b) Complementation with replicative vector	pKC1139; <sup>104</sup> replicative plasmid with low copy number, temperature sensitive replicon, with <i>ermE*</i> promoter	<ul style="list-style-type: none"> <li>▲ Literature precedence for heterologous gene expression<sup>111,112</sup></li> <li>▲ <i>E. coli/Streptomyces</i> conjugation to introduce plasmid</li> <li>▲ Rapid selection of transformant (&lt;2 weeks)</li> <li>▼ Apramycin selection required to maintain plasmid</li> <li>▼ Low copy number, temperature sensitive replicon, pSG5, has no function above 34°C<sup>113</sup></li> </ul>
(2c) Complementation with integrative vector	pSEE152; vector derived from pSET152, <sup>104</sup> containing $\phi$ C31 integrase, with <i>ermE*</i> promoter	<ul style="list-style-type: none"> <li>▲ Widely used for heterologous gene expression</li> <li>▲ <i>E. coli/Streptomyces</i> conjugation to introduce plasmid</li> <li>▲ Rapid selection of single crossover mutant (&lt;2 weeks)</li> <li>▲ Replicates with <i>Streptomyces</i> genomic DNA</li> <li>▼ Apramycin selection required to maintain integration</li> </ul>

## Method 1: Construction of a *S. venezuelae* *urdGT2*( $\Delta$ *jadS*) mutant

This approach used simple genetic manipulation to generate a marker-less mutant with *urdGT2* directly within the L-digitoxyl biosynthetic gene cluster. Despite the limited literature precedent for this heterologous expression method, it was deemed ideal to directly replace the *jadS* with *urdGT2* by homologous recombination. Given the cryptic nature of the jadomycin gene cluster expression, having a stable mutant without the need for selective antibiotics (which could be disruptive to bacterial growth and secondary metabolite production) and having the heterologous gene expression co-regulated with the gene cluster was preferential. It had been previously demonstrated that insertion of apramycin (*aa3(IV)*) disruption cassettes within the genes involved in dideoxysugar biosynthesis did not produce polar effects,<sup>103</sup> so it was presumed the in-frame replacement of *jadS* with *urdGT2*, a gene of similar size and G+C content, would not disrupt the transcription of the downstream genes.

For direct replacement of *jadS* with *urdGT2* by homologous recombination (Figure 17), the insertion site within the *S. venezuelae* genome was controlled by vector cassette design, wherein the *urdGT2* gene was flanked by 1 kb of chromosomal DNA immediately up- and downstream of the insertion site (i.e. *jadQ* upstream and *jadT*/partial *jadU* downstream). This *jadQ::urdGT2::jadT* gene cassette was synthesized (BioBasic, refer to 8.1

UrdGT2 Gene and Protein Sequences), with the *jadQ* and *jadT* identical to the chromosomal DNA of *S. venezuelae* and the *urdGT2* as a codon-optimized sequence of the reported *S. fradiae* gene. The cassette design also introduced a His<sub>6</sub>-tag before the *urdGT2* stop codon and a series of restriction enzyme recognition sites at the junctions between the vector and genes. This cassette was digested from the pUC57 vector and

ligated into the conjugative vector pKC1139. The plasmid was passed through *E. coli* ET12567 pUZ8002 and subsequently transferred to *S. venezuelae* by conjugation. Selection of a double crossover *S. venezuelae urdGT2* ( $\Delta jadS$ ) mutant proceeded as previously described.<sup>114</sup> Screening for the insert was accomplished by colony PCR using primers specific to the *urdGT2* insert (Table 15).

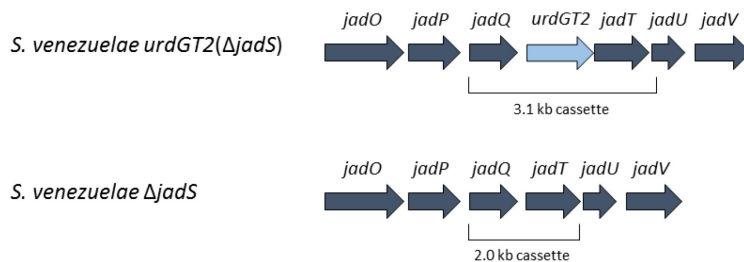


**Figure 17.** L-digitoxose biosynthetic gene cluster in the *jadS* replacement and deletion *S. venezuelae* mutants.

#### Method 2: Construction of *S. venezuelae ΔjadS* mutant

For *urdGT2* vector complementation studies, a *jadS* deletion mutant of *S. venezuelae* was prepared (Figure 17). Designing an in-frame  $\Delta jadS$  mutant strain was problematic, as the *jadS* and *jadT* genes are overlapped but *jadT* is frame-shifted. Additionally, the end sequence of *jadS* resembles a ribosomal binding site (RBS) and may be crucial for transcription of *jadT* and the downstream genes. The *jadQ::urdGT2::jadT* cassette had no overlapping genes and maintained the frame of *jadQ/ urdGT2* into *jadT*, and the end of *urdGT2* does not contain an RBS-like sequence. Ultimately, the  $\Delta jadS$  deletion cassette was designed to retain the last 15 base pairs of *jadS* and the shifted start codon for *jadT*. The *jadQ* and *jadT* flanking regions were amplified from *S. venezuelae* genomic DNA and unified by overlap extension PCR, ligated into the pKC1139 backbone, and transferred

into the wild-type *S. venezuelae* by conjugation. A double crossover *S. venezuelae*  $\Delta$ *jadS* mutant was selected and the *jadS* deletion was confirmed by PCR.

#### Method 2a: Replicative Expression using pSE34

The first complementation vector selected was the *Streptomyces* expression vector pSE34, which is maintained under selective pressure using thiostrepton (*tsr*) and contains the strong, constitutive promoter *ermE\** (*permE\**). The *urdGT2* gene was amplified from the pKC1139\_ *jadQ::urdGT2::jadT* vector using primers which incorporated a ribosomal binding site (RBS) ahead of *urdGT2* and a stop codon and restriction site at the end of the gene, before the His<sub>6</sub>-tag. The plasmid was ligated into the pSE34 vector and transformed into *E. coli* ET12567 to generate non-methylated copies of the plasmid. Since the pSE34 vector lacks an *oriT* necessary for conjugation, the furnished pSE34\_ *urdGT2* vector was introduced by *Streptomyces* protoplast transformation, following adapted literature procedures for *S. venezuelae*.<sup>115</sup> Unfortunately, the *tsr* selection of transformants proceeded slowly, and while several *tsr*-resistant colonies were identified, attempts to confirm to the presence of the plasmid by colony PCR and DNA isolation were unsuccessful. Some strains of *Streptomyces*, including *S. venezuelae*, may display pseudo-resistance to thiostrepton, resulting in a high number of false positives in selective screening.<sup>110,115</sup> Given the challenges encountered in the screening process and a failure to confidently identify any *S. venezuelae* colonies carrying pSE34\_ *urdGT2*, this method was not pursued.

#### Method 2b: Replicative Expression using pKC1139

With the failure of *tsr*-based mutant selection, we next attempted heterologous expression using the pKC1139 replicative vector, which requires apramycin selection. The entire *permE\**, RBS, and *urdGT2* cassette was digested from the pSE34\_urdGT2 vector and ligated into pKC1139. The pSG5 replicon maintains a low copy number in *Streptomyces* and is temperature sensitive, preventing plasmid replication above 34°C, a feature allowing the facile generation and selection of single-crossover mutants.<sup>113</sup> As a replicative vector, the temperature sensitive replication was not anticipated as a limitation to the method, as mutant selection and jadomycin productions proceed at 30°C. However, the pKC1139 vector complement displayed limited growth above 28°C, resulting in extended durations for both the selection and confirmation of *S. venezuelae* colonies carrying the plasmid (termed SV\_11Urd).

#### Method 2c: Integrative Expression using pSET152

The vector pSET152 possesses a *Streptomyces*  $\phi$ C31 integrase that recognizes *attB* sites in the chromosome.<sup>104</sup> Integration of pSET152 is the result of a single crossover in which the entire plasmid is inserted into the *attB* site and is maintained under selective pressure with apramycin. To retain constitutive expression of *urdGT2*, a pSET152-derived vector was prepared by Gibson Assembly to incorporate the *permE\**. The *urdGT2* gene with the RBS were amplified from the pSE34\_urdGT2 construct and ligated into the new integrative vector, termed pSEE152. The pSEE152\_urdGT2 plasmid was transformed into *S. venezuelae* wild-type and  $\Delta$ *jadS* and single-crossover mutants (SV\_WUrd and SV\_52Urd, respectively) were selected and confirmed by PCR.

### *Jadomycin Production in S. venezuelae Wild-type and Mutant Strains*

The *Streptomyces* strains generated by homologous recombination were cultured in jadomycin production conditions using the amino acids glycine and D-serine, to direct biosynthesis of JdG and JdDS (Figure 16), respectively. These jadomycons contain small E-rings and R-substituents, and were selected to best mimic the size and polarity of the previously identified *urdGT2* substrates, prejadomycin and tetrangulol.<sup>102,116</sup> Productions were monitored at 600 nm ( $OD_{600}$ ), for bacterial proliferation, and at 526 nm ( $A_{526}$ ), to estimate jadomycin production. Productions were filtered and initially purified by silica-phenyl flash chromatography, wherein natural products were bound to a pre-conditioned silica-phenyl column which was washed with water to elute media components before eluting the natural products with methanol. This crude methanolic extract was analyzed by high performance liquid chromatography (HPLC) and tandem liquid chromatography mass spectrometry (LC-MS) to identify the natural products, as compared to non-complemented control productions. LC-MS analysis included non-selective electrospray ionization scans (Q1) scans, as well as the MS/MS enhance product ion (EPI, selective) and precursor ion (PREC) scans in positive mode. The EPI experiments scan for the molecular ion peak from a narrowed mass range and the precursor ion experiments identify the molecular ion peaks from known or presumed fragment ions; precursor scans used fragments phenanthroviridin  $m/z$  306 and L-digitoxosyl phenanthroviridin  $m/z$  436 (Figure 18), fragments common to all jadomycons arising from loss of the amino acid and sugar.<sup>48,49,51,53</sup>

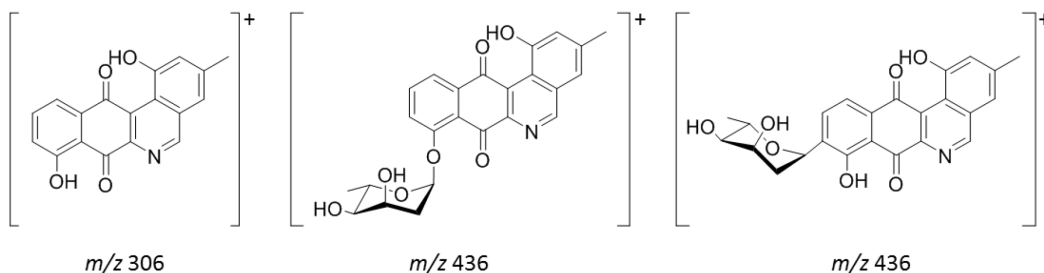


**Figure 18.** Jadomycin fragments ions used in precursor ion scans (PREC).

Method 1: *S. venezuelae urdGT2*( $\Delta$ *jadS*) mutant jadomycin production

Jadomycin productions using the *S. venezuelae urdGT2* ( $\Delta$ *jadS*) were performed with both glycine and D-serine. HPLC traces of these crude materials indicated only the presence of the corresponding aglycone (JdG or JdDS) in addition to chloramphenicol (Cam, discussed further in later section). LC-MS Q1 positive scans did not identify a peak for the predicted C-glycoside jadomycins, nor any other potential C-glycoside jadomycin precursor. Further LC/MS analysis of the JdG crude using PREC 306 gave the JdG aglycone  $m/z$  364 as the major signal detected, corroborating HPLC evidence that no glycosylated jadomycins were produced (Figure 19).

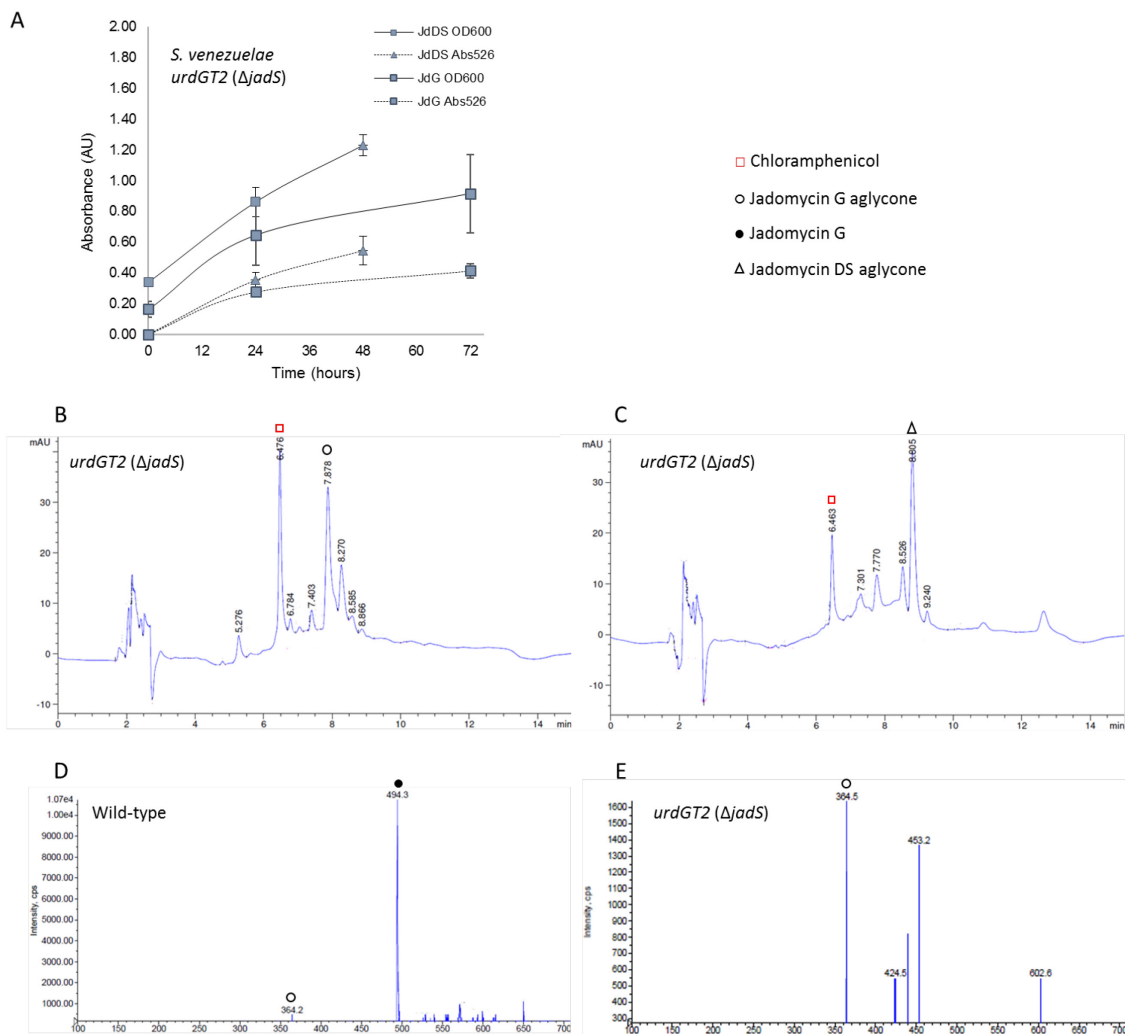


**Figure 19.** *S. venezuelae urdGT2* ( $\Delta$ *jadS*) culture analysis; (A) Jadomycin production growth curves; HPLC traces of (B) JdG crude extract, (C) JdDS crude extract; PREC 306 ion scans of (D) wild-type JdG crude extract and (E) *S. venezuelae urdGT2* ( $\Delta$ *jadS*) JdG crude extract.

The inability of the mutant to produce detectable quantities of jadomycin C-glycosides may be attributed to one or several failed hypotheses. The method design assumes that 1) the synthetic gene will be appropriately co-transcribed with the other jadomycin deoxysugar genes, 2) the gene will be translated appropriately and completely and that the His-6 tag will not interfere with the protein folding, 3) the downstream genes will still be transcribed and translated, and most importantly, 4) the UrdGT2 can accommodate and



turnover the acceptor and donor substrates.

Method 2b: pKC1139-complemented *S. venezuelae*  $\Delta$ *jadS* mutant jadomycin production

Jadomycin productions using the pKC1139-derived *urdGT2* and *jadS* complementation strains (SV\_11Urd and SV\_11JS, respectively) were performed with glycine at 28°C, as limited by the pSG5 replicon temperature sensitivity. The temperature restriction, compounded by the apramycin supplementation in the media, caused an overall slow doubling time of the *S. venezuelae* strains, which contributed to difficulty generating *S. venezuelae* inoculum and greatly reduced the yield of the jadomycin productions (Figure 32). Crude extracts were analyzed by HPLC and LC-MS, but again only data supporting formation of JdG aglycone and Cam were attained in both SV\_11Urd and SV\_11JS (Figure 20).

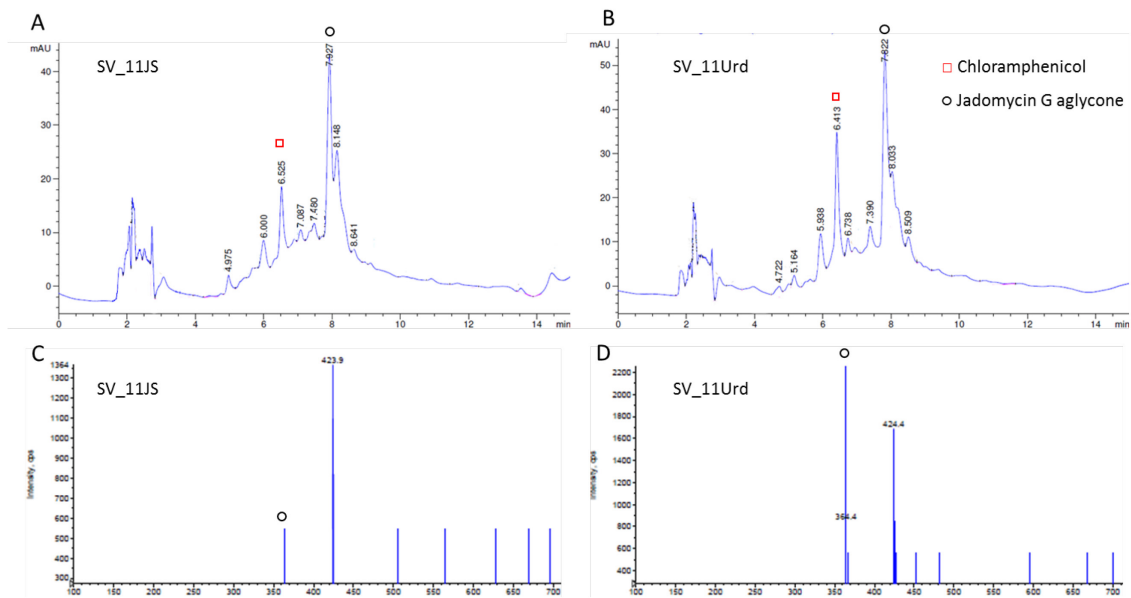


**Figure 20.** JdG and JdDS productions of pKC1139-derived *urdGT2* and *jadS* complemented *S. venezuelae*  $\Delta$ *jadS* (SV\_11Urd and SV\_11JS, respectively); HPLC traces of (A) SV\_11JS and (B) SV\_11Urd; PREC 306 ion scans of (C) SV\_11JS and (D) SV\_11Urd.

Method 2c: pSEE152-complemented *S. venezuelae*  $\Delta$ *jadS* mutant jandomycin production

The integrative-vector complementation strains were also cultured in JdG producing conditions. HPLC analysis of the *jadS* complementation strain, SV\_52JS, had a small peak suggestive of L-digitosoylated JdG formation, subsequently confirmed by PREC 306 scans in which *m/z* 364, 494 and 526 were detected, corresponding to JdG aglycone, JdG, and glucosylated JdG  $[M+H]^+$  (Figure 21). These data indicated a successful deletion and complementation strategy for *jadS*, confirming the expression of both the *O*-GT JadS and the products of the genes downstream from *jadS* (JadT, JadU, JadV) which are involved in L-digitoxose biosynthesis. The JdG aglycone was the major peak in the HPLC trace and PREC 306 scan, demonstrating that *O*-glycosylation is only partially restored. Notably, detection of the glucosylated JdG in the PREC 306 scan shows the JadQ product of L-digitoxose biosynthesis (Figure 15) being appended by JadS, suggesting that the *jadTUV* gene expression may have been adversely effected, although not abolished, by deletion of *jadS*.

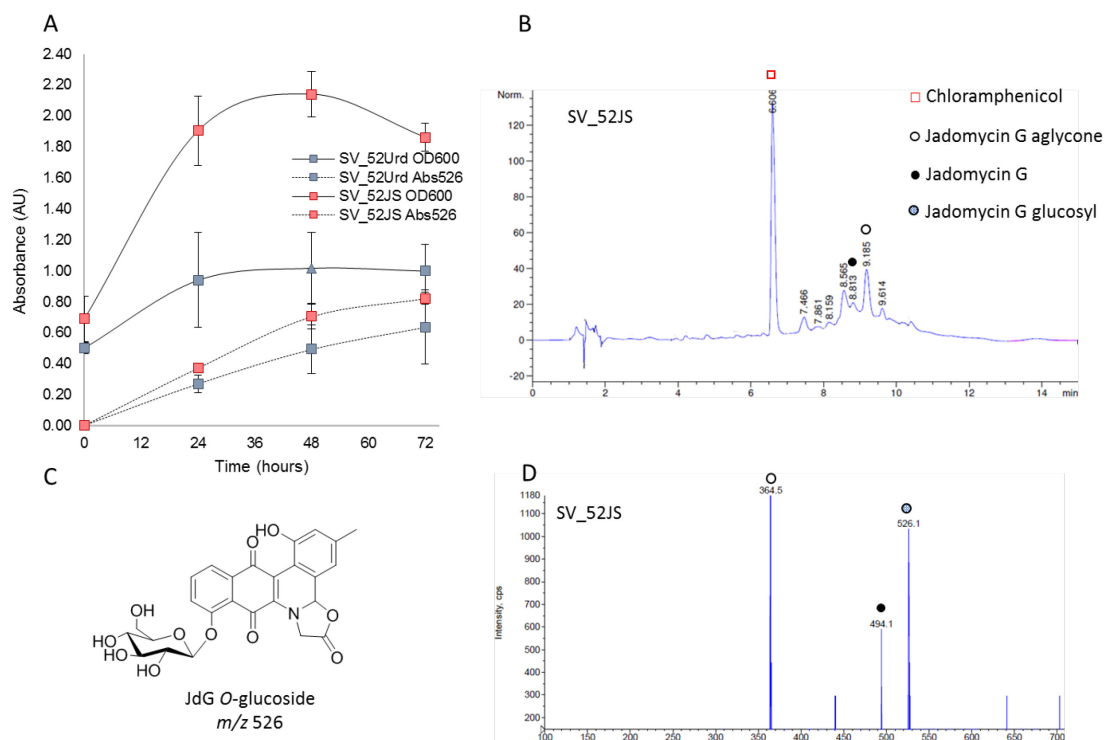


**Figure 21.** Growth and JdG production in integrative *urdGT2* and *jadS* complemented *S. venezuelae*  $\Delta$ *jadS*. (SV\_52Urd and SV\_52JS, respectively); SV\_52JS JdG crude analysis by (B) HPLC and (D) LC-MS PREC 306 indicating formation *O*-glycosylated jadomycins, including jadomycin *O*-glucoside (C).

The HPLC trace of the *urdGT2* complementation strain, SV\_52Urd, also had small peak at a  $R_t$  similar to the glycosylated JdG (Figure 22), but probing the crude by LC-MS did not identify any peaks which were not also detected in the *S. venezuelae*  $\Delta$ *jadS* control productions (Figure S56). SV\_52Urd was further cultured in a JdDS production, but similar results were obtained (Figure S57, Figure S58). The SV\_52Urd JdG production was scaled up to 2 L to generate more crude material, wherein a pink compound was identified by TLC which did not appear in the *S. venezuelae*  $\Delta$ *jadS* control production TLC. The scaled-up production crude was fractionated by normal phase preparative TLC, but none of the fractions appeared to contain a *C*-glycoside by LC-MS or NMR (Figure S59).

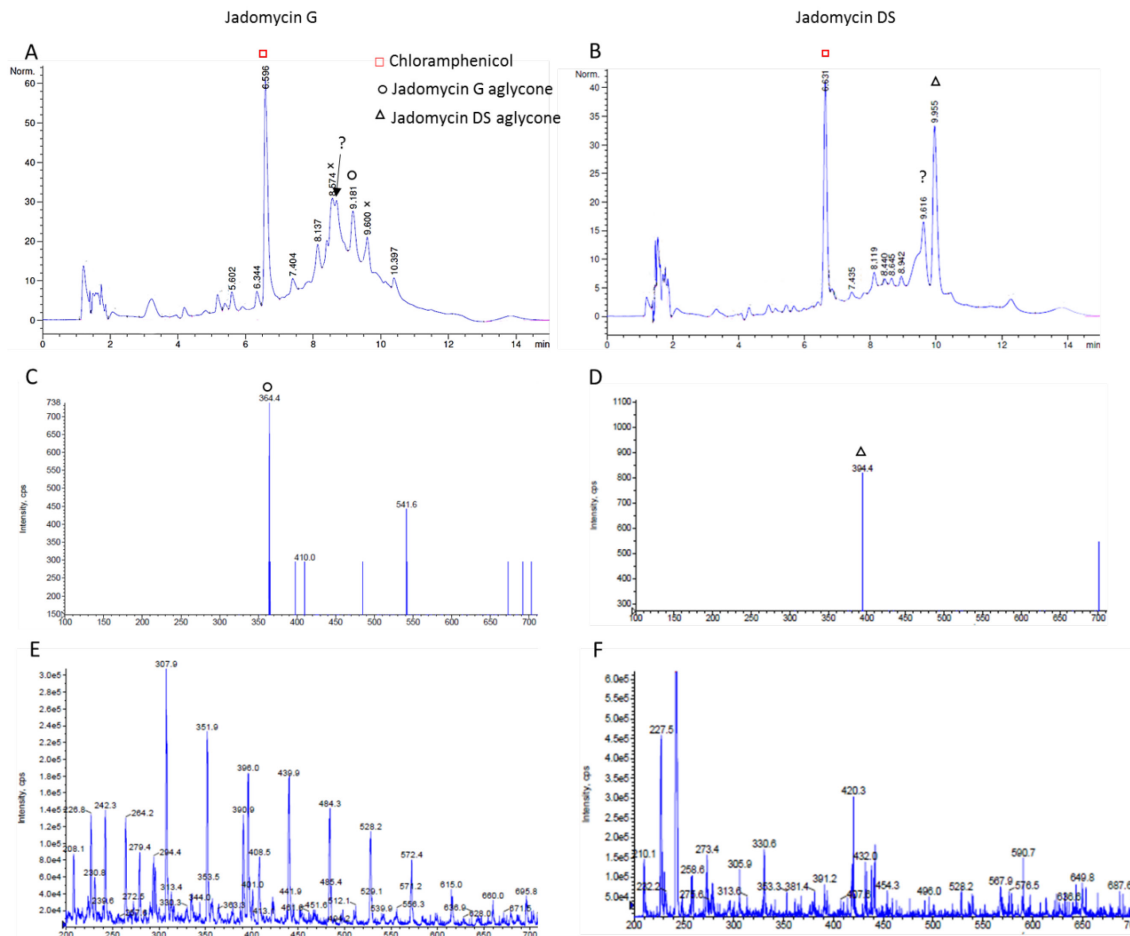


**Figure 22.** Analysis of JdG and JdDS productions in SV\_52Urd; HPLC traces of (A) JdG and (B) JdDS; PREC 306 scans of (C) JdG and (D) JdDS; ESI<sup>+</sup> non-selective scans of (E) JdG and (F) JdDS.

### *Chloramphenicol production in complementation and deletion mutants*

Generally, chloramphenicol (Cam) biosynthesis is negligible or minimal during jadomyacin production, as a result of the complex reciprocal regulation of the two *S. venezuelae* natural products.<sup>117</sup> The jadomyacin gene cluster contains a series of regulatory genes, including JadR1, which represses Cam gene transcription and activates Jd gene expression, and JadR2, which is a higher-level regulatory protein that represses the transcription of *jadR1*. Changes to JadR2, whether by ethanol shock or antibiotic binding, causes de-repression of *jadR1* transcription, and subsequent activation of jadomyacin biosynthesis by JadR1.<sup>118,119</sup>

In all cases, the *S. venezuelae* strains which were manipulated by gene replacement, deletion, or vector-based complementation saw increased Cam production. This shift in natural product biosynthesis could be attributed to the disruption of the jadomycin biosynthetic gene cluster or to media supplementation with the antibiotic apramycin. The  $\Delta$ *jadS* and *urdGT2*( $\Delta$ *jadS*) *S. venezuelae* strains were cultured without apramycin selective media and produced only Jd aglycone (in modest yields) and Cam. We speculate the reversion from Jd to Cam production in these strains may occur through JadR2-mediated mechanism, where changes to JadR2 after ethanol shock allow formation of JadR1, thereby activating Jd biosynthesis and repressing Cam. Then, as the cells recover from the ethanol shock, JadR2 would generally bind the furnished jadomycin, allowing *jadR1* expression to continue.<sup>118</sup> However, since only Jd aglycone is produced in these strains, the JadR2 binds *jadR1* to repress it, and as JadR1 diminishes, Cam production is activated and Jd production diminished. In the complemented strains, including the wild-type *S. venezuelae* with the pSEE152 (empty) integrative vector, apramycin in the production media may higher-level pleiotropic regulators to modulate the natural product biosynthesis. We have not made attempts to further substantiate these proposed mechanisms of cross-regulation.

### 3.5 Conclusions

To generate hydrolytically stable jadomycin C-glycosides, four methods for heterologous expression of *urdGT2* in *S. venezuelae* were explored. While C-glycosylated jadomycons or jadomycin analogues were not detected, the O-glycosylation of JdG was observed using integrative, constitutive expression of *jadS* in the *S. venezuelae*  $\Delta$ *jadS* mutant, verifying that the vector expression system was viable. In addition, both L-digitoxosylated and glucosylated JdG congeners were detected in LC-MS experiments, suggesting that the

entire L-digitoxose biosynthetic sub-cluster was functional, but transcription of the genes downstream of *jadS* (*jadTUV*) may be diminished. The complex co-transcription, frame-shifting, and overlapping of the biosynthetic genes in the jadomycin cluster makes preparation of a deletion mutant without polar effects difficult. Interestingly, the deletion and complementation mutants of *S. venezuelae* produced increased chloramphenicol as compared to wild-type *S. venezuelae*, suggesting the antibiotic supplementation and lack of furnished jadomycin production contribute to the complex co-regulation of the two natural products.

As *jadS* complementation did not fully restore production glycosylated jadomycins, the constitutive expression of *jadS* may still be lower than in the wild-type *S. venezuelae*. To fully assess the transcription of the integratively-expressed gene (*jadS* or *urdGT2*) and the *jadTUV*, mRNA analysis as a surrogate marker for protein production would be beneficial. Constitutive complementation of any genes which demonstrate reduced transcription in  $\Delta$ *jadS* mutant as compared to wild-type would improve production of NDP-L-digitoxose donor. Alternatively, or additively, performing further heterologous expression studies in mutants which overexpress jadomycin and have chloramphenicol production blocked would increase substrate concentration and simplify analysis of the crude natural products. Performing heterologous gene expression studies on a cryptic natural product may have been ambitious.

With improved *jadS* complementation, continued attempts at C-glycoside production using *urdGT2* could be made using the native jadomycin dideoxysugar, L-digitoxose, or the dideoxy gene cluster could be manipulated and complemented to affect the production of the native *urdGT2* donor sugar, D-olivose. The heterologous production and O-

glycosylation of jadomycins with D-olivose has been recently reported, using a similar integrative expression system and the donor-flexible JadS.<sup>120</sup>

### 3.6 Experimental Methods

**Table 14.** List of bacterial strains and plasmids used in Chapter 3.

Strain or Plasmid	Description	Source
NEB 5-alpha competent <i>E. coli</i>	Commercial cloning strain (high efficiency)	New England Biolabs
<i>E. coli</i> ET12567 (pUZ8002)	Produces non-methylated DNA; <i>dam</i> <sup>-</sup> <i>dcm</i> <sup>-</sup> <i>hsdS</i> <sup>-</sup> , carrying <i>oriT</i> mobilizing plasmid	<sup>121</sup>
<i>S. venezuelae</i> ISP5230 (WT)	Wild-type jadomycin and chloramphenicol producing strain	ATCC 10712
SV_WT5	Wild-type <i>S. venezuelae</i> complemented with empty pSEE152	This work
SV_WUrd	Wild-type <i>S. venezuelae</i> complemented with pSEE152_urdGT2	This work
<i>S. venezuelae</i> urdGT2( $\Delta$ jadS)	<i>S. venezuelae</i> mutant with urdGT2 replacing <i>jadS</i>	This work
<i>S. venezuelae</i> $\Delta$ jadS	<i>jadS</i> deletion mutant of <i>S. venezuelae</i>	This work
SV_11Urd	<i>S. venezuelae</i> $\Delta$ jadS complemented with pKC1139_urdGT2	This work
SV_52DS	<i>S. venezuelae</i> $\Delta$ jadS complemented with empty pSEE152	This work
SV_52Urd	<i>S. venezuelae</i> $\Delta$ jadS complemented with pSEE152_urdGT2	This work
SV_11JS	<i>S. venezuelae</i> $\Delta$ jadS complemented with pKC1139_jadS	This work
SV_52JS	<i>S. venezuelae</i> $\Delta$ jadS complemented with pSEE152_jadS	This work
pUC57_jadQ:: <i>urdGT2</i> :: <i>jadT</i>	<i>E. coli</i> vector; <i>amp</i> <sup>R</sup> , containing synthetic, codon-optimized <i>urdGT2</i> with terminal His <sub>6</sub> -tag, flanked by <i>jadQ</i> and <i>jadT</i> (sequence identical to native <i>S. venezuelae</i> )	BioBasic Inc.
pKC1139	<i>E. coli</i> - <i>Streptomyces</i> conjugation vector; <i>oriT</i> RK2, <i>ori</i> pBR322, <i>ori</i> pSG5, <i>aa(3)IV</i>	<sup>104</sup>
pKC1139_jadQ:: <i>urdGT2</i> :: <i>jadT</i>	pKC1139 containing synthetic <i>jadQ</i> :: <i>urdGT2</i> :: <i>jadT</i> cassette	This work
pKC1139_jadQT	pKC1139 containing <i>jadS</i> deletion cassette	This work
pKC1139_urdGT2	pKC1139 containing <i>permE</i> <sup>*</sup> , RBS, and <i>urdGT2</i>	This work
pKC1139_jadS	pKC1139 containing <i>permE</i> <sup>*</sup> , RBS, and <i>jadS</i>	This work
pSE34	<i>Streptomyces</i> expression vector; <i>ori</i> pIJ101, <i>ori</i> pUC19, <i>bla</i> , <i>tsr</i>	<sup>105</sup>
pSE34_urdGT2	pSE34 containing RBS and <i>urdGT2</i>	This work
pSE34_jadS	pSE34 containing RBS and <i>jadS</i>	This work
pSET152	Integrative vector; <i>oriT</i> RK2, <i>ori</i> pUC18, <i>int</i> $\phi$ C31, <i>aa(3)IV</i>	<sup>104</sup>
pSEE152	pSET152 containing <i>permE</i> <sup>*</sup>	This work
pSEE152_urdGT2	pSEE152 containing RBS and <i>urdGT2</i>	This work
pSEE152_jadS	pSEE152 containing RBS and <i>jadS</i>	This work



**Table 15.** List of primers used in Chapter 3.

Primer identification	Primer sequence (Restriction sites underlined, RBS italicized)
JadQ Fwd OE ( $\Delta$ JadS)	GGT <u>TCTAGACGAATTC</u> CTGGCCGGAGGCCACGGC
JadQ Rev OE ( $\Delta$ JadS)	GCCGTCCCTCCGAGGGTCTCTCTCCGCGG
JadT Fwd OE ( $\Delta$ JadS)	CCTCGGAGGGACGGCATGAGGATCCTCGTCACC
JadT Rev OE ( $\Delta$ JadS)	GGT <u>AAGCTT</u> GGGTACCTGCATGGTCGTCG
pSEurd Fwd	CGTCTAGAA <u>GGAGGT</u> ACGGACGTGTTCCGCCCTCGCCCCG
pSEurd Rev	GGT <u>AAGCTT</u> TCACGCGAGCTGCTCCAGCGCCG
pSEjadS Fwd	CGT <u>TCTAGAC</u> CCCGCCCCGCGGAGAG
pSEjadS Rev	GGT <u>AAGCTT</u> CCGCCGGTGACGAGGATCC
ermEpSE Fwd	GATGCTAGCATGAATTCGAGCTCGGTACC
ermE GA Fwd	CTATGACATGATTACGAATTCGATCGATGTCGGACCGGAGTTC GAGGTAC
ermE GA Rev	AGCTTGGGCTGCAGGTCTGACTCATATGC <u>GGTACCCCTTCTAGA</u> GGATCCTACC
pSETurd Rev	GTCATATGGT <u>TACCC</u> GCGAGCTGCTCCAGCGCCG
pSETjadS Rev	GTCATATGGGT <u>TACCC</u> GCCGGTGACGAGGATCC
urdtg2_spec Fwd	GGTGGTACCCCAGGAGGAGAGAAC
urdtg2_spec Rev	GGTGGTCTCCGCGTCGAG

### 3.6.1 General Laboratory Procedures

All chemical and biological reagents were purchased from commercial sources and used without further purification. All solvents were HPLC grade, unless otherwise indicated. Sterile water used for all molecular biology and aseptic requirements indicates autoclaved distilled deionized water. All media was prepared with distilled water and was sterilized by autoclaving at 121°C for 20 minutes. Apramycin (50  $\mu$ g/mL), thiostrepton (25 or 50  $\mu$ g/mL) as stated, nalidixic acid (25  $\mu$ g/mL), chloramphenicol (25  $\mu$ g/mL), kanamycin (50  $\mu$ g/mL), and/or ampicillin (100  $\mu$ g/mL), were added to media as required.

All buffers used in the described procedures were prepared as indicated or were provided with the commercial kits, as referenced. Genomic DNA and were kept at -20°C, while

plasmid isolates and in-progress samples were stored at 4°C. Primers were purchased from Integrated DNA Technologies.

#### *General Bacteria Handling*

*Streptomyces venezuelae* strains were grown on MYM-agar at 30°C. Liquid cultures of MYM were inoculated with *S. venezuelae* lawn was scrapings from sporulated plates and grown at 30°C and 250 rpm. Spore solutions were prepared by harvested from plates grown for a minimum of 10 days, with dense white or green spores scraping the *S. venezuelae* lawn into sterile water, vortexing and vigorously shaking to separate spores, then filtering through sterile cotton wool. For preparation of glycerol stocks, the spores were immediately diluted 1:1 with 50% sterile glycerol. Alternatively, the spore solution was pelleted at 5000 g for 10 minutes, supernatant decanted, and the spores were re-suspended in sterile water before being diluted 1:1 with 50% sterile glycerol. The glycerol stocks were aliquoted and stored at -70 °C.

*E. coli* cultures were grown overnight at 37°C, 250 rpm in LB media with antibiotics as required, and stored as solutions supplemented with 25% glycerol at -70°C.

#### *Genomic DNA Extraction*

Overnight liquid cultures of *S. venezuelae* in MYM were used to collect bacteria for genomic DNA isolation using a spin column genomic DNA kit (Qiagen or BioBasic) following manufacturer guidelines for bacterial samples. An aliquot of culture media was pelleted at 12000 rpm for 5 minutes. The supernatant was removed and the cell pellet re-suspended in 200 µL cold TE buffer, then 400 µL of the Digestion solution and 3 µL Proteinase K solution were added. The sample was heated at 55°C for 20 minutes or until

cells were lysed, with intermittent vortexing. The sample was allowed to cool, then 260  $\mu\text{L}$  ethanol was added, and the solution was applied to a spin column. The column was centrifuged for 2 minutes (or longer as needed) at 10000 rpm. The column flow-through was discarded and 500  $\mu\text{L}$  of Wash solution was applied to the column, and the column was spun once again, and the flow-through discarded. The wash step was repeated. The column was spun for an additional minute to remove residual wash solution. The column was placed in a clean micro-centrifuge tube and 50  $\mu\text{L}$  of Elution buffer was applied. After allowing the Elution buffer to incubate for several minutes at room temperature, the column was centrifuged to elute the genomic DNA.

#### *PCR and Colony PCR methods*

For use in PCR reactions, 10  $\mu\text{M}$  working solutions of primers in sterile water were prepared. A 10 mM dNTP stock solution in sterile water was prepared from dNTP stock solutions (100 mM, BioBasic). PCR reactions contained 10  $\mu\text{L}$  buffer (5  $\times$ ), 10  $\mu\text{L}$  NEB Q5 GC enhancer (5  $\times$ ) or 5  $\mu\text{L}$  DMSO (10% total volume), 1  $\mu\text{L}$  dNTP (10 mM), 5  $\mu\text{L}$  forward primer (10  $\mu\text{M}$ ), 5  $\mu\text{L}$  reverse primer (10  $\mu\text{M}$ ), 0.5-2  $\mu\text{L}$  template DNA (as indicated), 0.5  $\mu\text{L}$  DNA polymerase, and sterile water to a 50  $\mu\text{L}$  total volume. PCR reactions using Phusion DNA polymerase (ThermoFisher) were performed with the provided High G+C buffer and DMSO, while reactions using Q5 DNA Polymerase (NEB) were performed with the provided Q5 reaction buffer and Q5 GC enhancer.

Colony PCR screening was carried out with Phusion DNA polymerase. Colony PCR templates were prepared by scraping the colony into 10  $\mu\text{L}$  DMSO in a microtube, then vortexing, heating at 95°C for 10 minutes in the thermocycler, then centrifuging down the

cell debris. PCR reactions were performed using a BIOMETRA Tpersonal thermocycler with the program in the table below.

Step	Temp (°C)	Time (s)	cycles
0	95	600	1
1	98	30	15 (steps 1-3)
2	82.6 (- 0.5 per cycle)	30	
3	72	As indicated	
4	98	30	20 (steps 4-6)
5	55	30	
6	72	As indicated	
7	4	hold	1

#### *Agarose Gel Running Conditions and Visualization*

Agarose (300 mg) was melted in 30 mL TAE buffer (1.0%) in a microwave. The dissolved agarose was cast into the gel boat and allowed to set. DNA samples were mixed with loading dye (6x). Samples were run alongside a 1 kb reference ladder (NEB 1kb DNA ladder Thermo Scientific GeneRuler 1kb ladder). The TAE running buffer contained 30 µL of 1 mg/mL ethidium bromide and gels were run with an applied current of 120 mV. Developed gels were visualized under a UV light (392 nm) and images captured using an Olympus C-4000 Zoom camera and DOC ITLS 5.5.5 software (UVP, Inc). Adobe Photoshop Elements 2.0 was used for manipulation of images such as colour inversion and contrast adjustments. For gel extraction, 240 mg of agarose was used in 30 mL TAE buffer (0.8%). For small bands of interest (<800 bp), 390 mg of agarose was used in 30 mL TAE buffer (1.3%) and samples were run alongside a 100bp reference ladder (NEB). All other running conditions were identical.

### *Gel Densitometry*

DNA concentrations of linearized vectors and PCR products were determined by gel densitometry. DNA samples were run alongside two dilutions of a 1kb DNA ladder (NEB or Thermo Scientific) on an agarose gel and imaged, and the intensity of the bands closest in size to band of interest were used to generate a standard curve using ImageJ (NIH) with which to interpolate the concentration of the DNA of interest.

### *Media and Buffer Recipes*

Refer to Section 2.5.1 for additional media recipes

*Lysogeny broth (LB)*: 5 g yeast extract, 10 g NaCl, 10 g tryptone, water to 1.0 L, pH 7.5

Malt yeast maltose (MYM): 10 g malt extract, 4 g yeast extract, 4 g maltose, water to 1.0 L, pH 7.0.

*Mannitol soya flour (MS)*: 4 g each of mannitol, soya flour, and agar, water to 200 mL.

*YEME medium*: 3 g yeast extract, 5 g peptone, 3 g malt extract, 10 g glucose, 340 g sucrose, water to 1.0 L, pH 7.5. After autoclaving, the solution was supplemented with separately autoclaved glycine (5 mL of 20% aqueous solution) and MgCl<sub>2</sub> (400 µL of 2.5 M solution).

*Modified P buffer*: 0.25 g K<sub>2</sub>SO<sub>4</sub>, 17.5 g NaCl, 2.02 g MgCl<sub>2</sub>·6H<sub>2</sub>O, 2 mL trace element solution, 800 mL water, aliquot into 10 × 80 mL solutions and autoclave. To each 80 mL autoclaved solution, the following filter-sterilized solutions are added: 1 mL KH<sub>2</sub>PO<sub>4</sub> (0.5%), 10 mL CaCl<sub>2</sub> (3.68%), 10 mL TES (5.73%, pH 7.2).

*Modified T buffer:* 17.5 g NaCl, distilled water to 1.0 L. After autoclaving, add separately autoclaved: 2 mL trace element solution, 10 mL K<sub>2</sub>SO<sub>4</sub> (2.5%). To a 9.3 mL aliquot, add separately sterilized: 0.2 mL CaCl<sub>2</sub> (3.68%), 0.5 mL Tris HCl (pH 8).

*Modified L buffer:* 17.5 g NaCl, water to 800 mL. After autoclaving, add separately sterilized: 2 mL trace element solution, 10 mL K<sub>2</sub>SO<sub>4</sub> (2.5%), 10 mL CaCl<sub>2</sub> (0.25 M), 10 mL KH<sub>2</sub>PO<sub>4</sub> (0.5%), 1 mL MgCl<sub>2</sub> (2.5 M), 100 mL TES buffer (5.73%, pH 7.2).

*Trace element solution:* 40 mg ZnCl<sub>2</sub>, 200 mg FeCl<sub>3</sub>·6H<sub>2</sub>O, 10 mg CuCl<sub>2</sub>·2H<sub>2</sub>O, 10 mg MnCl<sub>2</sub>·4H<sub>2</sub>O, 10 mg Na<sub>2</sub>B<sub>4</sub>O<sub>7</sub>·10H<sub>2</sub>O, and 10 mg (NH<sub>4</sub>)<sub>6</sub>Mo<sub>7</sub>O<sub>24</sub>·4H<sub>2</sub>O in water to 1.0 L.

*Modified R5N Medium:* 0.25 g K<sub>2</sub>SO<sub>4</sub>, 17.5 g NaCl, 10 g maltose, 0.1 g casamino acids, 2.2 g agar, water to 800 mL. Autoclave in 80 mL aliquots. To each autoclaved aliquot add separately autoclaved: 0.2 mL trace element solution, 1 mL KH<sub>2</sub>PO<sub>4</sub> (0.5%), 8 mL CaCl<sub>2</sub> (3.68%), 1.5 mL proline (20%), 5 mL yeast extract (10%), 10 mL TES buffer (5.73%), 0.5 mL NaOH (1 N).

*Soft nutrient agar (SNA):* 0.8 g Difco nutrient broth powder, 0.5 g agar, water to 100 mL

*TAE buffer (50X):* 242 g TRIS, 57.1 mL glacial acetic acid, and 18.6 g disodium ethylenediaminetetraacetic acid (EDTA), water to 1.0 L. Diluted for use with distilled water.

*TE Buffer:* 10 mL 1 M TRIS (60.6 g in 500 mL water, pH 7.5), 2 mL 0.5 M EDTA (18.6 g EDTA in 100 mL water, pH 8.0), water to 1.0 L.

### 3.6.2 Vector Construction

#### *Plasmid Ligation*

Linearized plasmids were treated with calf intestinal alkaline phosphatase (CIP, NEB) by adding 1  $\mu\text{L}$  (10 U) to heat-inactivated restriction digestion reactions, and incubating for 1 h at 37°C. Linearized, CIP-treated vectors were purified using a gel extraction kit, or, if previously gel extracted, using a PCR clean up kit (Qiagen). Digested PCR products were either purified using a PCR clean up kit or using a gel extraction kit following manufacturer protocols.

Ligation reactions were set up using various ligand:vector ratios, generally between 3:1 and 10:1 depending on the concentrations and sizes of the vector and insert DNA. Ligations used T4 ligase per manufacturer procedure (NEB) and reactions were overnight at room temperature. A typical ligation reaction contained 1  $\mu\text{L}$  T4 ligase, 1  $\mu\text{L}$  T4 ligase buffer, x  $\mu\text{L}$  linearized vector, and 8-x  $\mu\text{L}$  insert and sterile water to a total volume of 10  $\mu\text{L}$ . Aliquots (2-5  $\mu\text{L}$ ) of ligation mixtures were directly used to transform NEB 5-alpha competent *E. coli* (high efficiency).

#### *Transformation of NEB 5-alpha or ET12567 pUZ8002 Competent E. coli*

An aliquot of competent cells was allowed to thaw on crushed ice, then 2-5  $\mu\text{L}$  of plasmid or ligation mixture was added and the contents gently mixed. The cells were kept on ice for 30 minutes, heated in a hot water bath (42°C) for 30 seconds, then returned to the ice for 5 minutes. The cells were then diluted into 950  $\mu\text{L}$  SOC media (provided with NEB

competent cells) and incubated for 1 h at 37°C with shaking. Aliquots of 50-500 µL were spread onto LB selection plates and the plates were incubated overnight at 37°C.

#### *Plasmid Isolation from E. coli*

Isolation of plasmids was accomplished using EZ-10 spin column plasmid DNA mini-prep kit (BioBasic). *E. coli* bearing the plasmid of interest was grown overnight in 25 mL LB with the appropriate selective antibiotic(s). An aliquot (1-2 mL) was spun down at 12000 rpm, and the supernatant decanted. To the cell pellet was added 200 µL Solution I. Following one minute incubation, 200 µL Solution II was added and the tube gently inverted to mix, and incubated another minute. Solution III (350 µL) was added and the solution was mixed gently and thoroughly, and then incubated again for one minute. The suspension was centrifuged for 5-10 minutes at 12000 rpm. The supernatant was then transferred to an EZ-10 spin column, and centrifuged for 2 minutes at 10000 rpm. The column was then washed twice with 750 µL Wash buffer, discarding the flow through after each step. After the second wash, the column was spun down once again for an additional minute to remove residual wash buffer. Elution buffer (50 µL) was then added to the column and incubated for two minutes at 37 °C. The column flow through was then collected in a clean 1.5 mL Eppendorf tube and stored at -20 °C. To confirm successful ligation and transformation, plasmids were screened by restriction digestion with indicated enzymes to confirm the presence of the insert.

#### *Restriction Digestion*

Restriction digestion of PCR products and plasmids for ligation reactions or colony screening were performed per the manufacturer suggestions (NEB) for buffer selection and



incubation times. Restriction digestions were generally performed at a total volume of 10  $\mu$ L (7  $\mu$ L DNA, 1  $\mu$ L restriction enzyme A, 1  $\mu$ L restriction enzyme B, 1  $\mu$ L commercial buffer) incubated at 37 °C for 2 h. Incubation times were extended or restriction enzyme concentration were increased, as required.

#### *Competent Cell Preparation (E. coli ET12567 pUZ8002)*

*E. coli* ET12567 pUZ8002 was grown overnight in LB with kanamycin and chloramphenicol at 37°C, 250 rpm. The overnight growth was sub-cultured into new LB media with antibiotics, which was grown at 37°C and 250 rpm until an OD<sub>600</sub> of 0.4-0.6 was reached. The sub-culture was transferred to a conical tube on crushed ice and kept for 10 minutes, then pelleted at 4°C, 4000 rpm for 10 minutes. The supernatant was discarded and the cell pellet re-suspended in cold 0.1 M CaCl<sub>2</sub>, then incubated on crushed ice for 20 minutes. The cell suspension was centrifuged as before and the supernatant was discarded. The cell pellet was re-suspended in chilled 0.1 M CaCl<sub>2</sub> and 50  $\mu$ L aliquots were dispensed into chilled micro-centrifuge tubes containing 50  $\mu$ L of cold, sterile 50% glycerol. Frozen competent cells were kept at -70°C until use.

#### *Construction of pKC1139\_jadQ::urdGT2::jadT*

A codon optimized *urdGT2* gene was synthesized by BioBasic Inc. The gene included a His<sub>6</sub>-tag and was flanked by *jadQ* (upstream) and *jadT* with partial *jadU* (downstream). The entire *jadQ::urdGT2::jadT* cassette was provided on a pUC57 vector. The vector was transformed into competent NEB 5-alpha cells, using ampicillin for transformant selection. The pUC19\_*jadQ::urdGT2::jadT* vector was isolated and digested with EcoR1 and HindIII, allowing the 3.1 kb fragment to be gel extracted and purified. The pKC1139 was

similarly digested with EcoR1 and HindIII and subsequently CIP treated. The linearized pKC1139 and *jadQ::urdGT2::jadT* insert were ligated and transformed into NEB 5-alpha competent *E. coli*. Transformant colonies were screened by EcoR1 and HindIII double restriction digest (Figure 23A). Plasmid identity was confirmed by additional restriction digestion (Figure 23B).

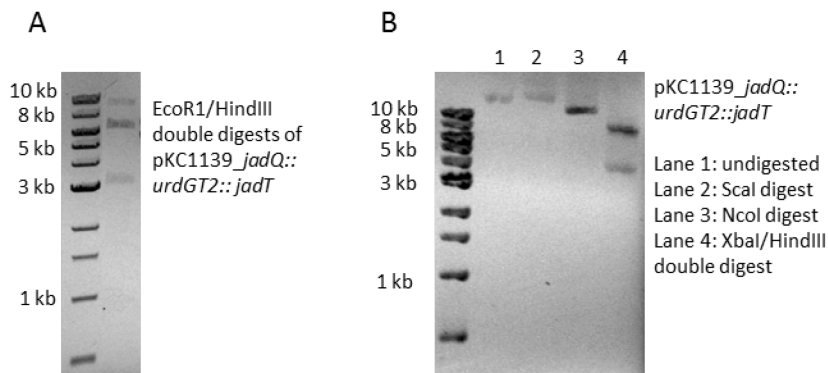


**Figure 23.** pKC1139\_ *jadQ::urdGT2::jadT* construction; (A) EcoR1 and HindIII double restriction digest of transformant colony plasmid isolates; (B) Confirmatory data; undigested plasmid (coiled), ScaI digest (no digestion, coiled), NcoI digest (linearized plasmid), XbaI and HindIII double digest (3.1 kb drop out).

#### *Assembly of pKC1139\_jadQT*

Overlap extension fragments were amplified by PCR from *S. venezuelae* genomic DNA.

The 0.9 kb upstream region *jadQ* was amplified using primers JadQ Fwd OE ( $\Delta$ JadS):

GGTTCTAGACGAATTCCTGGCCGGAGGCCACGGC (XbaI and EcoRI sites underlined) and JadQ Rev OE ( $\Delta$ JadS):

GCCGTCCCTCCGAGGGTTCTCTCTCCGCGG and the 1.0 kb downstream region *jadT*

was amplified using JadT Fwd OE ( $\Delta$ JadS):

CCTCGGAGGGACGGCATGAGGATCCTCGTCACC and JadT Rev OE ( $\Delta$ JadS):

GGTAAGCTTGGGTCACCTGCATGGTCGTCG (HindIII site underlined). The PCR

products were purified by gel extraction. An overlap extension PCR reaction to unify the

*jadQ* and *jadT* flanking regions was performed using the purified PCR products as template DNA with the outermost primers, JadQ Fwd OE ( $\Delta$ JadS) and JadT Rev OE ( $\Delta$ JadS). The resulting 1.9 kb *jadQT* PCR product was ligated into pCK1139 using restriction sites XbaI and HindIII and transformed to NEB 5-alpha competent *E. coli*. Isolated plasmids were screened by XbaI and HindIII double restriction digest (Figure 24).

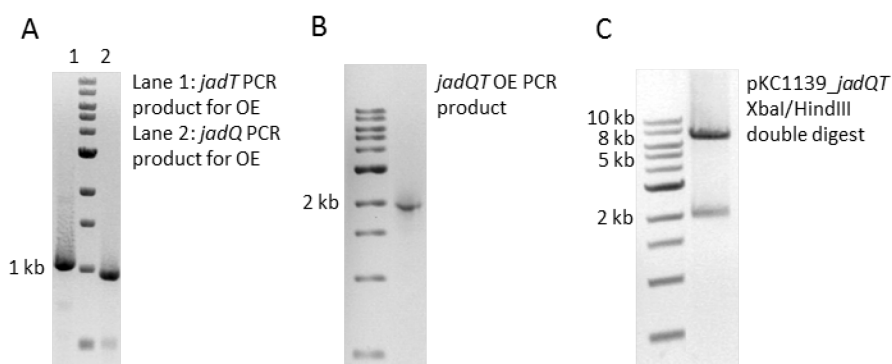


**Figure 24.** Construction of pKC1139\_ *jadQT*; (A) *jadT* and *jadQ* PCR fragments for overlap extension; (B) *jadQT* overlap extension PCR product; (C) XbaI and HindIII double restriction digest of NEB 5-alpha transformant pKC1139\_ *jadQT*.

#### *Construction of pSE34\_urdGT2*

The synthetic *urdGT2* gene was cloned from the pKC1139 *jadQ::urdGT2::jadT* vector, with primers designed to insert a ribosomal binding site (RBS, upstream) and a stop codon ahead of the His<sub>6</sub>-tag (downstream). The gene was amplified using primers pSEurd Fwd: CGTCTAGA*AAGGAGGTACGGACGTGTT*CGCCCTCGCCCCG (XbaI site underlined, RBS italicised) and pSEurd Rev: GGTAAAGCTTTCACGCGAGCTGCTCCAGCGCCG (HindIII site underlined). The 1.1 kb PCR product and pSE34 vector were ligated using HindIII and XbaI digestion sites. Following ligation and transformation to NEB-5 alpha competent *E. coli*, isolated plasmids were screened by HindIII and XbaI double restriction digest.

### *Construction of pSE34\_jadS*

The *jadS* gene was amplified from *S. venezuelae* ISP5230 genomic DNA with primers pSEjadS Fwd: CGTTCTAGACCCCGCCCCGCGGAGAG (XbaI site underlined) and pSEjadS Rev: GGTAAAGCTTCCGCCGGTGACGAGGATCC (HindIII site underlined). The 1.2 kb PCR product and pSE34 vector were ligated using HindIII and XbaI digestion sites. Following ligation and transformation to NEB-5 alpha competent *E. coli*, isolated plasmids were screened by HindIII and XbaI double restriction digest.

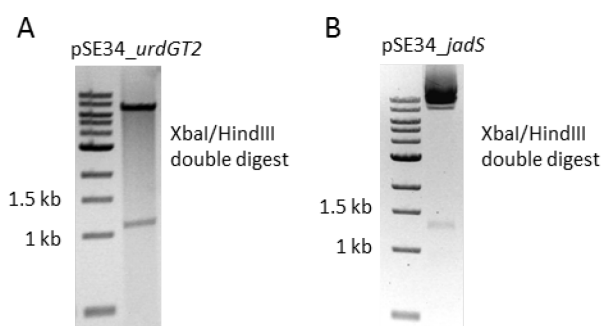


**Figure 25.** (A) XbaI/HindIII double digest of pSE34\_urdGT2; (B) XbaI/HindIII double digest of pSE34\_jadS.

### *Construction of pKC1139\_urdGT2*

The *ermE\** promoter, RBS, and *urdGT2* gene were cloned from the pSE34\_urdGT2 vector with primers ermEpSE Fwd: GATGCTAGCATGAATTCGAGCTCGGTACC (NheI and EcoR1 sites underlined) and pSEurd Rev. The 1.4 kb PCR product and pSE34 vector were ligated using EcoR1 and HindIII digestion sites. Following ligation and transformation to NEB-5 alpha competent *E. coli*, isolated plasmids were screened by EcoR1 and HindIII double restriction digest.

### Construction of pKC1139\_jadS

The *ermE*\* promoter and *jadS* gene were cloned from the pSE34\_urdGT2 vector with primers ermEpSE Fwd and pSEjadS Rev. The 1.5 kb PCR product and pSE34 vector were ligated using EcoR1 and HindIII digestion sites. Following ligation and transformation to NEB-5 alpha competent *E. coli*, isolated plasmids were screened by EcoR1 and HindIII double restriction digest.

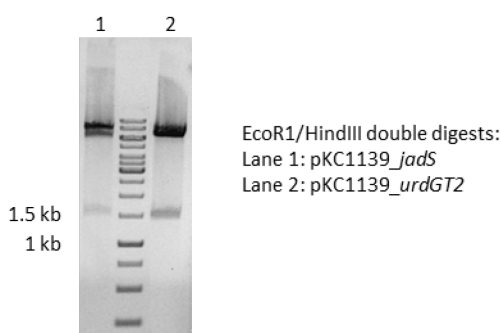


**Figure 26.** EcoR1/HindIII double digests of pKC1139\_urdGT2 and pKC1139\_jadS.

### Construction of pSEE152

The *ermE*\* promoter was amplified from pSE34\_urdGT2 using primers ermE GA Fwd: CTATGACATGATTACGAATTCGATCGATGTCGGACCGGAGTTCGAGGTAC and ermE GA Rev: AGCTTGGGCTGCAGGTCGACTCATATGCGGTACCCCTTCTAGAGGATCCTAC C (KpnI and XbaI sites underlined). The PCR product did not require digestion and was purified by gel extraction. The pSET152 vector was digested with XbaI and EcoRV and purified by gel extraction without CIP treatment. The vector and ligand were joined by Gibson Assembly (GA), performed using the NEB Gibson Assembly Kit per the manufacturer procedure. The linearized vector (5  $\mu$ L) and PCR product (2  $\mu$ L, 5:1 ratio) were combined in 10  $\mu$ L GA Master Mix (2x) and sterile water was added to a total volume

of 20  $\mu$ L. The reaction was heated at 50°C for 15 minutes, then allowed to cool before being directly used to transform NEB 5-alpha competent *E. coli*. Isolated plasmids were screened by KpnI digestion in addition to XbaI and XhoI double digestion.

#### *Construction of pSEE152\_urdGT2*

The *urdGT2* gene was cloned from pSE34\_urdGT2 with primers pSEurd Fwd: CGTCTAGA*A*GGAGGTACGGACGTGTTTCGCCCTCGCCCCG (XbaI site underlined, RBS italicied) and pSETurd Rev: GTCATATGGGTACCCGCGAGCTGCTCCAGCGCCG (NdeI and KpnI sites underlined). The 1.1 kb PCR product and pSEE152 vector were ligated using XbaI and KpnI digestion sites. Following ligation and transformation to NEB-5 alpha competent *E. coli*, isolated plasmids were screened by XbaI and KpnI double restriction digest

#### *Construction of pSEE152\_jadS*

The *jadS* gene was cloned from pSE34\_jadS with primers pSEjadS Fwd: CGTTCTAGACCCCGCCCCGCGGAGAG (XbaI site underlined) and pSETjadS Rev: GTCATATGGGTACCCGCGGTGACGAGGATCC (NdeI and KpnI sites underlined). The 1.2 kb PCR product and pSEE152 vector were ligated using XbaI and KpnI digestion sites. Following ligation and transformation to NEB-5 alpha competent *E. coli*, isolated plasmids were screened by XbaI and KpnI double restriction digest.

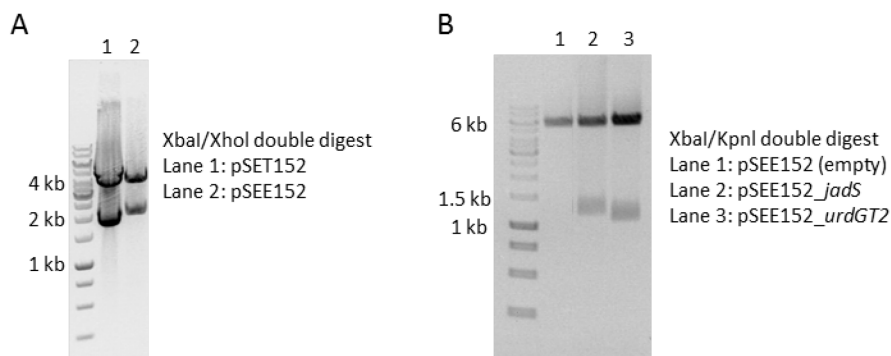


**Figure 27.** (A) XbaI/XhoI double digest of pSET152 (1.8 kb dropout) and pSEE152 (2.1 kb dropout); (B) XbaI/KpnI double digest of pSEE152 plasmids.

### 3.6.3 Mutant Preparation

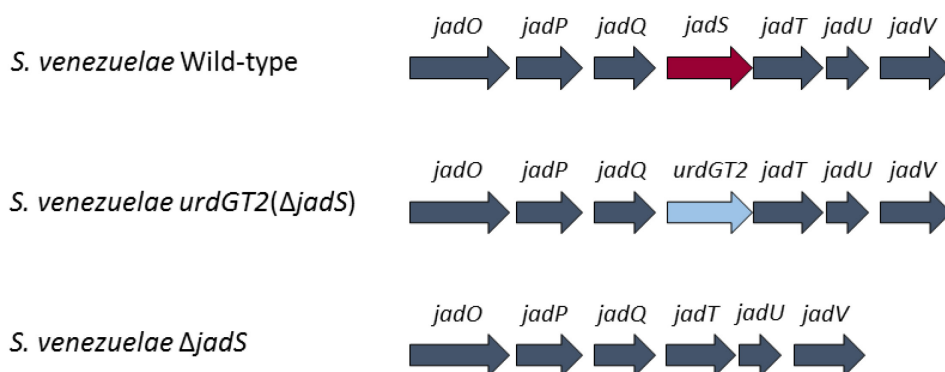


**Figure 28.** L-digitoxose biosynthetic genes of *S. venezuelae* wild-type, *urdGT2(ΔjadS)*,  $\Delta$ *jadS*.

#### *E. coli*-*Streptomyces* Conjugation

*E. coli* ET12567 pUZ8002 with the desired vector (e.g. pKC1139\_ *jadQ*::*urdGT2*::*jadT*) was inoculated into LB media supplemented with apramycin, kanamycin and chloramphenicol and grown overnight. An aliquot from an overnight culture was sub-cultured into new LB media with selective antibiotics. The sub-culture was grown 37°C and 250 rpm until an OD<sub>600</sub> of 0.4-0.6 was reached, the culture was transferred to a conical tube and centrifuged (3 min, 5000 rpm). The supernatant was decanted, and the cell pellet re-suspended in LB without antibiotics, and pelleted again. This wash procedure was

repeated twice, after which the pellet was suspended in 500  $\mu$ L LB. Concurrently, a spore solution of *Streptomyces venezuelae* ISP5230 was prepared as previously described. The solution was diluted with sterile water to an OD<sub>450</sub> of 0.03 and heated at 50°C for 10 minutes. The *Streptomyces* spore suspension was then allowed to cool to room temperature, then 500  $\mu$ L was added to the 500  $\mu$ L of the *E. coli* solution and gently mixed. The solution was then centrifuged at 4°C, 13000 rpm for 3 minutes. The supernatant was removed and the cell pellet was re-suspended in LB without antibiotics and were plated directly ( $10^0$ ) or diluted in LB ( $10^{-1}$ ). These solutions (100  $\mu$ L) were plated on MS-agar and transferred to a 30°C incubator. After 18-24 h incubation, a soft nutrient agar overlay containing nalidixic acid and apramycin was applied to each of the plates. Once the agar set, the plates were returned to 30°C.

#### Homologous Recombination (Double Crossover) Mutant Selection

Exconjugant *Streptomyces* colonies were patched to MYM-agar with nalidixic acid and apramycin and grown at 37°C to select for single crossover mutants. The single crossover mutants were patched to MYM with apramycin (MYM-Apr) and grown at 30°C. Colonies were further patched to MYM and grown at 30°C and retained colonies were patched twice more after spore growth at each step. Colonies were patched to MYM-Apr and grown at 30°C to select out which colonies retained single crossover. Colonies sensitive to apramycin (thereby likely to have undergone a double crossover recombination event) were used to generate spore solutions, which were streaked on MYM for single colonies. Single colonies were screened by colony PCR.



The *S. venezuelae* *urdGT2*( $\Delta$ *jadS*) mutant was confirmed by colony PCR using primers *urdgt2\_spec* Fwd: GGTGGTACCCCAGGAGGAGAGAAC and *urdgt2\_spec* Rev: GGTGGTCTCCGCGTCGAG. The *S. venezuelae*  $\Delta$ *jadS* mutant was confirmed colony PCR with primers *JadQ* Fwd OE ( $\Delta$ *JadS*) and *JadT* Rev OE ( $\Delta$ *JadS*).

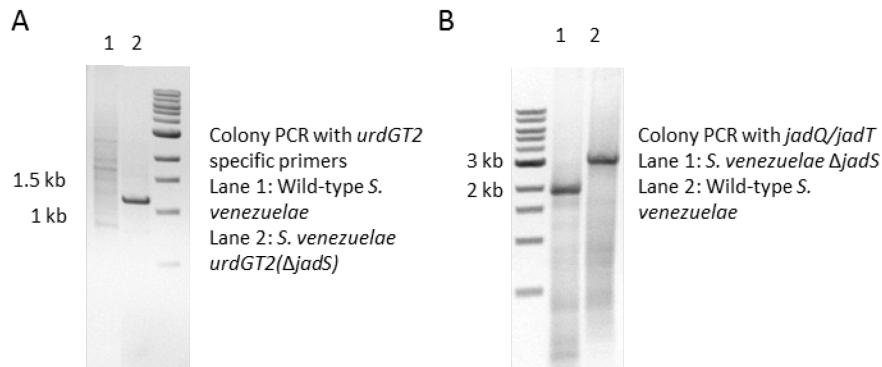


**Figure 29.** (A) Colony PCR of wild-type and *urdGT2*( $\Delta$ *jadS*) *S. venezuelae*; (B) Colony PCR *S. venezuelae*  $\Delta$ *jadS* and wild-type.

#### Integration (Single Crossover) and Replicative Plasmid Mutant Selection

Exconjugant *Streptomyces* colonies were patched to MYM-agar with nalidixic acid and apramycin and grown at 30°C. Retained colonies were used to generate spore solutions, which were streaked on MYM for single colonies. Single colonies were grown in liquid culture (MYM) for genomic DNA extraction for PCR screening. Primers flanking the insert or the *permE*\* were used to identify the desired mutants.

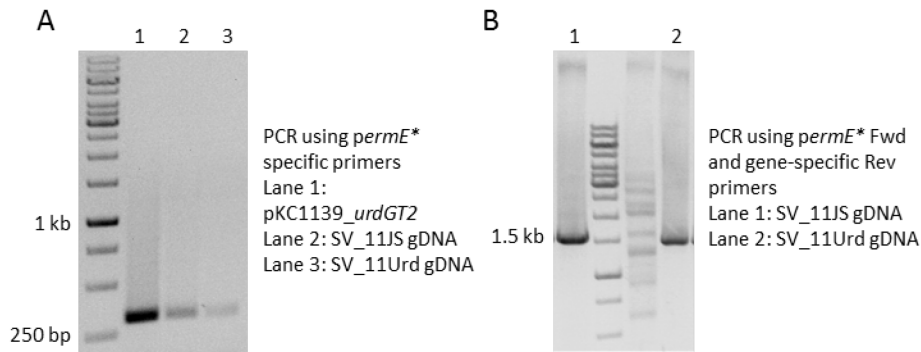


**Figure 30.** (A) PCR of pKC1139\_urdGT2, and gDNA from the SV\_11JS and SV\_11Urd transformants, amplified using *permE\** primers; (B) PCR of gDNA from the SV\_11JS and SV\_11Urd transformants, amplified using *permE\** Fwd primer and gene-specific Rev primer.

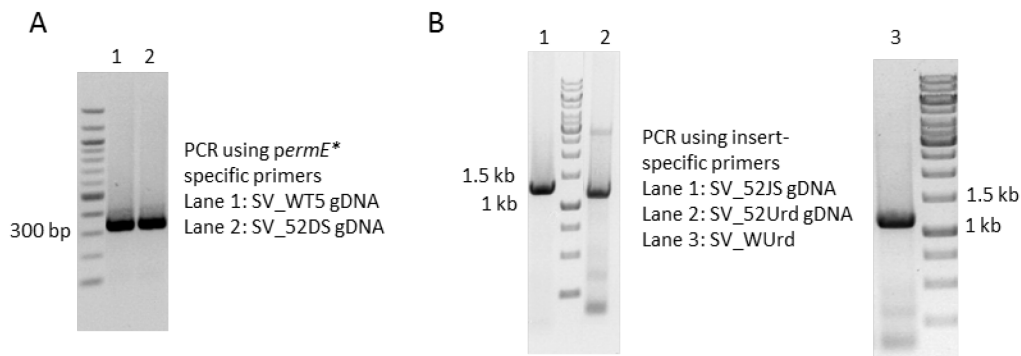


**Figure 31.** (A) PCR of gDNA from the SV\_WT5 and SV\_52DS transformants, amplified using *permE\** primers; (B) PCR of gDNA from the transformants SV\_52JS, SV\_52Urd, and SV\_WUrd, amplified using insert-specific primers.

### *Streptomyces* Protoplast Preparation and Transformation

Protoplast transformation procedures were adapted from Vining.<sup>115</sup> A 30 h culture of *S. venezuelae* ISP5230 in YEME was harvested by centrifugation at 4°C, 3000 rpm for 10 minutes. The cells were washed with 1.5 mL modified L buffer, centrifuged again, then the supernatant was discarded and the pellet was re-suspended in 1 mL modified Buffer L (with 3 mgmL<sup>-1</sup> lysozyme), followed by one hour incubation at 30°C. The mixture was gently agitated twice throughout incubation. Then 1.5 mL modified P buffer was added and the mixture was incubated a further 15 minutes at room temperature. The protoplast

solution was filtered through sterile cotton wool into a micro-centrifuge tube then the protoplasts were collected by centrifugation at 3000 rpm at 4 °C, 10 min. The supernatant was discarded and the protoplasts were re-suspended in 100 µL modified P buffer.

Prior to use in protoplast transformations, the incoming vector (pSE34\_urdGT2 or pSE34\_jadS) was passed through *E. coli* ET12567 pUZ80002 to generate non-methylated plasmid for introduction to *S. venezuelae* and diluted to a concentration of 10-15µgmL<sup>-1</sup> (based on A<sub>260</sub> values) into TE buffer. The plasmid (20 µL) was added to the protoplast suspension, followed immediately by 500 µL modified T buffer prepared with 25% PEG 1000, and gently pipetted once to mix. The mixture rested for 3 minutes, then was diluted with 1.5 mL modified P buffer, centrifuged at 3000 rpm at 4 °C, 10 min. The supernatant was discarded and the protoplasts re-suspended in 200 µL modified P buffer. Aliquots (50 and 150 µL) of this solution were spread on modified R5N agar plates. The plates were incubated overnight at 30°C, and then a soft nutrient agar overlay containing 50 µg/mL thiostrepton (tsr) was applied to the plates.

Exconjugants were visible within three days. Colonies were patched to MYM containing 25 µg/mL tsr and incubated at 30°C. Colonies were patched twice more to MYM-tsr before sporulation was observed. Spores were isolated and streaked for single colonies, which were subsequently patched for confluent growth on MYM-tsr. Potential transformants were screened by colony PCR using insert-specific primers. Colonies were then cultured overnight in 25 mL MYM-tsr for genomic DNA isolation, which was used to screen for presence of the plasmid by PCR. However, no evidence obtained to support that the tsr-

resistant colonies carried the vectors of interest (pSE34\_urdGT2 or pSE34\_jadS). The method was not further investigated.

### 3.6.4 Jadomycin Production Conditions

Jadomycin productions were performed and monitored as described in 2.5.2.

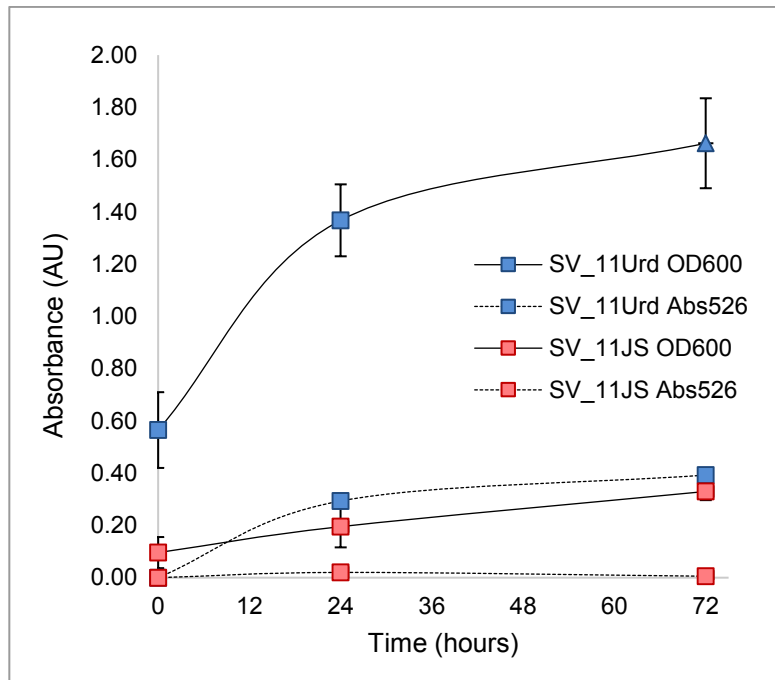


**Figure 32.** JdG and JdDS productions of pKC1139-derived *urdGT2* and *jadS* complemented *S. venezuelae*  $\Delta$ *jadS*. (SV\_11Urd and SV\_11JS, respectively).

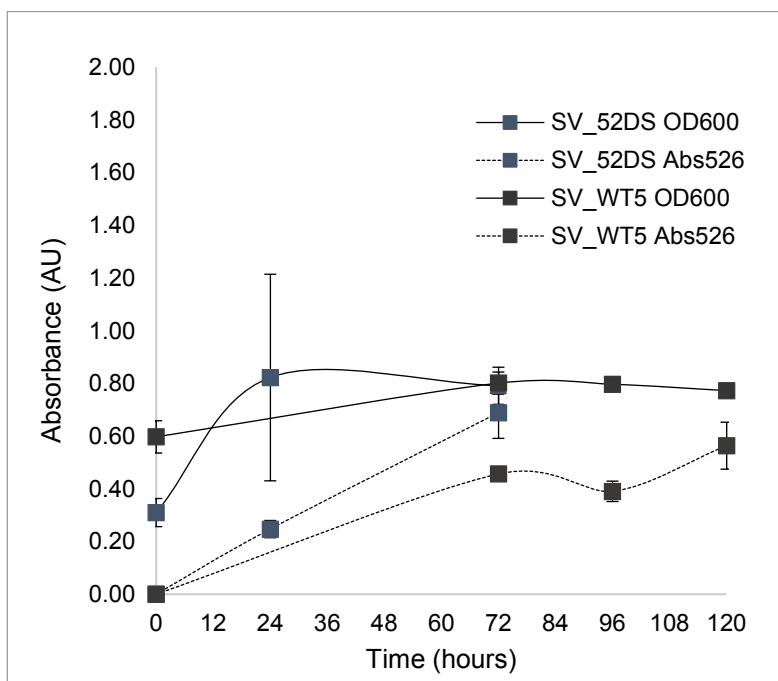


**Figure 33.** JdG productions of pSEE152 (empty) control strains of *S. venezuelae* wild-type (SV\_WT5) and *S. venezuelae*  $\Delta$ jadS SV\_52DS.

### 3.6.5 Jadomycin Purification Methods

Jadomycin productions were purified as described in 2.5.3.

### 3.6.6 Extract Characterization

Jadomycin production extracts were characterized as described in 2.5.4.

For low resolution LC-MS/MS, the instrument was used in positive mode (ESI+) for acquisition of jadomycin data. Enhanced product ionization (EPI) was performed with scans conducted over a range of 100-900  $m/z$  scanning for  $[M+H]^+$  and the appropriate jadomycin fragmentation. Precursor ion scans with parent ion  $[M+H]^+$   $m/z$  306 or 436 were also performed. Spectra were analyzed using Analyst software version 1.4.1 (Applied Biosystems).

## CHAPTER 4: EXPLORATION OF SILENT BIOSYNTHETIC GENE CLUSTERS

### 4.1 Cryptic and Silent Biosynthetic Gene Clusters

Natural products are chemical structures produced by an organism outside of primary metabolism, and are therefore also termed secondary metabolites. Largely, the genes responsible for producing these secondary metabolites are clustered together in the genome, forming biosynthetic gene clusters (BGCs) that vary from several genes to over 100 kb<sup>122</sup> to enjoy the evolutionary benefits of co-transcription and horizontal gene transfer.<sup>13</sup> Analysis of the bacterial genomes of known producers of one or several natural products has demonstrated a vast and diverse catalogue of BGCs which are un- or under-expressed in laboratory conditions, termed *silent* BGCs.<sup>123</sup> As DNA sequencing technologies have improved over the past decade, the number of available genome sequences and assemblies has risen exponentially and with them the number of uncharacterized silent BGCs.<sup>124</sup>

There are a host of approaches and methods to switching on the expression of these silent BGCs, many of which have been compiled and described in recent reviews.<sup>7,125,126</sup> Methods which target specific BGCs, including manipulation of pathway-specific (cluster-situated) regulators, require identification of specific genes for overexpression or repression and *in silico* genome mining tools specific to natural product BGCs such as the previously mentioned antiSMASH,<sup>23</sup> as well as PRISM,<sup>127</sup> ClusterFinder,<sup>123</sup> and IMG-ABC<sup>128</sup> aid in the identification of these targets. These programs analyze sequenced and annotated genomes for conserved sequences which correlate to secondary metabolite biosynthetic proteins clustered with genes for regulatory, resistance, and tailoring proteins.<sup>7</sup> Further, these tools can compare the sequence known clusters and sub-cluster

for homology to identify known clusters or to predict the potential structure for the natural product produced by the coded enzymes, making them powerful tools for novel natural product discovery.<sup>9</sup> A central and comprehensive resource for these databases and tools, the Secondary Metabolites Bioinformatics Portal, has recently been launched.<sup>129</sup> As the throughput rates of bacterial genome sequencing are increasing with advanced technologies, more researchers are likely to turn to genomic based natural product discovery projects, and this portal will be an invaluable tool.<sup>124</sup>

Upon selection of priority or target gene clusters with predicted novel chemistry, there are a multitude of approaches to activate the expression of these gene clusters, the predominant methods have been detailed in recent reviews.<sup>7,11,126</sup> The methods can be broadly divided into two categories, non-genetic and genetic.<sup>7</sup> Non-genetic methods may include varying culture conditions (temperature, nutrients, pH) or adding sub-inhibitory concentrations of antibiotics<sup>130</sup> to imitate stress conditions, adding histone deacetylases to induce increased transcription, or adding stressors which mimic cell signaling molecules in secondary metabolite regulation. Genetic methods are generally variable techniques to overexpress structural or regulatory genes (activators) in the cluster, but also includes deletion of regulatory genes (repressors).<sup>126</sup>

The Jakeman group has worked extensively with *S. venezuelae* ISP5230 for over a decade investigating the biosynthetic potential of the strain with the jadomycin family of natural products.<sup>19-21</sup> *S. venezuelae* is a model strain of *Streptomyces*, exhibiting facile growth and sporulation and is recognized as a potentially valuable host strain for heterologous production of natural products,<sup>10,24,131,132</sup> as such it's genome has been sequenced.<sup>22</sup> These

qualities made *S. venezuelae* a good candidate for exploration and activation of silent BGCs. Herein, we report the selection and putative activation of a BGC by overexpression of a pathway-specific activator.

## **4.2 Regulation of Biosynthesis**

There are complex regulatory systems for natural product biosynthesis, which may be co-regulated with morphological development and differentiation,<sup>14</sup> quorum sensing, environmental stress conditions, or nutrient availability.<sup>15</sup> The regulatory elements in biosynthetic gene clusters may be pathway-specific regulators, which act only upon neighboring genes, or pleiotropic (global or high-level) regulators, which may act upon multiple gene clusters.<sup>14,15</sup> In *Streptomyces*, most pleiotropic regulators are part of two-component systems which regulate secondary metabolite production with nutrient availability and morphological differentiation, while most pathway specific regulators are transcription factors which bind DNA to directly affect gene expression.<sup>16</sup>

Transcription factors are identified by the presence of a DNA-binding domain, often a helix-turn-helix domain, and a ligand binding domain and are categorized based on sequence- and structural-homology with similar proteins.<sup>11</sup> Transcription factors can act as activators or repressors of their target genes. Simple activators will act by stabilizing the initial RNA polymerase–promoter complex or by accelerating the transition to the open complex (where the promoter DNA is unwound and the template strand is complexed with the RNA polymerase active site), but transcriptional activation by these proteins can be much more complex.<sup>133</sup> Repressors may act by binding the promoter region of a gene,



preventing an activator or RNA polymerase from binding; repressors may also bind downstream of a promoter region, preventing transcriptional elongation.<sup>15</sup>

Identification and manipulation of pathway-specific regulatory genes has been demonstrated in the literature as a successful method to activate a targeted silent gene cluster and obtain access to novel natural products.<sup>134-139</sup> There are two main families of pathway-specific activators in *Streptomyces*: SARPs (*Streptomyces* antibiotic regulatory proteins) family and the LALs (large ATP-binding regulators of the LuxR family).<sup>134</sup> The SARP family are widely recognized as valuable pathway-specific regulators of antibiotic production in *S. coelicolor*, but there is an increasing assembly of LAL family proteins as PKS transcriptional regulators.<sup>122</sup>

#### **4.2.1 LuxR Family**

Certain families of transcription factors are more associated with secondary metabolite biosynthesis, however, the regulatory protein cross-talk makes it difficult to definitively indicate the behavior of a given family.<sup>11</sup> For the purpose of selecting target gene clusters for exploration, one family of activator proteins which has promising literature precedence was chosen for overexpression, the LuxR family.

The LuxR family of regulatory proteins is primarily comprised of proteins which are typically 250 residues and are involved in quorum sensing and pathway specific activation of secondary metabolite production.<sup>15,140</sup> However, a subset of large (900 residues), atypical LuxR proteins which bind ATP (LAL family LuxR proteins) are more highly correlated to secondary metabolite production. LAL family members are involved in the positive control of natural products such as avermectin, rapamycin and pikromycin.<sup>141</sup>

LAL regulators were first identified in proteobacteria,<sup>142</sup> but have become largely associated with natural product regulation.<sup>141</sup> These large proteins have a nucleotide triphosphate binding motif (N-terminus) and a helix-turn-helix motif characteristic of the LuxR family of DNA-binding proteins (C-terminus).<sup>15,142</sup> The overexpression of these LAL protein homologues has been used to improve the production of known natural products as well as induce the production of novel natural products, including the ansatrienins.<sup>143,144</sup>

**Table 16.** Collection of LAL-family activators involved in positive secondary metabolite regulation.

Strain	Gene	Natural Product
<i>Streptomyces natalensis</i>	<i>pimR</i> <sup>145</sup>	pimaricin
<i>Streptomyces</i> sp. CK4412	<i>tmcN</i> <sup>146</sup>	tautomycetin
<i>Streptomyces avermitilis</i>	<i>aveR</i> <sup>147</sup>	avermectin
<i>Streptomyces venezuelae</i> ATCC 15439	<i>pikD</i> <sup>148</sup>	pikromycin
<i>Streptomyces coelicolor</i>	<i>sco0877</i> , <i>sco7173</i> <sup>149</sup>	actinorhodin
<i>Streptomyces hygroscopicus</i>	<i>rpH</i> <sup>150</sup>	rapamycin
<i>Streptomyces tsukubaensis</i> NRRL 18488	<i>fkbN</i> <sup>151</sup>	FK506 (Tacrolimus)
<i>Saccharothrix aerocolonigenes</i> ATCC 39243	<i>rebR</i> <sup>152,153</sup>	rebeccamycin
<i>Streptomyces</i> sp. XZQH13	<i>astG1</i> <sup>144</sup>	ansatrienins
<i>Streptomyces hygroscopicus</i> JCM4427	<i>gell4</i> , <i>gell7</i> <sup>154</sup>	geldanamycin
<i>Streptomyces noursei</i>	<i>nysRI</i> , <i>nysRIII</i> <sup>155</sup>	Nystatin
<i>Streptomyces</i> sp. LZ35	<i>hgcI</i> <sup>143</sup>	Hygrocin
<i>Streptomyces wuyiensis</i> CK-15	<i>wysR</i> <sup>156</sup>	wuyiencin
<i>Amycolatopsis orientalis</i>	<i>eco-orf4</i> <sup>157</sup>	ECO-0501
<i>Streptomyces ambofaciens</i> ATCC 23877	<i>samR084</i> <sup>136</sup>	stambomycin
<i>Streptomyces bingchenggensis</i>	<i>milR</i> <sup>112</sup>	milbemycin

### 4.3 Cryptic Gene Cluster Selection

Within the thirty-one BGCs identified by antiSMASH (Table 1), six putative LuxR proteins were included (Table 17). Four of the LuxR genes belong to the LAL subfamily of activators, and within those four, three were contained in BGC with associated natural products. In fact, during the course of this research, the overexpression of the LAL activator in Cluster R3 was found to aid in the isolation of venemycin.<sup>25</sup>

**Table 17.** LuxR genes identified within the *S. venezuelae* BGC

Cluster	Locus Tag	Residues
Cluster R2	SVEN_RS01305	929*
Cluster R3	SVEN_RS36965	949*
Cluster R4	SVEN_RS02605	1015*
Cluster R6	SVEN_RS03645	1065*
Cluster R17	SVEN_RS26885	222
Cluster R22	SVEN_RS30835	203

\*Denotes LAL-family activator

Notably, R6 contains a sub-cluster with homology to the indolocarbazole producing genes in in staurosporine,<sup>158</sup> K-252A,<sup>159,160</sup> rebeccamycin,<sup>152,153</sup> and AT2433<sup>161</sup> biosynthesis. The indolocarbazoles are potent protein kinase inhibitors with anticancer applications.<sup>162</sup> Cluster R6 (Figure 34) was therefore selected as the target. The entirety of Cluster R6 genes are described in Table 18.

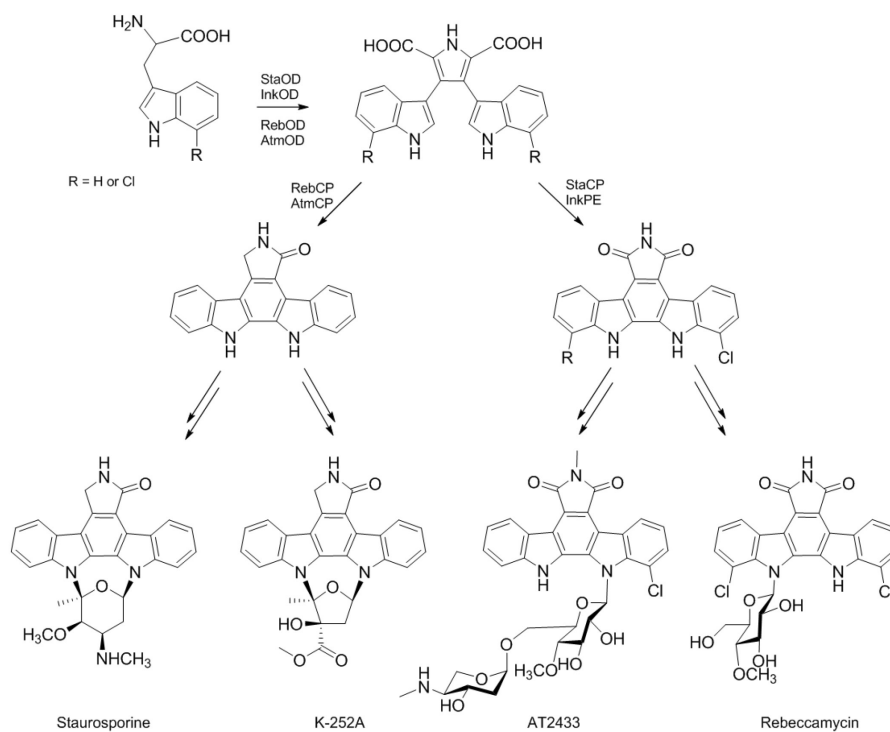
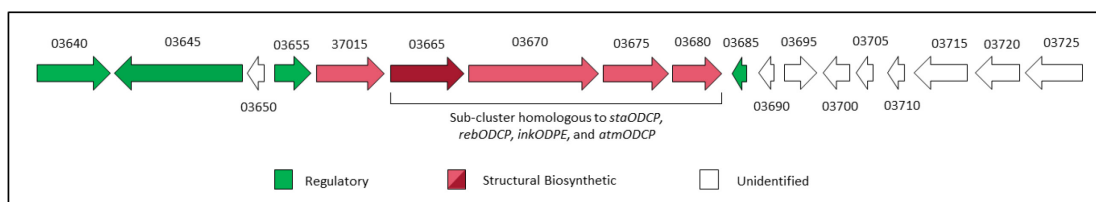


**Figure 34.** (Inset) organization of the genes in Cluster R6; biosynthesis of indolocarbazoles from tryptophan.

**Table 18.** Cluster R6 genes and putative functions.

<b>Locus Tag</b>	<b>Amino Acids</b>	<b>Annotation</b>
SVEN_RS03640	616	Serine/threonine protein kinase
SVEN_RS03645	1065	HTH transcriptional activator
SVEN_RS03650	144	DUF2000 domain-containing family
SVEN_RS03655	301	AraC family transcriptional regulator
SVEN_RS37015	567	2-polyprenyl-6-methoxyphenol hydroxylase
SVEN_RS03665	605	Tryptophan-2 monooxygenase
SVEN_RS03670	1068	VioB polyketide synthase
SVEN_RS03675	545	FAD Binding Monooxygenase
SVEN_RS03680	415	CYP P450
SVEN_RS03685	115	ArsR family Transcriptional Regulator
SVEN_RS03690	128	Anti-sigma factor antagonist
SVEN_RS03695	273	NADP Oxidoreductase
SVEN_RS03700	222	Isochorismatase (cysteine hydrolase superfamily)
SVEN_RS03705	144	Anti-sigma factor antagonist
SVEN_RS03710	146	Membrane protein (NTF2-like superfamily)
SVEN_RS03715	443	DUF418 domain-containing membrane protein
SVEN_RS03720	373	Exo-alpha sialidase
SVEN_RS03725	470	M24 family peptidase

#### 4.4 Cryptic Gene Cluster Activation

##### 4.4.1 Generation of pLuxR Mutant of *S. venezuelae*

An overexpression mutant was prepared by inserting the strong *ermE\** constitutive promoter (*permE\**)<sup>108</sup> as well as a short ribosomal-binding site (RBS)<sup>134</sup> immediately upstream of the LuxR activator (SVEN\_RS03645). Mutant preparation was facilitated by the *Streptomyces/E. coli* conjugative vector pKC1139<sup>104</sup> containing a pLuxR cassette, comprised of the *permE\** and RBS flanked by a portion of SVEN\_RS03645 (upstream) and SVEN\_RS03650/5 (downstream) (Figure 35). The vector was transformed into

ET12567/pUZ8002, which was then used to conjugate with the wild-type *S. venezuelae*. *S. venezuelae* single- and double-crossover mutants were selected using apramycin and incubation temperature. Desired homologous recombination mutants were screened by PCR for amplicons containing the *permE\** (+300 bp) (Figure 36).

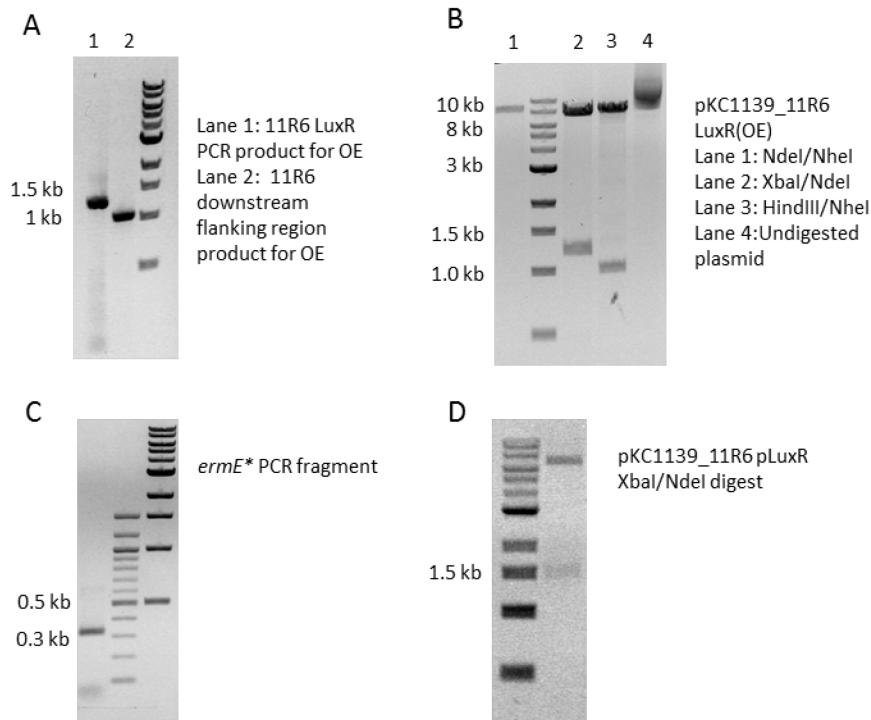


**Figure 35.** Vector construction; (A) R6 LuxR fragment and downstream flanking region PCR fragments for overlap extension; (B) digestions of NEB 5-alpha transformant pKC1139\_R6 LuxR(OE) to confirm plasmid identity; (C) *ermE\** PCR fragment from pSE34; (D) XbaI and NdeI double digestion of NEB 5-alpha transformant pKC1139\_R6 pLuxR to confirm plasmid identity.

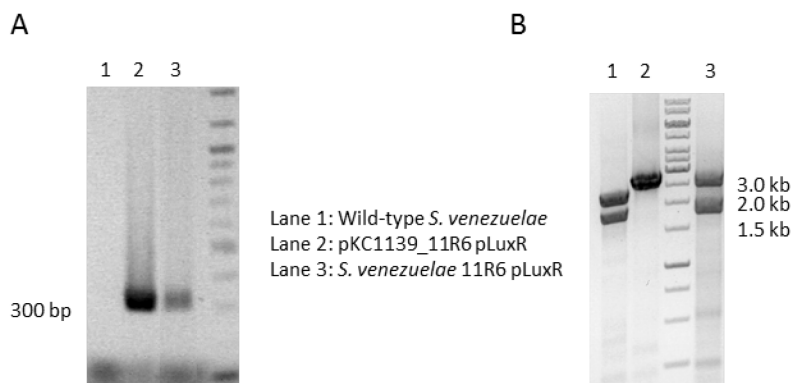


**Figure 36.** Mutant confirmation; (A) PCR using *permE\** primers; (B) PCR using LuxR cassette flanking primers.

#### 4.4.2 Evaluation of Natural Product Biosynthesis

With the *S. venezuelae* pLuxR mutant in hand, a series of growth conditions and media were explored, including those used for jadomycin and the indolocarbazole rebeccamycin production, to evaluate the production of novel natural products. Herein, will focus on “rebeccamycin fermentation media” (RFM) with DL-tryptophan supplementation post inoculation.

Initial productions with RFM were performed as paired *S. venezuelae* wild-type (WT)/R6 pLuxR mutant (R6) cultures, then were further stratified as non-supplemented and supplemented with DL-tryptophan (DL-W). These productions were extracted with ethyl acetate and the crude extracts were analyzed by TLC and HPLC. The DL-W supplemented culture of R6 displayed a remarkably different TLC from both the supplemented WT and the non-supplemented R6, suggesting R6 had an altered biosynthetic profile and that it involved the metabolism of DL-W (Figure 37).

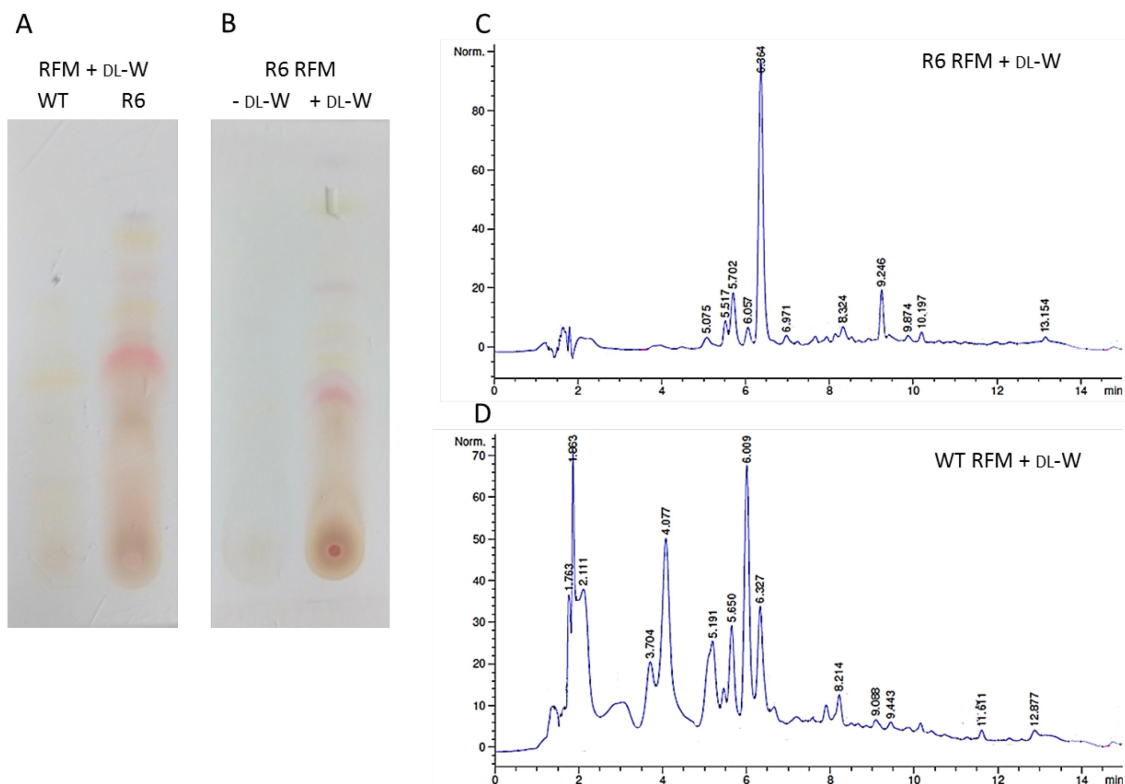


**Figure 37.** Comparative analysis of R6 and WT paired productions; (A) TLC of WT and R6 extract from DL-W supplemented productions; (B) TLC of R6 extract from non-supplemented and DL-W supplemented productions; (C) HPLC trace of R6 extract from DL-W supplemented production; (D) HPLC trace of WT extract from DL-W supplemented production.

Productions using R6 were repeated with RFM, comparing DL-W supplementation at 0 h or 24 h to the established 48 h, but no discernable difference was observed between the three conditions. To scale-up and optimize extractions, the next productions were executed as 1.5 L RFM supplemented with the adsorbent resin Diaion HP20 (5% w/v), which was collected, washed, and extracted with methanol and then ethyl acetate at the end of the production. From these crude production extracts, several compounds were identified as target for isolation and characterization based these HPLC traces.

The first target compound appeared in the HPLC trace of R6 extract but not the WT, with a strong UV absorbance and a retention time of 6.3 minutes (Figure 37). Upon isolation of



the compound through hexanes/methanol extraction and several iterations of normal phase chromatography, it was identified as tryptophol, a derivative of tryptophan which has been previously reported from *Streptomyces* species<sup>163,164</sup> in indole-type natural product isolation studies (Figure S60). Spiked HPLC experiments with commercially sourced tryptophol confirmed the identification (Figure S62).

The next target compound also appeared in the HPLC trace of R6 extract but not the WT, with a retention time of 9.2 minutes (Figure 37). This peak was partially purified by hexanes/methanol extraction and normal phase chromatography. The NMR spectrum contained an aromatic motif suggestive of an indole-containing natural product, but the singlet at 7.1 ppm correlated to an indole ring H2 (Figure S63), which would not be present in an indolocarbazole scaffold. The compound was presumptively identified as another tryptophan metabolite, and therefore this compound was not pursued further.

To combat the difficulties observed in target selection and isolation based on UV intensity (by TLC or HPLC), small-scale RFM productions were repeated using DL-5-fluorotryptophan (5F-W) supplementation as a probe to determine the metabolic fate of tryptophan in both *S. venezuelae* WT and R6 with <sup>19</sup>F NMR spectroscopy. Precursor-directed biosynthesis of fluorinated rebeccamycin analogues by including DL-5-fluorotryptophan or DL-6-fluorotryptophan in the production media had been previously reported,<sup>165</sup> so enzyme flexibility towards these substrates was not anticipated as a limitation. Both the ethyl acetate (EtOAc) extract and water layer of the 5F-W supplemented productions were analyzed by <sup>19</sup>F NMR spectroscopy (Figure 38, Figure S61). Based on the spectra, the 5-FW had been metabolized similarly in the WT and R6, generating predominant peaks at 124.8 ppm in the water layers and 131.5 ppm in the

EtOAc extracts. Minor constituents generally correlated between the WT and R6, with some small peaks appearing only in the R6 crude material (110.2, 115.6, 119.4, 120.5, 121.3, 124.7, 128.1, 132.9 ppm, visible in Figure S64).

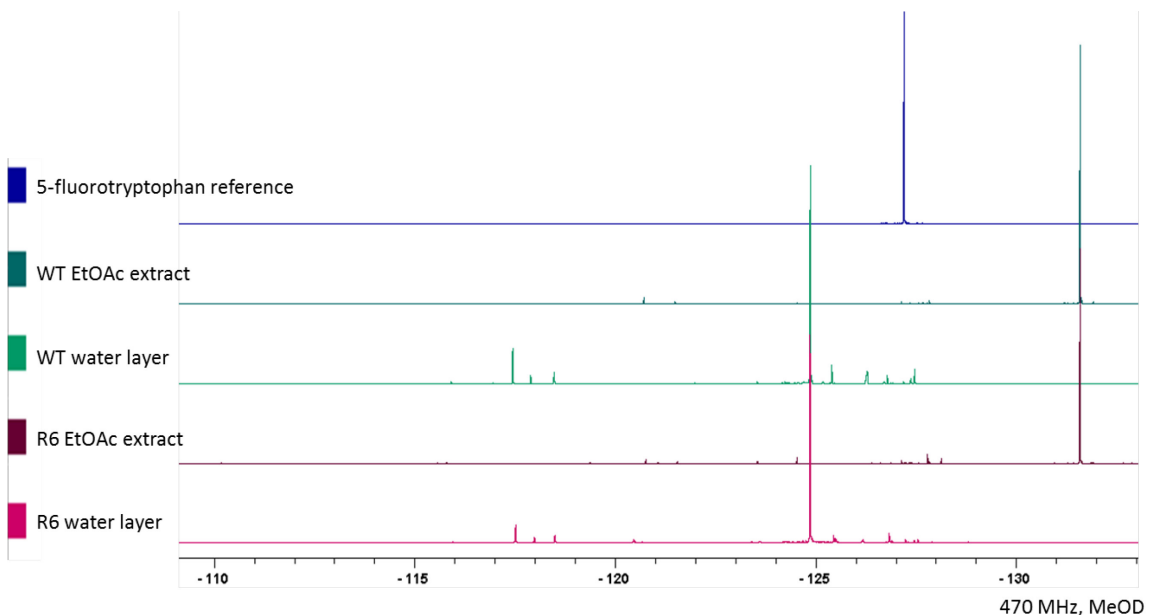


**Figure 38.** NMR spectra of RFM productions with 5F-W supplementation ( $^{19}\text{F}$ :470 MHz).

Throughout the evaluations of R6 and WT in RFM media, the formation of chloramphenicol or jadomycin were not evident by HPLC and UV-Vis spectroscopy. To determine if the constitutive overexpression of the R6 LuxR activator had abolished production of these established *S. venezuelae* natural products, jadomycin productions were performed using D-serine and L-phenylalanine to affect the production of JdDS and JdF, respectively. Additionally, the productions were divided into replicates with ethanol shock (E+), to induce jadomycin (Jd) production, and without ethanol shock (E-), to encourage chloramphenicol (Cam) production.<sup>117</sup> The production material was filtered and passed through a pre-conditioned silica-phenyl column (2 g), which was then rinsed with water and eluted with methanol. This crude material was analysed by HPLC to identify chloramphenicol and the jadomycins (Figure 39). The HPLC traces indicated that JdDS and JdF were produced in the WT and R6 *S. venezuelae* strains and that omitting the ethanol shock caused the expected reversion to chloramphenicol biosynthesis, with reduced jadomycin production observed. There were no peaks observed in the R6 crude

which were not in the WT crude HPLC traces, signifying that the regulation and biosynthesis of the major natural products Cam and Jd take priority under conditions favourable for their production.

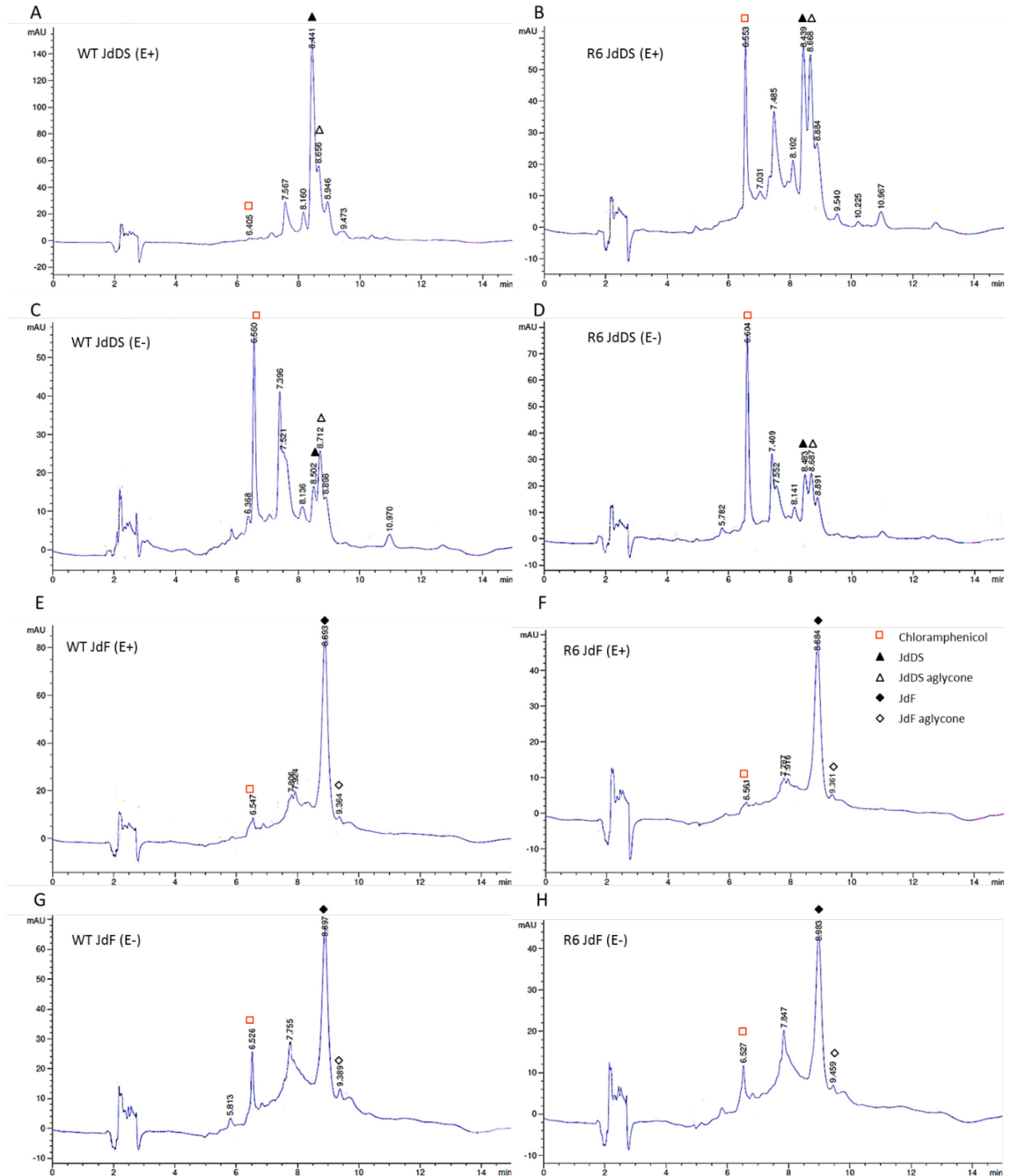


**Figure 39.** Jadomycin production crude material HPLC traces. JadDS productions with ethanol shock from (A) WT and (B) R6; JadDS productions without ethanol shock from (C) WT and (D) R6; JadG productions with ethanol from (E) WT and (F) R6; JadG productions without ethanol from (G) WT and (H) R6.

## 4.5 Conclusions

A silent *Streptomyces venezuelae* gene cluster was studied for its ability to produce novel natural products. Cluster R6 was selected for activation as it contained a putative LAL family activator and an indolocarbazole biosynthetic sub-cluster. The LAL activator was constitutively overexpressed through insertion of an *ermE*\* promoter ahead of the gene by homologous recombination. The mutant *S. venezuelae* strain was cultured in several media types and supplementation conditions and the resultant extracts were analyzed for novel natural products.

While the changes to the biosynthetic profile were apparent in the overexpression mutant, production of a novel natural product was not observed in appreciable quantities. The major metabolites observed were derivatives of tryptophan, but there was no evidence of indolocarbazole formation under the studied conditions. Given the intricacy of natural product biosynthesis regulation, as evidenced by jadomycin and chloramphenicol production regulation,<sup>117-119</sup> it is possible that the target of the LAL activator may also be another regulatory gene in the cluster, or a non-functional gene containing a mutation. Even if a secondary metabolic gene cluster encodes a single regulator for the control of the structural genes, transcription of this regulatory gene may be very complex.<sup>134</sup>

The collection and analysis of mRNA data to quantitate R6 gene transcription would help inform further study of this cluster. With that data in hand, alternate approaches (i.e. integrative expression of the LAL regulator to avoid polar effects in the gene cluster, overexpression or disruption of other cluster-situated regulators, or direct overexpression of the indolocarbazole structural genes) could be pursued.

## 4.6 Experimental Methods

**Table 19.** List of bacterial strains and plasmids used in this study.

Strain	Description	Source
NEB 5-alpha competent <i>E. coli</i>	High efficiency commercial cloning strain	New England Biolabs
<i>E. coli</i> ET12567 (pUZ8002)	Methylation deficient strain; <i>dam</i> <sup>-</sup> , <i>dcm</i> <sup>-</sup> <i>hsdS</i> <sup>-</sup> carrying <i>oriT</i> mobilizing plasmid	<sup>121</sup>
<i>Streptomyces venezuelae</i> ISP5230	Wild-type strain	ATCC 10712
<i>S. venezuelae</i> R6 pLuxR	Mutant strain overexpressing putative LAL (LuxR) gene sven_RS03645	This work
Plasmids	Description	Source
pKC1139	<i>E. coli</i> - <i>Streptomyces</i> conjugation vector; <i>oriT</i> RK2, <i>ori</i> pBR322, <i>ori</i> pSG5, <i>aa(3)IV</i>	<sup>104</sup>
pSE34	<i>Streptomyces</i> expression vector; <i>ermE</i> <sup>*</sup> promoter, <i>ori</i> pIJ101, <i>ori</i> pUC19, <i>bla</i> , <i>tsr</i>	<sup>105</sup>
pKC1139_R6 LuxR(OE)	pKC1139 vector containing sven_03640/5 fragments	This work
pKC1139_R6 pLuxR	pKC1139 vector containing sven_03645 (LuxR gene) overexpression cassette	This work

### 4.6.1 General Laboratory Procedures

Refer to 2.5.1 and 3.6.1 for General Procedures and Media Recipes.

*ISP Media 4 (ISPM4)*: 3.7 g inorganic salt starch agar (Difco) in 100 mL water.

*A-Media (A-med)*: 10 g glucose, 5 g yeast extract, 20 g soluble starch, 5 g peptone, 4 g NaCl, 0.5 g K<sub>2</sub>HPO<sub>4</sub>, 0.5 g MgSO<sub>4</sub>·7H<sub>2</sub>O, and 2 g CaCO<sub>3</sub> water to 1.0 L, pH 7.0.

*Rebeccamycin fermentation media (RFM)*: 10 g soluble starch, 2.5 g L-threonine, 1 g MgCl<sub>2</sub>, 2 g KH<sub>2</sub>PO<sub>4</sub>, 2 g CaCO<sub>3</sub>, water to 1.0 L, pH 7.0.

*Modified Staurosporine vegetative media (SVM)*: 20 g glucose, 5 g meat peptone, 5 g malt extract, 3 g yeast extract, 4 g CaCO<sub>3</sub>, water to 1.0 L.

*Modified Staurosporine fermentation media (SFM)*: 30 g glucose, 15 g soytone, 4 g CaCO<sub>3</sub>, water to 1.0 L.

#### 4.6.2 Vector Construction

##### *Construction of pKC1139\_R6 LuxR(OE)*

Overlap extension fragments were amplified by PCR from *S. venezuelae* genomic DNA. A 1.0 kb region of the LuxR gene sven\_RS03645 was amplified using primers 11R6 (L) OE Fwd: GGTAAGCTTCCGGTGC GTACGGGCATG (HindIII site underlined) and 11R6 (L) OE Rev: GCTAGCAGACATATGGTGGACACTTCCGCG (NheI and NdeI sites underlined) with a 40 second extension time and the 1.2 kb downstream flanking region was amplified using 11R6 (D) OE Fwd: CATATGTCTGCTAGCCGTGGTCCGTGGCCG (NdeI and NheI sites underlined) and 11R6 (D) OE Rev: GGTTCTAGAGCGCGTCGAGGAGCTCGC (XbaI site underlined) with a 40 second extension time. The PCR products were purified by gel extraction. The fragments were unified by overlap extension PCR with the outermost primers 11R6 (L) OE Fwd and 11R6 (D) OE Rev using the purified PCR products as template DNA. The resulting 2.2 kb 11R6 LuxR(OE) PCR product was digested with NdeI to confirm the fragment identity, then was ligated into pCK1139 using restriction sites XbaI and HindIII and transformed to NEB 5-alpha competent *E. coli*. Isolated plasmids were screened by XbaI and HindIII double restriction digest, then confirmed by XbaI/NdeI and HindIII/NheI double digests.

##### *Construction of pKC1139\_R6 pLuxR*

The *ermE*\* promoter was amplified by PCR from the plasmid pSE34 using primers pSE34 ermE Fwd (NE): GATGCTAGCATGAATTCGAGCTCGGTACC (NheI and EcoRI sites underlined) and pSE34 ermE Rev (XN):

AATCATATGTCCTCCTTCTAGAGGATCCTACC (NdeI and XbaI sites underlined) with a 30 second extension time. The resulting 320 bp fragment was purified by gel extraction, then ligated into pCK1139\_R6 LuxR(OE) using restriction sites NdeI and NheI and transformed to NEB 5-alpha competent *E. coli*. Isolated plasmids were screened by XbaI and NdeI double restriction digest.

#### 4.6.3 Mutant Preparation

The pKC1139\_R6 pLuxR plasmid was transformed into *E. coli* ET12567 pUZ8002. The transformant was inoculated into selective LB media (chloramphenicol, apramycin, kanamycin) and grown overnight. An aliquot from an overnight culture was sub-cultured into new LB media with the selective antibiotics. The sub-culture was grown 37°C and 250 rpm until an OD<sub>600</sub> of 0.4-0.6 was reached, the culture was transferred to a conical tube and centrifuged (3 min, 5000 rpm). The supernatant was decanted, and the cell pellet re-suspended in LB without antibiotics, and pelleted again. This wash procedure was repeated twice, after which the pellet was suspended in 500 µL LB. Concurrently, a spore solution of *Streptomyces venezuelae* ISP5230 was prepared as previously described. The solution was diluted with sterile water to an OD<sub>450</sub> of 0.03 and heated at 50°C for 10 minutes. The *Streptomyces* spore suspension was cooled to room temperature, then 500 µL was added to the 500 µL of the *E. coli* solution and gently mixed. The mixture was then centrifuged at 4°C, 13 000 rpm for 3 minutes. The supernatant was removed and the cell pellet was re-suspended in LB and plated directly (10<sup>0</sup>) or diluted in LB (10<sup>-1</sup>) and plated on MS-agar. After 18-24 h incubation at 30°C, a soft nutrient agar overlay

containing nalidixic acid and apramycin was applied to each of the plates. Once the agar set, the plates were returned to 30°C and allowed to grow for three days.

Exconjugant *Streptomyces* colonies were patched to MYM-agar with nalidixic acid and apramycin and grown at 37°C to select for single crossover mutants, which grew within three days. The single crossover mutants were patched to MYM with apramycin (MYM-Apr) and grown at 30°C. Colonies were further patched to MYM and grown at 30°C and retained colonies were patched twice more after spore growth at each step. Colonies were patched to MYM-Apr and grown at 30°C to select out which colonies retained single crossover. Colonies sensitive to apramycin (indicating double crossover) were used to generate spore solutions, which were streaked on MYM for single colonies. Single colonies were grown in liquid culture (MYM) for genomic extraction and PCR screening. Primers pSE34 ermE Fwd (NE) and pSE34 ermE Rev (XN) (30 second extension time) were used to identify the desired mutants, with subsequent confirmation using primers 11R6 (L) OE Fwd and 11R6 (D) OE Rev (110 second extension time).

#### **4.6.4 Production Conditions**

##### *S. venezuelae inoculum preparation*

A patch from a sporulating plate (>4 days of growth) was used to inoculate MYM and grown overnight at 30 °C with shaking (250 rpm) for 16 – 20 hours. The cultures were monitored by microscope until the mycelia were fibrous. For productions with minimal medias (RFM, MSM), the cells were pelleted in a conical tube by centrifugation at 3750 rpm (4°C) for 10-30 minutes and the cells were washed twice with MSM and re-suspended



in MSM, forming an inoculum slurry. For productions with rich media (SFM, A-medium), the overnight MYM cultures were used directly as inoculum.

#### *Production methods*

In all productions, media pH was corrected regularly to 7.5 using NaOH (5 M) or HCl (5 M) for the duration of the production period. All productions proceeded at 30°C with shaking (250 rpm).

MSM production media was separately prepared with the indicated amino acid (L-phenylalanine or D-serine 60 mM) and autoclaved, after which separately filter sterilized 30% glucose solution (2%, v/v) and separately autoclaved 9 mM phosphate solution (0.54%, v/v) were added. The re-suspended *S. venezuelae* slurry was then added to the production media to an optical density of 0.4-0.6 at 600 nm (OD<sub>600</sub>) using a SpectraMax Plus Microplate Reader (Molecular Devices). As indicated, the production media was ethanol shocked (3%, v/v) to induce jadomycin production. RFM production media were prepared with DL-W (1 mgmL<sup>-1</sup>) or HP20 supplementation (5% w/v) included before autoclaving, as indicated. Media was inoculated with the MSM *S. venezuelae* slurry at 3% v/v, as the calcium carbonate prevented accurate OD<sub>600</sub> measurements. Productions may also have been supplemented with DL-W (1, 2.5, or 5 mgmL<sup>-1</sup>) after 24 or 48 hours, as indicated.

#### **4.6.5 Natural Product Purification Methods**

Natural product purity and presumptive identity were monitored by thin layer chromatography (TLC) or high-pressure liquid chromatography (HPLC). TLC plates were

normal phase silica (250 µm thickness) and glass-backed. White light or ultraviolet (UV) light were used to visualize TLC.

#### *Adsorbent Resin Preparation and Extraction*

Diaion HP20 resin was supplemented into RFM, as indicated, to adsorb non-polar natural products. The HP20 was pre-conditioned with 3 volumes of water and 3 volumes of methanol, then rinsed with three volumes of water. HP20 was added to media prior to autoclaving, or after filtration at the end of the production. After shaking, the HP20 was separated from the culture media and bacteria, rinsed with at least 3 volumes of water, extracted with methanol, and finally extracted with ethyl acetate. The solvent was removed *in vacuo*.

#### *Liquid/Liquid Extraction*

Upon production completion, bacteria were removed from the solution by gravity (7500 rpm) or filtration (20 µm). The filtrate or supernatant were extracted with ethyl acetate. The solvent was removed *in vacuo*. Crude material was further extracted by methanol/hexanes extraction, as indicated.

#### *Flash chromatography (silica-phenyl)*

Refer to 2.5.3

#### *Flash chromatography (normal phase)*

Biotage SP1™ unit was used to perform flash chromatography, using pre-packed normal phase silica columns (25 g, 40 g, and 80 g) from SiliCycle®. Compounds were eluted using

a stepwise gradient with an ethyl acetate/hexanes or a methanol/dichloromethane solvent system.

#### *Preparative thin layer chromatography*

Refer to 2.5.3.

### **4.6.6 Natural Product Analysis and Characterization**

#### *High-performance liquid chromatography*

Refer to 2.5.4 for instrument and column parameters, and NUCTRAN method gradient. A second method, GTFAACN, was also used, which has a linear gradient from 85:15 A:B to 30:70 A:B over 11.0 min, followed by a plateau at 30:70 A:B from 11.0 to 13.0 min, a linear gradient back to 85:15 A:B over 1.5 min, and finally a re-equilibration at 85:15 A:B up to 15.0 min; where Buffer A is an aqueous solution of 0.1% trifluoroacetic acid and Buffer B is 100% acetonitrile. Samples were analyzed by injecting 20  $\mu$ L aliquots with 10-100  $\mu$ M concentrations.

#### *Mass Spectrometry*

Refer to 2.5.4.

#### *Nuclear magnetic resonance spectroscopy*

Refer to 2.5.4.

## CHAPTER 5: CONCLUSIONS

Precursor-directed jadomycin biosynthesis using 4-(aminomethyl)benzoic acid (4-AMBA), 3-(aminomethyl)benzoic acid (3-AMBA), and 8-aminooctanoic acid was facilitated by co-amino acid supplementation and generated a series of jadomycons incorporating these amino acids. Five novel jadomycons were isolated and characterized. Incorporation of 4-AMBA and 3-AMBA, amino acids unable to undergo intramolecular cyclization, broaden the library of jadomycons omitting an E-ring. Cytotoxic activity evaluation of the 3-AMBA jadomycons indicated reduced potency when compared to jadomycin F in drug-sensitive and drug-resistant breast cancer cells, but the jadomycons retained their potency in *ABCBI*-overexpressing, taxane-resistant cancer cells in contrast to the doxorubicin control. Incorporation of 8-aminooctanoic acid provided the eleven-membered E-ring containing jadomycin Undec, which further demonstrates the flexibility of the non-enzymatic incorporation of amino acids for E-ring formation in jadomycin biosynthesis.

Four methods of heterologous expression of *urdGT2* in *S. venezuelae* were explored to generate jadomycin C-glycosides. Unfortunately, C-glycosylation of jadomycons or jadomycin intermediates was not observed in jadomycin productions using the integrative or alternate expression methods, suggesting that UrdGT2 donor substrate specificity may not extend to L-digitoxose. The O-glycosylation of JdG using integrative, constitutive expression of *jadS* in the *S. venezuelae*  $\Delta$ *jadS* mutant, verified that the vector expression was viable and that the genes downstream of the *jadS* deletion site were functional.

A silent *Streptomyces venezuelae* gene cluster, Cluster R6, was studied for its ability to produce novel natural products. Cluster R6 was selected for activation as it contained a

putative LAL family activator and an indolocarbazole biosynthetic sub-cluster. The LAL activator was constitutively overexpressed under an *ermE*\* promoter and the mutant *S. venezuelae* strain was cultured in several media types and supplementation conditions. While the changes to the biosynthetic profile were apparent in the overexpression mutant, the major metabolites observed were derivatives of tryptophan.

## REFERENCES

1. Cragg, G. M.; Newman, D. J. *BBA - General Subjects* **2013**, *1830*, 3670-3695.
2. Patridge, E.; Gareiss, P.; Kinch, M. S.; Hoyer, D. *Drug Discov. Today* **2016**, *21*, 204.
3. Drews, J. *Science* **2000**, *287*, 1960-1964.
4. Newman, D. J.; Cragg, G. M. *J. Nat. Prod.* **2016**, *79*, 629.
5. Moloney, M. G. *Trends Pharmacol. Sci.* **2016**, *37*, 689-701.
6. Crawford, J. M.; Clardy, J. *Chem. Commun.* **2011**, *27(47)*, 7559.
7. Zarins-Tutt, J.; Barberi, T. T.; Gao, H.; Mearns-Spragg, A.; Zhang, L.; Newman, D. J.; Goss, R. J. M. *Nat. Prod. Rep.* **2015**, *33*, 54-72.
8. Bode, H. B.; Bethe, B.; Höfs, R.; Zeeck, A. *ChemBioChem* **2002**, *3*, 619-627.
9. Ziemert, N.; Alanjary, M.; Weber, T. *Nat. Prod. Rep.* **2016**, *33*, 988-1005.
10. Kim, E.; Yang, I.; Yoon, Y. *Arch. Pharm. Res.* **2015**, *38*, 1606-1616.
11. Chen, J.; Wu, Q.; Hawas, U.; Wang, H. *Appl. Microbiol. Biotechnol.* **2016**, *100*, 2953-2965.
12. Smanski, M. J.; Zhou, H.; Claesen, J.; Shen, B.; Fischbach, M. A.; Voigt, C. A. *Nature Reviews Microbiology* **2016**, *14*, 135.
13. Lawrence, J. *Curr. Opin. Genet. Dev.* **1999**, *9*, 642-648.
14. Liu, G.; Chater, K. F.; Chandra, G.; Niu, G.; Tan, H. *Microbiol. Mol. Biol. Rev.* **2013**, *77*, 112-143.
15. Romero-Rodríguez, A.; Robledo-Casados, I.; Sánchez, S. *BBA-Gene Regul. Mech.* **2015**, *1849*, 1017-1039.
16. Rodríguez, H.; Rico, S.; Díaz, M.; Santamaría, R. I. *Microb. Cell. Fact.* **2013**, *12*, 127.
17. Bentley, S. D.; Chater, K. F.; Cerdeno-Tarraga, A. M.; Challis, G. L.; Thomson, N. R.; James, K. D.; Harris, D. E.; Quail, M. A.; Kieser, H.; Harper, D.; Bateman, A.; Brown, S.; Chandra, G.; Chen, C. W.; Collins, M.; Cronin, A.; Fraser, A.; Goble, A.; Hidalgo, J.; Hornsby, T.; Howarth, S.; Huang, C. H.; Kieser, T.; Larke, L.; Murphy, L.; Oliver, K.; O'Neil, S.; Rabinowitsch, E.; Rajandream, M. A.; Rutherford, K.; Rutter, S.; Seeger, K.; Saunders, D.; Sharp, S.; Squares, R.; Squares, S.; Taylor, K.; Warren, T.;

- Wietzorrek, A.; Woodward, J.; Barrell, B. G.; Parkhill, J.; Hopwood, D. A. *Nature* **2002**, *417*, 141-147.
18. Shapiro, S.; Vining, L. C. *Can. J. Microbiol.* **1983**, *29*, 1706-1714.
  19. Ayer, S. W.; McInnes, A. G.; Thibault, P.; Wang, L.; Doull, J. L.; Parnell, T.; Vining, L. C. *Tetrahedron Lett.* **1991**, *32*, 6301-6304.
  20. Doull, J. L.; Ayer, S. W.; Singh, A. K.; Thibault, P. *J. Antibiot.* **1993**, *46*, 869-871.
  21. MacLeod, J. M.; Forget, S. M.; Jakeman, D. L. *Can. J. Chem.* **2017**, Submitted.
  22. Pullan, S. T.; Chandra, G.; Bibb, M. J.; Merrick, M. *BMC Genomics* **2011**, *12*, 75.
  23. Weber, T.; Blin, K.; Duddela, S.; Krug, D.; Kim, H. U.; Bruccoleri, R.; Lee, S. Y.; Fischbach, M. A.; Müller, R.; Wohlleben, W.; Breitling, R.; Takano, E.; Medema, M. H. *Nucleic Acids Res.* **2015**, *43*, W237-W243.
  24. Phelan, R. M.; Sekurova, O. N.; Keasling, J. D.; Zotchev, S. B. *ACS Synth. Biol.* **2015**, *4*, 393.
  25. Thanapipatsiri, A.; Gomez-Escribano, J. P.; Song, L.; Bibb, M. J.; Al-Bassam, M.; Chandra, G.; Thamchaipenet, A.; Challis, G. L.; Bibb, M. J. *ChemBioChem* **2016**, *17*, 2189-2198.
  26. Inahashi, Y.; Zhou, S.; Bibb, M. J.; Song, L.; Al-Bassam, M.; Bibb, M. J.; Challis, G. L. *Chem. Sci.* **2017**, *8*, 2823-2831.
  27. Rabe, P.; Rinkel, J.; Klapschinski, T. A.; Barra, L.; Dickschat, J. S. *Org. Biomol. Chem.* **2015**, *14*, 158-164.
  28. Goto, Y.; Li, B.; Claesen, J.; Shi, Y.; Bibb, M. J.; van der Donk, W. A. *PLoS Biology* **2010**, *8*, e1000339.
  29. Sidda, J. D.; Song, L.; Poon, V.; Al-bassam, M.; Lazos, O.; Buttner, M. J.; Challis, G. L.; Corre, C. *Chem. Sci.* **2014**, *5*, 86-89.
  30. Mingzi, M. Z.; Fong, T. W.; Wang, Y.; Luo, S.; Yee, H. L.; Heng, E.; Wan, L. Y.; Ryan, E. C.; Enghiad, B.; Ee, L. A.; Zhao, H. *Nat. Chem. Biol.* **2017**, *13*, 607-609.
  31. Kodani, S.; Komaki, H.; Suzuki, M.; Kobayakawa, F.; Hemmi, H. *Biometals* **2015**, *28*, 791-801.
  32. Chatterjee, S.; Vining, L. C.; Westlake, D. W. S. *Can. J. Microbiol.* **1983**, *29*, 247-253.

33. Doull, J. L.; Singh, A. K.; Hoare, M.; Ayer, S. W. *J. Ind. Microbiol.* **1994**, *13*, 120-125.
34. Schöller, C. E. G.; Gürtler, H.; Pedersen, R.; Molin, S.; Wilkins, K. *J. Agric. Food Chem.* **2002**, *50*, 2615.
35. Molle, V.; Buttner, M. J. *Mol. Microbiol.* **2000**, *36*, 1265-1278.
36. Hertweck, C. *Angew. Chem. Int. Ed.* **2009**, *48*, 4688-4716.
37. Cummings, M.; Breitling, R.; Takano, E. *FEMS Microbiol. Lett.* **2014**, *351*, 116-125.
38. Hertweck, C.; Luzhetskyy, A.; Rebets, Y.; Bechthold, A. *Nat. Prod. Rep.* **2007**, *24*, 162-190.
39. Kharel, M. K.; Pahari, P.; Shepherd, M. D.; Tibrewal, N.; Nybo, S. E.; Shaaban, K. A.; Rohr, J. *Nat. Prod. Rep.* **2012**, *29*, 264-325.
40. Rix, U.; Zheng, J.; Remsing Rix, L. L.; Greenwell, L.; Yang, K.; Rohr, J. *J. Am. Chem. Soc.* **2004**, *126*, 4496-4497.
41. Jakeman, D. L.; Farrell, S.; Young, W.; Doucet, R. J.; Timmons, S. C. *Bioorg. Med. Chem. Lett.* **2005**, *15*, 1447-1449.
42. Jakeman, D. L.; Graham, C. L.; Reid, T. R. *Bioorg. Med. Chem. Lett.* **2005**, *15*, 5280-5283.
43. Borissow, C. N.; Graham, C. L.; Syvitski, R. T.; Reid, T. R.; Blay, J.; Jakeman, D. L. *ChemBioChem* **2007**, *8*, 1198-1203.
44. Jakeman, D. L.; Bandi, S.; Graham, C. L.; Reid, T. R.; Wentzell, J. R.; Douglas, S. E. *Antimicrob. Agents Chemother.* **2009**, *53*, 1245-1247.
45. Jakeman, D. L.; Dupuis, S. N.; Graham, C. L. *Pure Appl. Chem.* **2009**, *81*, 1041-1049.
46. Dupuis, S. N.; Veinot, T.; Monroe, S. M. A.; Douglas, S. E.; Syvitski, R. T.; Goralski, K. B.; McFarland, S. A.; Jakeman, D. L. *J. Nat. Prod.* **2011**, *74*, 2420-2424.
47. Dupuis, S. N.; Robertson, A. W.; Veinot, T.; Monroe, S. M. A.; Douglas, S. E.; Syvitski, R. T.; Goralski, K. B.; McFarland, S. A.; Jakeman, D. L. *Chem. Sci.* **2012**, *3*, 1640-1644.
48. Robertson, A. W.; Martinez-Farina, C. F.; Syvitski, R. T.; Jakeman, D. L. *J. Nat. Prod.* **2015**, *78*, 1942-1948.



49. Robertson, A. W.; Martinez-Farina, C.; Smithen, D. A.; Yin, H.; Monro, S.; Thompson, A.; McFarland, S. A.; Syvitski, R. T.; Jakeman, D. L. *J. Am. Chem. Soc.* **2015**, *137*, 3271-3275.
50. Martinez-Farina, C. F.; Robertson, A. W.; Yin, H.; Monro, S. M. A.; McFarland, S. A.; Syvitski, R. T.; Jakeman, D. L. *J. Nat. Prod.* **2015**, *78*, 1208-1214.
51. Martinez-Farina, C. F.; Jakeman, D. L. *Chem. Commun.* **2015**, *51*, 14617-14619.
52. Robertson, A. W.; MacIntyre, L. W.; MacLeod, J. M.; Forget, S. M.; Jakeman, D. L. *Chem. Sci.* **2017**, *Submitted*.
53. Forget, S. M.; Robertson, A. W.; Overy, D. P.; Kerr, R. G.; Jakeman, D. L. *J. Am. Chem. Soc.* **2017**, *80 (6)*, 1860-1866.
54. MacLeod, J. M.; Martinez-Farina, C. F.; Jakeman, D. L. *Can. J. Chem.* **2017**, *Submitted*.
55. Wang, L. Dalhousie University, Halifax, Nova Scotia, 2002.
56. Tibrewal, N.; Pahari, P.; Wang, G.; Kharel, M. K.; Morris, C.; Downey, T.; Hou, Y.; Bugni, T. S.; Rohr, J. *J. Am. Chem. Soc.* **2012**, *134*, 18181-18184.
57. Syvitski, R. T.; Borissow, C. N.; Graham, C. L.; Jakeman, D. L. *Org. Lett.* **2006**, *8*, 697-700.
58. Jakeman, D. L.; Graham, C. L.; Young, W.; Vining, L. C. *J. Ind. Microbiol. Biotechnol.* **2006**, *33*, 767-772.
59. Robertson, A. W.; Forget, S. M.; Martinez-Farina, C. F.; McCormick, N. E.; Syvitski, R. T.; Jakeman, D. L. *J. Am. Chem. Soc.* **2016**, *138*, 2200-2208.
60. Issa, M. E.; Hall, S. R.; Dupuis, S. N.; Graham, C. L.; Jakeman, D. L.; Goralski, K. B. *Anticancer Drugs* **2014**, *25*, 255-269.
61. Hall, S. R.; Blundon, H. L.; Ladda, M. A.; Robertson, A. W.; Martinez-Farina, C.; Jakeman, D. L.; Goralski, K. B. *Pharmacol. Res. Perspect.* **2015**, *3 (2)*, e00110.
62. Hall, S. R.; Toulany, J.; Bennett, L. G.; Martinez-Farina, C. F.; Robertson, A. W.; Jakeman, D. L.; Goralski, K. B. *J. Pharmacol. Exp. Ther.* **2017**, *363(1)*.
63. Subik, K.; Lee, J.; Baxter, L.; Strzepak, T.; Costello, D.; Crowley, P.; Xing, L.; Hung, M.; Bonfiglio, T.; Hicks, D. G.; Tang, P. *Breast Cancer (Auckl)* **2010**, *4*, 35-41.
64. Rivera, E. *Breast J.* **2010**, *16*, 252-263.

65. Morris, P. G.; McArthur, H. L.; Hudis, C. A. *Expert Opin. Pharmacother.* **2009**, *10*, 967.
66. Gottesman, M. M. *Annu. Rev. Med.* **2002**, *53*, 615-627.
67. Chen, C.; Chin, J. E.; Ueda, K.; Clark, D. P.; Pastan, I.; Gottesman, M. M.; Roninson, I. B. *Cell* **1986**, *47*, 381-389.
68. Ramachandra, M.; Ambudkar, S. V.; Chen, D.; Hrycyna, C. A.; Dey, S.; Gottesman, M. M.; Pastan, I. *Biochemistry* **1998**, *37*, 5010.
69. Gottesman, M. M.; Fojo, T.; Bates, S. E. *Nat. Rev. Cancer* **2002**, *2*, 48-58.
70. Wind, N. S.; Holen, I. *Int. J. Breast Cancer* **2011**, *2011*.
71. Shen, F.; Chu, S.; Bence, A. K.; Bailey, B.; Xue, X.; Erickson, P. A.; Montrose, M. H.; Beck, W. T.; Erickson, L. C. *J. Pharmacol. Exp. Ther.* **2008**, *324*, 95.
72. Lee, F. Y.; Borzilleri, R.; Fairchild, C. R.; Kim, S. H.; Long, B. H.; Reventos-Suarez, C.; Vite, G. D.; Rose, W. C.; Kramer, R. A. *Clin. Cancer Res.* **2001**, *7*, 1429.
73. MacLeod, J. M.; Robertson, A. W.; Hall, S. R.; Bennett, L. G.; Correa, H.; Goralski, K. B.; Kerr, R. G.; Jakeman, D. L. *J. Org. Chem.* **2017**, *Submitted*.
74. Liang, D.; Liu, J.; Wu, H.; Wang, B.; Zhu, H.; Qiao, J. *Chem. Soc. Rev.* **2015**, *44*, 8350-8374.
75. Thibodeaux, C.; Melançon, C.; Liu, H. *Angew. Chem. Int. Ed.* **2008**, *47*, 9814-9859.
76. Salas, J. A.; Mendez, C. *J. Mol. Microbiol. Biotechnol.* **2005**, *9*, 77-85.
77. Elshahawi, S. I.; Shaaban, K. A.; Kharel, M. K.; Thorson, J. S. *Chem. Soc. Rev.* **2015**, *44*, 7591-7697.
78. Erb, A.; Weiß, H.; Härle, J.; Bechthold, A. *Phytochemistry* **2009**, *70*, 1812-1821.
79. Menzella, H. G.; Reeves, C. D. *Curr. Opin. Microbiol.* **2007**, *10*, 238-245.
80. Brazier-Hicks, M.; Evans, K. M.; Gershater, M. C.; Puschmann, H.; Steel, P. G.; Edwards, R. *J. Biol. Chem.* **2009**, *284*, 17926.
81. Pérez, M.; Lombó, F.; Baig, I.; Braña, A. F.; Rohr, J.; Salas, J. A.; Méndez, C. *Appl. Environ. Microbiol.* **2006**, *72*, 6644-6652.

82. Trefzer, A.; Blanco, G.; Remsing, L.; Kunzel, E.; Rix, U.; Lipata, F.; Brana, A. F.; Mendez, C.; Rohr, J.; Bechthold, A.; Salas, J. A. *J. Am. Chem. Soc.* **2002**, *124*, 6056-6062.
83. Li, L.; Wang, P.; Tang, Y. *J. Antibiot* **2014**, *67*, 65-70.
84. Shepherd, M. D.; Liu, T.; Mendez, C.; Salas, J. A.; Rohr, J. *Appl. Environ. Microbiol.* **2011**, *77*, 435.
85. Künzel, E.; Faust, B.; Oelkers, C.; Weissbach, U.; Bearden, D. W.; Weitnauer, G.; Westrich, L.; Bechthold, A.; Rohr, J. *J. Am. Chem. Soc.* **1999**, *121*, 11058-11062.
86. Drautz, H.; Zähler, H.; Rohr, J.; Zeeck, A. *J. Antibiot.* **1986**, *39*, 1657.
87. Chu, M.; Yarborough, R.; Schwartz, J.; Patel, M. G.; Horan, A. C.; Gullo, V. P.; Das, P. R.; Puar, M. S. *J. Antibiot.* **1993**, *46*, 861-865.
88. Gladstone, S. ProQuest Dissertations Publishing, Utah State University, 2016.
89. Balitz, D. M.; O'Herron, F. A.; Bush, J.; Vyas, D. M.; Nettleton, D. E.; Grulich, R. E.; Bradner, W. T.; Doyle, T. W.; Arnold, E.; Clardy, J. *J. Antibiot.* **1981**, *34*, 1544-1555.
90. Liu, T.; Kharel, M. K.; Fischer, C.; McCormick, A.; Rohr, J. *ChemBioChem* **2006**, *7*, 1070-1077.
91. Takano, S.; Hasuda, K.; Ito, A.; Koide, Y.; Ishii, F. *J. Antibiot.* **1976**, *29*, 765.
92. Ichinose, K.; Ozawa, M.; Itou, K.; Kunieda, K.; Ebizuka, Y. *Microbiology* **2003**, *149*, 1633-1645.
93. Séquin, U.; Bedford, C. T.; Chung, S. K.; Scott, A. I. *Helv. Chim. Acta* **1977**, *60*, 896-906.
94. Bililign, T.; Hyun, C.; Williams, J. S.; Czisny, A. M.; Thorson, J. S. *Chem. Biol.* **2004**, *11*, 959-969.
95. Antal, N.; Fiedler, H.; Stackebrandt, E.; Beil, W.; Stroch, K.; Zeeck, A. *J. Antibiot* **2005**, *58*, 95-102.
96. Erb, A.; Luzhetskyy, A.; Hardter, U.; Bechthold, A. *ChemBioChem* **2009**, *10*, 1392-1401.
97. Schimana, J.; Fiedler, H.; Groth, I.; Suebmuth, R.; Bell, W.; Walker, M.; Zeeck, A. *J. Antibiot.* **2000**, *53*, 779-787.

98. Trefzer, A.; Pelzer, S.; Schimana, J.; Stockert, S.; Bihlmaier, C.; Fiedler, H. P.; Welzel, K.; Vente, A.; Bechthold, A. *Antimicrob. Agents Chemother.* **2002**, *46*, 1174.
99. Hatsu, M.; Sasaki, T.; Gomi, S.; Kodama, Y.; Sezaki, M.; Inouye, S.; Kondo, S. *J. Antibiot.* **1992**, *45*, 325-330.
100. Faust, B.; Hoffmeister, D.; Weitnauer, G.; Westrich, L.; Haag, S.; Schneider, P.; Decker, H.; Kunzel, E.; Rohr, J.; Bechthold, A. *Microbiology-(UK)* **2000**, *146*, 147-154.
101. Hoffmeister, D.; Drager, G.; Ichinose, K.; Rohr, J.; Bechthold, A. *J. Am. Chem. Soc.* **2003**, *125*, 4678-4679.
102. Baig, I.; Kharel, M.; Kobylansky, A.; Zhu, L.; Rebets, Y.; Ostash, B.; Luzhetskyy, A.; Bechthold, A.; Fedorenko, V. A.; Rohr, J. *Angew. Chem. Int. Ed.* **2006**, *45*, 7842-7846.
103. Wang, L.; White, R. L.; Vining, L. C. *Microbiology* **2002**, *148*, 1091-1103.
104. Bierman, M.; Logan, R.; O'Brien, K.; Seno, E. T.; Rao, R. N.; Schoner, B. E. *Gene* **1992**, *116*, 43-49.
105. Yoon, Y. J.; Beck, B. J.; Kim, B. S.; Kang, H.; Reynolds, K. A.; Sherman, D. H. *Chem. Biol.* **2002**, *9*, 203-214.
106. Han, A. R., S.; Park, S. R., E.; Park, J. W., E.; Lee, E. Y., K.; Kim, D. M., C.; Kim, B. G., S.; Yoon, Y. J., E. *J. Microbiol. Biotechnol.* **2011**, *6*, 613-616.
107. Kim, E.; Song, M. C.; Kim, M. S.; Beom, J. Y.; Jung, J. A.; Cho, H. S.; Yoon, Y. J. *ACS Comb. Sci.* **2017**, *19*, 262-270.
108. Bibb, M. J.; White, J.; Ward, J. M.; Janssen, G. R. *Mol. Microbiol.* **1994**, *14*, 533-545.
109. Kieser, T.; Hopwood, D. A.; Wright, H. M.; Thompson, C. J. *Mol. Gen. Genet.* **1982**, *185*, 223-238.
110. Cundliffe, E. *Nature* **1978**, *272*, 792.
111. Wang, L.; Hu, Y.; Zhang, Y.; Wang, S.; Cui, Z.; Bao, Y.; Jiang, W.; Hong, B. *BMC Microbiol.* **2009**, *9*, 14.
112. Zhang, Y.; He, H.; Liu, H.; Wang, H.; Wang, X.; Xiang, W. *Microb. Cell. Fact.* **2016**, *15*, 152.

113. Muth, G.; Nußbaumer, B.; Wohlleben, W.; Pühler, A. *Mol. Gen. Genet.* **1989**, *219*, 341-348.
114. Forget, S. M.; Na, J.; McCormick, N. E.; Jakeman, D. L. *Org. Biomol. Chem.* **2017**, *15*, 2725-2729.
115. Aidoo, D. A.; Barrett, K.; Vining, L. C. *Microbiology* **1990**, *136*, 657-662.
116. Luzhetskyy, A.; Taguchi, T.; Fedoryshyn, M.; Dürr, C.; Wohler, S.; Novikov, V.; Bechthold, A. *ChemBioChem* **2005**, *6*, 1410.
117. Sekurova, O. N.; Zhang, J.; Kristiansen, K. A.; Zotchev, S. B. *Microb. Cell. Fact.* **2016**, *15*, 1.
118. Xu, G. M.; Wang, J. A.; Wang, L. Q.; Tian, X. Y.; Yang, H. H.; Fan, K. Q.; Yang, K. Q.; Tan, H. R. *J. Biol. Chem.* **2010**, *285*, 27440-27448.
119. Wang, L.; Tian, X.; Wang, J.; Yang, H.; Fan, K.; Xu, G.; Yang, K.; Tan, H. *Proc. Natl. Acad. Sci. U. S. A.* **2009**, *106*, 8617-8622.
120. Li, L.; Pan, G.; Zhu, X.; Fan, K.; Gao, W.; Ai, G.; Ren, J.; Shi, M.; Olano, C.; Salas, J. A.; Yang, K. *Appl. Microbiol. Biotechnol.* **2017**, 1-10.
121. Flett, F.; Mersinias, V.; Smith, C. P. *FEMS Microbiol. Lett.* **1997**, *155*, 223-229.
122. Bibb, M. J. *Curr. Opin. Microbiol.* **2005**, *8*, 208-215.
123. Cimermancic, P.; Medema, M.; Claesen, J.; Kurita, K.; Weiland Brown, L.; Mavrommatis, K.; Pati, A.; Godfrey, P.; Koehrsen, M.; Clardy, J.; Birren, B.; Takano, E.; Sali, A.; Lington, R.; Fischbach, M. *Cell* **2014**, *158*, 412-421.
124. Gomez-Escribano, J.; Alt, S.; Bibb, M. J. *Marine drugs* **2016**, *14*.
125. Ren, H.; Wang, B.; Zhao, H. *Curr. Opin. Biotechnol.* **2017**, *48*, 21-27.
126. Rutledge, P. J.; Challis, G. L. *Nat. Rev. Microbiol.* **2015**, *13*, 509-523.
127. Skinnider, M. A.; Dejong, C. A.; Rees, P. N.; Johnston, C. W.; Li, H.; Webster, A. L. H.; Wyatt, M. A.; Magarvey, N. A. *Nucleic Acids Res.* **2015**, *43*, 9645.
128. Hadjithomas, M.; Chen, I.; Chu, K.; Ratner, A.; Palaniappan, K.; Szeto, E.; Huang, J.; Reddy, T. B. K.; Cimerman, P.; Fischbach, M. A.; Ivanova, N. N.; Markowitz, V. M.; Kypides, N. C.; Pati, A. *mBio* **2015**, *6*, e00932-15.
129. Weber, T.; Kim, H. U. *Synthetic and Systems Biotechnology* **2016**, *1*, 69-79.

130. Goh, E.; Yim, G.; Tsui, W.; McClure, J.; Surette, M. G.; Davies, J. *Proc. Natl. Acad. Sci. U. S. A.* **2002**, *99*, 17025-17030.
131. Lopatniuk, M.; Ostash, B.; Luzhetskyy, A.; Walker, S.; Fedorenko, V. *Russ. J. Genet.* **2014**, *50*, 360-365.
132. Yin, S.; Li, Z.; Wang, X.; Wang, H.; Jia, X.; Ai, G.; Bai, Z.; Shi, M.; Yuan, F.; Liu, T.; Wang, W.; Yang, K. *Appl. Microbiol. Biotechnol.* **2016**, *100*, 10563-10572.
133. Lee, D. J.; Minchin, S. D.; Busby, S. J. W. *Annu. Rev. Microbiol.* **2012**, *66*, 125-152.
134. Aigle, B.; Corre, C. *Meth. Enzymol.* **2012**, *517*, 343-366.
135. Du, D.; Katsuyama, Y.; Onaka, H.; Fujie, M.; Satoh, N.; Shin-Ya, K.; Ohnishi, Y. *ChemBioChem* **2016**, *17*, 1464-1471.
136. Laureti, L.; Song, L.; Huang, S.; Corre, C.; Leblond, P.; Challis, G. L.; Aigle, B. *Proc. Natl. Acad. Sci. U. S. A.* **2011**, *108*, 6258.
137. Jiang, L.; Wang, L.; Zhang, J.; Liu, H.; Hong, B.; Tan, H.; Niu, G. *Scientific Reports* **2015**, *5*.
138. Zhou, Z.; Xu, Q.; Bu, Q.; Guo, Y.; Liu, S.; Liu, Y.; Du, Y.; Li, Y. *Chembiochem : a European journal of chemical biology* **2015**, *16*, 496.
139. Li, S.; Li, Y.; Lu, C.; Zhang, J.; Zhu, J.; Wang, H.; Shen, Y. *Org. Lett.* **2015**, *17*, 3706.
140. Mo, S.; Yoon, Y. J. *Journal of microbiology and biotechnology* **2016**, *26*, 66.
141. Huang, M.; Li, M.; Feng, Z.; Liu, Y.; Chu, Y.; Tian, Y. *World J. Microbiol. Biotechnol.* **2011**, *27*, 2103-2109.
142. De Schrijver, A.; De Mot, R. *Microbiology* **1999**, *145* (6), 1287.
143. Li, S.; Wang, H.; Li, Y.; Deng, J.; Lu, C.; Shen, Y.; Shen, Y. *ChemBioChem* **2014**, *15*, 94-102.
144. Xie, C.; Deng, J.; Wang, H. *Curr. Microbiol.* **2015**, *70*, 859-864.
145. Anton, N.; Mendes, M. V.; Martin, J. F.; Aparicio, J. F. *J. Bacteriol.* **2004**, *186*, 2567.
146. Hur, Y.; Choi, S.; Sherman, D.; Kim, E. *Microbiology* **2008**, *154*, 2912-2919.
147. Guo, J.; Zhao, J.; Li, L.; Chen, Z.; Wen, Y.; Li, J. *Mol. Genet. Genomics* **2010**, *283*, 123-133.

148. Wilson, D. J.; Xue, Y.; Reynolds, K. A.; Sherman, D. H. *J. Bacteriol.* **2001**, *183*, 3468.
149. Guerra, S. M.; Rodríguez-García, A.; Santos-Aberturas, J.; Vicente, C. M.; Payero, T. D.; Martín, J. F.; Aparicio, J. F. *PLoS ONE* **2012**, *7*, e31475.
150. Kuscer, E.; Coates, N.; Challis, I.; Gregory, M.; Wilkinson, B.; Sheridan, R.; Petkovic, H. *J. Bacteriol.* **2007**, *189*, 4756.
151. Mo, S.; Yoo, Y. J.; Ban, Y. H.; Lee, S.; Kim, E.; Suh, J.; Yoon, Y. J. *Appl. Environ. Microbiol.* **2012**, *78*, 2249.
152. Onaka, H.; Taniguchi, S.; Igarashi, Y.; Furumai, T. *Biosci. Biotechnol. Biochem.* **2003**, *67*, 127-138.
153. Sánchez, C.; Butovich, I. A.; Braña, A. F.; Rohr, J.; Méndez, C.; Salas, J. A. *Chem. Biol.* **2002**, *9*, 519-531.
154. Kim, W.; Lee, J. J.; Paik, S. G.; Hong, Y. S. *J. Microbiol. Biotechnol.* **2010**, *20*, 1484-1490.
155. Sekurova, O. N.; Brautaset, T.; Sletta, H.; Borgos, S. E. F.; Jakobsen, O. M.; Ellingsen, T. E.; Strom, A. R.; Valla, S.; Zotchev, S. B. *J. Bacteriol.* **2004**, *186*, 1345.
156. Liu, Y.; Ryu, H.; Ge, B.; Pan, G.; Sun, L.; Park, K.; Zhang, K. *J. Microbiol. Biotechnol.* **2014**, *24*, 1644.
157. Shen, Y.; Huang, H.; Zhu, L.; Luo, M.; Chen, D. *J. Basic Microbiol.* **2014**, *54*, 104-110.
158. Onaka, H.; Tanifguchi, S.; Igarashi, Y.; Furamai, T. *J. Antibiot.* **2002**, *55*, 1063-1071.
159. Kim, S.; Park, J.; Chae, C.; Hyun, C.; Choi, B.; Shin, J.; Oh, K. *Appl. Microbiol. Biotechnol.* **2007**, *75*, 1119-1126.
160. Chiu, H.; Chen, Y.; Chen, C.; Jin, C.; Lee, M.; Lin, Y. *Mol. Biosyst.* **2009**, *5*, 1180-1191.
161. Gao, Q.; Zhang, C.; Blanchard, S.; Thorson, J. S. *Chem. Biol.* **2006**, *13*, 733-743.
162. Nakano, H.; Satoshi Ōmura *J. Antibiot.* **2009**, *62*, 17.
163. Elleuch, L.; Shaaban, M.; Smaoui, S.; Mellouli, L.; Karray-Rebai, I.; Fourati-Ben Fguira, L.; Shaaban, K.; Laatsch, H. *Appl. Biochem. Biotechnol.* **2010**, *162*, 579-593.

164. Zendah, I.; Riaz, N.; Nasr, H.; Frauendorf, H.; Schueffler, A.; Raies, A.; Laatsch, H.  
*J. Nat. Prod.* **2012**, *75*, 2-8-2-8.
165. Lam, K.; Schroeder, D.; Veitch, J.; Colson, K.; Matson, J.; Rose, W.; Doyle, T.;  
Forenza, S. *J. Antibiot.* **2001**, *54*, 1-9.



## APPENDIX I: SUPPLEMENTARY INFORMATION FOR CHAPTER 2

### 7.1 Jadomycin 4-AMBA Amide (1) Data

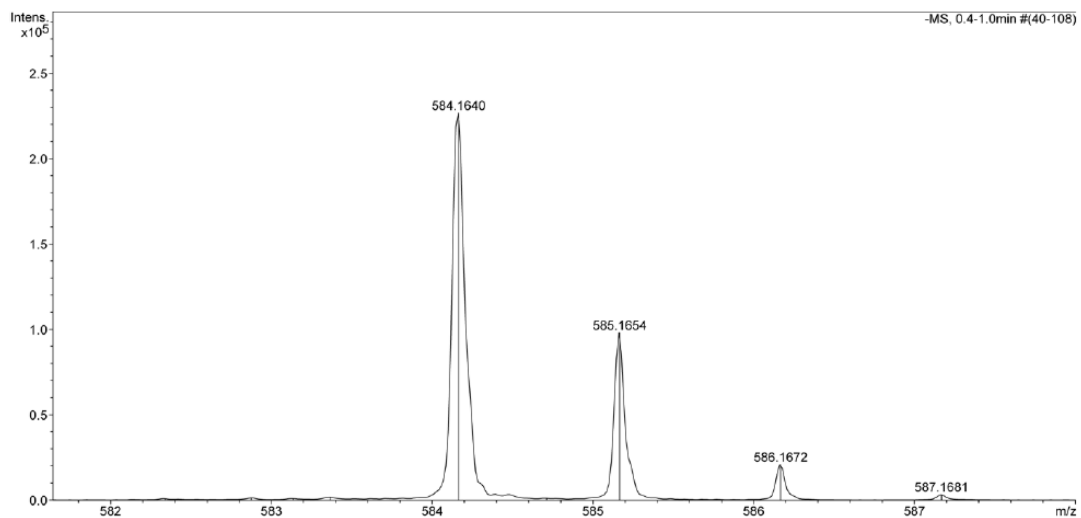


Figure S1. ESI- of 1 for  $C_{32}H_{26}NO_{10}$   $[M-H]^-$  (584.1640 found, 584.1562 calculated).

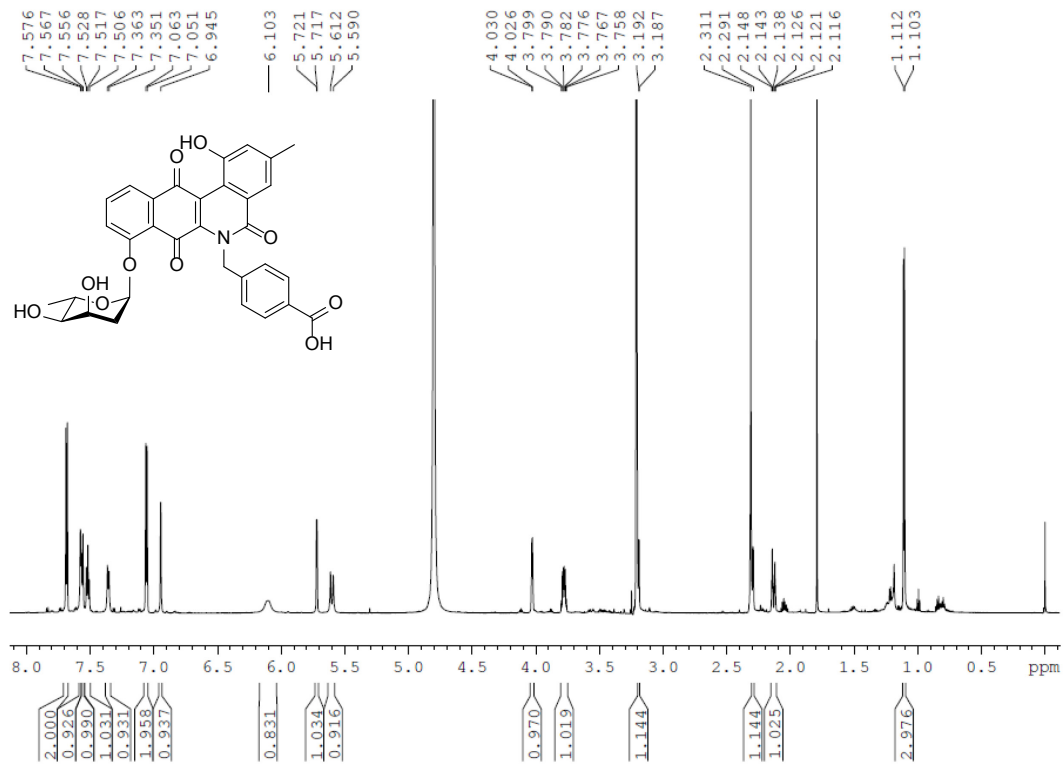


Figure S2.  $^1H$ -NMR spectrum of 1 in MeOD (1H: 700 MHz).

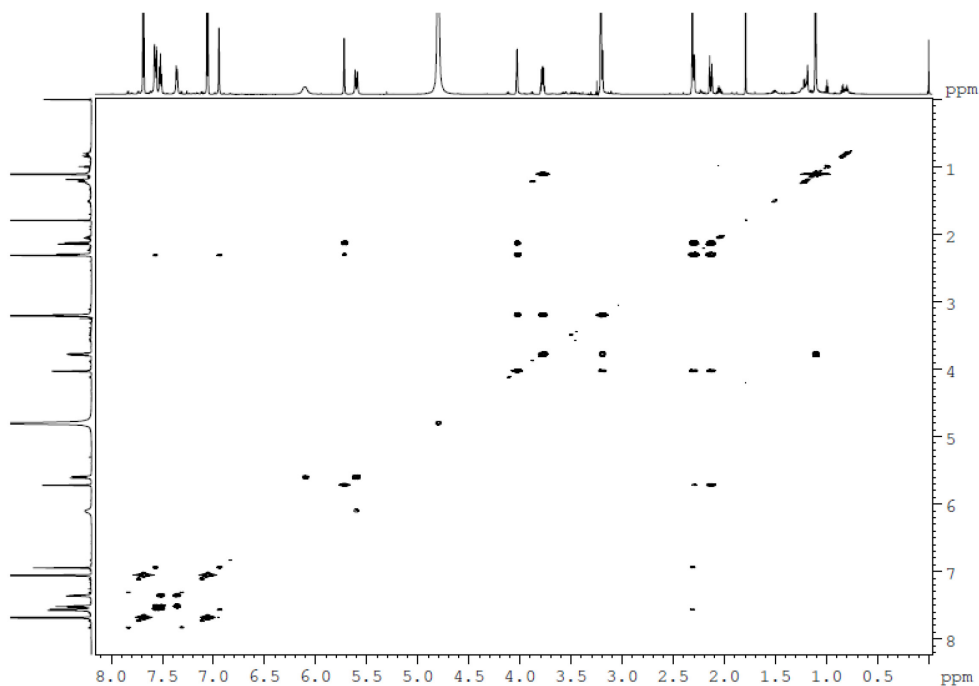


Figure S3.  $^1\text{H}$ - $^1\text{H}$  COSY spectrum of **1** in MeOD.

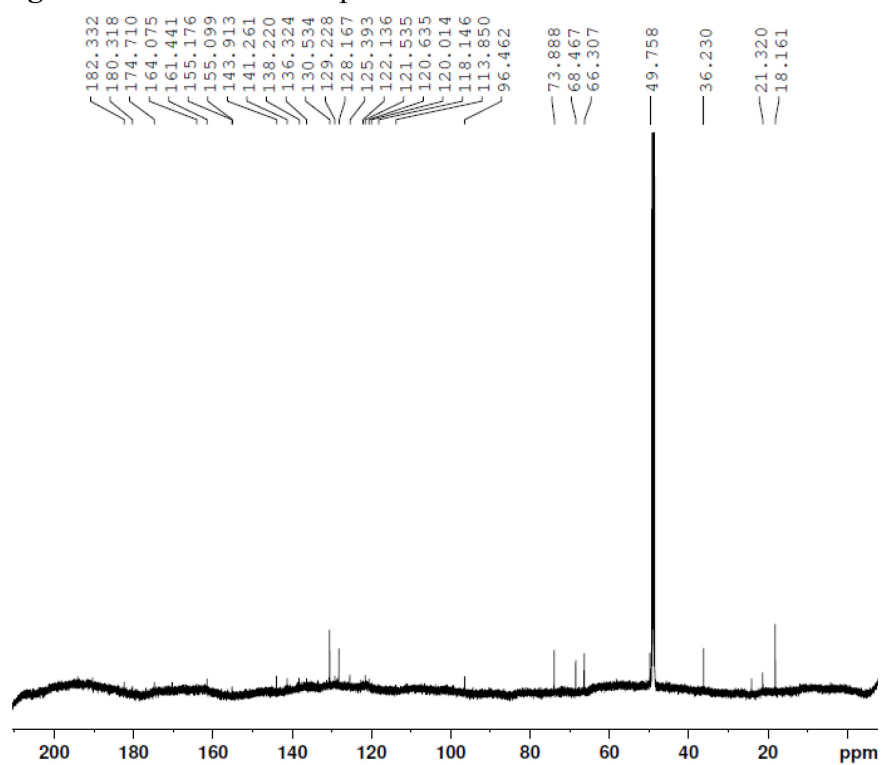
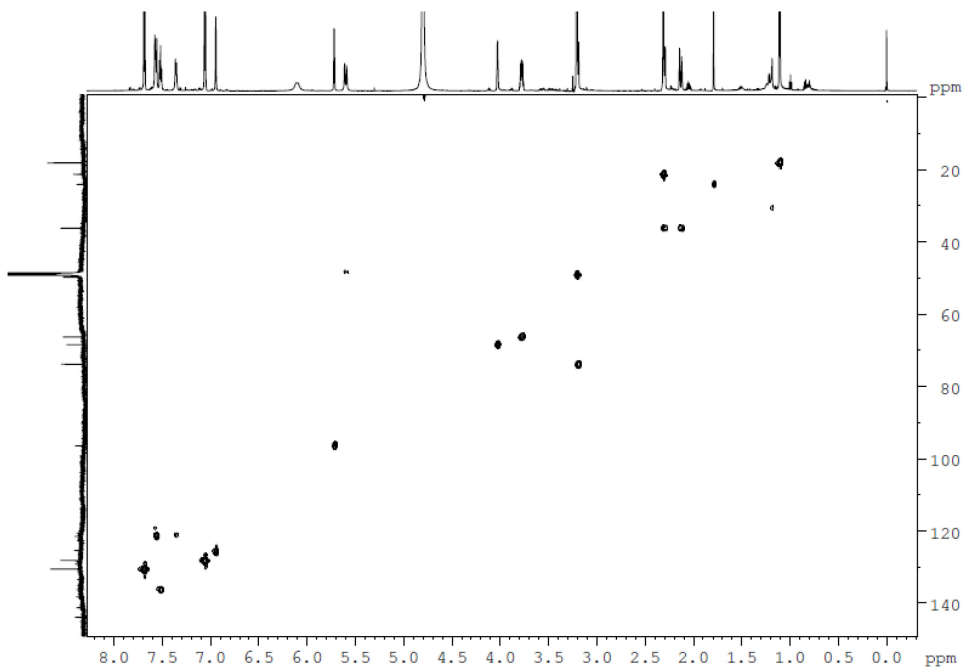
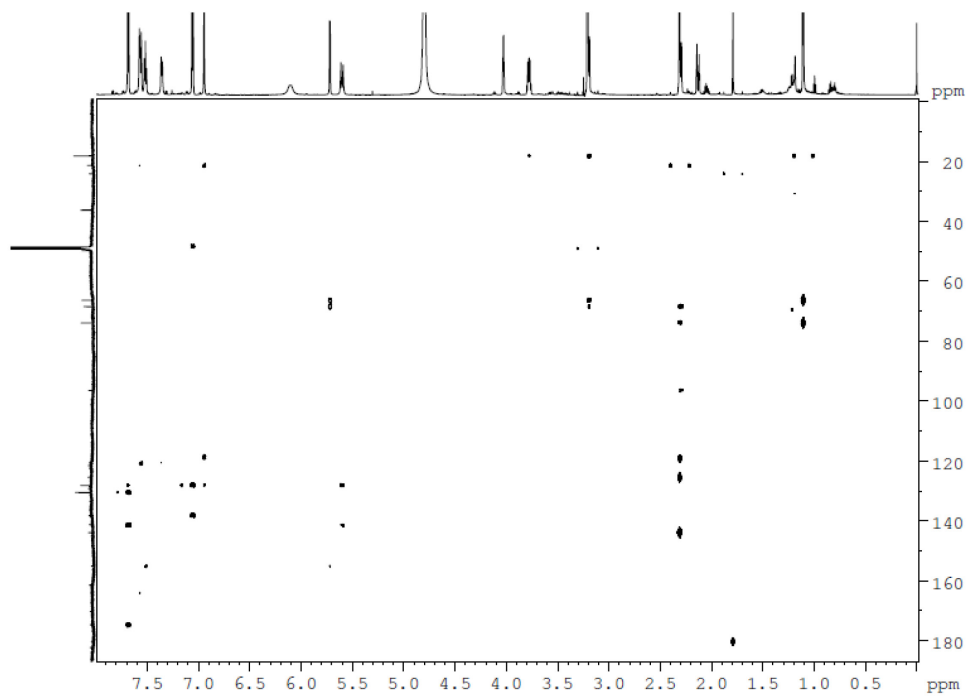


Figure S4.  $^{13}\text{C}$ -NMR spectrum of **1** in MeOD ( $^{13}\text{C}$ : 176 MHz).



**Figure S5.** Edited-HSQC ( $^1\text{H}$ - $^{13}\text{C}$ ) spectrum of **1** in MeOD,  $\text{CH}_3/\text{CH}$  phased up (blue),  $\text{CH}_2$  phased down (green).



**Figure S6.**  $^1\text{H}$ - $^{13}\text{C}$  HMBC spectrum of **1** in MeOD.

## 7.2 Jadomycin 3-AMBA Data

### 7.2.1 Jadomycin 3-AMBA Acetate Major (2a)

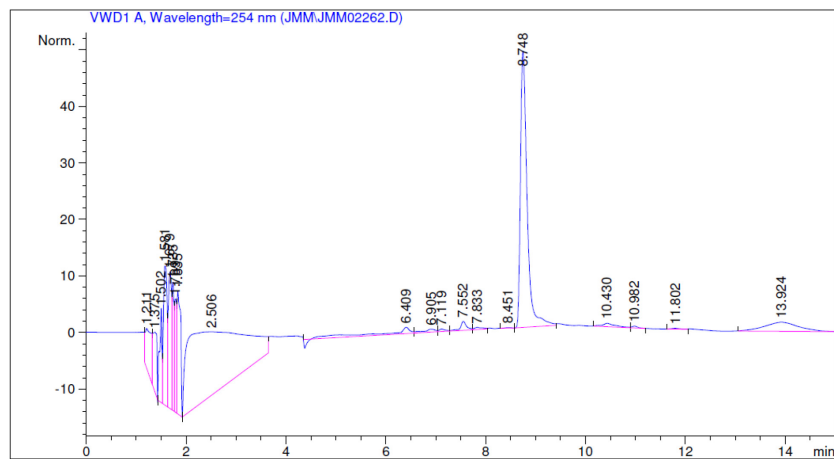


Figure S7. Analytical HPLC trace of 1a.

Acquisition Parameter		Ion Polarity	Negative	Set Corrector Fill	47 V
Source Type	ESI	Capillary Exit	-100.0 V	Set Pulsar Pull	382 V
Scan Range	n/a	Hexapole RF	140.0 V	Set Pulsar Push	382 V
Scan Begin	50 m/z	Skimmer 1	-50.0 V	Set Reflector	1300 V
Scan End	1500 m/z	Hexapole 1	-24.0 V	Set Flight Tube	9000 V
				Set Detector TOF	2200 V

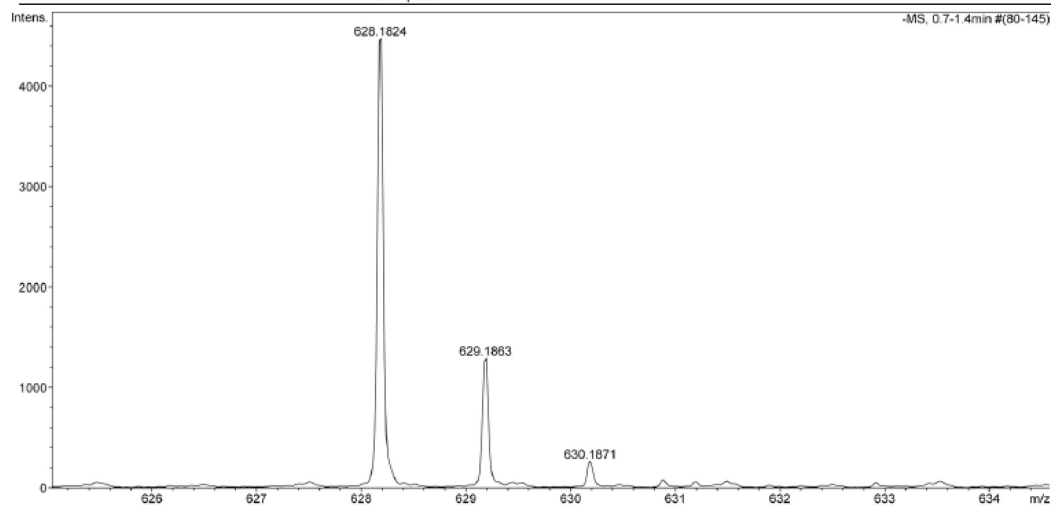
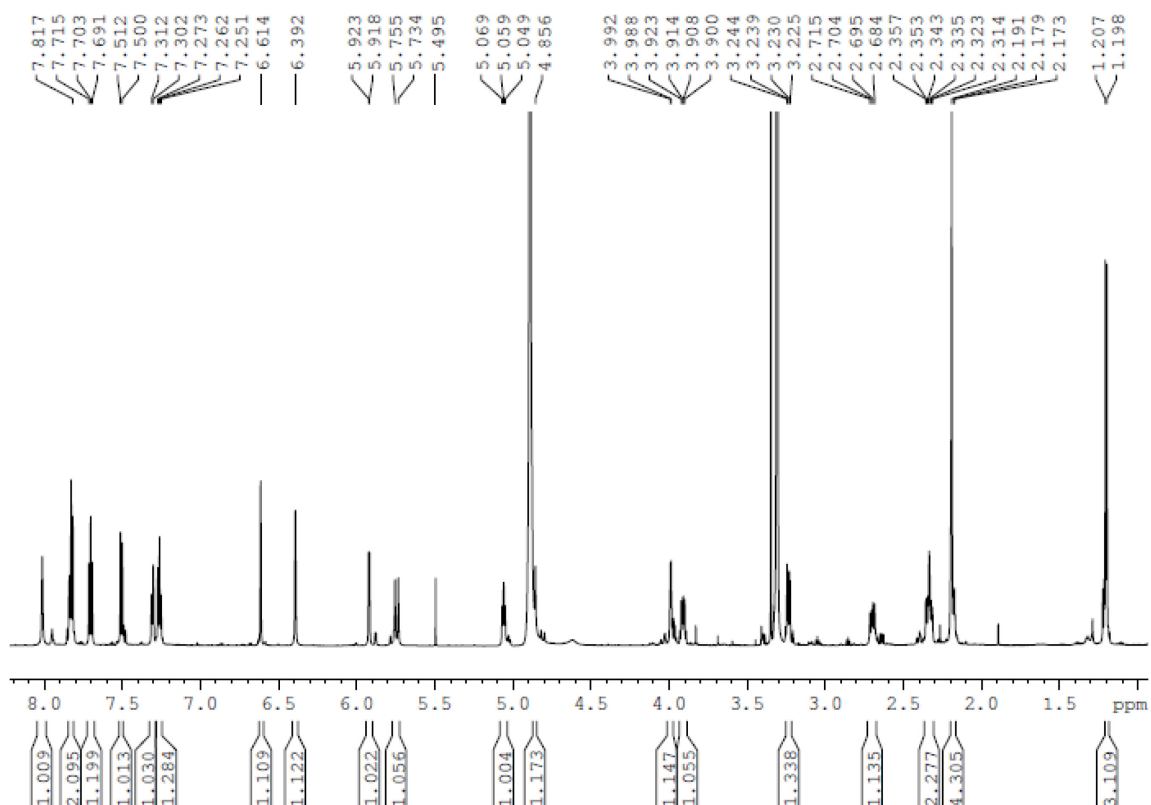
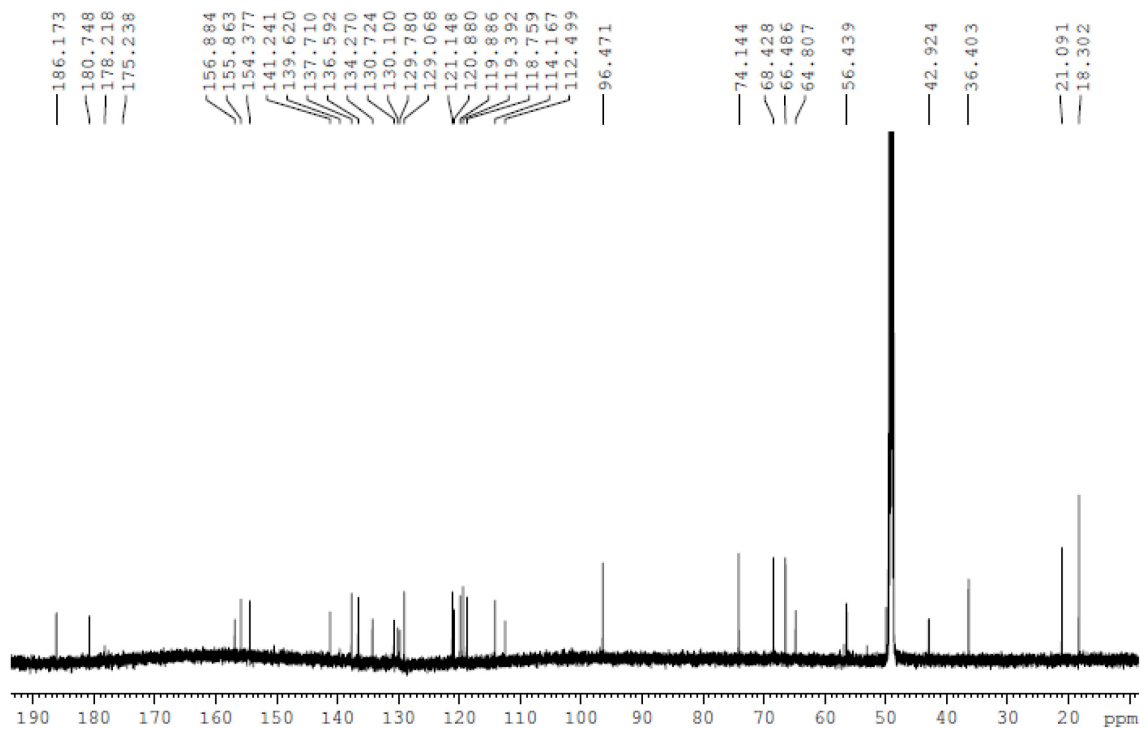


Figure S8. High resolution MS of 1a. HRMS (ESI-) for  $C_{34}H_{30}NO_{11}$   $[M-H]^-$ , 628.1824 found, 628.1824 calculated.



**Figure S9.**  $^1\text{H}$  NMR of **2a** in MeOD (1H: 700 MHz).



**Figure S10.**  $^{13}\text{C}$  NMR of **2a** in MeOD (13C: 176 MHz).

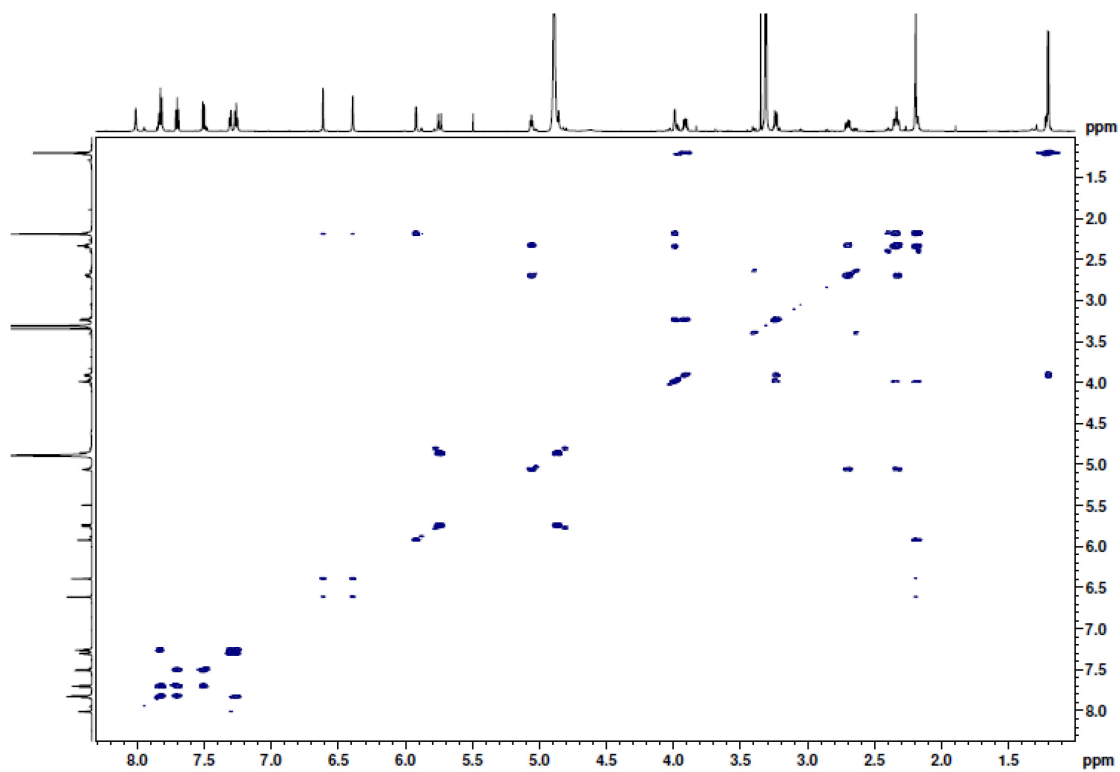


**Figure S11.**  $^1\text{H}$ - $^1\text{H}$  COSY of **2a** in MeOD.

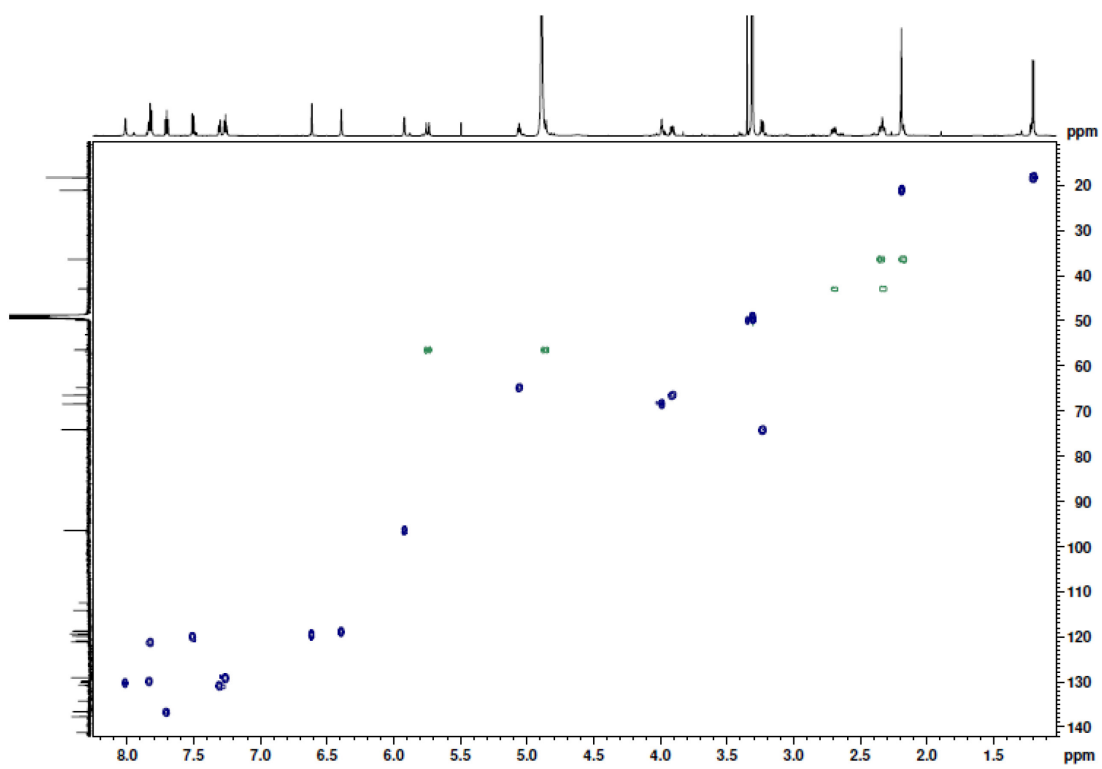


**Figure S12.**  $^1\text{H}$ - $^{13}\text{C}$  Edited HSQC of **2a** in MeOD.  $\text{CH}_3/\text{CH}$  phased up (blue),  $\text{CH}_2$  phased down (green).

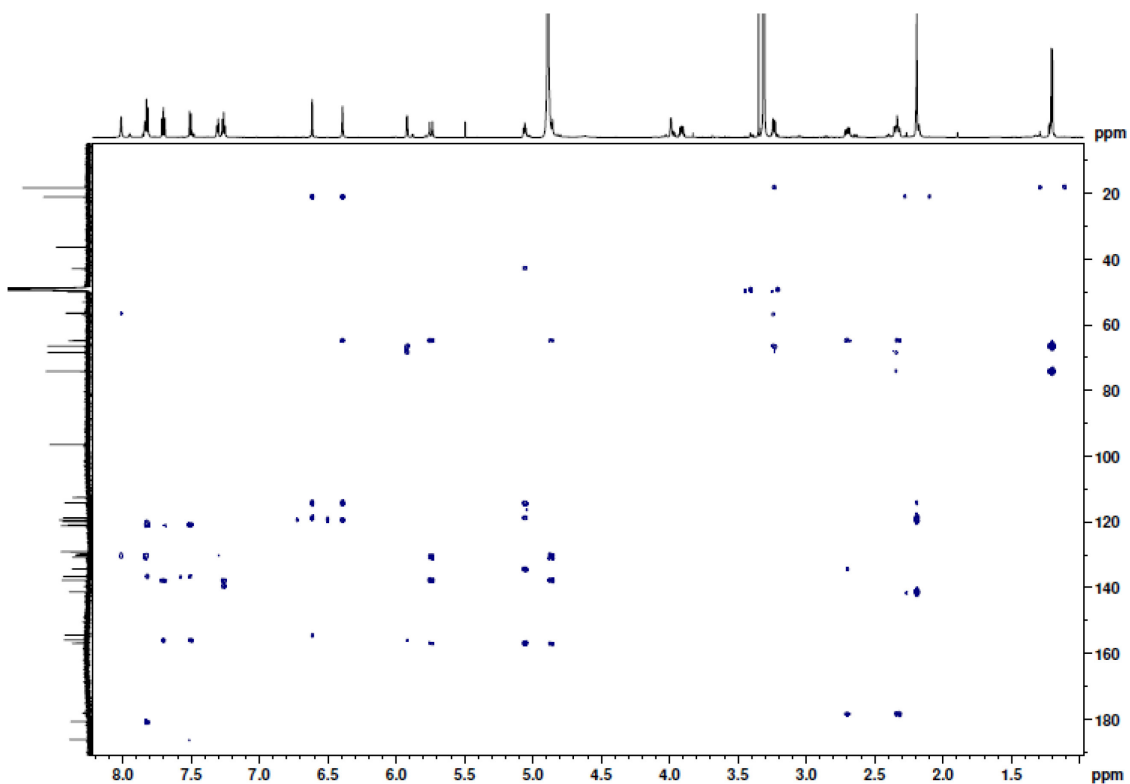


Figure S13.  $^1\text{H}$ - $^{13}\text{C}$  HMBC spectrum of **2a** in MeOD.

## 7.2.2 Jadomycin 3-AMBA Acetate Minor (**2b**)

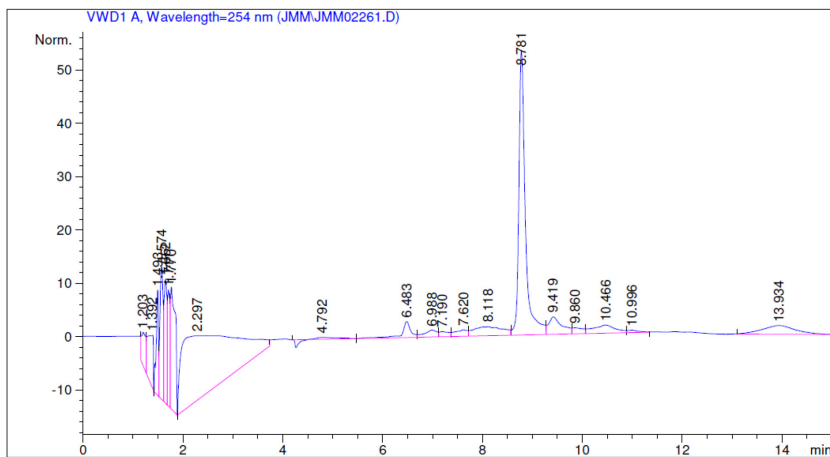
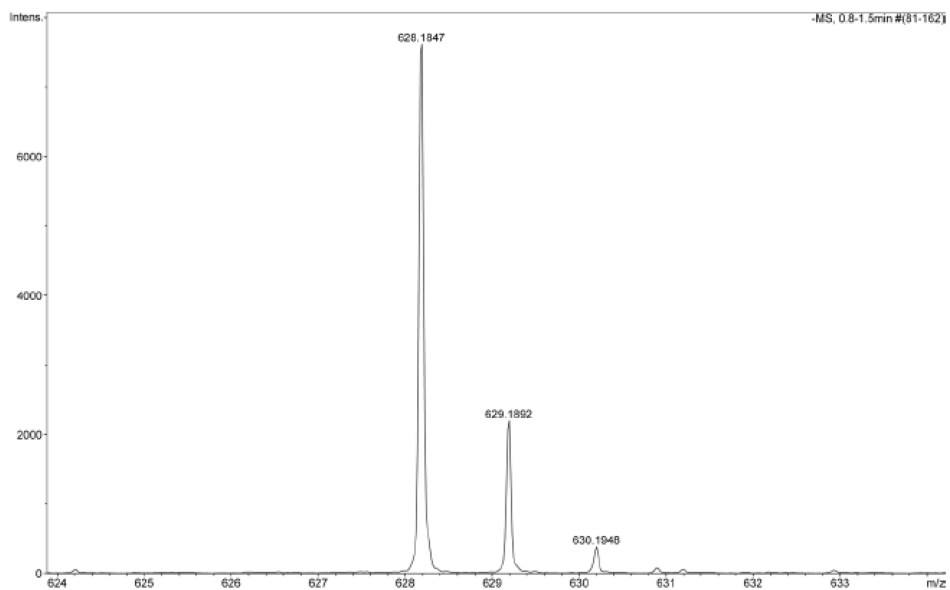
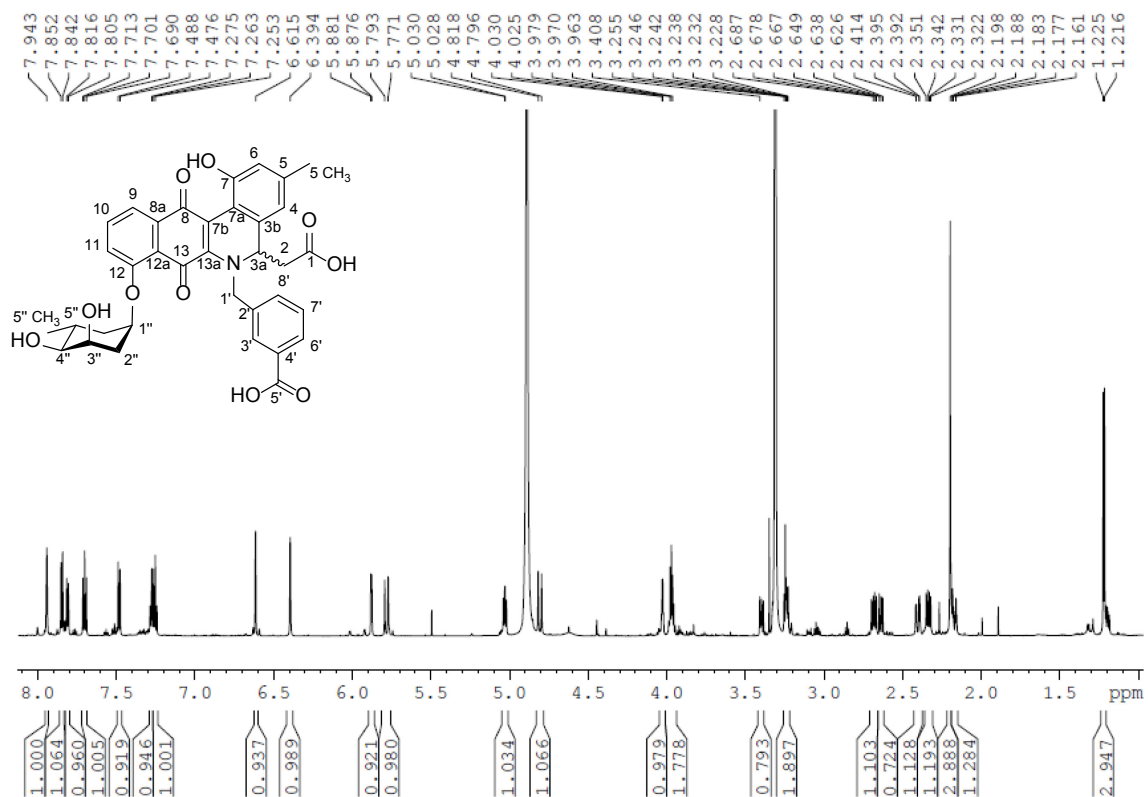


Figure S14. Analytical HPLC trace of **2b**.



**Figure S15.** High resolution MS of **2b**. HRMS (ESI-) for  $C_{34}H_{30}NO_{11}$   $[M-H]^-$ , 628.1847 found, 628.1824 calculated.



**Figure S16.**  $^1H$  NMR of **2b** in MeOD (1H: 700 MHz).



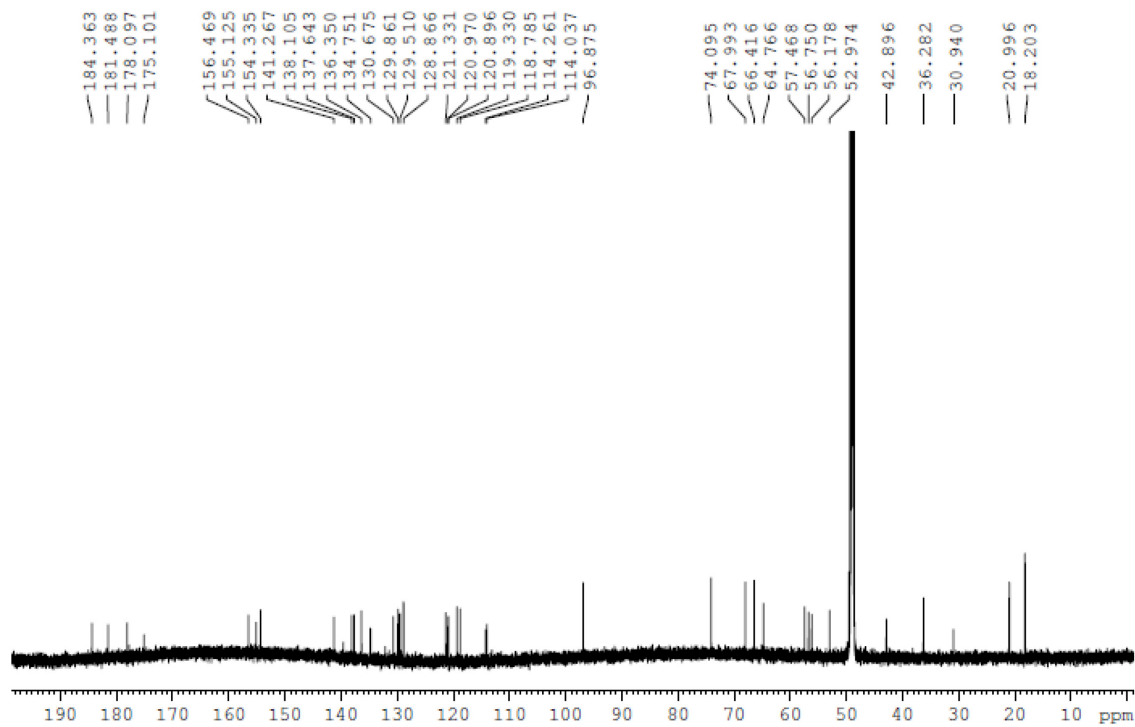


Figure S17.  $^{13}\text{C}$  NMR of **2b** in MeOD ( $^{13}\text{C}$ : 176 MHz).

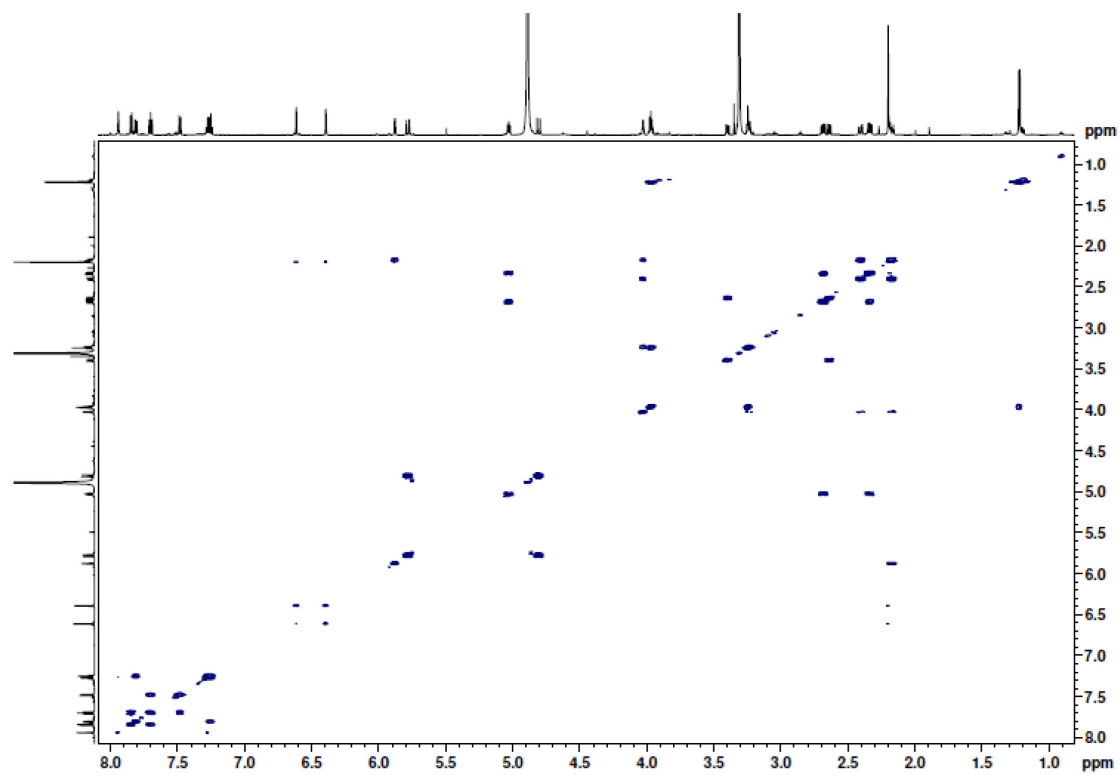
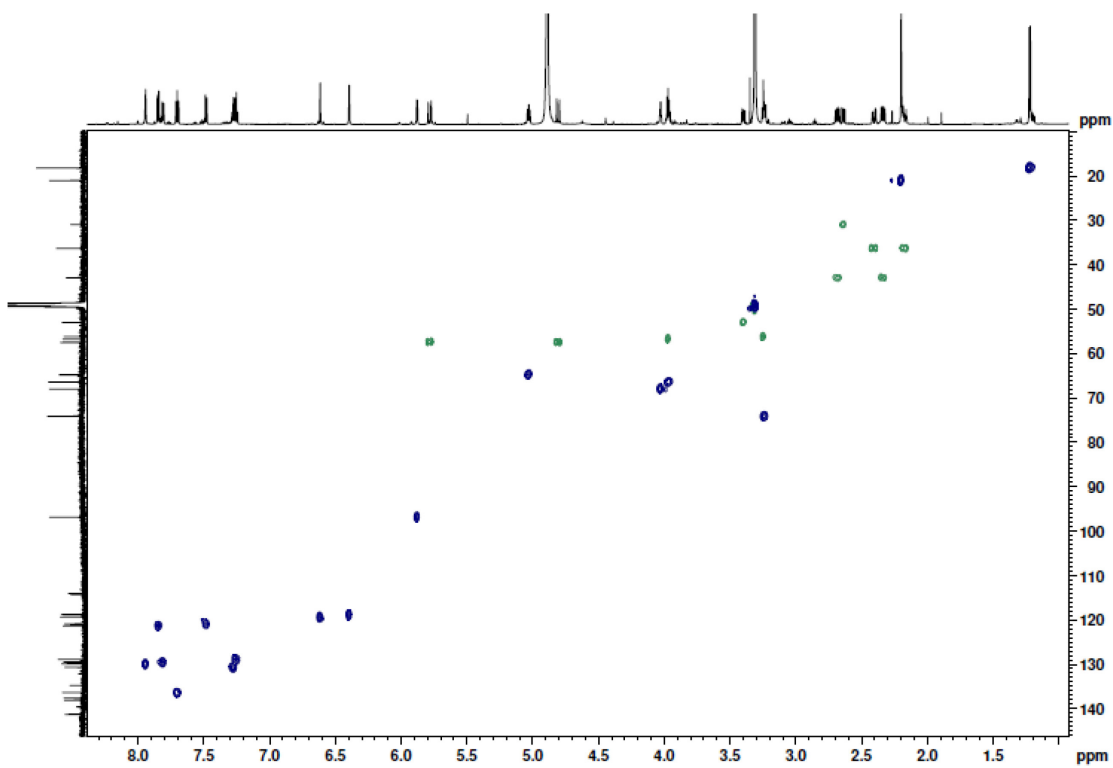
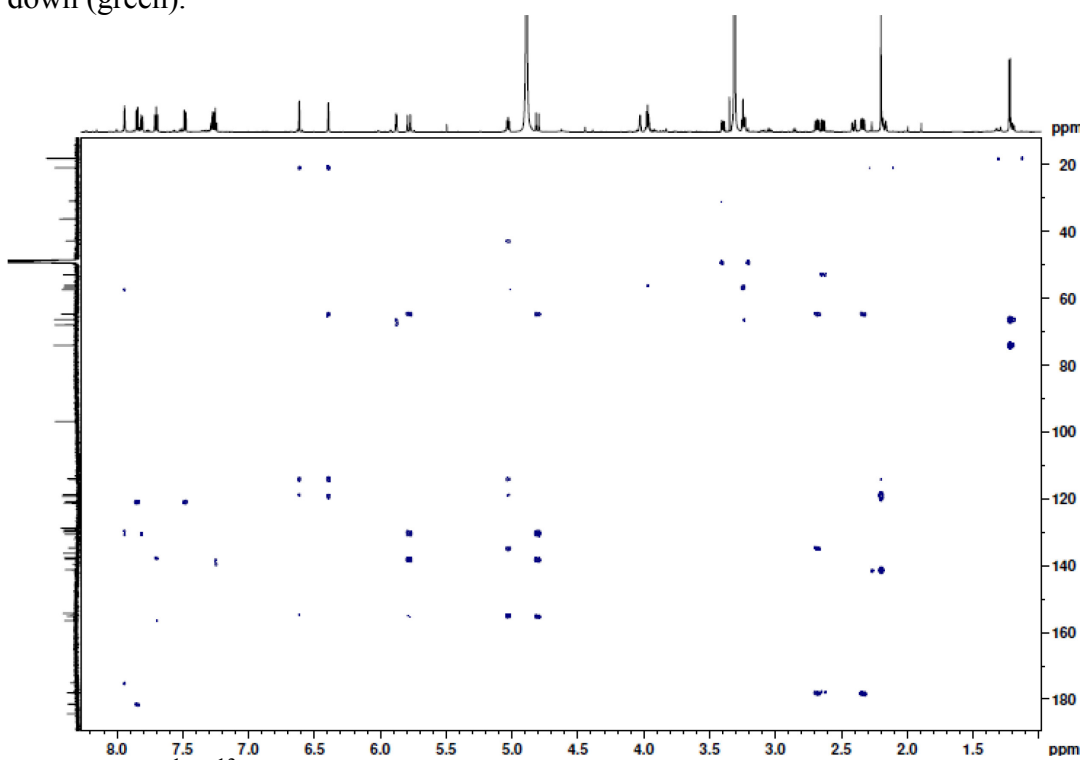


Figure S18.  $^1\text{H}$ - $^1\text{H}$  COSY of **2b** in MeOD.



**Figure S19.**  $^1\text{H}$ - $^{13}\text{C}$  Edited HSQC of **2b** in MeOD.  $\text{CH}_3/\text{CH}$  phased up (blue),  $\text{CH}_2$  phased down (green).



**Figure S20.**  $^1\text{H}$ - $^{13}\text{C}$  HMBC spectrum of **2b** in MeOD.

### 7.2.3 Jadomycin 3-AMBA 3a-Methoxy (3)

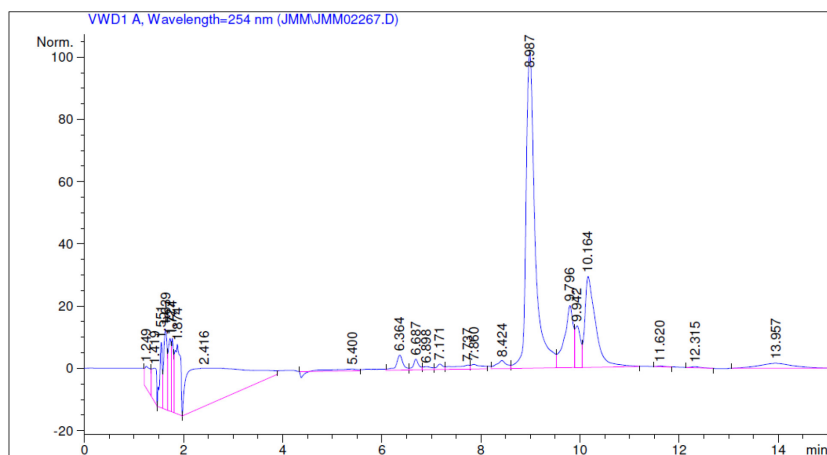


Figure S21. Analytical HPLC trace of **3**.

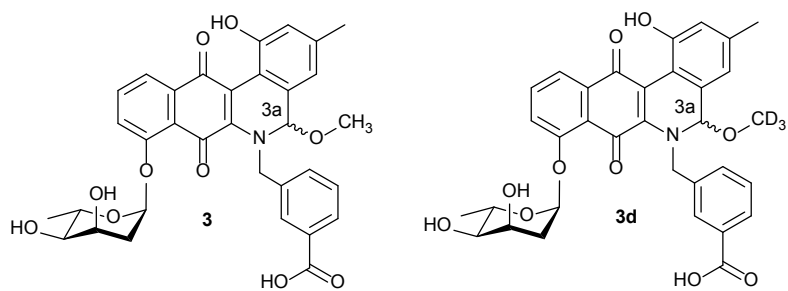
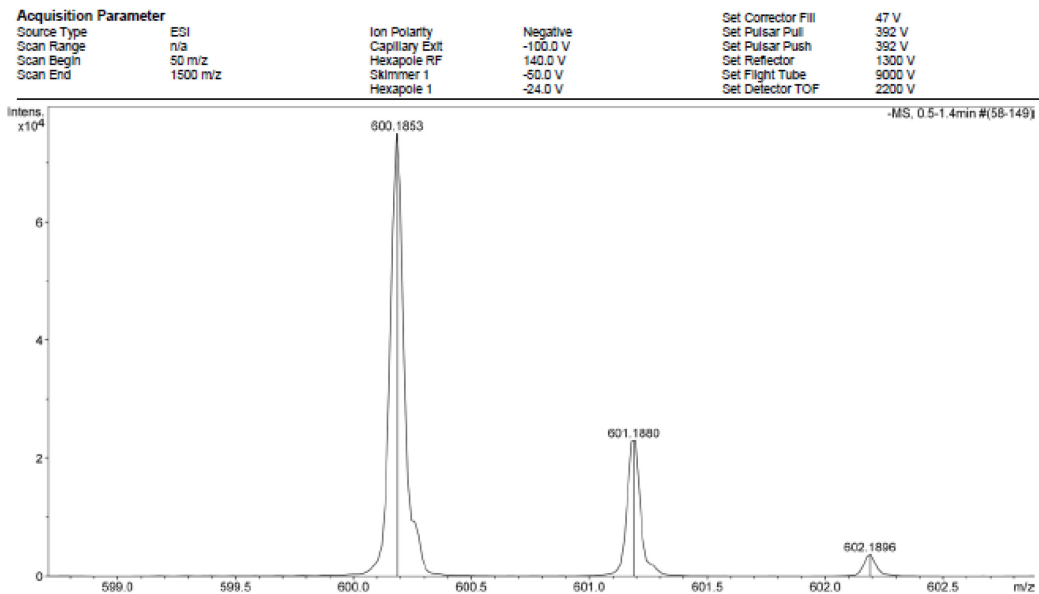
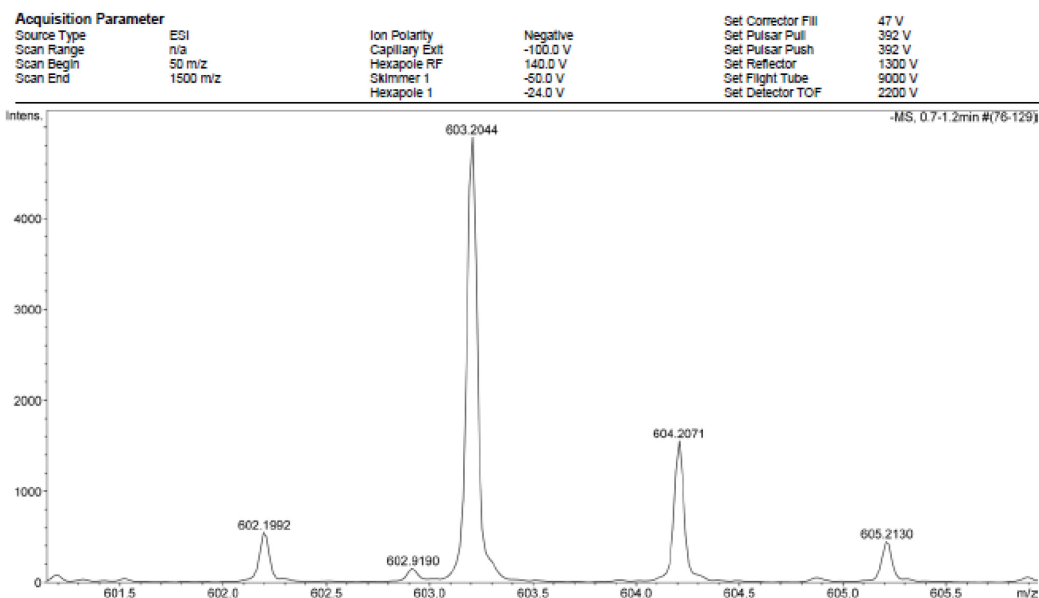


Figure S22. Structures of **3** and **3d**.



**Figure S23.** High resolution MS of **3**. HRMS (ESI-) for  $C_{33}H_{30}NO_{10}$   $[M-H]^-$ , 600.1853 found, 600.1875 calculated.



**Figure S24.** High resolution MS of **3d**. HRMS (ESI-) for  $C_{33}H_{27}D_3NO_{10}$   $[M-H]^-$ , 603.2044 found, 603.2064 calculated.

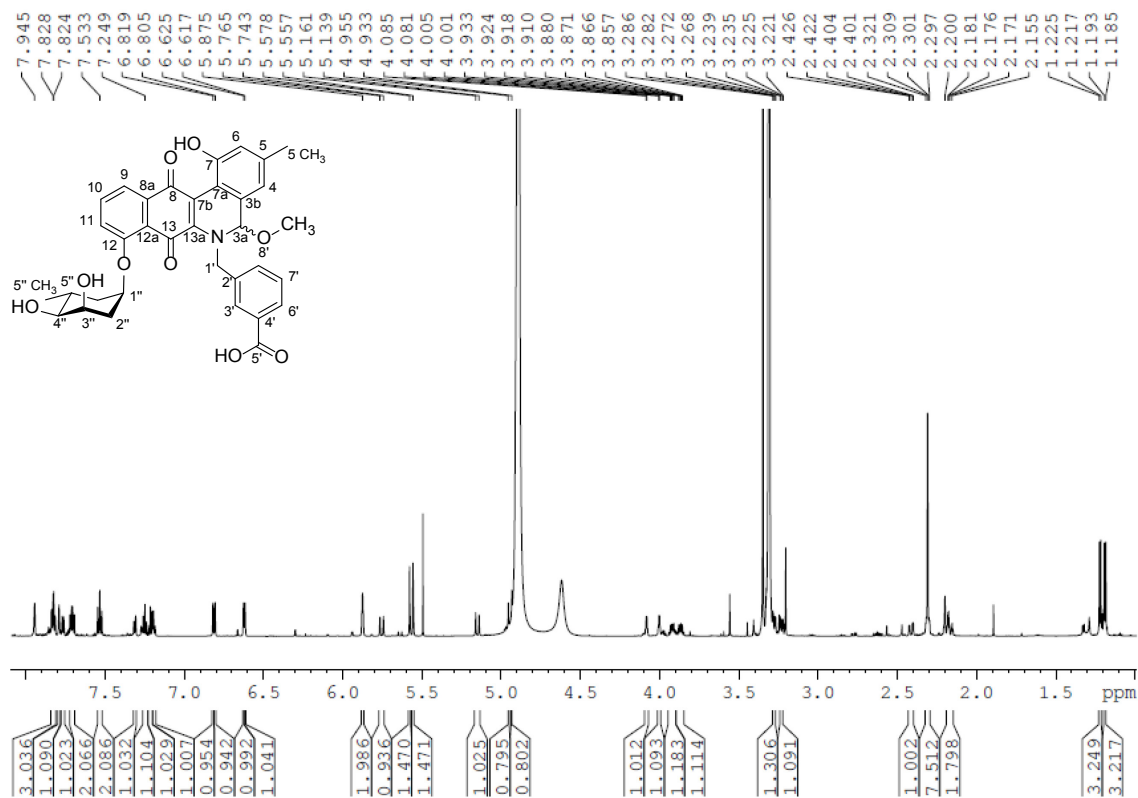


**Figure S25.** <sup>1</sup>H NMR of **3** (mixture of diastereomers) in MeOD (1H: 700 MHz).

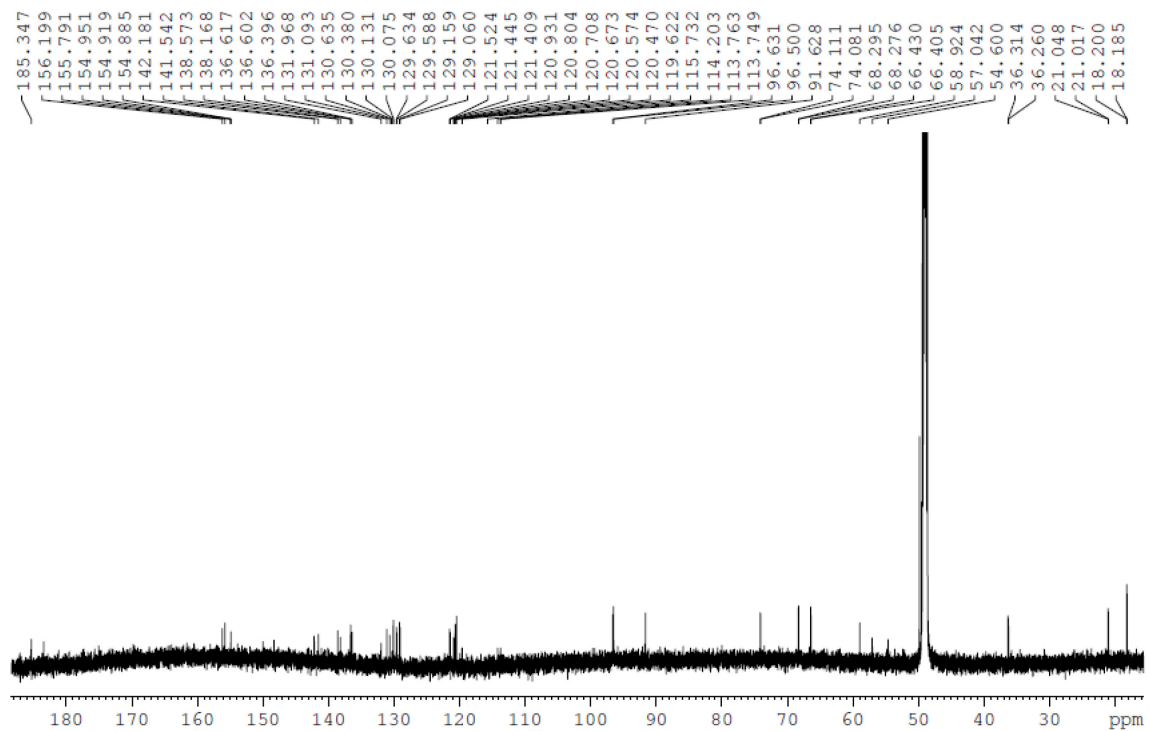


**Figure S26.** <sup>13</sup>C NMR of **3** (mixture of diastereomers) in MeOD (13C: 176 MHz).

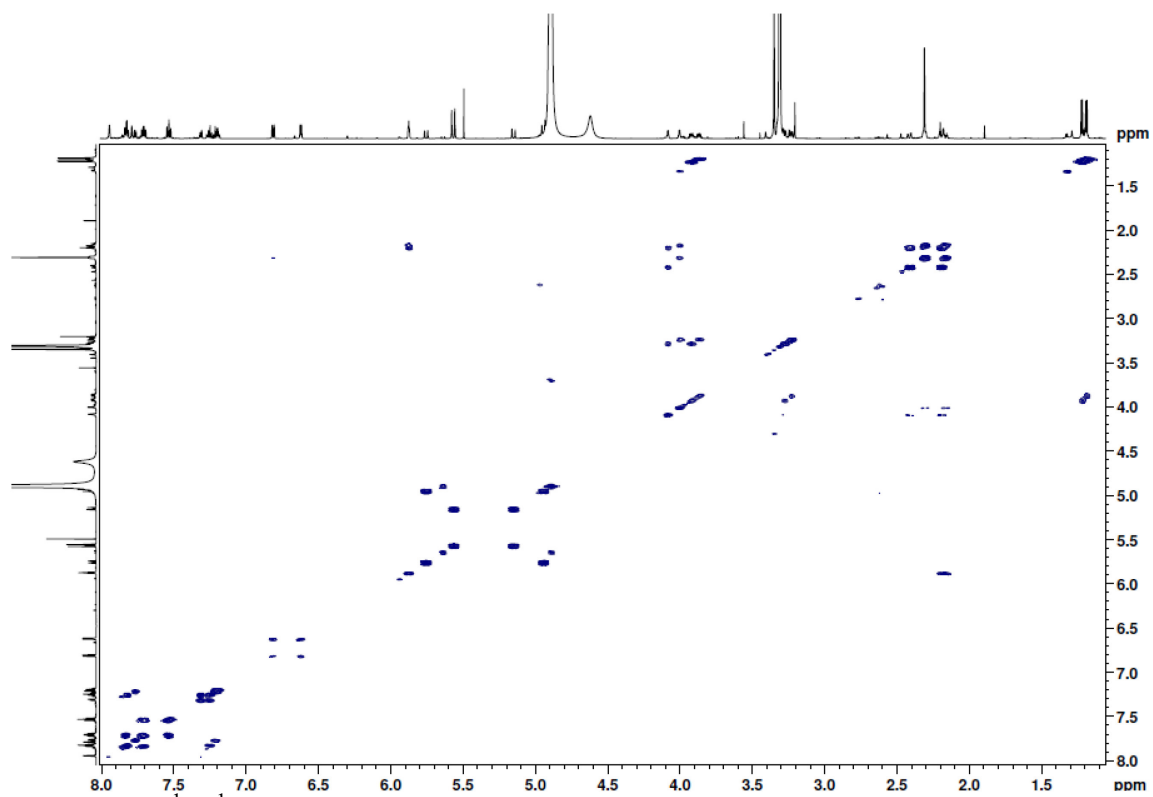


Figure S27.  $^1\text{H}$ - $^1\text{H}$  COSY of 3 (mixture of diastereomers) in MeOD.

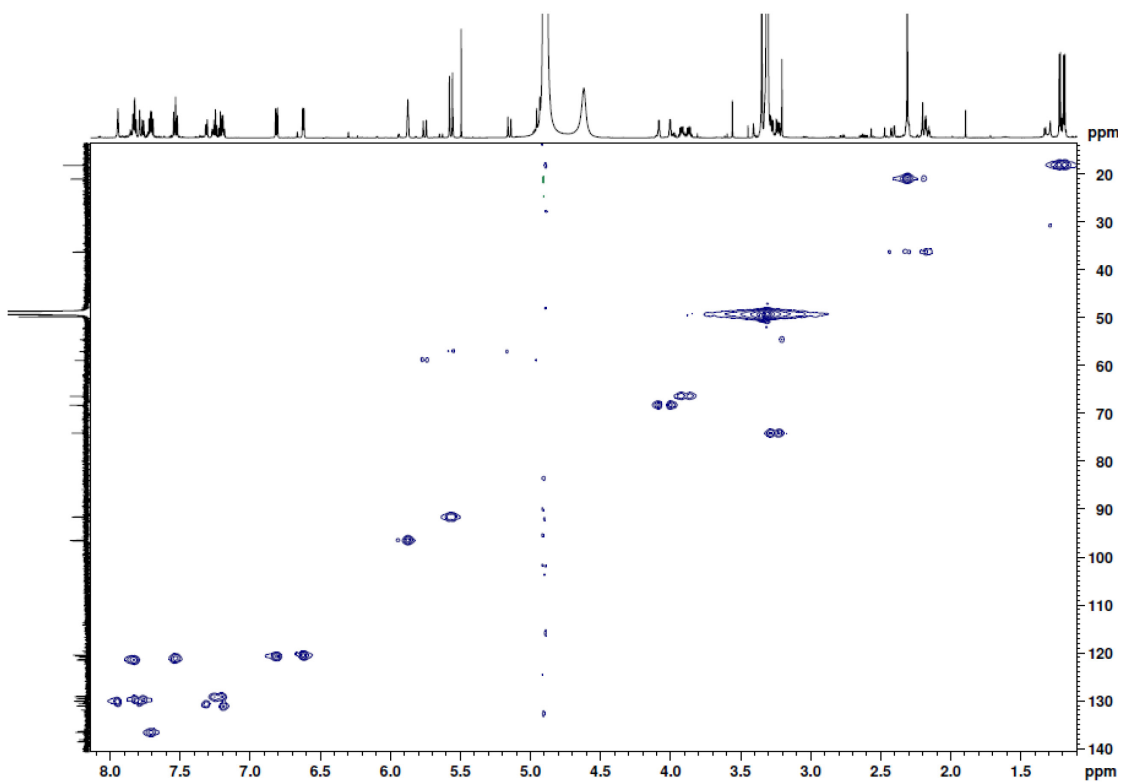


Figure S28.  $^1\text{H}$ - $^{13}\text{C}$  HSQC of 3 (mixture of diastereomers) in MeOD.

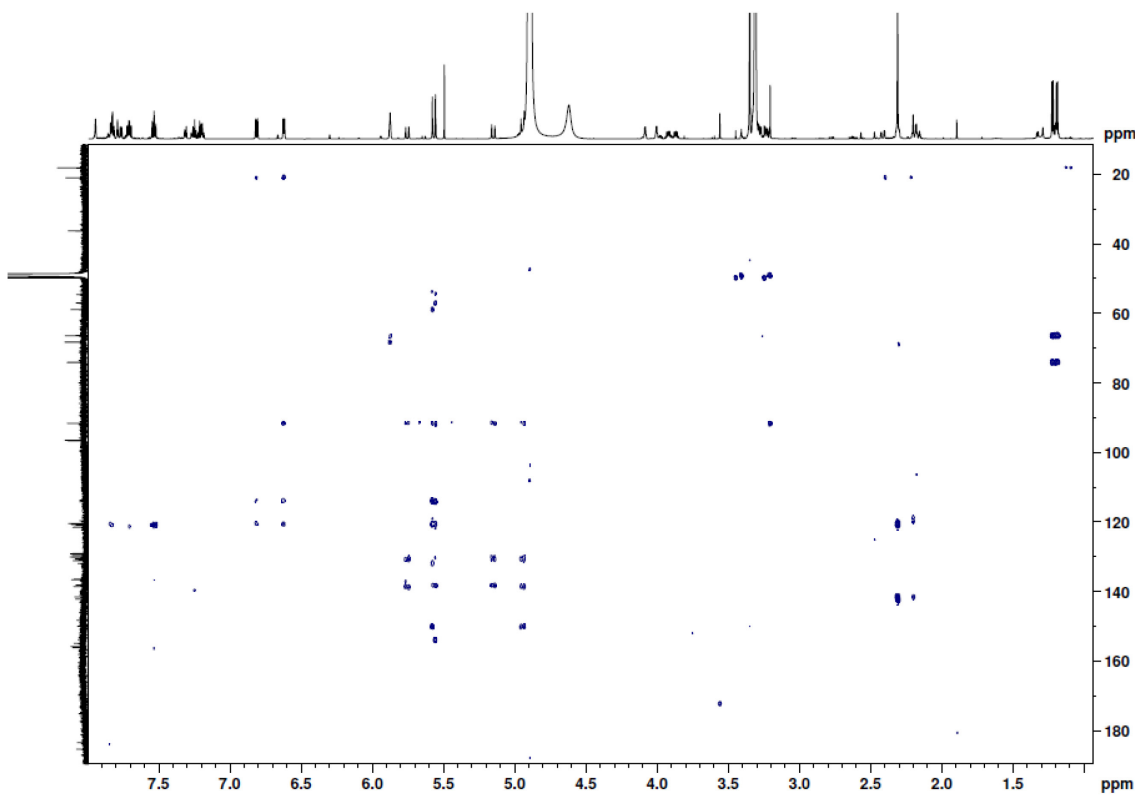


Figure S29.  $^1\text{H}$ - $^{13}\text{C}$  HMBC spectrum of **3** (mixture of diastereomers) in MeOD.

## 7.2.4 Jadomycin 3-AMBA Lactam (**4**)

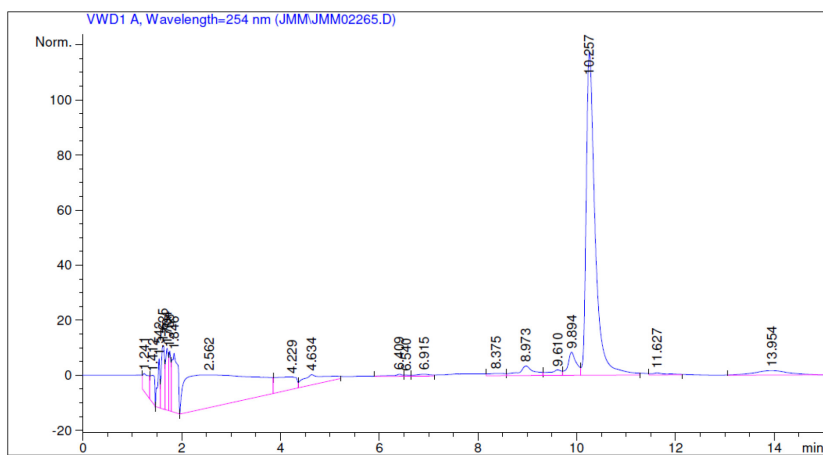
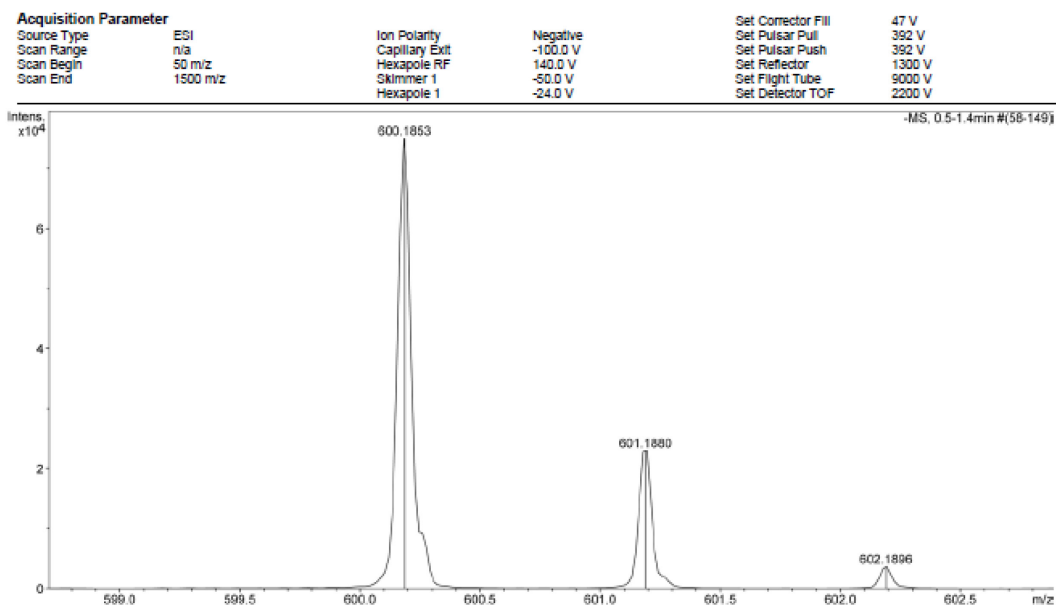
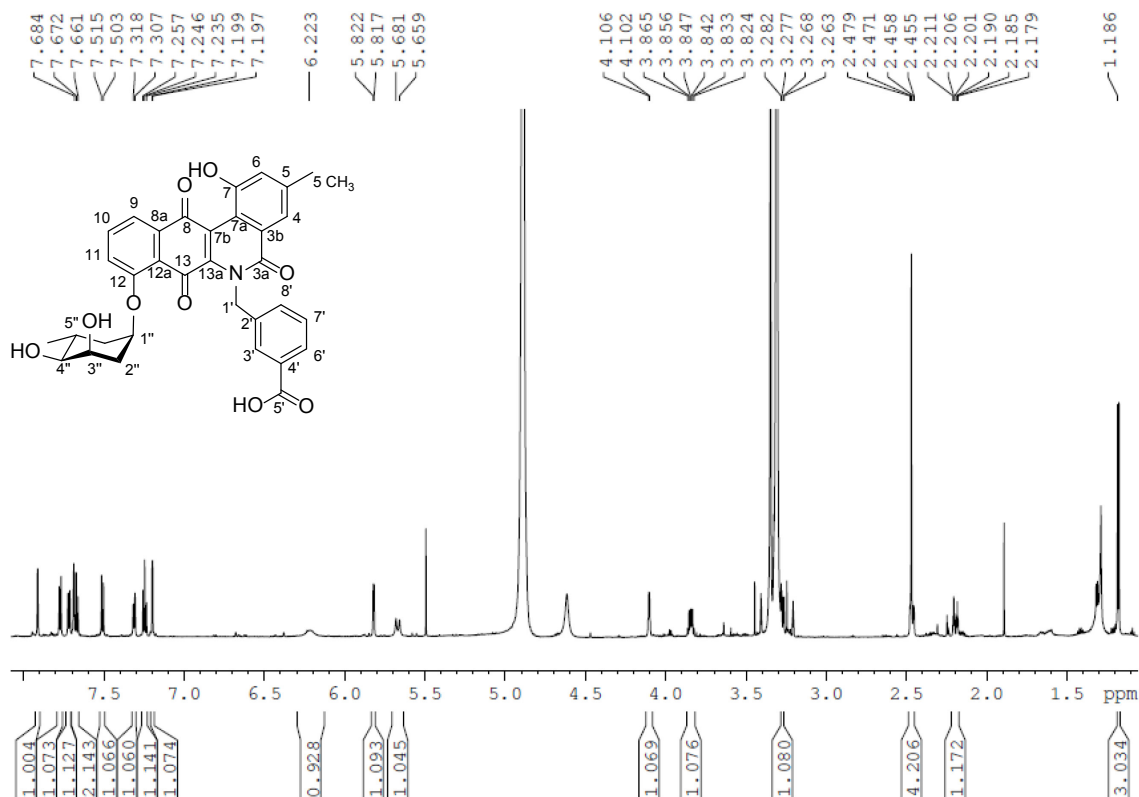


Figure S30. Analytical HPLC trace of **4**.



**Figure S31.** High resolution MS of **4**. HRMS (ESI-) for  $C_{32}H_{26}NO_{10}$   $[M-H]^-$ , 584.1542 found, 584.1562 calculated.



**Figure S32.**  $^1H$  NMR of **4** in MeOD (1H: 700 MHz).



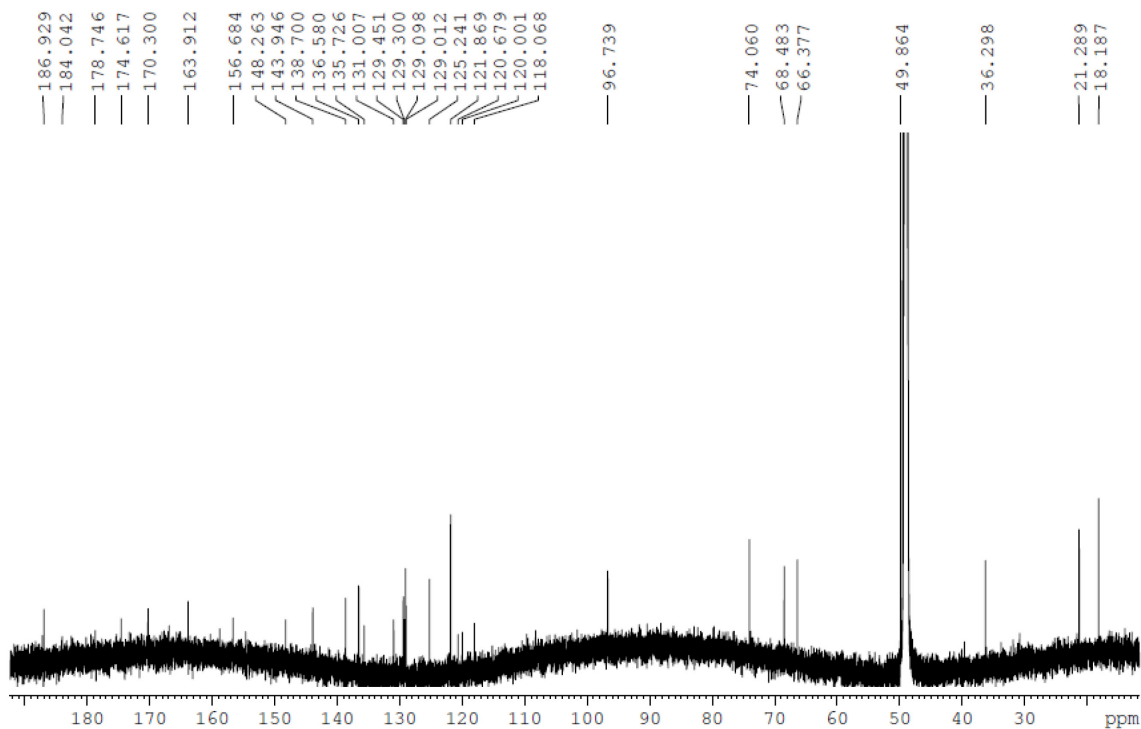


Figure S33.  $^{13}\text{C}$  NMR of **4** in MeOD ( $^{13}\text{C}$ : 176 MHz).

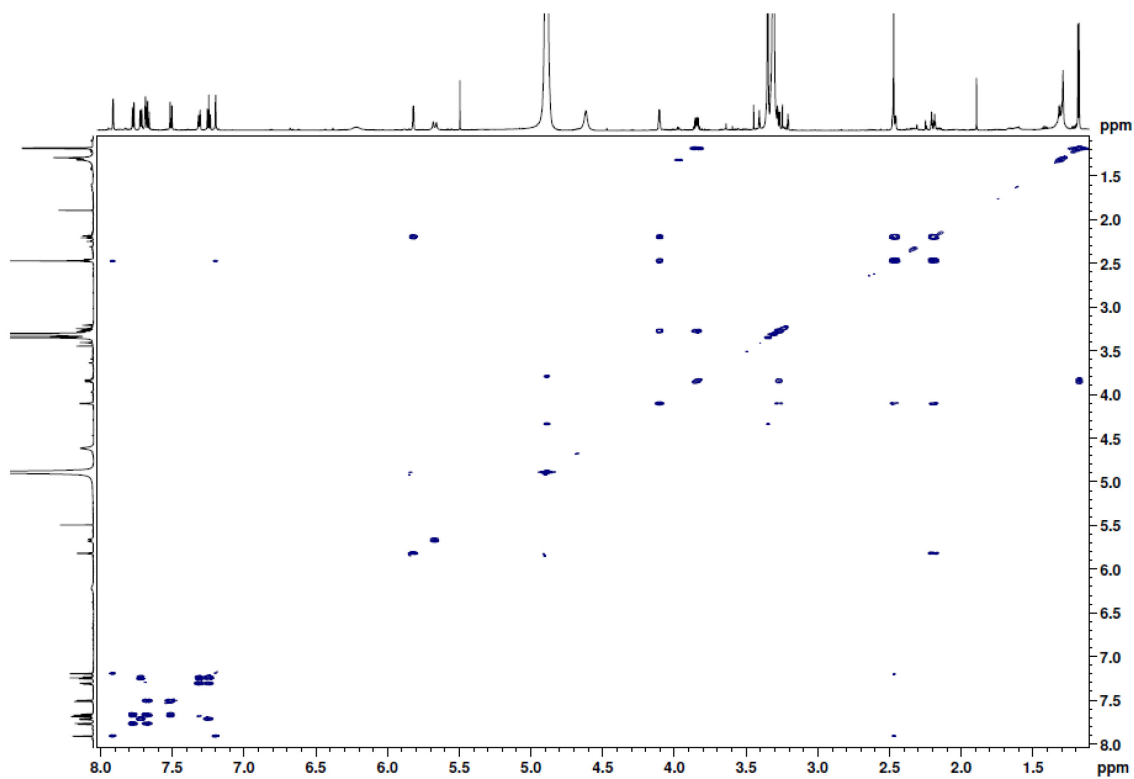


Figure S34.  $^1\text{H}$ - $^1\text{H}$  COSY of **4** in MeOD.

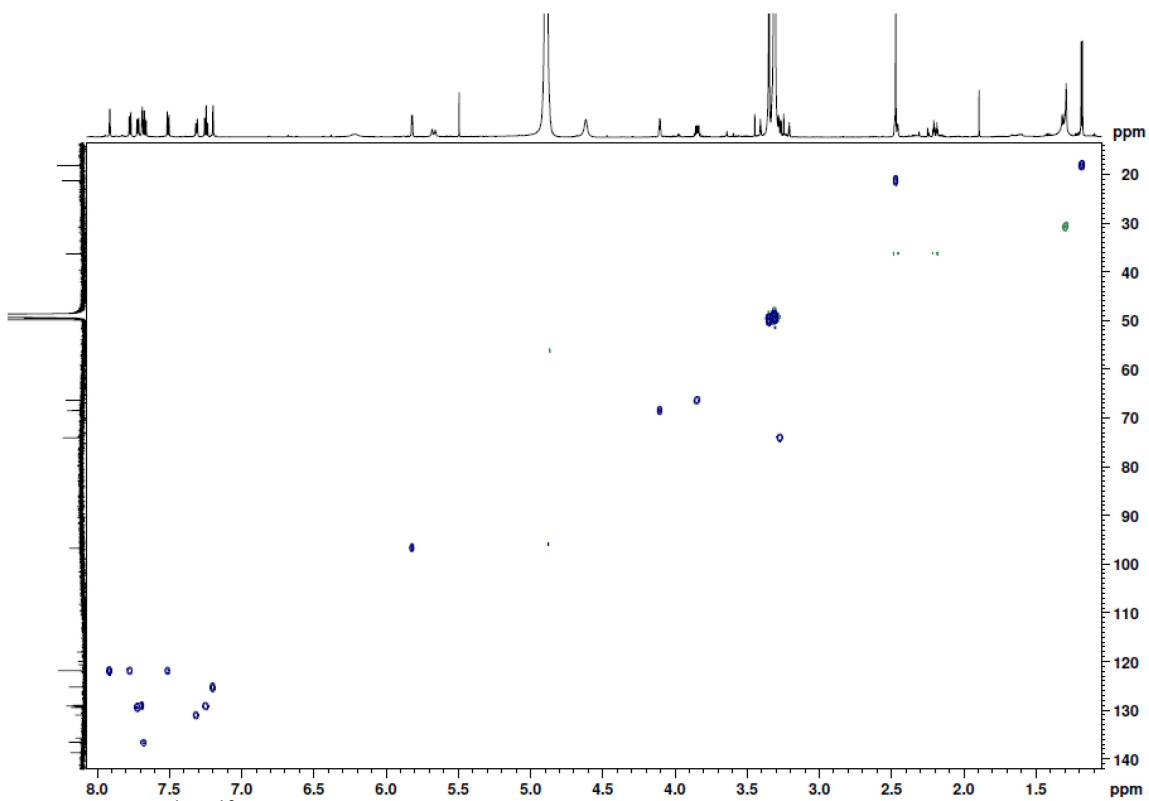


Figure S35.  $^1\text{H}$ - $^{13}\text{C}$  Edited HSQC of **4** in MeOD.

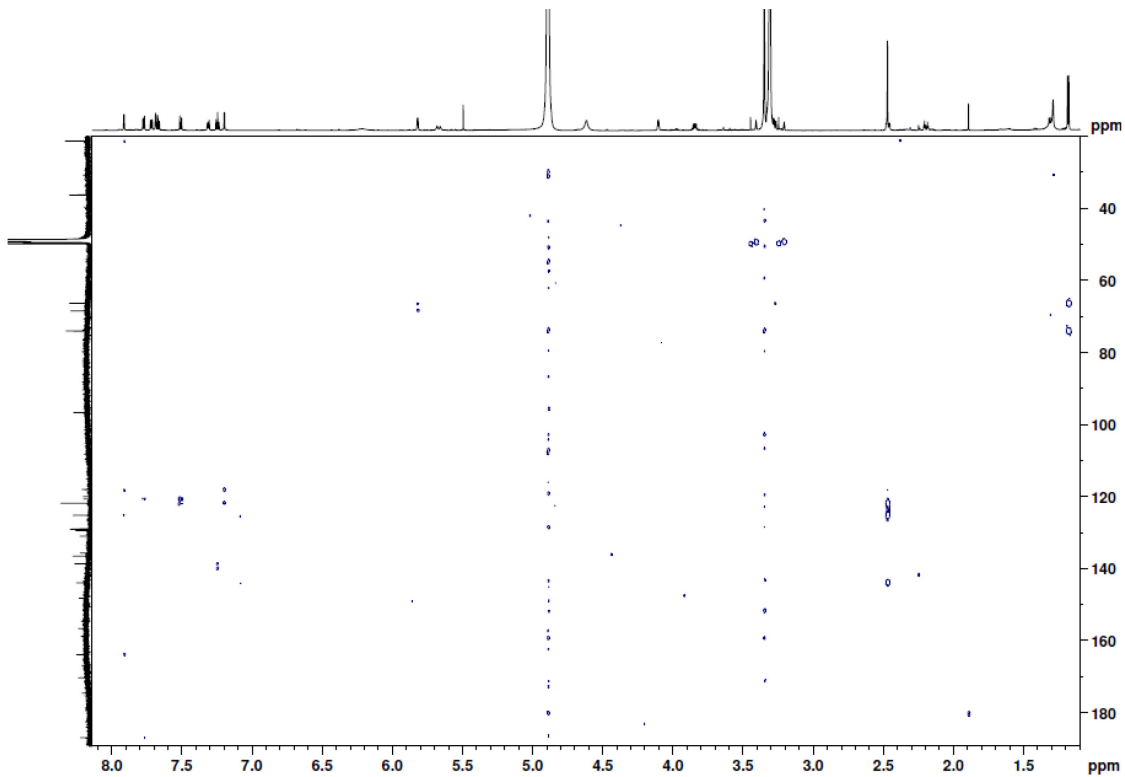
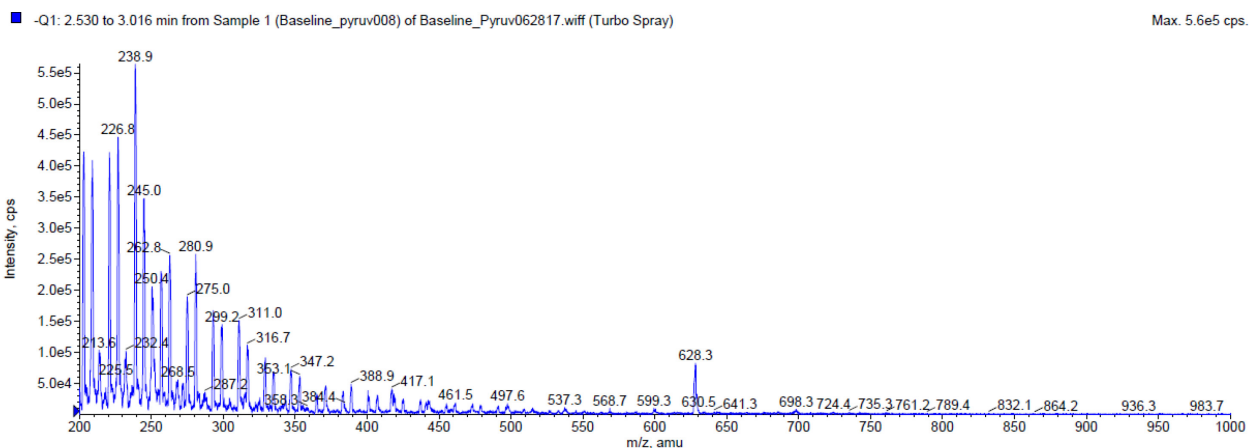


Figure S36.  $^1\text{H}$ - $^{13}\text{C}$  HMBC spectrum of **4** in MeOD.



**Figure S37.** Low resolution mass spectra Q1 (-) scan of crude culture material showing no evidence of 3-AMBA pyruvate analogue  $[M-H]^-$ .

### 7.3 Jadomycin Undec Data

#### 7.3.1 Jadomycin Undec Major (5a)

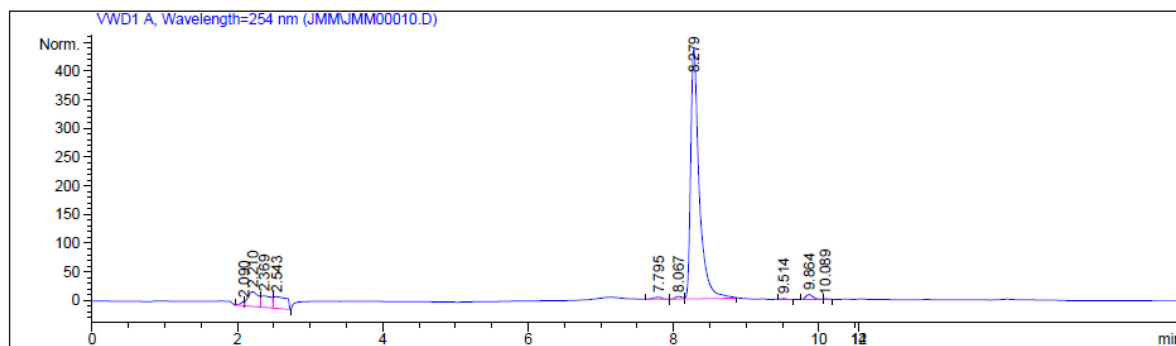


**Figure S38.** Analytical HPLC of 5a.

jadomycinundecmaj\_100ugpermL #129 RT: 1.39 AV: 1 NL: 4.11E4  
T: FTMS + p ESI Full ms2 578.30@cid0.00 [155.00-2000.00]

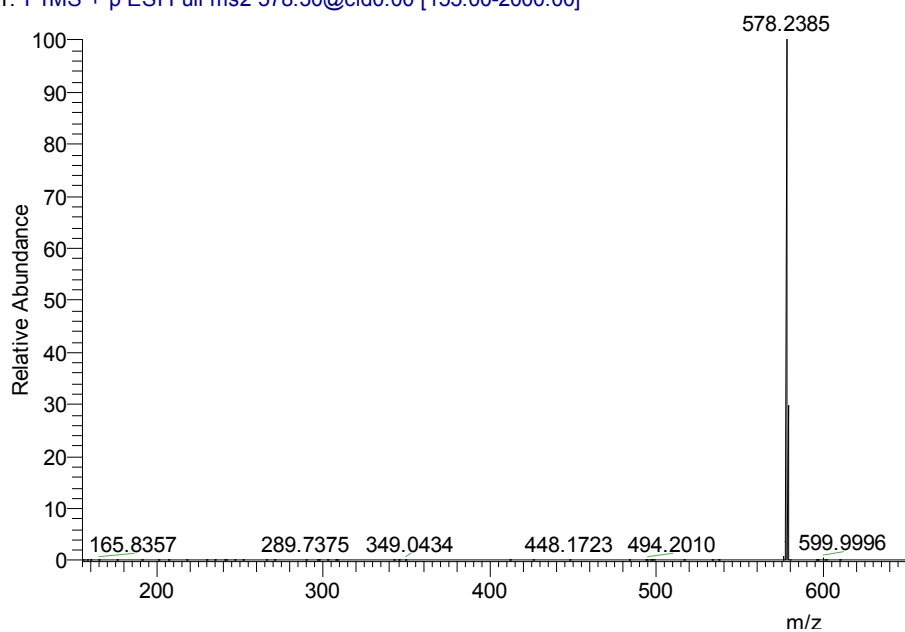
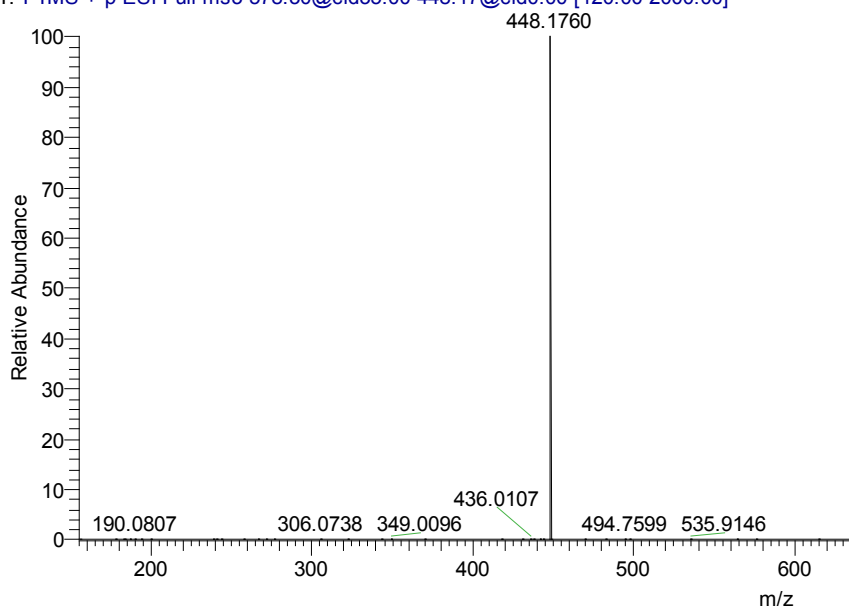


**Figure S39.** EPI<sup>+</sup> of **5a** for C<sub>32</sub>H<sub>35</sub>NO<sub>9</sub> [M+H]<sup>+</sup> (578.2385 found, 578.23846 calculated).

jadomycinundecmaj\_100ugperml #146 RT: 2.15 AV: 1 NL: 6.58E4  
T: FTMS + p ESI Full ms3 578.30@cid35.00 448.17@cid0.00 [120.00-2000.00]



jadomycinundecmaj\_100ugperml #147 RT: 2.19 AV: 1 NL: 7.00E4  
T: FTMS + p ESI Full ms3 578.30@cid35.00 448.17@cid35.00 [120.00-2000.00]

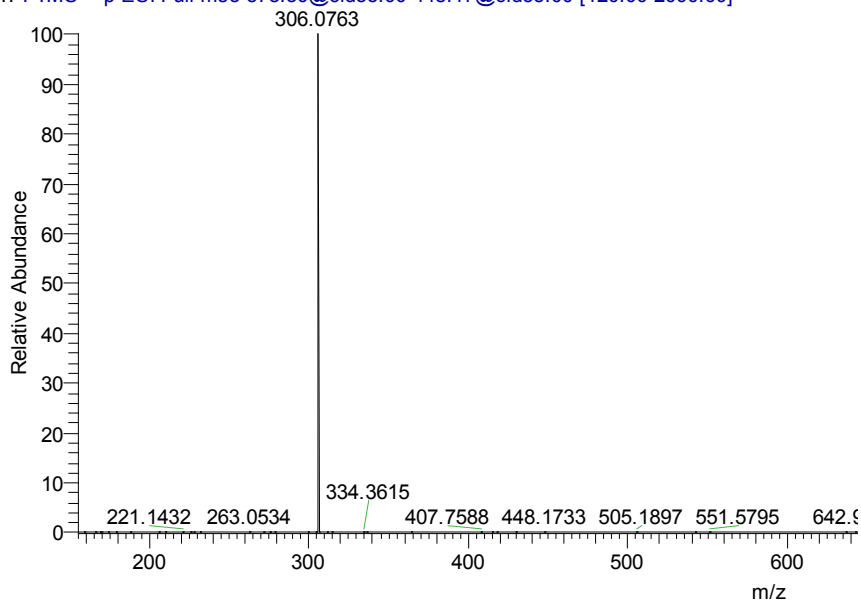


**Figure S40.** EPI+ MS/MS/MS of **5a** (578.30) found 578.2385  $[M+H]^+$ , 448.1760  $[M+H\text{-digitoxose}]^+$ , 306.0763  $M+H\text{-digitoxose-C}_8\text{H}_{14}\text{O}_2]^+$ .

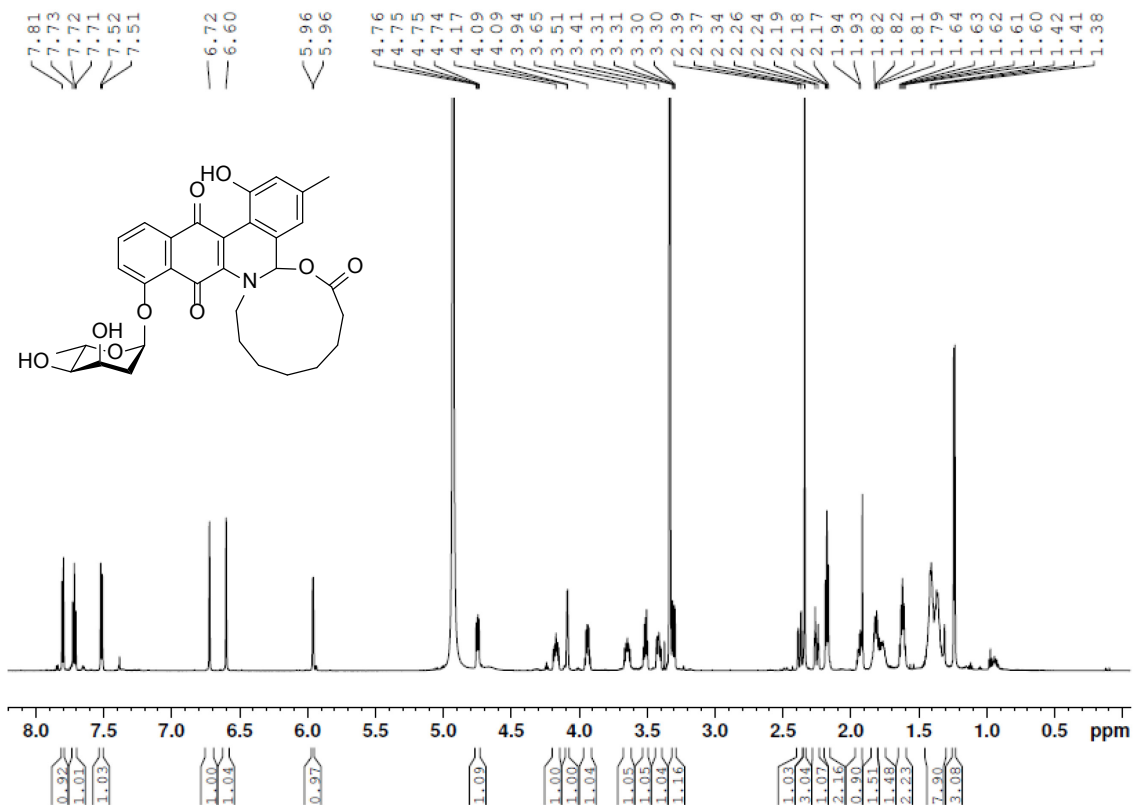


**Figure S41.** <sup>1</sup>H-NMR spectrum of **5a** in MeOD (1H: 700 MHz).

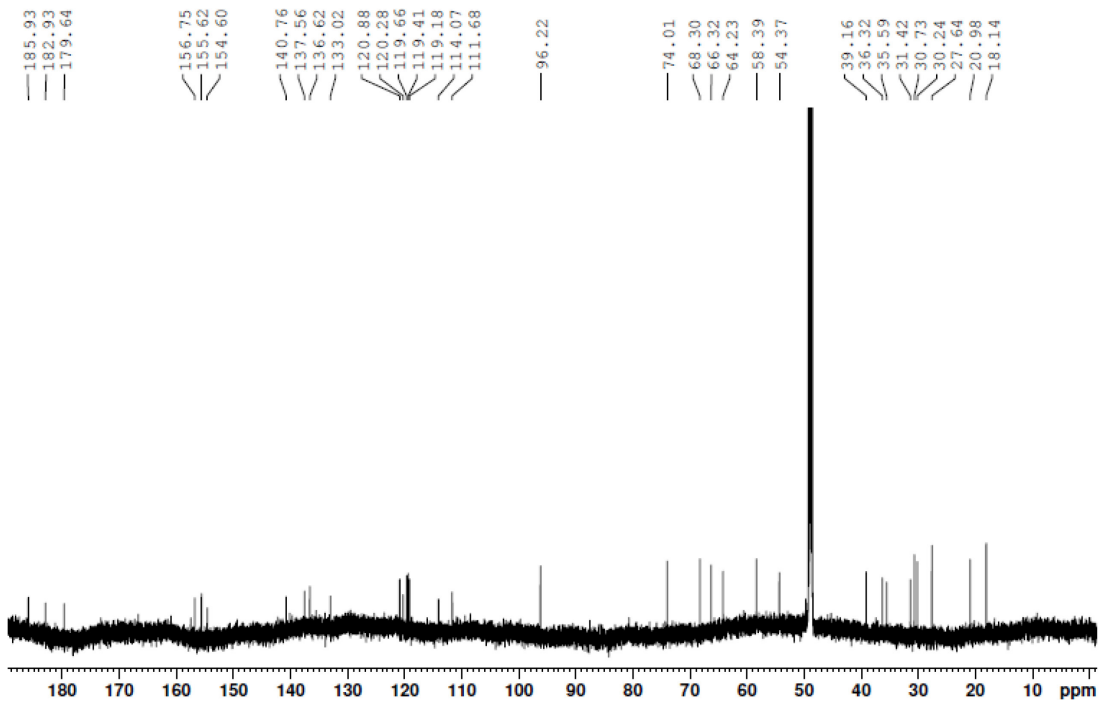


**Figure S42.** <sup>13</sup>C-NMR spectrum of **5a** in MeOD (13C: 176 MHz).

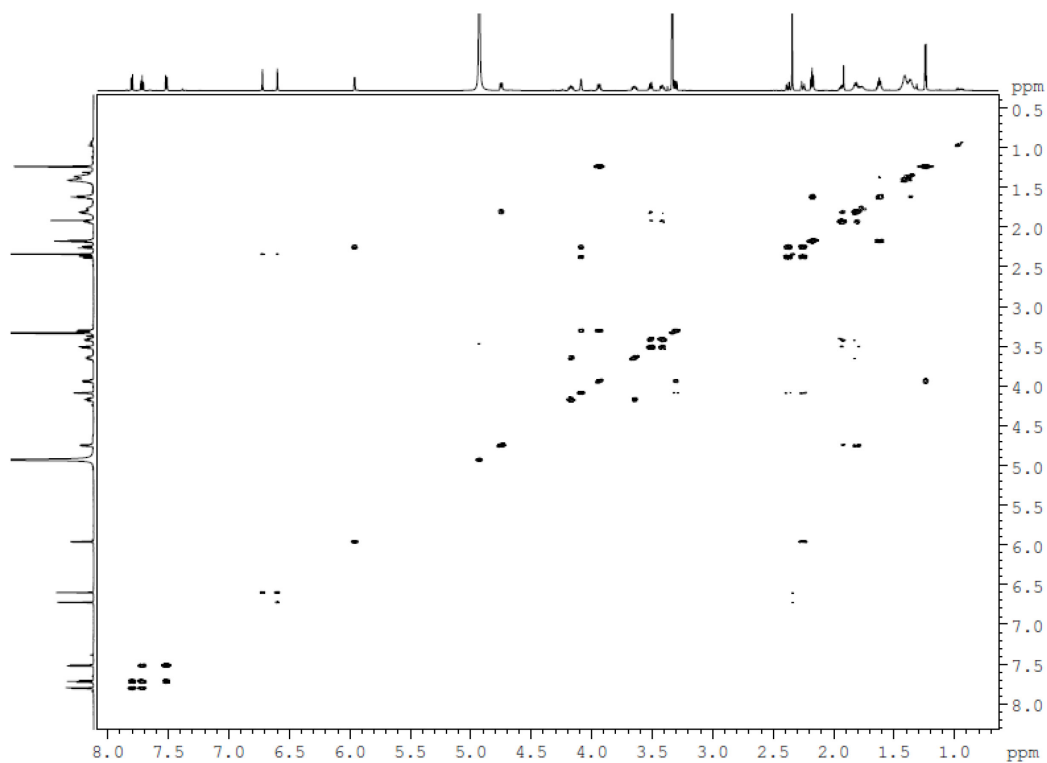


**Figure S43.**  $^1\text{H}$ - $^1\text{H}$  COSY spectrum of **5a** in MeOD.

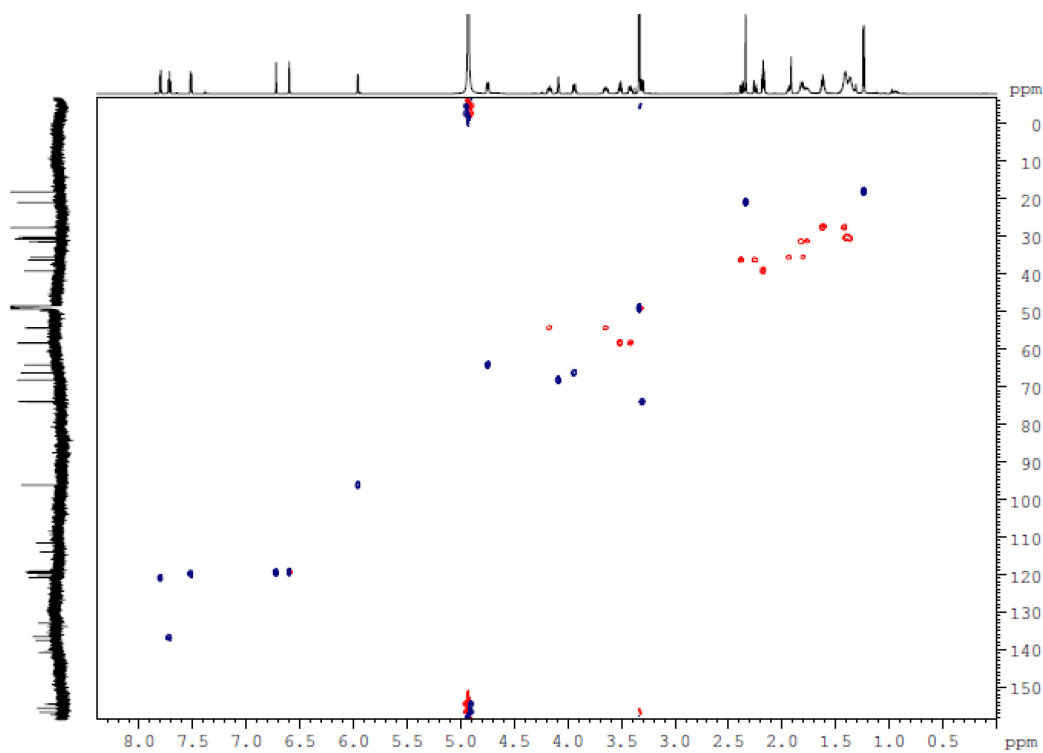


**Figure S44.** Edited-HSQC ( $^1\text{H}$ - $^{13}\text{C}$ ) spectrum of **5a** in MeOD,  $\text{CH}_3/\text{CH}$  phased up (blue),  $\text{CH}_2$  phased down (red).

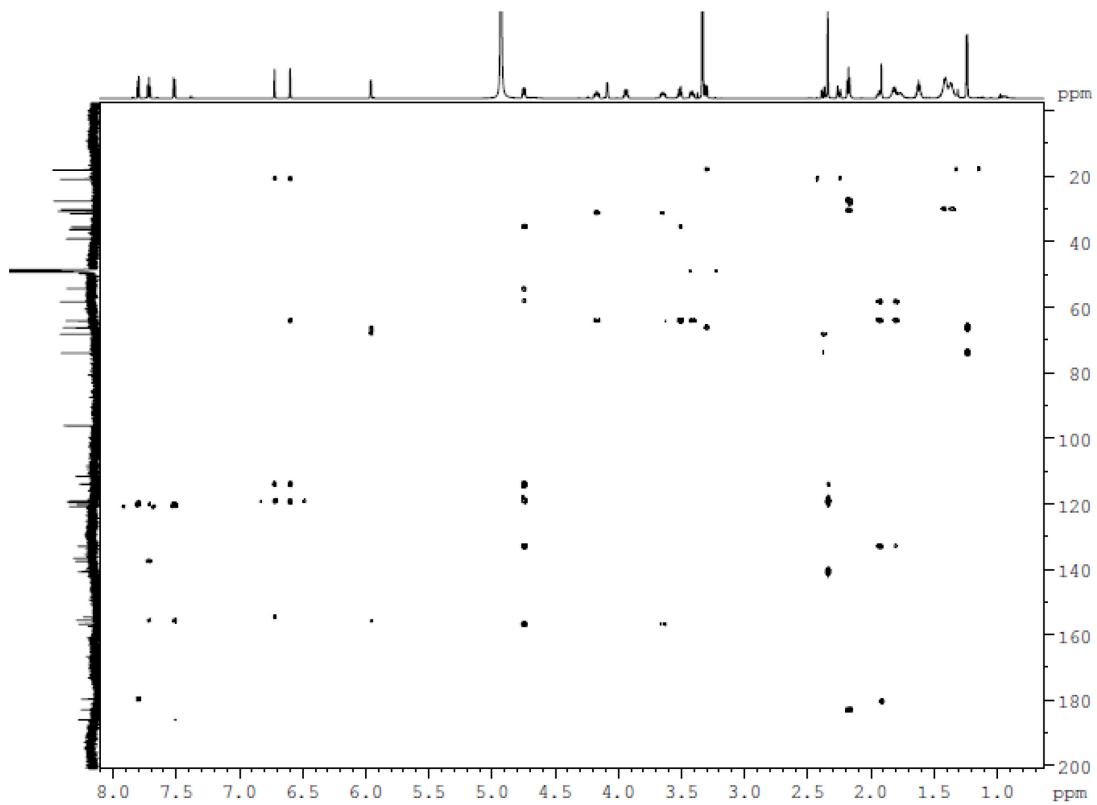


Figure S45.  $^1\text{H}$ - $^{13}\text{C}$  HMBC spectrum of **5a** in MeOD.

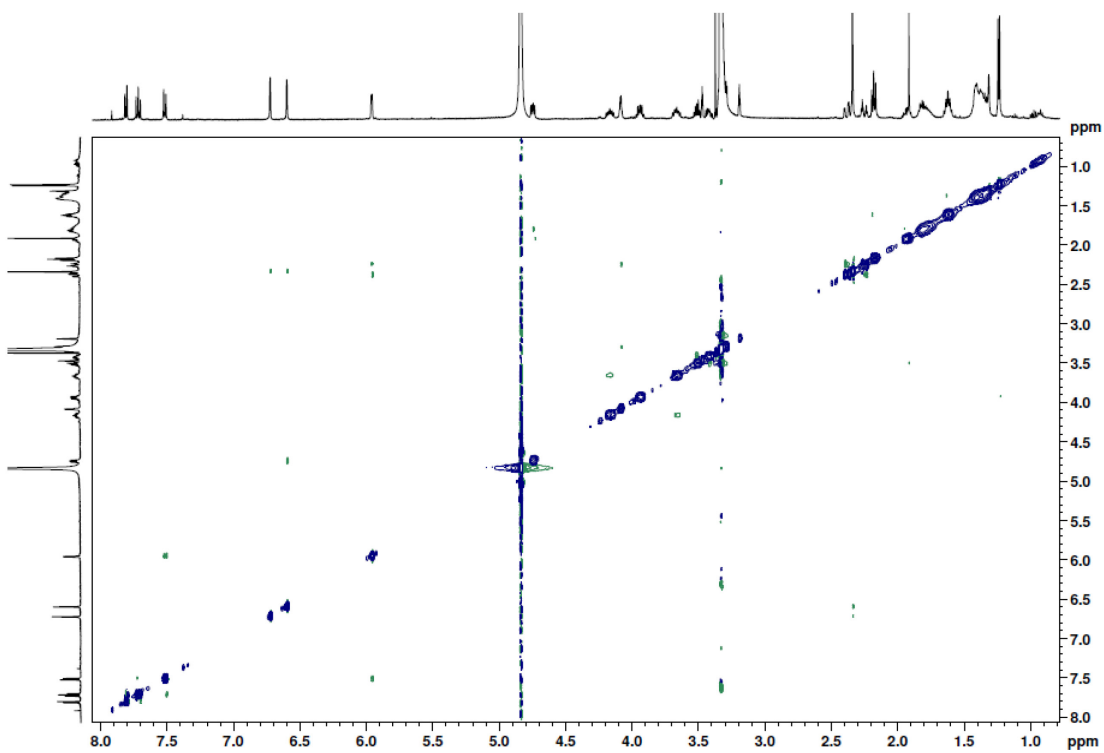


Figure S46.  $^1\text{H}$ - $^1\text{H}$  2D NOESY spectrum of **5a** in MeOD (mixing time 0.04  $\mu\text{s}$ ).



### 7.3.2 Jadomycin Undec Minor (5b)

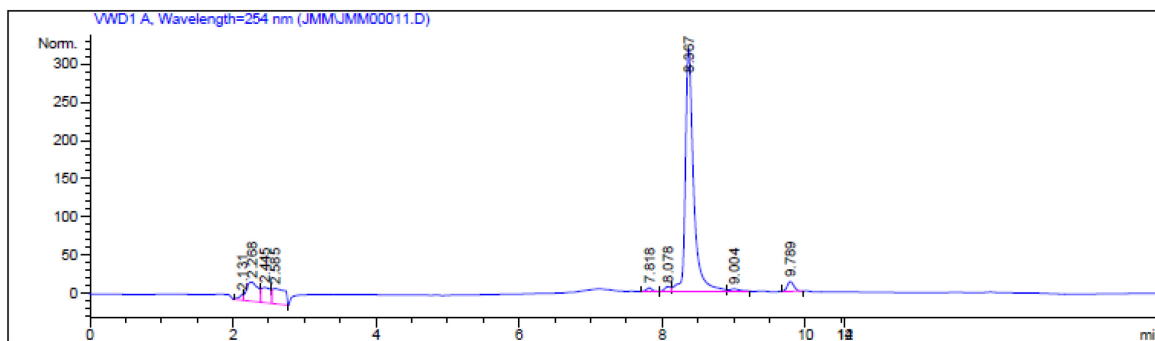


Figure S47. Analytical HPLC of **5b**.

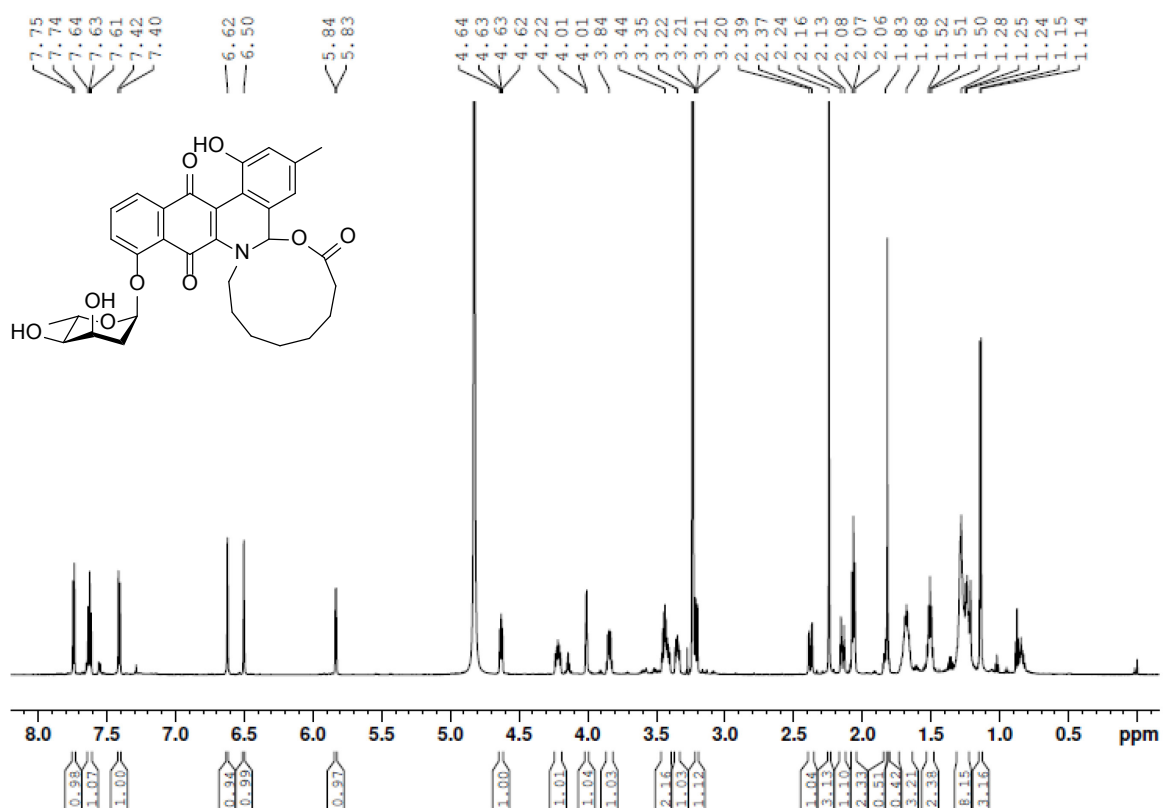
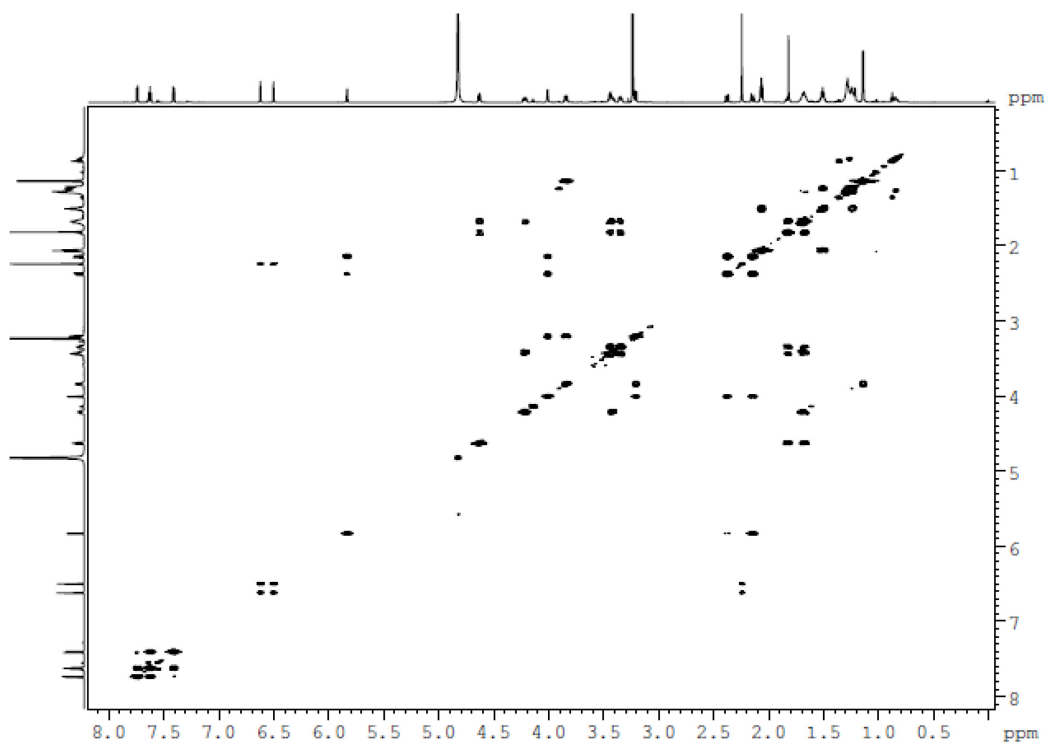
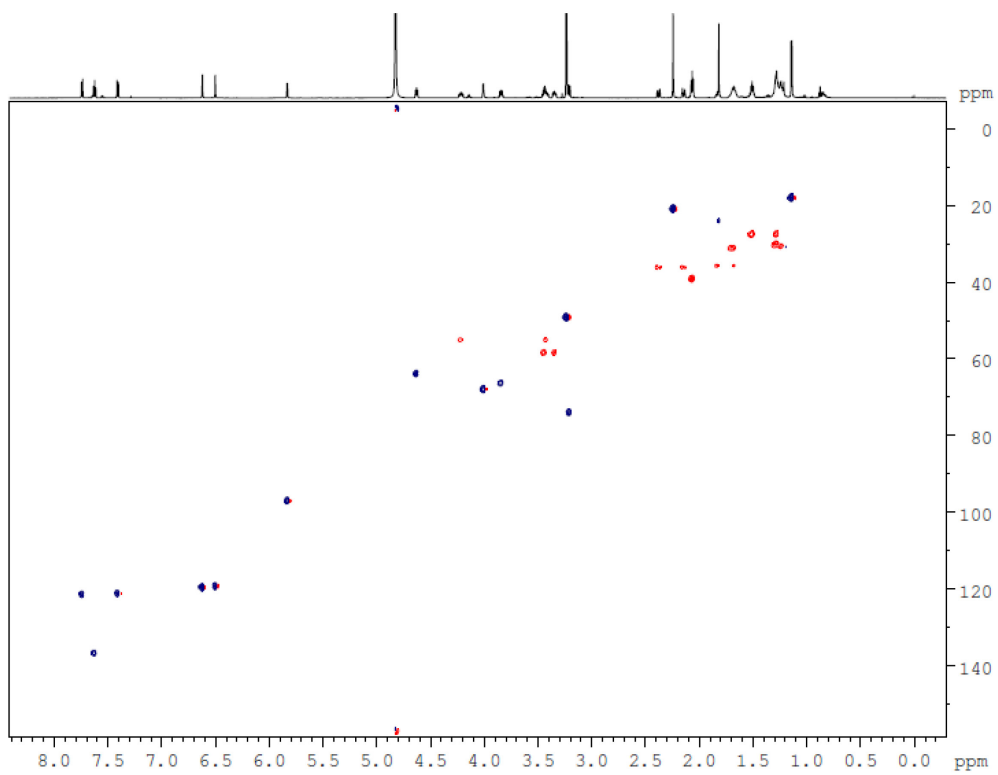


Figure S48.  $^1\text{H}$  NMR of **5b** in MeOD (1H: 700 MHz).



**Figure S49.**  $^1\text{H}$ - $^1\text{H}$  COSY spectrum of **5b** in MeOD.



**Figure S50.**  $^1\text{H}$ - $^{13}\text{C}$  Edited HSQC spectrum of **5b** in MeOD.  $\text{CH}_3/\text{CH}$  phased up (blue),  $\text{CH}_2$  phased down (red).

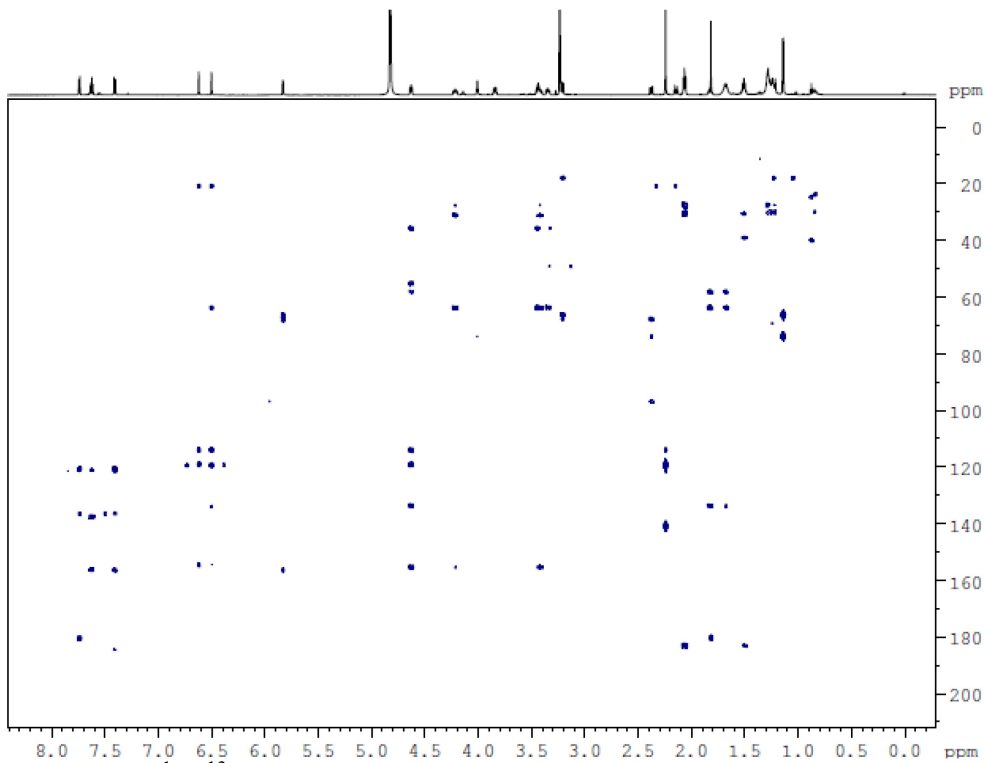


**Figure S51.**  $^1\text{H}$ - $^{13}\text{C}$  HMBC spectrum of **5b** in MeOD.

### 7.3.3 Jadomycin Undec Open E-ring Analogues (6, 7)

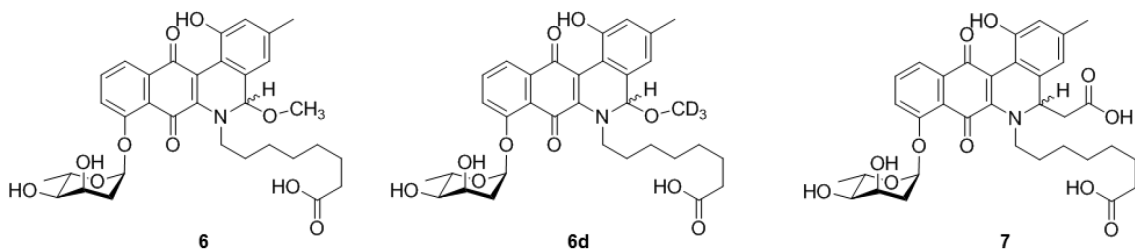


**Figure S52.** Jd analogues with open E-rings.

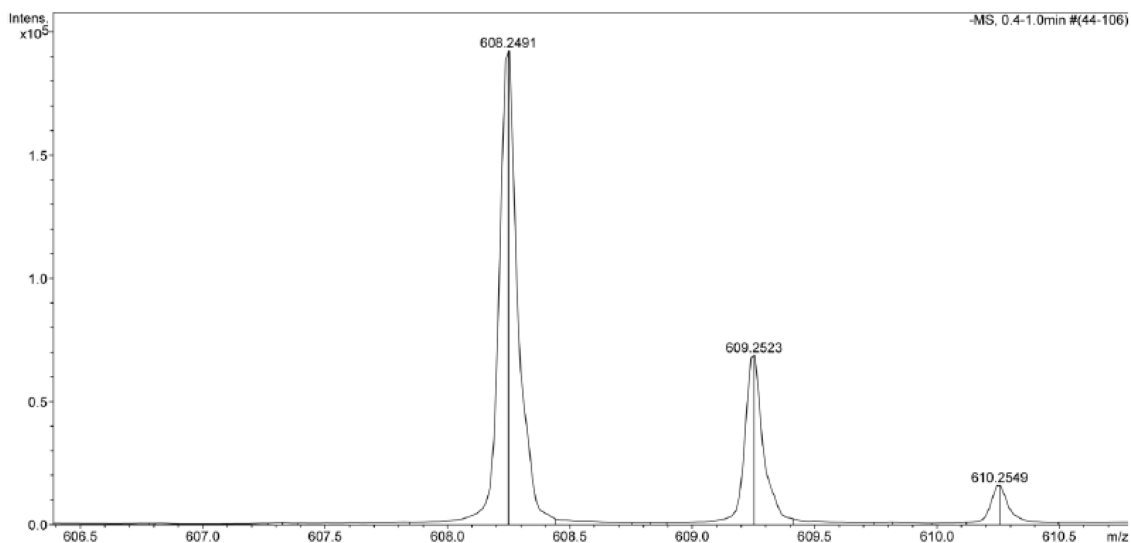


**Figure S53.** High resolution mass spectrum of **6**.  $[M-H]^-$  608.2491 found, 608.2496 calculated.

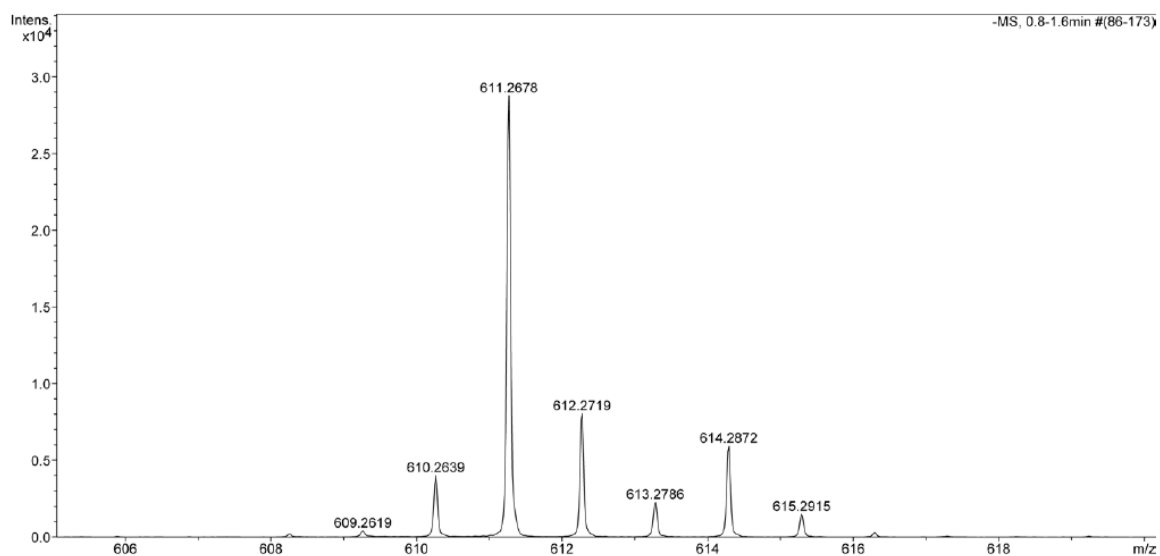


**Figure S54.** High resolution mass spectrum of **6d**.  $[M-H]^-$  611.2678 found, 611.2690 calculated.

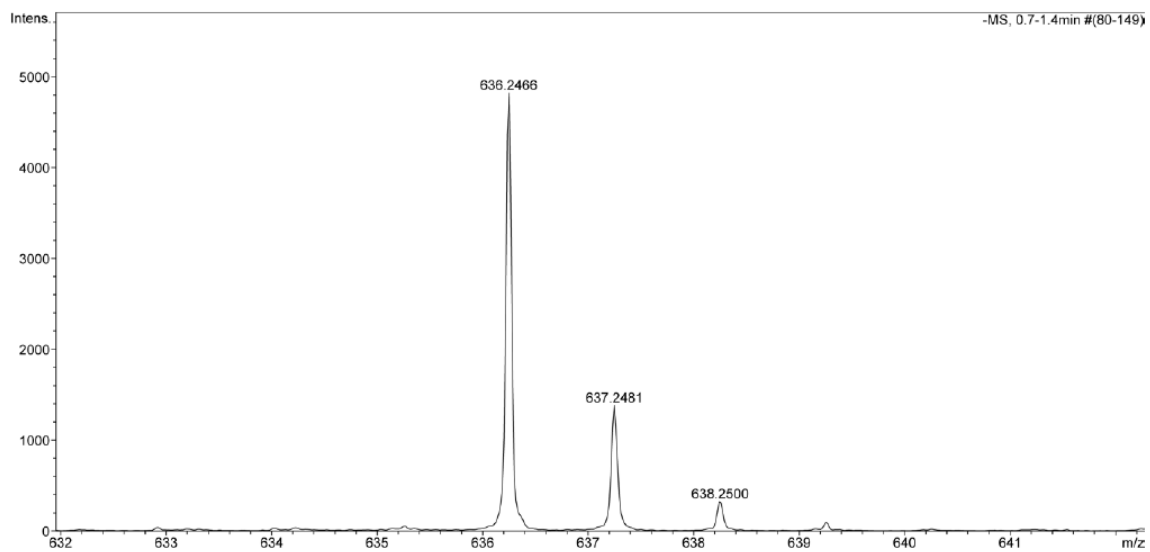


**Figure S55.** High resolution mass spectrum of **7**.  $[M-H]^-$  636.2468 found, 636.2450 calculated.

## APPENDIX II: SUPPLEMENTARY INFORMATION FOR CHAPTER 3

### 8.1 UrdGT2 Gene and Protein Sequences

Native <i>urdGT2</i> nucleotide sequence	gtttcgcgctggccccgctggccaccgcccccgaacgccggccaccaggtcgtcatggcggccaaccaggacatg ggaccggtcgttaccggagtgggcctgccggcggtcgcgaccaccgacctgccgatccgccactcatcaccacggacc gggagggcctcccaggccatccctccgatcccgtggcacaggcacgttaccggccgctggtcggccatgccc gctccagcctgccgcatgctgacttcagccgtgctggcgtcccggacctatcgtcggcggcacgatgactacgtc gccccctgctgcccctgcatctggcgctgccgcacccccgagacatgggatgctgctgatccgacggcatccacc cgtgccgatccgaactcggcccagctgagtgaaactggctggaacggctgccgccccggatctgttcacgacat ctccccccgagcctcgcgccgcgaacgccgcgccccggatgatcggcacgctcgcgacgagccgacagtcc cgtggaaccgtgatgtacaccgcgacaccgtcagcgtgttctgtaacctccggcagcagggctcgcgaaggagag ctacgacaggaactcgaactcctgcgcggcctggccaagatctcgtccgctgggatgctgagctcatcgtcggcccc gacaccgtcggcaggccctccgcggcagggtgccgaggcacgggtcggctggacaccctggatgctggtggccc acctcgcacctgctggtccaccatggggcggtgctcagcacactgaccggcctgagcggggtgagccgcaactgctcat cccaaggctcctcctggaggcggcgctcgcgcgtcggcactacggagcggccatcggcctgctcgggggtga ggactcagccgagcgtcggactcctgccaggagctgcacccaaggacacctatgccggcgagcccaggacct ctccccggagatctccggaatgccctgccgcgaccgtcgtcacagcgtcgaacagctggcgtga
Native UrdGT2 amino acid sequence	VFALAPLATAARNAGHQVMAANQDMGPVVTGVGLPAVATTDLPIRHFITTD REGRPEAIPSDPVAQARFTGRWFARMAASSLPRMLDFSRAWRPDLIVGGTMS YVAPLLALHLGVPHARQTWDAVDADGIHPGADAELRPELSELGLERLPAPDLF IDICPPSLRPANAAPARMMRHVATSRQCPLPVMYTRDTRQRVLVTSGSRVA KESYDRNFDFLRGLAKDLVRWDVELIVAAPDTVAEALRAEVPQARVWGWTPL DVVAPTCDLLVHHAGGVSTLTGLSAGEPQLLIPKGSVLEAPARRVADYGAIA LLPGEDSTEAIAIDSCQELHAKDTYARRAQDLSREISGMPLPATVVTALEQLA*
Optimized <i>urdGT2</i> nucleotide sequence with His-6 tag	gtttcgcctcggccccgctgccaccgcccccgaacgccggcaccaggtcgtcatggcggccaaccaggacatgg ggcggcgtcgtcaccggggtcggctcctcccggcggtcgcgaccaccgacctccgatccgccactcatcaccacggaccg ggaggggcggccccgagccatcccgtccgaccccggtggcccaggcccgggtcaccggctcgtggtcggccatggc cgctcctcctcccgcgcatgctggacttcagccggcctggcggcccgaactcctcgtcggcggcacgatgtcctacgt cgcgccccctgctgcccctgcacctggcgctgccgcacccccgagacgtgggacggcgtggacggcagccatcca ccccggcggcagccgaactccggcccagctgctggaactggcctggagcggctgccgccccggacctgttcac gacatcgtcccgcgagcctcgcgccgcgaacgccgcgccccggatgatcggcacgctcgcgacgagccgcca gtccccgctggagcgtgatgtacaccgcgacaccgccagcgcgtcgtcgtgacctccggcagccgggtggcgaa ggagtgctagcagccggaactcgaactcctcgcggcctggccaaggacctcgtccgctgggacgtcagctgatcgtc ccgccccggacaccgtcgcgagccctccgcggcaggtgccgagggcgggtgggctggacggccctggagctc gtggcggccacctcggacctcctcgtccaccacggggcggtctcgtcagcgtcaccggcctcctcggcggggagccgc agctcctatccccagggtcctcctggaggcggcgccgcccgcgtcggcactacggcggccatcggcctcct ggcgggggagactcagccagggcgtcggactcctgccaggagctgcacccaaggacacctacggcggcggc cccaggacctcagccgggagatctccggcatgccctcccggcgaccgtcgtgacggcgtggagcagctcgcgcacc accaccaccactga
Optimized UrdGT2 amino acid sequence with His-6 tag	VFALAPLATAARNAGHQVMAANQDMGPVVTGVGLPAVATTDLPIRHFITTD REGRPEAIPSDPVAQARFTGRWFARMAASSLPRMLDFSRAWRPDLIVGGTMS YVAPLLALHLGVPHARQTWDAVDADGIHPGADAELRPELSELGLERLPAPDLF IDICPPSLRPANAAPARMMRHVATSRQCPLPVMYTRDTRQRVLVTSGSRVA KESYDRNFDFLRGLAKDLVRWDVELIVAAPDTVAEALRAEVPQARVWGWTPL DVVAPTCDLLVHHAGGVSTLTGLSAGEPQLLIPKGSVLEAPARRVADYGAIA LLPGEDSTEAIAIDSCQELHAKDTYARRAQDLSREISGMPLPATVVTALEQLA HHHHH*

## 8.2 Control Production Analysis

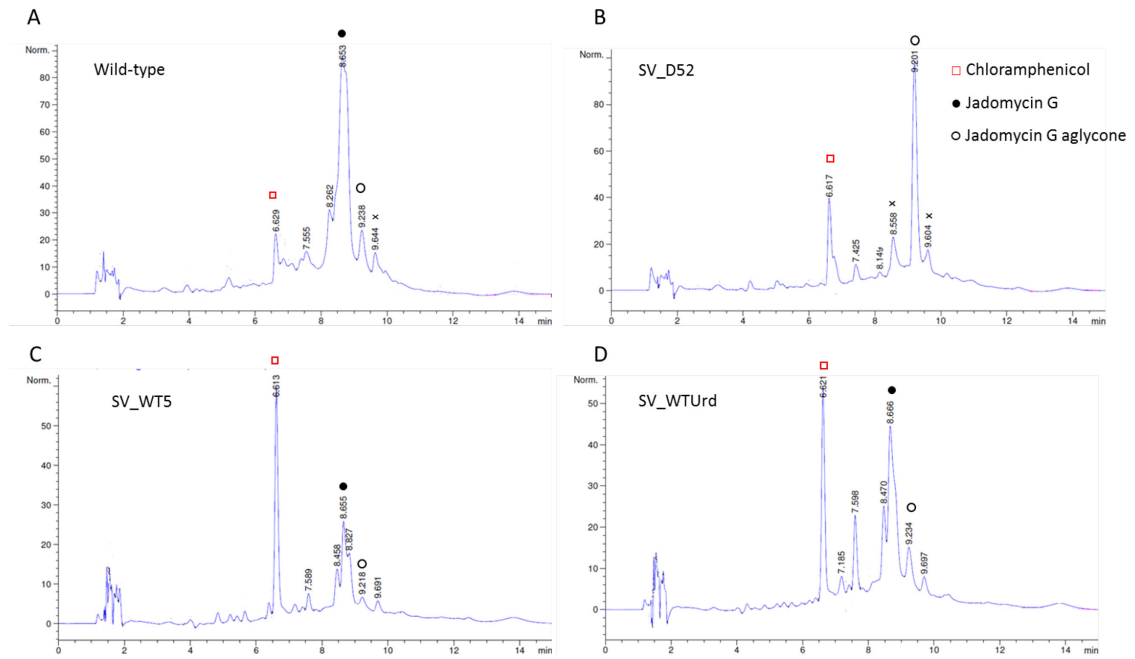


**Figure S56.** HPLC traces of JdG control productions from *S. venezuelae* (A) wild-type, (B) SV\_D52, (C) SV\_WT5, and (D) SV\_WTUrD.

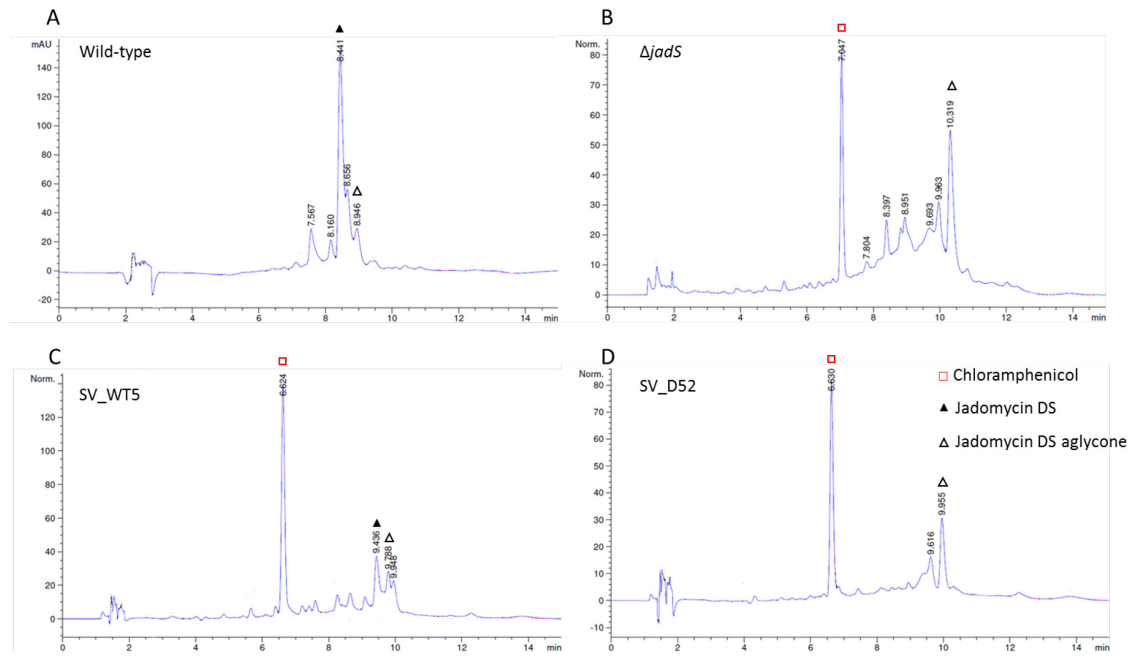


**Figure S57.** HPLC traces of JdDS control productions from *S. venezuelae* (A) wild-type, (B)  $\Delta$ *jadS*, (C) SV\_WT5, and (D) SV\_D52.

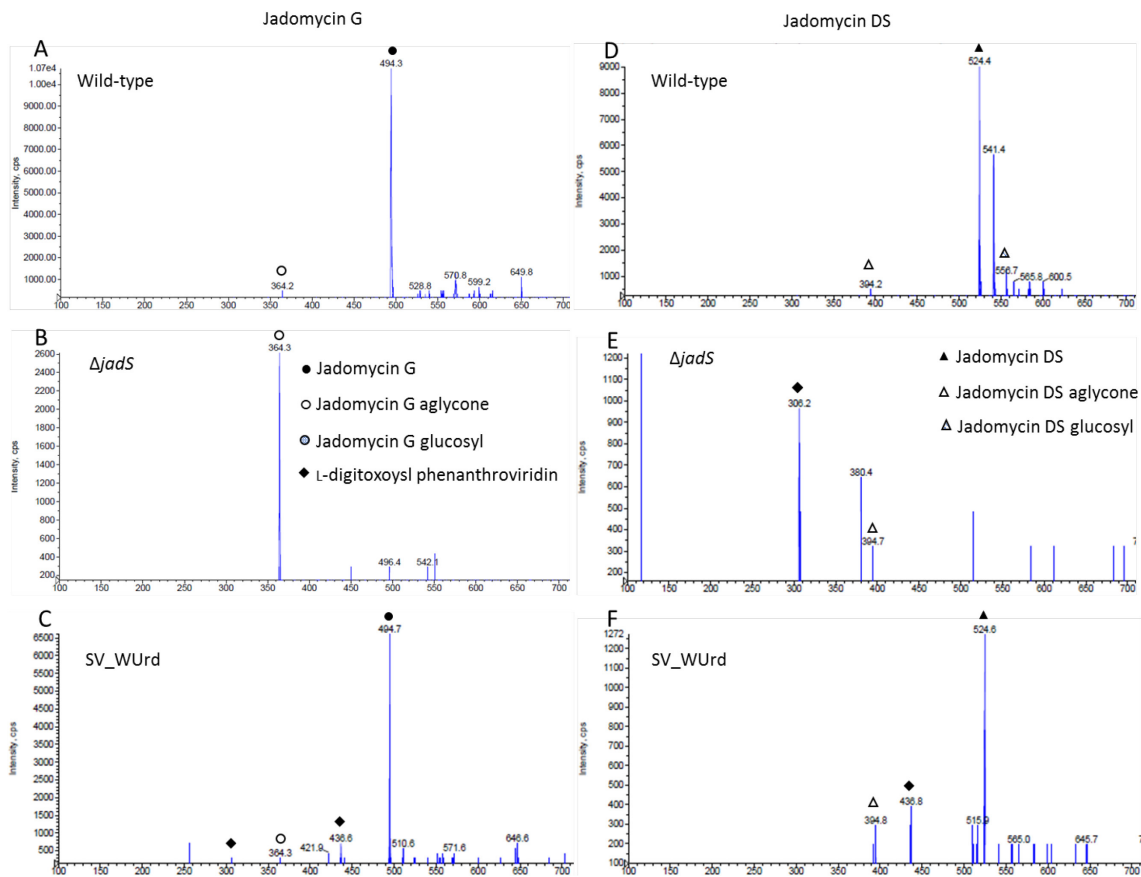


**Figure S58.** PREC 306 scans JdG and JdDS control production crude extracts using JdG from *S. venezuelae* wild-type (A),  $\Delta jadS$  (B), wild-type pSEE152\_urdGT2 (C); and using JdDS from *S. venezuelae* wild-type (D),  $\Delta jadS$  (E), wild-type pSEE152\_urdGT2 (F).



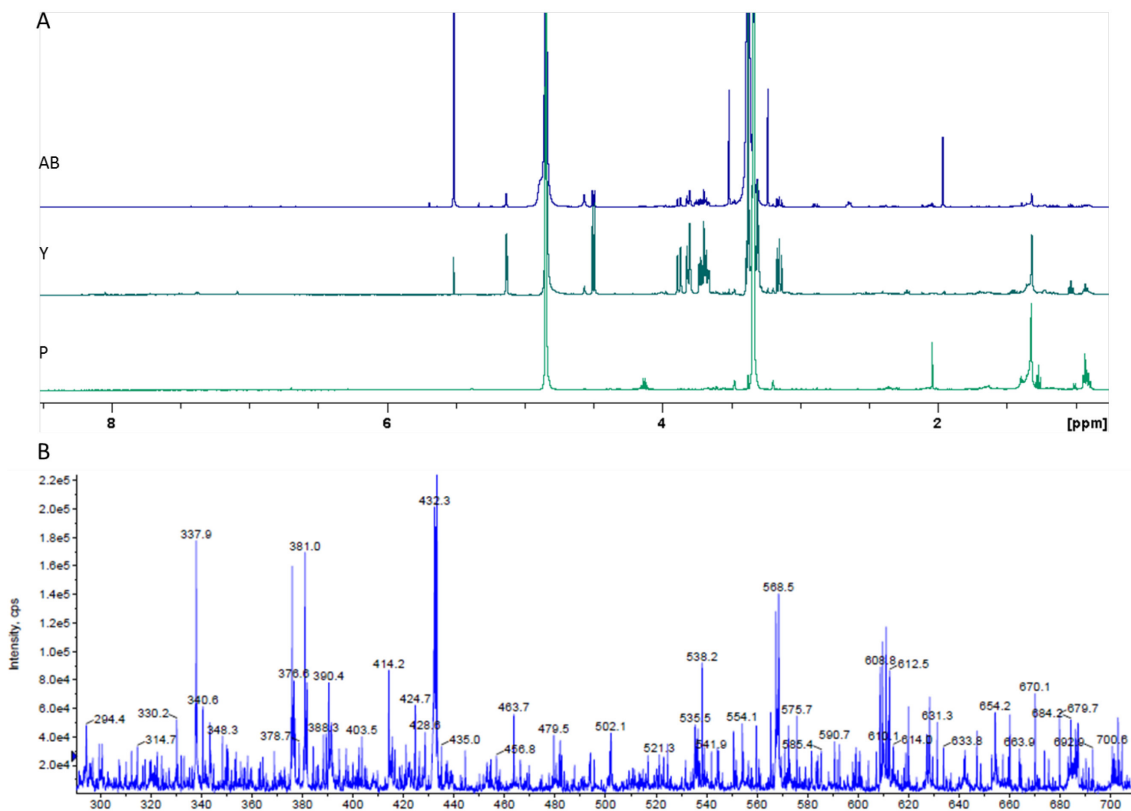


**Figure S59.** Analysis of scaled up JdG crude from SV\_52Urd; (A) <sup>1</sup>H NMR (500 MHz) in MeOD of three prep-TLC fractions; (B) ESI<sup>+</sup> scan of fraction P (pink coloured pre-TLC fraction).

## APPENDIX III: SUPPLEMENTARY INFORMATION FOR CHAPTER 4

### 9.1 Control Compound Data

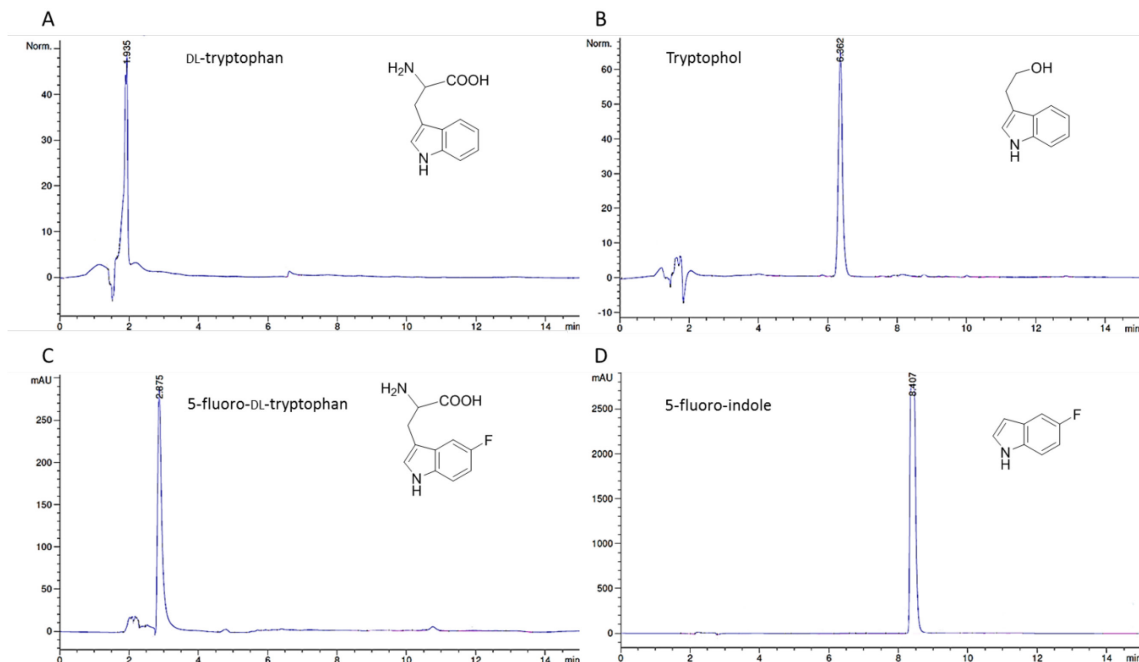


**Figure S60.** Reference HPLC traces of commercially sourced compounds; (A) DL-tryptophan; (B) tryptophol; (C) 5-fluoro-DL-tryptophan; (D) 5-fluoroindole.

### 9.2 Supplemental Production Data

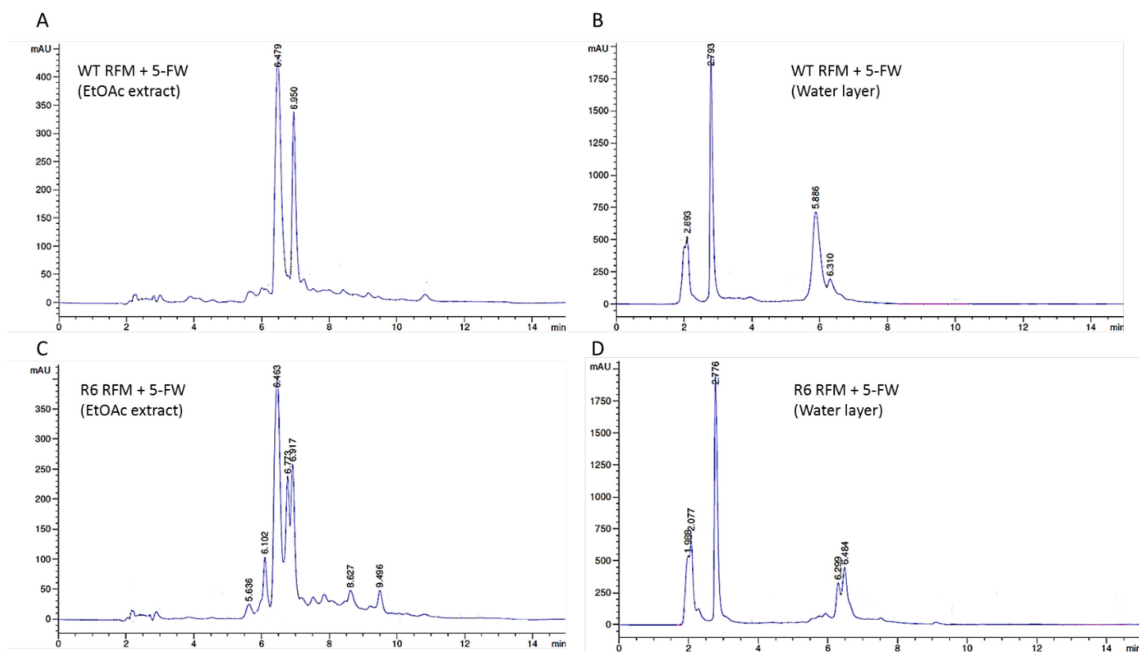


**Figure S61.** HPLC traces of RFM productions supplemented with 5-FW; wild-type production ethyl acetate (A) and water (B) extracts; R6 production ethyl acetate (C) and water (D) extracts.

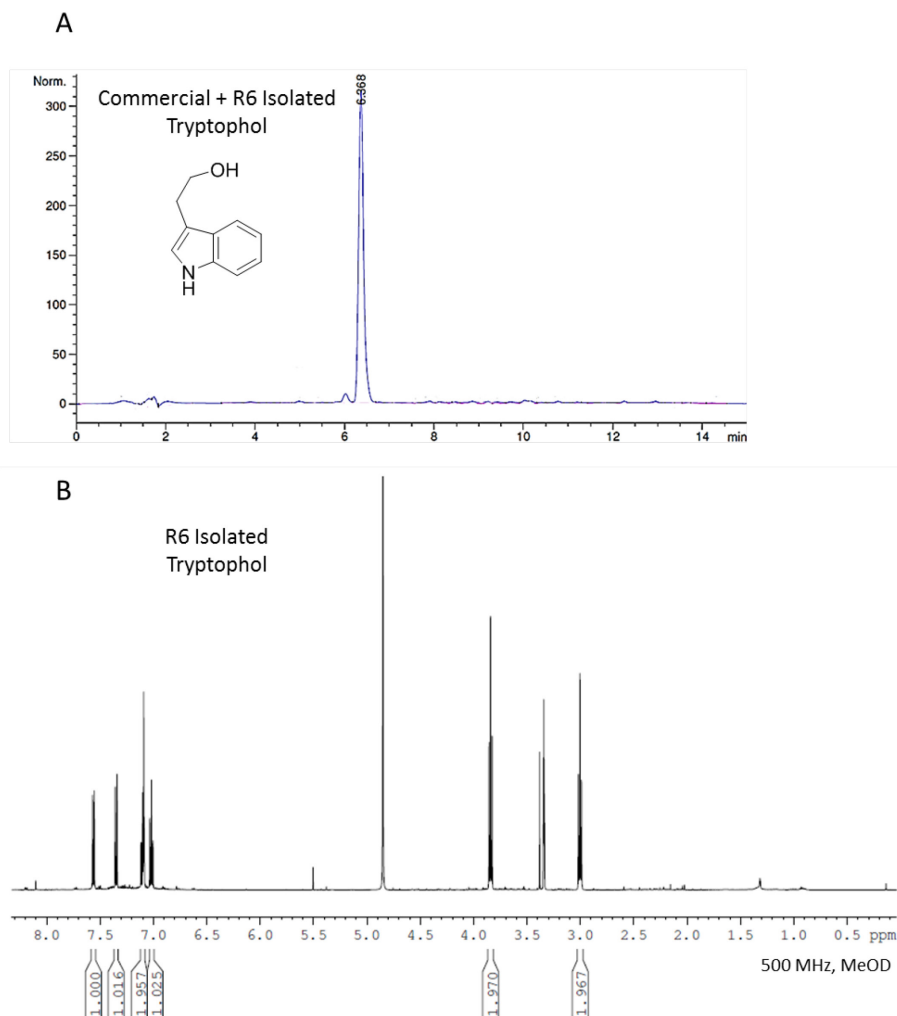


**Figure S62.** (A) HPLC of R6 isolated tryptophol spiked with commercially-sourced tryptophol to confirm identity; (B) NMR of R6 isolated tryptophol in methanol-*d*<sub>4</sub>

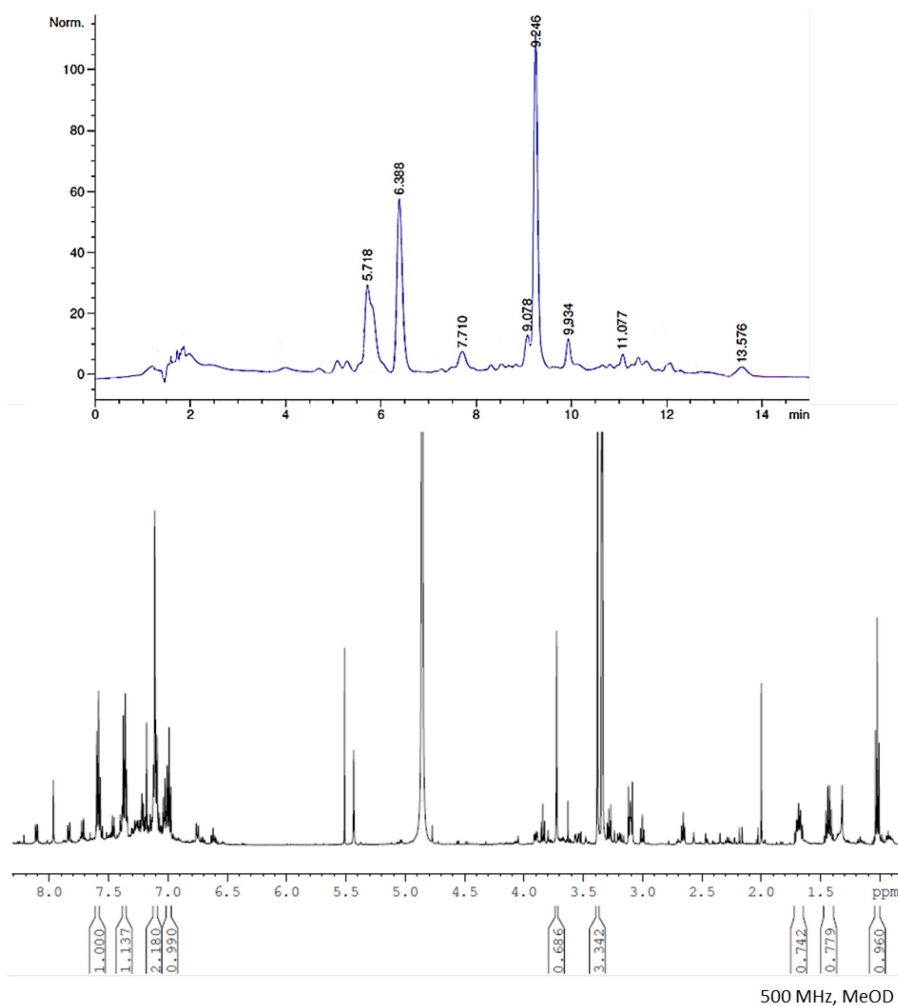


**Figure S63.** (A) HPLC of R6 isolated tryptophan derivative (presumed 3-methylindole); (B) NMR of same isolate in methanol-*d*<sub>4</sub>.

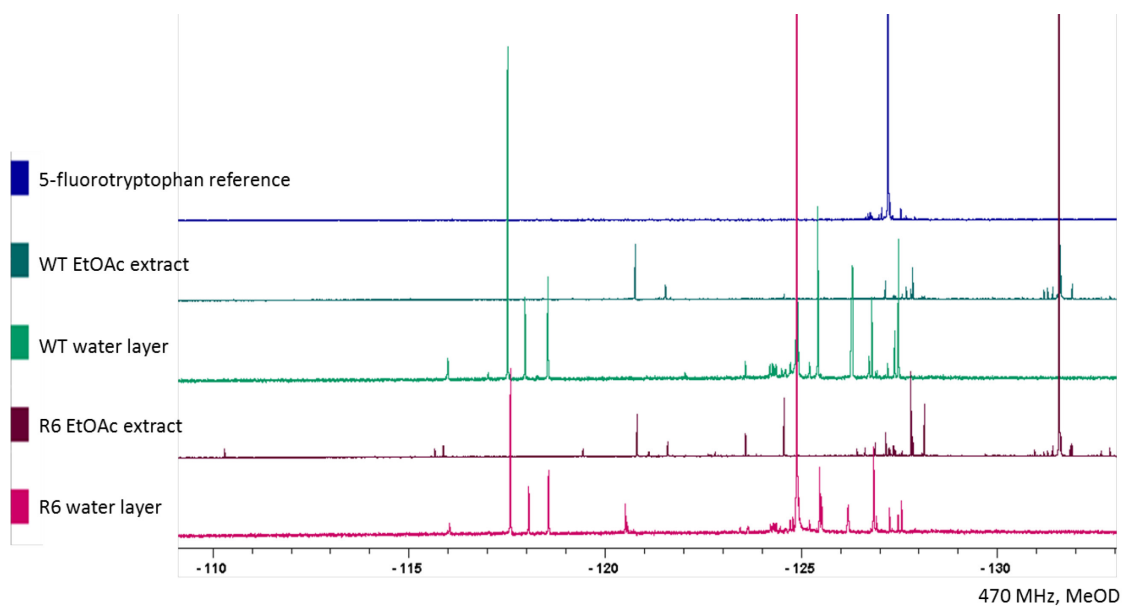


**Figure S64.** NMR spectra of RFM productions with 5F-W supplementation ( $^{19}\text{F}$ : 470 MHz) (baseline intensity increased).